THE UNIVERSITY OF HULL

MICROWAVE EFFECTS ON SOME ZEOLITE CATALYSED REACTIONS

being a Thesis submitted for the Degree of

Doctor of Philosophy

in the University of Hull

by

STEPHEN DAVID POLLINGTON, BSc. Hons.

October 1993

ACKNOWLEDGEMENTS

I am grateful to my supervisors Dr. R. B. Moyes and Dr. D. A. Whan for their invaluable help and support throughout this work and to SERC for the award of a postgraduate studentship under the CASE scheme. I express my thanks to my industrial supervisor Dr. I. J. S. Lake and to the Hydrocarbons Group at ICI Wilton for their financial and material support. I am also grateful to Dr. C. A. Hamilton and the Melinar Group at ICI Wilton for the collaborative study which was undertaken in their laboratories. Thanks to all the members of the Catalysis Group at Hull for their help and advice. I must also acknowledge the help, throughout this work, from the technical staff at the School of Chemistry.

Special thanks to Dr. G. Bond for all his time, advice and enthusiasm.

A big thank you to my wife and parents for all their support and encouragement.

SUMMARY

This research was prompted by the growing body of information accumulating in the literature which refers to the advantages of microwave irradiation as opposed to normal conventional heating. Many of the reports claim that activation by microwave radiation results in enhanced rates and changes in product selectivities. Of special interest were reports that microwave irradiation had beneficial effects on heterogeneous catalysed reactions. Microwave irradiation should be able to activate specifically the actual catalytic sites and hence could be used to affect reactions where the bulk of the catalyst, the reactants and products are transparent to microwaves. Investigation of this effect was conducted on zeolite catalysed reactions, namely the disproportionation of toluene and the alkylation of toluene with methanol.

Most of the reports fail to address the problem of accurate temperature measurement within a microwave field. This is of paramount importance and this study describes the development and use of a gas thermometer to overcome this problem. This development has been used to measure the temperature of solvents under thermal and microwave conditions. Using this device it was discovered that polar solvents could attain temperatures in excess of 20°C above their normal boiling point and this phenomenon was investigated further to quantify the effect as a function of the microwave power, the volume of the solvent, the dielectric properties associated with the solvent and the surface of the container used.

A comprehensive study of the effect of microwave radiation on disproportionation and alkylation of toluene has been made using hydrogen forms of mordenite and ZSM-5 catalysts. The aim of this reaction is to make paraxylene which is then used in the production of terephthalic (1,4-benzenedicarboxylic) acid. This reaction has been studied under both microwave and thermal conditions at various temperatures. Microwave radiation has shown to have no beneficial effect on the reaction selectivity for the disproportionation and alkylation of toluene. Experiments on disproportionation of toluene under high pressure thermal conditions have shown that partial regeneration of the catalyst can be performed by raising the partial pressure of hydrogen.

The study describes in detail the comparison between microwave radiation and normal conventional heating, the influence of carbon laydown on the catalyst under conventional and microwave conditions, and the possibilities of catalyst regeneration. Carbon is deposited on the catalyst and observations have shown that it preferentially absorbs microwaves offering novel techniques for regeneration of the catalyst.

Contents.

Chapter Three. Toluene Disproportionation.

Chapter One.

Catalysis With Microwaves: A Review.

1.1. Reasons for this study.

The development of microwave technology since the 1940's has had a great impact in the 20th Century. Industrial, scientific and medical applications using this technology have been developed and utilised[1-2]. Microwaves have been used for applications such as cooking, curing and hardening, dye fixation, drying, heating and melting. The advantages of microwaves over conventional techniques have been summarised by Perkin[3].

(1). More efficient in drying.
(2). Drying times may be reduced.
(3). The system is more compact than conventional systems.
(4). Selective energy absorption by lossy constituents.
(5). Heat transfer is independent of air stream and mass transfer is increasingly independent of air stream as solid temperature increases.
(6). Energy dissipated throughout volume of material - deeper penetration.
(7). Overdrying can be avoided.
(8). Substitution of an expensive raw material with a cheaper one.
(9). Relatively low maintenance costs.

This study was prompted by the growing number of publications detailing the use of microwave radiation as an alternative mode of heating in chemical reactions. Early reports claimed rate enhancements of between five and one thousand were achieved when using microwave radiation compared to normal conventional heating[4]. Early explanations for this effect stated that it was due to specific bond activation by microwaves[5]. However, little attention in these early reports was made to temperature measurement of the reactants during irradiation. An excellent review of applications of microwaves in chemistry has been conducted by Mingos and Baghurst[6].

Interest in microwave applications for use in heterogeneous catalysis was prompted by several reports in the literature which suggested that heterogeneously catalysed reactions may be systems which might benefit from the effects of microwave irradiation. Attention was focused on three areas where microwave irradiation could have an effect, namely preparation of catalysts, characterisation of catalysts and catalytic reactions.

1.2. Catalyst Preparation.

The theory of microwave heating will be discussed in chapter two. Most microwave appliances are tuned to a frequency of 2.45 GHz, which is quite effective in heating water and other compounds with OH groups. Catalyst preparation by impregnation often involves drying of the support material to form stable strong bonds between the support and the active phase. Many catalytic supports (alumina, silica etc.) have an extensive surface covered with hydroxyl groups, so microwave irradiation to dry the support could beneficial to produce a more stable material. Bond et al.[7] report that drying of alumina pellets, impregnated with aqueous nickel nitrate solution, by microwave irradiation results in reduced drying times, a more homogenous distribution of nickel and the pellets were significantly stronger when compared to conventional methods.

The use of microwave radiation, for drying purposes, has been well established in the ceramics industry[1, 2, 8-12]. Microwave tunnel ovens and specially constructed microwave ceramic dryers have been built for the treatment of ceramics[2]. Drying of polymers by microwave radiation is recommended because the polymers are mostly non-polar materials while the solvents to be evaporated are usually polar materials. Thermal methods can damage the products and produce changes in molecular weight, so drying using microwave radiation has significant advantages. Other drying processes where microwaves have been used are spray drying, vacuum drying and freeze drying[1].

Preparation of catalysts can not just be limited to drying. Roy et al.[12] have heated gels (silica or alumina) to very high temperatures in a microwave oven, providing an alternative method of preparing sol-gels in the ceramics industry. This could be developed for preparing more homogenous phases of alumina for catalytic purposes.

Microwave energy for a more rapid preparation of zeolite materials has been performed. Roussy et al.[13] observed that water can be desorbed from the internal surface of a zeolite cage (13X) when heated under microwave irradiation. Microwave drying of 13X zeolite has been experimentally studied[14]. Water has been shown to circulate throughout the zeolite porous space in the form of water vapour and that water

molecules adsorbed on the zeolite surfaces are less free than water molecules in the liquid water. The synthesis of zeolites using microwave radiation has not received much attention until recently. Chu et al.[15] have patented the use of microwave technology for preparation of zeolites namely NaA and ZSM-5. A range of zeolites has been synthesised using a 650 W microwave oven and a Parr autoclave[6]. The samples were highly uniform with particles sizes >2μm and some differences in sample morphology between thermal and microwave products were observed. Jansen et al.[16-17] have applied microwave energy to achieve faster reaction times (>10 times) compared with normal conventional heating for ZSM-5 and zeolites A and Y. The crystal size distribution was found to be smaller when compared with thermal samples. This was attributed to heterogeneous nucleation being avoided during microwave heating. The conclusion from their experiments was that microwave irradiation is a useful method for preparation of zeolites. Zerger et al.[18] have used a microwave discharge to prepare highly dispersed and reduced metal atom clusters in zeolites and other substances such as alumina and silica. This microwave discharge method has been shown to have advantages over other activation methods, the metal particle size can be selected by optimisation of the time of the microwave discharge, amount of metal and the type of metal and support used.

1.3. Catalyst Characterisation.

Temperature programmed techniques have been widely used in the characterisation of catalytic materials[19-20]. However, the problem with these techniques is that temperature gradients arise in the catalyst bed due to inefficient heat transfer from the walls of the furnace to the catalyst container and then to the catalyst itself. This results in poor resolution which leads to less data being extracted for the results.

Microwave energy provides more homogenous heating of the sample than conventional methods and temperature gradients should be minimised as only the sample should be heated under microwave irradiation. Karmaszin et al.[21-23] have used microwave radiation for thermal analysis of $CaHPO_4.2H_2O$ and $(CH_3COO)_2Zn.2H_2O$ and have obtained better resolution when compared with normal conventional methods.

Bond et al.[24] have conducted temperature programmed studies on a hydroxycarbonate catalyst (copper/zinc/aluminium) under thermal and microwave conditions and have concluded that microwave radiation provided a more linear heating rate, improved the resolution of data, and that the whole process was much quicker (due to the fact that under thermal conditions the furnace needs to cool before the next sample can be examined).

1.4. Catalytic Reactions using microwave radiation.

As stated earlier heterogeneous catalysis may be an area which could benefit from using microwave radiation as the mode of heating. Different product selectivities have been observed when catalysts are heated using microwave radiation when compared with the selectivity when heated conventionally. Villemin et al.[25-31] and Varma et al.[32-33] have studied "dry organic reactions" using microwave radiation. They have adsorbed organic reactants onto inorganic solids (such as silica, alumina or clay) and observed increased reaction rates compared with normal conventional heating. The explanation given for their observations was that the hydroxyl groups, water and the organic reactants present on the oxide surface absorb the microwave energy, while the bulk oxide is transparent to it.

Thiebaut et al.[34] have studied the reaction of 2-methylpentane on platinum supported on alumina and have shown that the product ratios were different when the reaction was performed under microwave conditions. The reaction of 2-methylpentane on Pt/Al_2O_3 gave a range of cracking and isomerisation products. Under microwave irradiation the conversion was enhanced, and the yield of benzene and butane was substantially greater than that from normal conventional heating. Their interpretation of the results was that the platinum was 25°C hotter than measured, but this does not explain the excess production of benzene and butane.

Herbst et al. [35] have subjected spent catalyst to microwave radiation before catalyst regeneration for use in catalytic cracking. In this process the microwave frequency ignores the catalytic cracking catalyst and preferentially excites the hydrocarbon or coke on the spent catalyst.

Suib et al.[36-37] have used microwave plasma methods for the catalytic conversion of methane to higher hydrocarbons. The plasma was initiated in argon at low pressure. The feed (methane, ethane, ethylene or a selected methane/oxygen ratio) was introduced to the plasma zone. The catalyst (Ni, Pt, Fe, MnO_2 or MoO_2) was placed outside the plasma zone to intercept the radicals as soon as they left the plasma. Conversion of methane gave ethane, ethylene and ethyne. Selectivity was influenced by

the power, flow rate and presence of a catalyst. Other researchers have also studied the catalytic conversion of methane using microwave plasma methods without a catalyst present[38-40]. Wan et al.[41-42] have studied the catalytic conversion of methane to higher hydrocarbons under microwave radiation using a different experimental procedure. The catalyst was heated under pulsed microwave radiation (typically millisecond pulses) at atmospheric pressure. Pulsed microwave heating of the catalyst gave C_2 and C_3 hydrocarbons depending on the power and duration of the pulses.

Wan and co-workers have investigated the application of microwave radiation for catalytic purposes for several years[41-51]. They have been developing experimental methods and procedures in microwave catalysis, and conclude that there is no general apparatus which is suitable for all applications. Their early experiments used a commercial microwave oven modified to concentrate the microwave energy on a flow reactor. The reactions of cyclohexane over a $CaNi_2$ catalysts under thermal and microwave conditions were studied[44]. Under microwave irradiation conversion of cyclohexane gave benzene which suggested that the surface temperature of the catalyst was hotter when compared with thermal heating. Microwave assisted catalytic hydrocracking has been also examined and claims that the water gas shift reaction can give conversion of water and CO to CO_2 and hydrogen in 80% at an apparent temperature of 40°C have been made[45]. However, temperature measurement within a microwave field is very difficult (see later). Methane to ethene has also been performed at an apparent temperature of 50°C, however, the microwave power used in the experiments had been sufficient to melt the surface of the nickel catalysts used (melting point of nickel is 1455°C), so it appears that catalytic surfaces can achieve very high temperatures, under microwave conditions, while the bulk remains relatively cool. Improved conversion and product selectivities have been obtained with a waveguide reactor system using higher microwave power pulses (3 kW) for short durations. Reactions which have been studied were the catalytic decomposition of organic halides[46]. The reactions were observed to be 100% efficient and a mechanism was proposed for the decomposition using microwave conditions. This technique has also been applied to the catalytic decomposition of alkenes[47]. Variations in microwave

energy, number of pulses and the duration of pulses lead to efficient conversions to selected aliphatic and aromatic hydrocarbons. Other decomposition reactions studied have been the catalytic decomposition of gaseous air pollutants[48] and the decomposition of the complex and viscous hydrocarbons contained in bitumen to extract volatile and economically useful organic products such as C_2 and C_3 hydrocarbons[49]. Addition of water to the tar sand material promoted the formation of useful liquid oxygenated hydrocarbon products. They have also demonstrated the feasibility of producing hydrocarbons via the microwave induced catalytic reaction of water and carbon[50]. The major reaction products were ethyne, methane, ethene and ethane with minor products of propene, propyne and cyclopropane. Again, judicious use of experimental variables such as irradiation time, microwave power, and duration of pulses gave different selected hydrocarbons. The reaction of carbon dioxide and water in a continuous flow system using a supported nickel catalyst has been investigated[51]. The major products from this reaction were methane, ethane, methanol, acetone and C_3 and C_4 alcohols.

However, there is still an inadequate understanding of the basic mechanisms of how microwaves interact with surface metallic sites and the subsequent energy transfer on the surface, so research has been directed towards a greater understanding of this phenomenon[52].

1.5. The nature of this study.

The Hydrocarbons Group at ICI Wilton developed an interest in microwave activated reactions as a result of the published reports, and the claim that activation by microwaves results in enhanced rates and produces different product distributions compared with reactions activated by conventional thermal methods. The CASE award for this study was negotiated with the Hydrocarbons Group at Wilton. The programme of work was to investigate the effect of microwave radiation on a catalytic reaction. The first reaction chosen was the disproportionation of toluene, which is a zeolite catalysed reaction. The hydrogen forms of mordenite and ZSM-5 were the catalysts used in the study. The first experiment was to irradiate a hydrogen mordenite catalyst in a microwave oven. Even at full power (650 W) the temperature attained was only 240°C. These ovens operate as a multi-mode cavity where microwaves are generated by a magnetron and pass to the cavity by way of a short section of waveguide (see later). Devices of this type have a crude means of power control which consists of switching the microwave supply on and off. The timescale of this switching is of the order of several seconds, thus making this form of equipment unsuitable for reactions in flowing systems. With this in mind the initial experiments were performed under thermal conditions and a Hewlett-Packard gas chromatograph was modified to incorporate a reactor which could be usable in both thermal and microwave environments. The microwave experiments were carried out using a microwave single mode cavity device.

The problem of temperature measurement was of paramount importance and needed to be addressed, so experiments were designed to investigate methods of measurement of temperature within a microwave field. When a suitable device was constructed (the gas thermometer) the next stage of the project was to investigate the claim of rate enhancement under microwave radiation. Experiments were then conducted on heating of solvents under thermal and microwave conditions.

1.6. References.

1. Metaxas A. C. and Meredith R. J., "Industrial Microwave Heating", Peter Peregrinus Ltd, (1983).
2. Thuery J., "Microwaves: Industrial, Scientific and Medical Applications", Artech House, Boston London, (1991).
3. Perkin R. M., J. Sep. Proc. Techn., **1**, 14, (1979).
4. Gedye R. N., Smith F. E., and Westway K. C., Can. J. Chem., **66**, 17, (1988).
5. Sun W-C., Guy P.M., Jahngen J. H., Rossomando E. F., and Jahangen G. E., J. Org. Chem., **53**, 4414, (1988).
6. Mingos D. M. P. and Baghurst D. R., Chem. Soc. Rev., **20**, 1, (1991).
7. Bond G., Moyes R. B., Pollington S. D., and Whan D. A., Proc. 10th Intern. Congr. Catal. Budapest 1992, Part B, p1805, Elsevier, Amsterdam.
8. Kenkre V. M., Skala L., Weiser M. W., and Katz J. D., J. Mat. Sci., **26**, 2483, (1991).
9. Mingos D. M. P., and Baghurst D. R., J. British Ceramics Trans., **91**, 124, (1992).
10. Palaith D., and Silberglitt R., Ceramic Bulletin, **68**, 1601, (1989).
11. Jones P., in "Drying 1992", Mujundar A. S. (Ed.), Elseveir Science Publishers B. V., 114, (1992).
12. Roy R., Komarneni S., and Yang L. J., J. Am. Ceram. Soc., **68**, 392, (1985).
13. Roussy G., Zoulalian A., Charreyre M., and Thiebaut J. M., J. Phys. Chem., **88**, 5702, (1984).
14. Thiebaut J. M., Akyel C., Roussy G., and Bosisio R., IEEE. Trans. Instr. Meas., **37**, 114, (1988).
15. Chu P., Dwyer F. G., and Caike V. J., Eur. Patent, No. **358,827**, (1990).
16. Jansen J. C., Arafat A., Barakat A. K., and van Bekkum H., in "Molecular Sieves: Synthesis of Microporous Materials". Occelli M. L. and Robson H. E. (Eds.), Vol. I, Van Nostrand Reinhold, 507, (1992).

17. Arafat A., Jansen J. C., Ebaid A. R., and van Bekkum H., Zeolites, **13**, 162, (1993).

18. Zerger R. P., McMahon K. C., Seltzer M. D., Michel R. G., and Suib S. L., J. Catal., **99**, 498, (1986).

19. Jones A., and McNicol B. D., Catal. Rev., **24**, 233, (1982).

20. Lemaitre J. L., in "Characterisation of Heterogeneous Catalysts", Delannay F. (Ed.), Marcel Dekker, New York, 27, (1984).

21. Karmazsin E., Barhoumi R., and Satre P., J. Thermal Analysis, **29**, 1269, (1984).

22. Karmazsin E., Barhoumi R., Satre P., and Gaillard F. G., J. Thermal Analysis, **30**, 43, (1985).

23. Karmazsin E., Thermochimica Acta., **110**, 289, (1987).

24. Bond G., Moyes R. B., and Whan D. A., in "Catalysis and Surface Characterisation", Dines T. J., Rochester C. H., and Thomson J., (Eds.), The Royal Society of Chemistry, 60, (1992).

25. Villemin D., and Alloum A. B., Syn. Comm., **21**, 63, (1991).

26. Alloum A. B., Labiad B., and Villemin D., J. Chem. Soc., Chem. Comm., **16**, 386, (1989).

27. Villemin D., and Alloum A. B., Syn. Comm., **20**, 925, (1990).

28. Villemin D., and Labiad B., Syn. Comm., **20**, 3333, (1990).

29. Villemin D., and Alloum A. B., Syn. Comm., **20**, 3325, (1990).

30. Villemin D., Alloum A. B., and Thibault-Starzyk F., Syn. Comm., **22**, 1359, (1992).

31. Villemin D., Alloum A. B., and Loupy A., Syn. Comm., **23**, 419, (1993).

32. Varma R. S., Varma M., and Chatterjee A. K., J. Chem. Soc. Perkin Trans. I, 999, (1993).

33. Varma R. S., Chatterjee A. K., and Varma M., Tet. Letts., **34**, 4603, (1993).

34. Thiebaut J. M., Roussy G., Maire G., and Garin F., Proc. High Frequency and Microwave Processing and Heating, KEMA, Arnhem, No. 6(5), 2, (1989).

35. Herbst J. A., Markham C. L., Sapre A. V., and Teitman G.J., U. S. Patent, No. **4,968,403**, (1990).

36. Suib S. L., Zerger R. P., and Zhang Z., Symposium on Natural Gas Upgrading II., Div. Petroleum Chem., ACS, Washington D. C., 344, (1992).

37. Suib S. L., and Zerger R. P., J. Catal., **139**, 383, (1993).

38. Kawahara Y., U. S. Patent, No. **3,663,394,** (1972).

39. Kawahara Y., J. Phys. Chem., **73**, 1648, (1969).

40. McCarthy R. L., J. Phys. Chem., **22**, 1360, (1954).

41. Wan J. K. S., U. S. Patent, No. **4,574,038**, (1986).

42. Wan J. K. S., Tse M Y., Husby H., and Depew M. C., J. Microwave Power and Electromagnetic Energy, **25**, 32, (1990).

43. Tse M. Y., Depew M. C., and Wan J. K. S., Res. Chem. Interm., **13**, 221, (1990).

44. Wolf K., Choi H. K. J., and Wan J. K. S., AOSTRA (Alberta Oil Sands Technology and Research) Journal of Research, **3**, 53, (1986).

45. Wan J. K. S., and Heyding R. D., Catalysis on the Energy Scene, 561, (1984).

46. Dinesen T. R. J., Tse M. Y., Depew M. C., and Wan J. K. S., Res. Chem. Interm., **15**, 113, (1991).

47. Cameron K. L. Depew M. C., and Wan J. K. S., Res. Chem. Interm., **16**, 57, (1991).

48. Depew M. C., Dinesen T. R. J., Tse M. Y., and Wan J. K. S., Proc. Environmental Research, Technology Transfer Conference, Toronto, 1990, **I**, 200.

49. Depew M. C., Lem S., and Wan J. K. S., Res. Chem. Interm., **16**, 213, (1991).

50. Bamwenda G., Moore E., and Wan J. K. S., Res. Chem. Interm., **17**, 243, (1992).

51. Wan J. K. S., Bamwenda G., and Depew M. C., Res. Chem. Interm., **16**, 241, (1991).

52. Wan J. K. S., Personal Communication.

Chapter Two.

Microwave Assisted Superheating Of Liquids.

2.1. Introduction.

2.1.1. Heating substances under microwave irradiation.

The effect of heat on reaction rates is well known; investigations of an alternative form of rate increase for chemical reactions have included studies on photochemical, catalytic, sonic and high pressure techniques[1]. Although microwave equipment for heating food has been available since the 1950's, it was not until the 1970's and 1980's that microwave ovens made an significant impact on domestic home cooking. There is a now a whole industry devoted to making microwave convenience meals. However, the response by chemists has been disappointing. This is probably due to a lack of understanding about microwave dielectric heating. This method of heating could be of great advantage to the chemist, since microwave dielectric heating is dependent upon the dielectric properties of the particular material being used. Therefore certain reactions could show different product selectivities depending upon the way the materials interact with microwave radiation.

2.1.2. Theory of Microwave heating.

The microwave region of the electromagnetic spectrum (figure 2.1) lies between the infrared and radio frequencies and corresponds to wavelengths between 1 cm and 1m (frequencies of 300 MHz to 300 000 MHz respectively). RADAR transmissions operate between 1 and 25 cm and the remaining wavelengths are used for telecommunication applications. For this reason, industrial, and domestic microwave appliances operate at four fixed frequencies, 915 ± 25, 2450 ± 13, 5800 ± 75 and 22125 ± 125 MHz; domestic microwave ovens operate at 2.45 GHz.

As shown in table 2.1 the energy of a microwave quantum is not sufficient to break a chemical bond, although the use of microwave technology for heating purposes has been established for 40 years. The theory of microwave heating has been developed by many workers[2-6], however, an in-depth approach to this topic is not the primary concern of this study although the relevant features will be discussed. A more detailed appraisal of the theory of heating under microwave irradiation is contained in several excellent reviews[6-8].

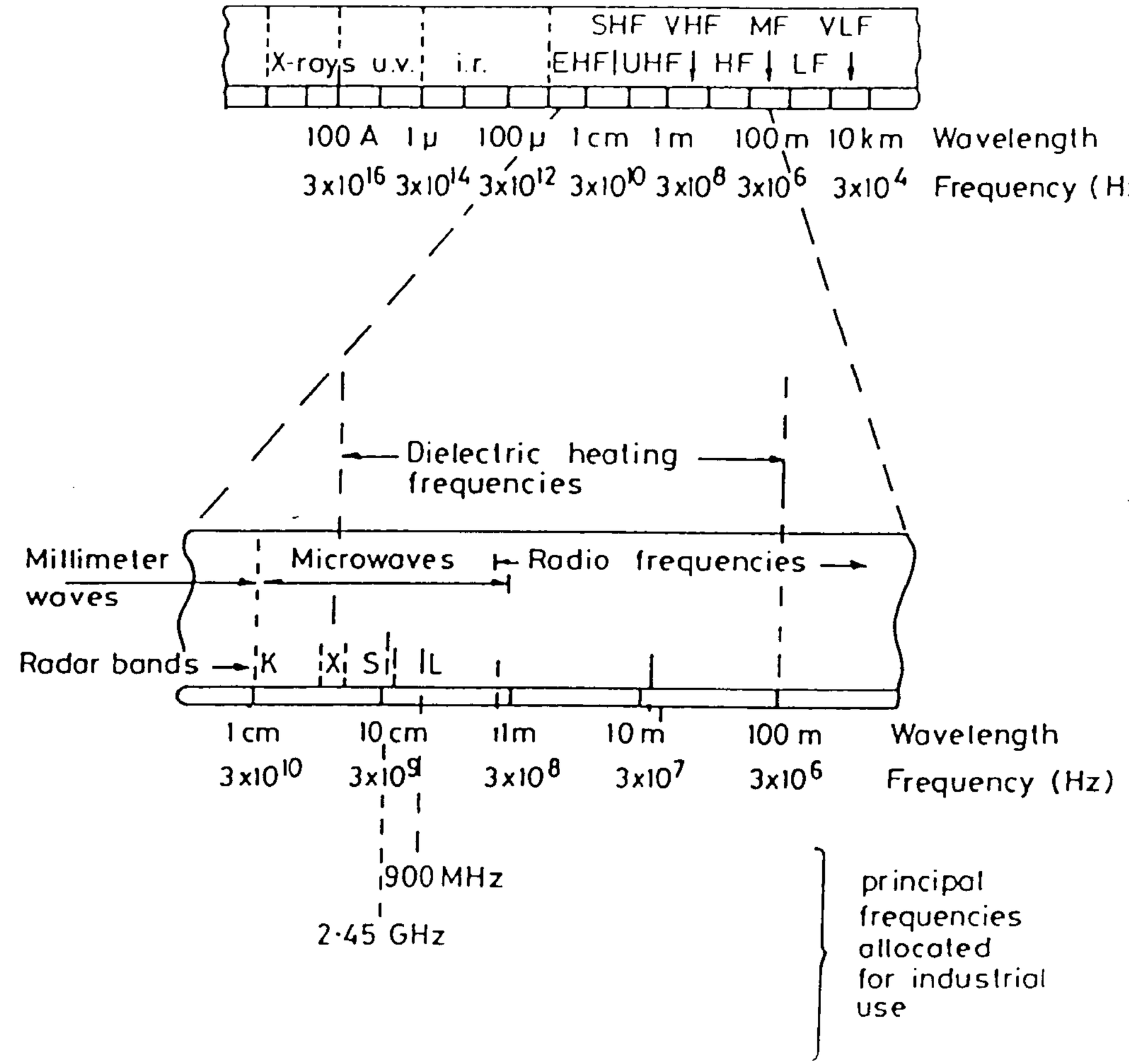

Figure 2.1. Schematic diagram of the electromagnetic spectrum showing the microwave region.

The two principal mechanisms for microwave heating are dipole rotation and ionic conductance.

Table 2.1.
Microwave energy versus other electromagnetic energy[9].

Radiation type	Typical frequency (MHz)	Quantum energy (eV)
Gamma rays	3.0×10^{14}	1.24×10^{6}
X-rays	3.0×10^{13}	1.24×10^{5}
Ultra violet	1.0×10^{9}	4.1
Visible	6.0×10^{8}	2.5
Infra-red	3.0×10^{6}	0.012
Microwave	2450	0.0016
Radio	1	4×10^{-9}

Chemical Bond Type	Chemical Bond Energy (eV)
H-OH	5.5
$H\text{-}CH_3$	4.5
H-NHCH	4.0
$H_3C\text{-}CH_3$	3.8
$PhCH_2\text{-}COOH$	2.4

2.1.2.1. Dipole rotation.

The origin of microwave heating lies in the ability of the electric field to rotate the charges in a material, and the inability of this rotation to follow extremely rapid reversals of the electric field.

2.1.2.2. Dielectric polarisation.

The total polarisation is the sum of the following factors:

$$\alpha_t = \alpha_e+\alpha_a+\alpha_d+\alpha_i+\alpha_v \qquad (2.1).$$

Where:

α_e is the electronic polarisation which arises from the realignment of electrons around specific nuclei.
α_a is the atomic polarisation which results from the relative displacement of nuclei due to unequal distribution of charge within the molecule.
α_d is the dipolar polarisation which results from the orientation of permanent dipoles by the electric field.
α_i is the interfacial polarisation (Maxwell - Wagner effect) (which occurs when there is a build up of charge at interfaces).
α_v is the vibrational polarisation (which occurs due to forces between atoms).

When an oscillating electric field (the result of electromagnetic radiation) is applied to a material, the polarisation and subsequent depolarisation of α_c and α_a are far too rapid and therefore do not contribute to the dielectric heating effect due to there being no phase lag and therefore no dielectric loss. However, α_d and possibly α_i are polarised and depolarised within a timescale which is comparable to microwave frequencies.

Dipolar polarisation, for water, is shown schematically in figure 2.2. It is due to its dipole moment which results from the differing electronegativities of the hydrogen and oxygen atoms involved. When an electric field is applied to a material at a low frequency, the dielectric polarisation keeps in phase with the electric field. This field has sufficient energy for the molecules to move into alignment. However, some of the energy is transferred each time a dipole is knocked out of alignment and then realigned. This transfer of energy is too small however to increase the temperature of the material. When the electric field is applied at high frequencies, it changes faster than the response time of the dipole. The dipoles cannot rotate so no energy is absorbed and hence there is no temperature increase.

When the timescale at which the electric field change is comparable to the response time of the dipole, the dipole rotates, but the resulting polarisation lags behind the changes of the electric field. When the field decreases, this resultant lag is always behind the oscillating electric field. When the field is removed and the molecules return to their natural disorder, thermal energy is released. At 2.45 GHz this occurs 4.9×10^9 times per second and so very rapid heating can result. This heating is dependent upon several factors such as the dielectric properties of the material and its characteristic relaxation time (which depends upon temperature).

Tan δ is defined as the ability of the material to convert electromagnetic energy into heat energy at a given temperature and pressure (equation 2.2). It is also called the dissipation factor. It is shown as the angle between the current density vector and the charging current axis as shown in figure 2.3.

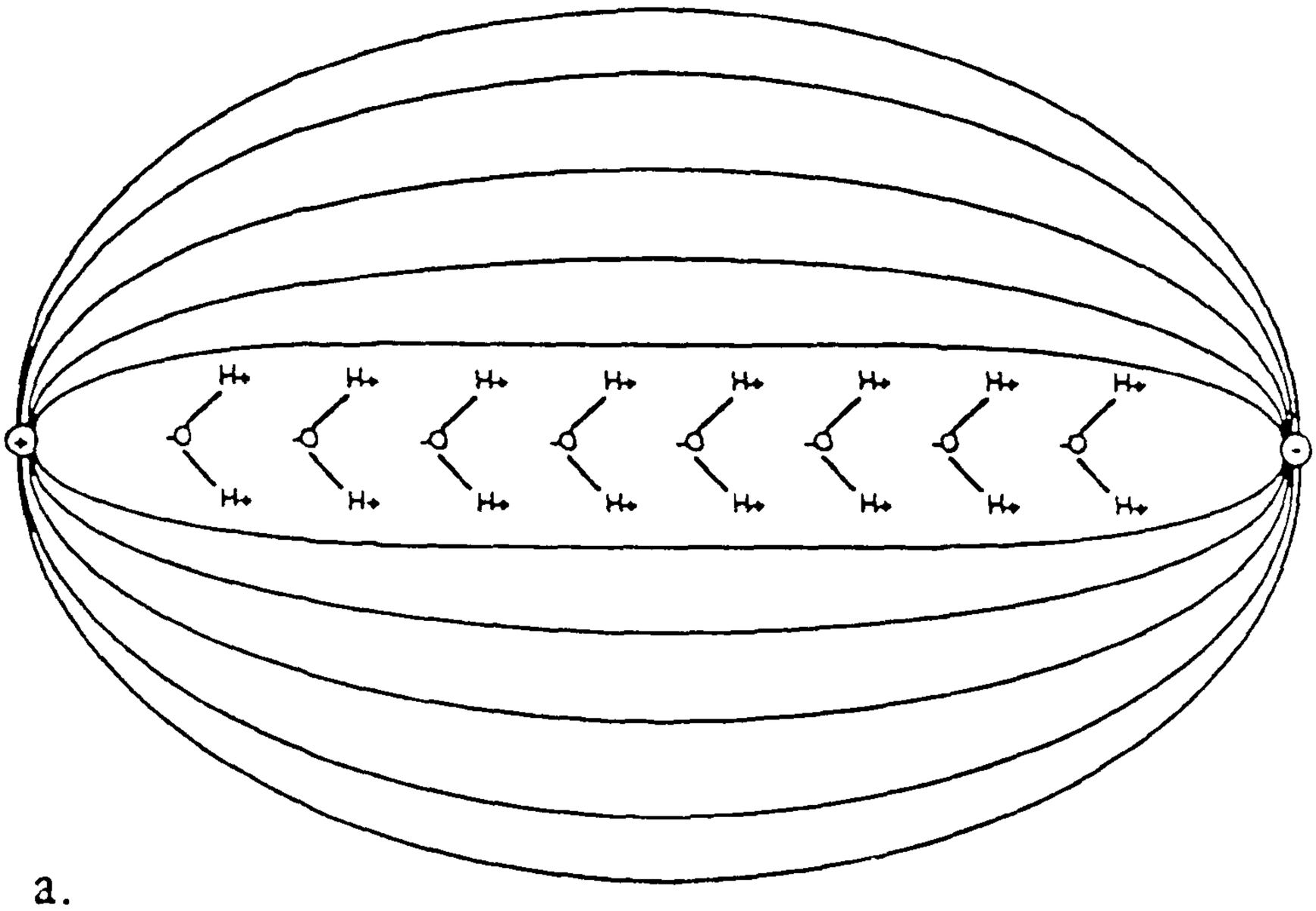

a.

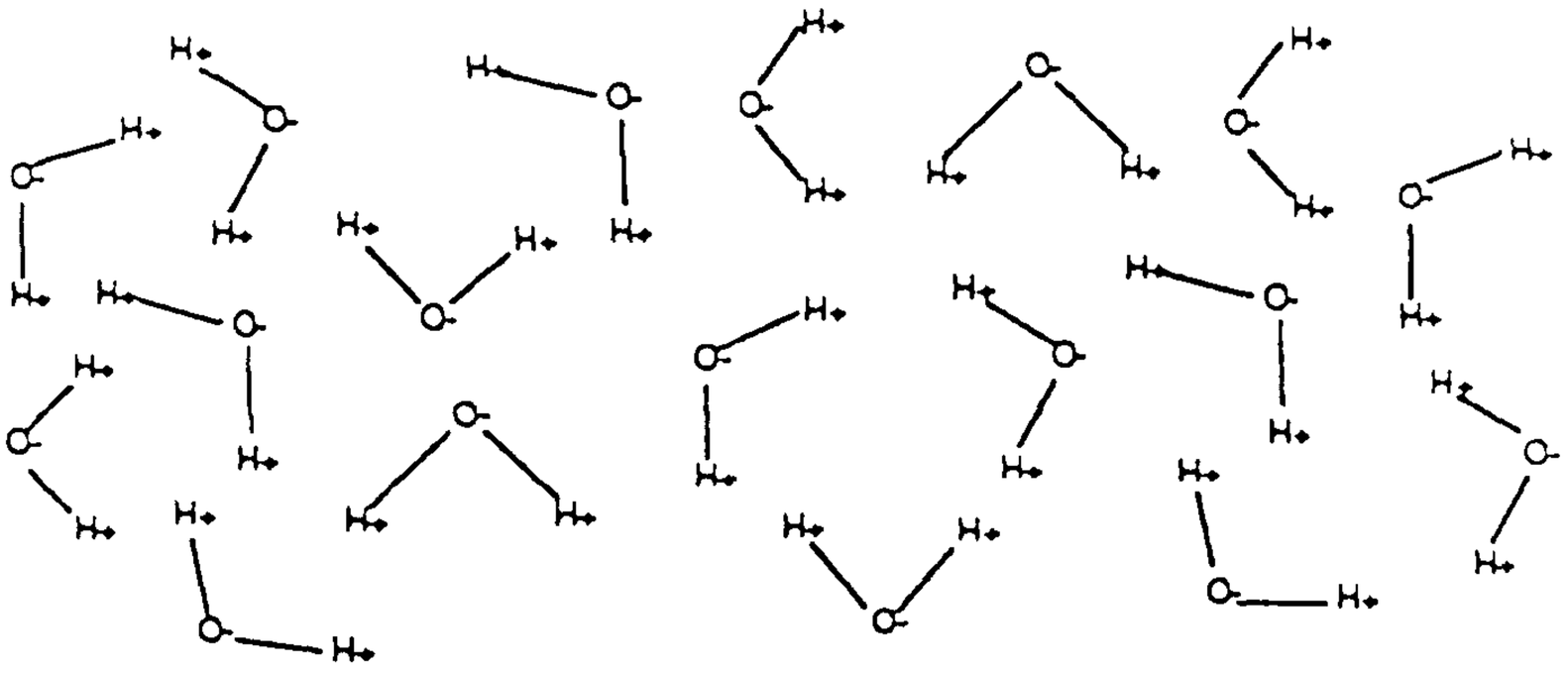

b.

Figure 2.2 Schematic diagram of the molecular response to an electromagnetic field.
(a) polarised molecules align with the field.
(b) thermally induced disorder as field is removed.

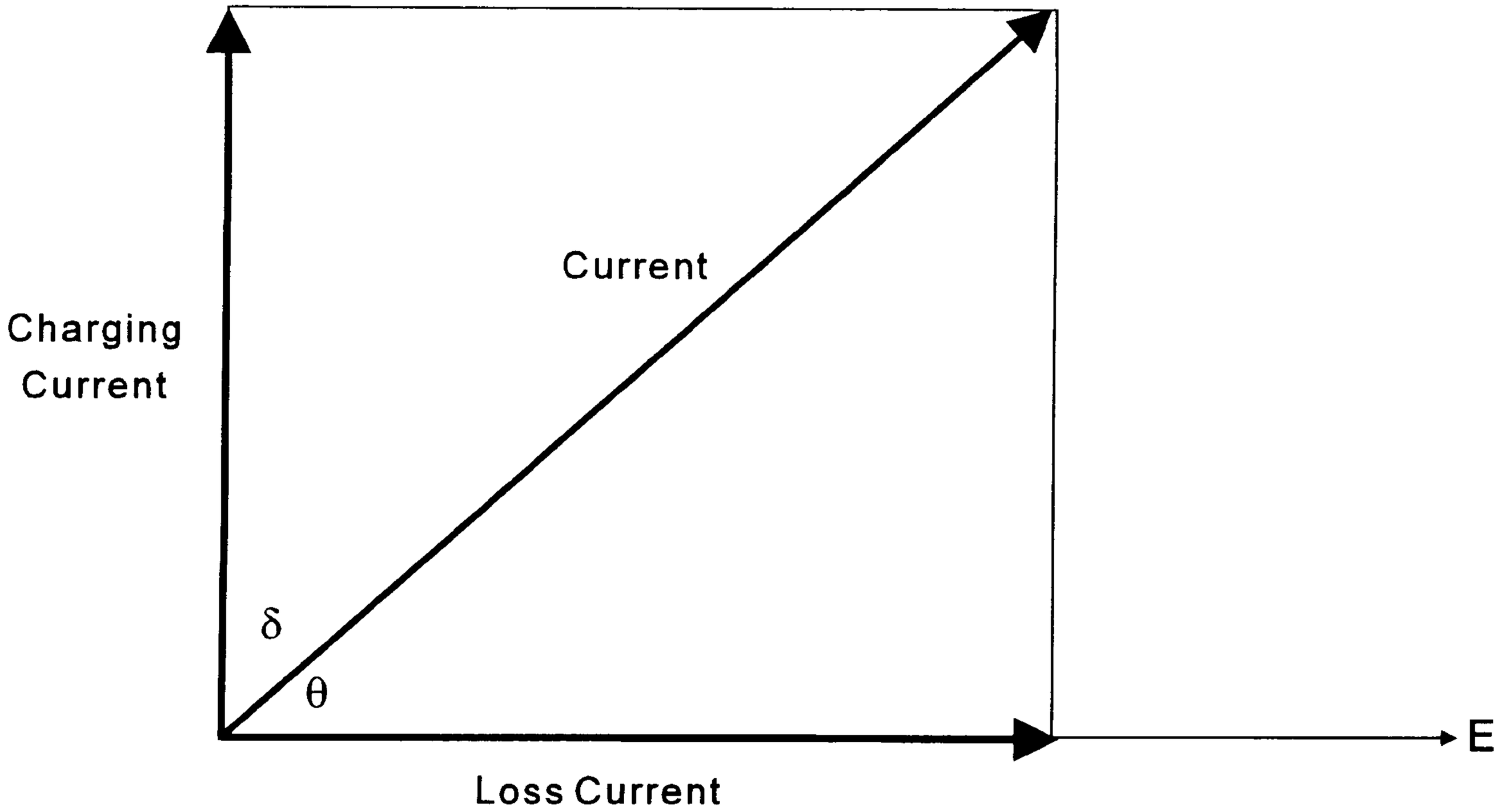

Figure 2.3. Schematic diagram of the dissipation factor Tan δ.[9]

$$\text{Tan}\,\delta = \frac{\varepsilon''}{\varepsilon'} \qquad (2.2).$$

The dielectric constant ε' describes the ability of the molecule to be polarised by the electric field.

$$\varepsilon' = \frac{C}{C_o} \qquad (2.3).$$

Where C=capacitance, ability to store charge.

The dielectric loss factor ε" measures the efficiency with which the energy of the electromagnetic radiation can be converted into heat (equation 2.4).

$$\varepsilon'' = \frac{\sigma}{2\pi f} \qquad (2.4)$$

Where σ is dielectric conductivity and f is microwave frequency.

Figure 2.4 shows how the dielectric properties of distilled water vary with frequency. The diagram shows that ε" is a maximum around 10 GHz while domestic microwave oven operate at 2.45 GHz. The reason for this is that microwaves at a frequency of 10 GHz would only penetrate a short distance into the food sample. Materials which are transparent to microwave energy have a penetration which is infinite, while materials which are reflective (e.g. metals) have a penetration which is almost zero. The penetration depth is therefore an important factor in microwave chemistry. It is defined as the depth into the material where the power falls to e^{-1} to that on the surface (equation 2.5).

Penetration depth $$D_p = \lambda_o \frac{\varepsilon'}{2\pi\sqrt{\varepsilon''}} \qquad (2.5).$$

Where ε" is small and λ_o is the wavelength of microwave radiation (microwaves generated at a frequency of 2.45 GHz have a wavelength of 12.2 cm).

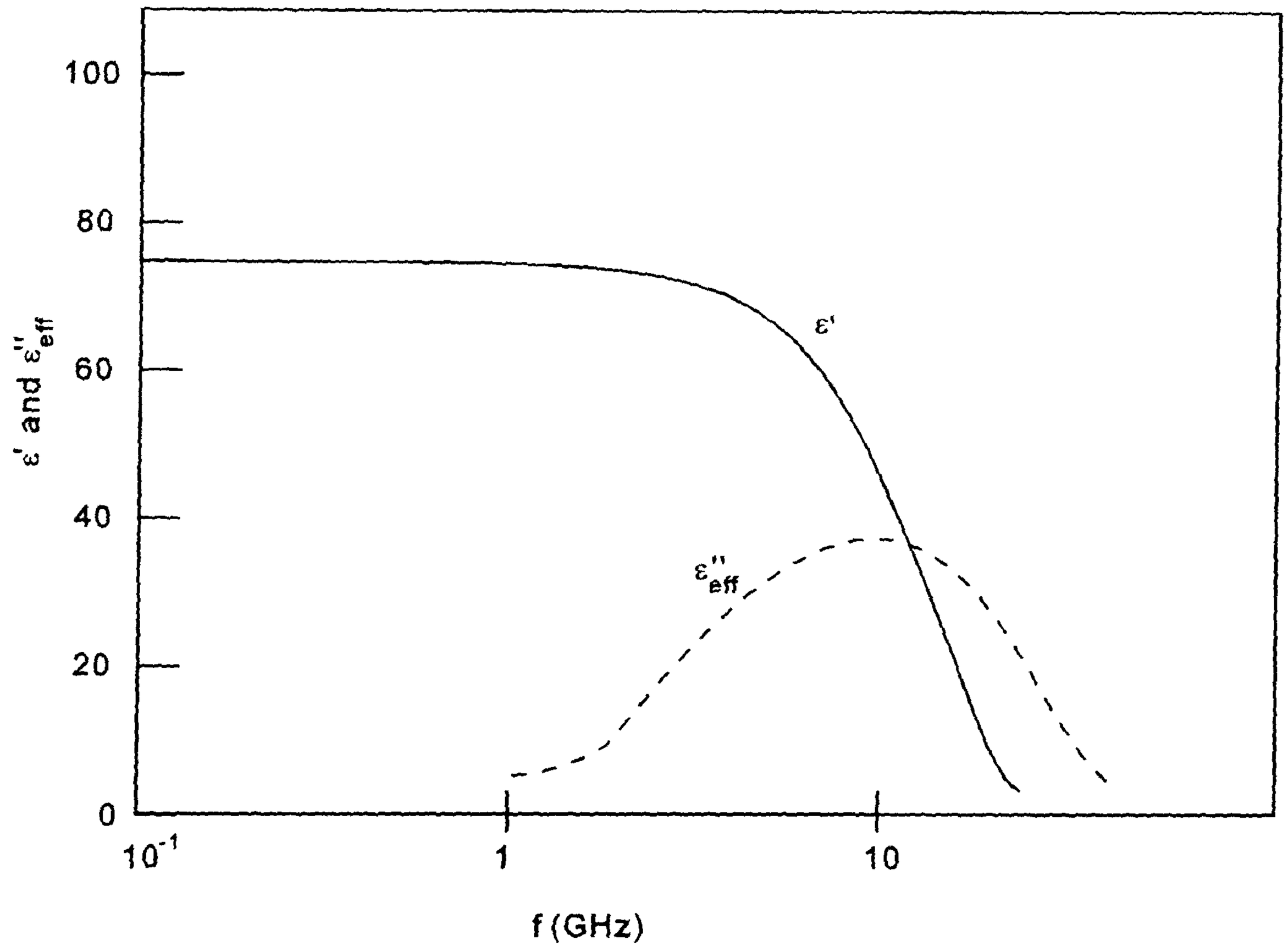

Figure 2.4. Dielectric properties of water as a function of frequency.

2.1.2.3. The Debye equation for relaxation time.

The classical approach to the treatment of permanent dipoles in liquids and in solutions of polar molecules in nonpolar solvents is to consider their behaviour in alternating fields arising from the rotation of a spherical dipole in a viscous medium dominated by friction. The general assumption in liquids is that dipoles can point in any direction and, due to thermal agitation, are continually changing[2]. Debye's interpretation of the relaxation is given in terms of dipole rotation against frictional force in the medium[3]. Using Stokes' theorem, he derived the following expression for the relaxation time of the spherical dipole.

$$\tau = \frac{4\pi r^3 \eta}{kT} \qquad (2.6).$$

Where:

τ is the relaxation time constant.
η is the viscosity of the medium.
r is the radius of the dipole molecule.
k is Boltzmann's constant.

However, many liquids and solid dielectric material have relaxation times which are much longer than those indicated by equation 2.6. Even when a correction factor is applied, this interpretation is inaccurate[3]. Viscosity is not usually the dominant factor in solid dielectrics. Debye introduced the idea of an activation energy U, which is the energy required for a dipole to acquire a different position. In gaseous substances $U<<kT$, so interatomic forces are relatively insignificant, where as in solid dielectrics $U>>kT$ where the interatomic forces predominate.

In solids a dipole has a number of equilibrium positions (due to interatomic forces). They are separated by potential barriers over which the dipole must pass in turning from one direction to another. In the simplest model only two equilibrium positions with opposite dipole directions exist and they are separated by an energy barrier U_a as shown in figure 2.5. Using Boltzmann's statistics, the number of dipole transitions from one state to the other is proportional to $(1-e^{t/\tau})$, where t is the time and τ is the relaxation time constant. In this system, the dielectric absorption decreases with increasing temperature[10-13].

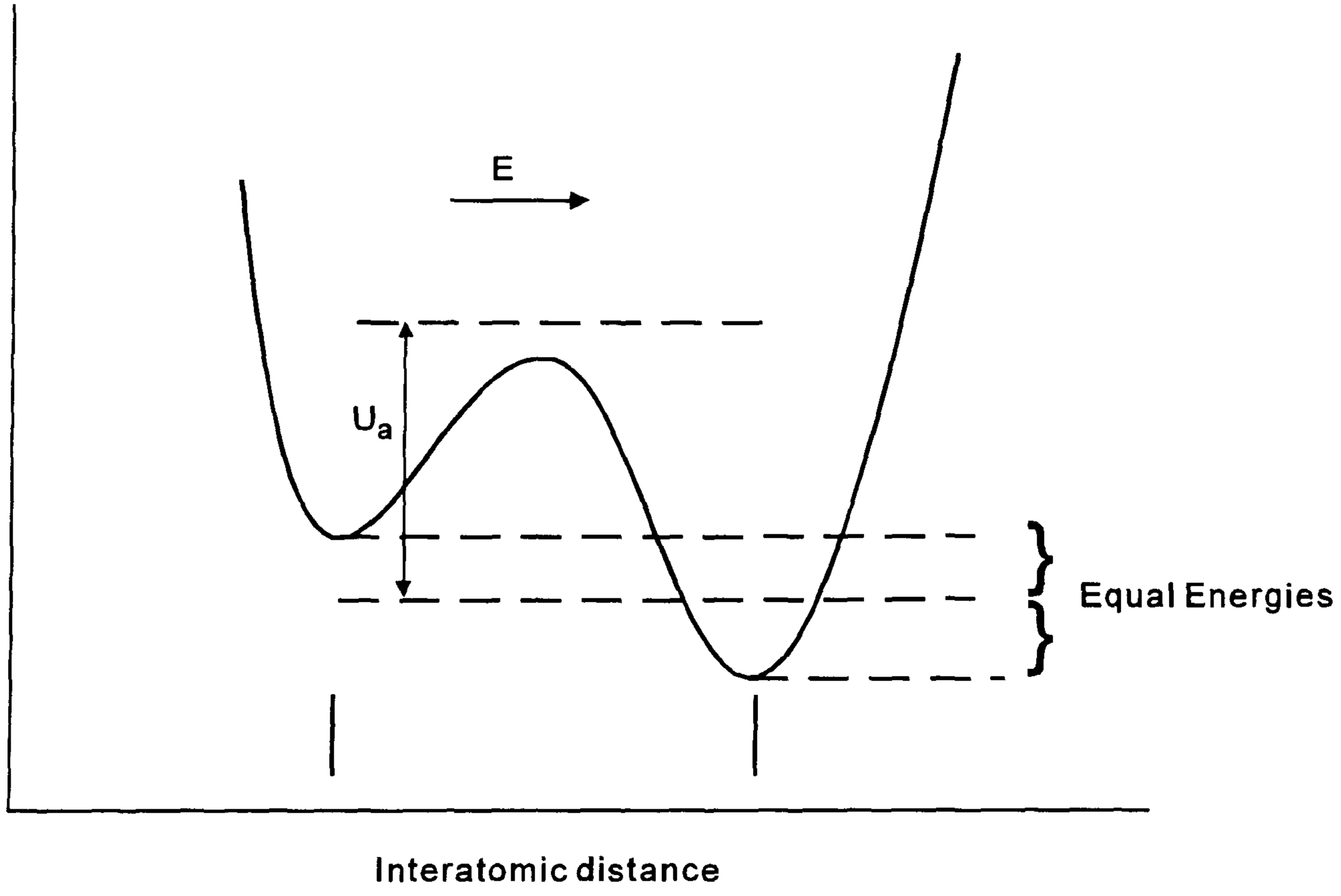

Figure 2.5. Potential energy diagram for two alternative positions of a dipole relative to an electric field.

Many polar solids (e.g. aliphatic long chain ketones) have small dielectric losses. This is because the energy differences between the equilibrium positions are very large. In other cases (e.g. long chain esters), there is absorption which decreases with increasing temperature.

2.1.2.4. Relaxation time.

The dielectric relaxation time is the time required for the molecules in the sample to achieve 63% of their return to disorder. This will occur when

$$\omega = \frac{1}{\tau} \qquad (2.7).$$

Where $\omega=2\pi f$.

If $1/\tau$ corresponds to the angular frequency of the microwave energy, as for a non-ionic polar sample, the dissipation factor will be high. If $1/\tau$ is different from ω, the dissipation factor will be low.

If the sample (e.g. water) is heated, this changes the dielectric relaxation time, the dissipation factor (Tan δ) and hence the penetration depth. If the temperature of water is raised Tan δ decreases because $1/\tau$ increases with temperature. This means that the rotation frequency of the sample is more out of phase with the microwave angular frequency and hence absorption decreases as shown in table 2.2. The absorbance also depends on the viscosity of the sample. If molecular motion of the molecules is restricted (as in the case of ice), the molecules cannot align with the field so the dissipation factor is low.

Table 2.2.
Effect of temperature on dissipation factor of water[7, 14].

Temperature / °C	Tan δ (x10^4) Measurement at 3000 MHz
1.5	3100
5.0	2750
15.0	2050
25.0	1570
35.0	1270
45.0	1060
55.0	890
65.0	765
75.0	660
85.0	547
95.0	470

2.1.2.5. Interfacial Polarisation.

Interfacial or Maxwell-Wagner polarisation is very important in heterogeneous dielectrics. The Maxwell-Wagner effect is seen as the build up of charge between the interfaces in a suspension of conducting particles in a non-conducting medium. Wagner[15] devised a simple model for this type of polarisation. His model consisted of conducting spheres distributed through a non-conducting medium, where the frequency variation of the loss factor is similar to that of dipolar relaxation. This theory can be extended to ionic conduction. A model for interfacial polarisation was suggested by Maxwell and Wagner in their two layer capacitor model (figure 2.6).

The total effect is seen as a combination of areas of differing dielectric constants and conductivity. The dielectric loss is related to d.c. conductivity. The contribution to the total loss due to this extra conductive parameter therefore depends on d.c. conductivity itself.

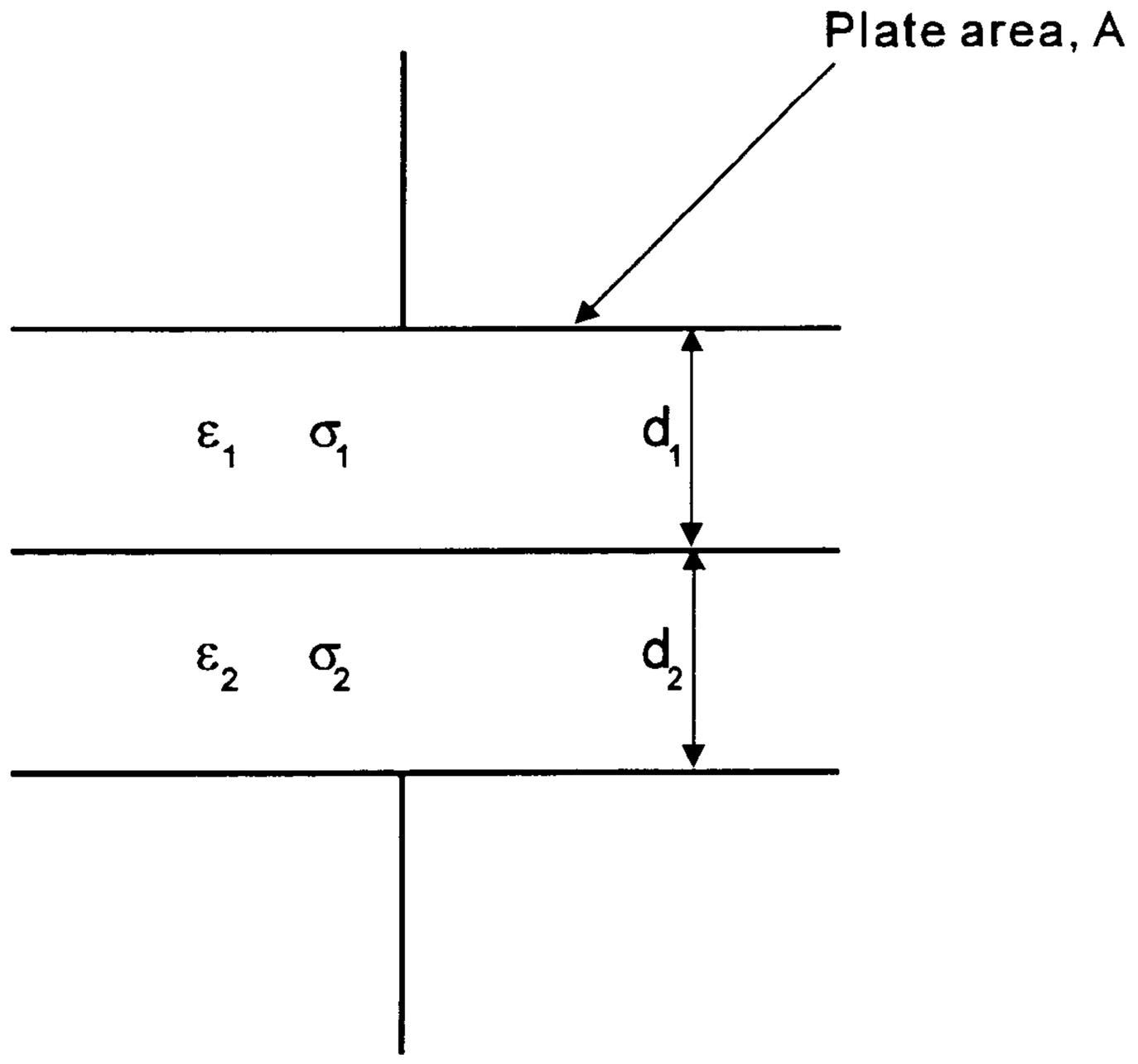

Figure 2.6. The Maxwell-Wagner two layer capacitor model.

2.1.2.6. Ionic conduction.

When the electromagnetic field is applied to the sample (e.g. NaCl in water) there is a migration of dissolved ions. This results in a flow of current which gives heat production (due to I^2R losses). These losses depend on the size, charge and conductivity of the dissolved ions. The factors which affect ionic conduction are ion concentration, ion mobility and temperature. Each sample will conduct current depending on its concentration and mobility of its ionic species. Table 2.3 shows the variation in Tan δ by increasing ion concentration.

Table 2.3.
Effect of increasing NaCl concentration on the dissipation factor[7, 14]

Molal Concentration	Tan δ ($x10^4$)
0.0 (water only)	1570
0.1	2400
0.3	4250
0.5	6250

2.1.2.7. Microwave heating.

The power dissipated by the material will depend upon the material's dielectric properties. Maxwell used Poynting's vector P=E x H to obtain an expression for the average power (equation 2.8).

$$P_{av} = 2\pi f \varepsilon'_o \varepsilon'' \int_V (E^*.E) dV \qquad (2.8).$$

E is not a constant quantity since it varies in space; but, in certain circumstances it can be assumed constant (as in the case of multimode devices), $E^2=E.E^*$ (however, it will certainly vary within the sample as it is absorbed).

$$P_{av} = 2\pi f \varepsilon'_o \varepsilon'' E^2_{rms} V \qquad (2.9).$$

Where E is in volt/m and V is in m^3. If the material exhibits magnetic losses the power will be

$$P_{av} = 2\pi f \varepsilon'_o \varepsilon'' E^2_{rms} V + 2\pi f \mu_o \mu'' H^2_{rms} V \qquad (2.10).$$

The electric field generated in microwave frequencies can be calculated. If the power dissipation is 10^7 W/m^3 and ε"=0.1, the electric field generated at 27.12 MHz and 2450 MHz are 257 kV/m and 27 kV/m respectively. The frequency and ε" are vital in

sity
ary
Hall

establishing the magnitude of the electric field to obtain the same power dissipation in a material. The electric field becomes thus the most important feature in microwave heating.

Temperature is the main factor for determining which mechanism, ionic conduction or dipole rotation predominates in microwave heating. For materials such as water, the dielectric loss decreases as temperature increases as explained by dipole rotation. However, dielectric loss increases as temperature rises due to ionic conduction. When an ionic sample (liquid or solid) is irradiated by microwave energy, the dielectric loss factor initially depends on dipole rotation, but as the temperature increases, dielectric loss is mainly due to ionic conduction.

The rate of temperature rise due to the electric field is given by Meek[17] (equation 2.11).

$$\frac{\delta T}{\delta t} = \frac{\text{constant}.\varepsilon'' f E^2_{rms}}{\rho C_P} \qquad (2.11).$$

Where:

E^2_{rms} is the field intensity,
ρ is the density
C_P is the specific heat capacity.

The losses due to radiation are defined in equation 2.12.

$$\frac{\delta T}{\delta t} = \frac{-e\sigma}{\rho C_P}\left(\frac{\text{area}}{\text{volume}}\right)T^4 \text{ sample} \qquad (2.12).$$

Where e is the sample emmissivity and σ is the Stefan-Boltzman constant.

The temperature rise in a given sample is thus dependent on the dielectric constant, specific heat capacity, emmissivity of the sample and the strength of the applied field. All of these factors (liquids or solids) are also temperature dependent.

2.1.2.8. Thermal runaway.

The "runaway" effect is the uncontrolled rise in temperature in a material under microwave irradiation (figure 2.7). The diagram shows that after the initial absorption of the microwave energy, ε" increases with temperature and at a critical temperature, Tan δ increases so that the material is converting so much of the microwave radiation into heat that a thermal runaway is observed. This can be potentially dangerous as the material may achieve temperatures well in excess of the desired temperature and damage to the sample (or to the vessel containing the sample) may occur.

This runaway effect is well known with materials such as nylon[17] and ceramics[18]. The interest of the ceramic industry in microwaves is because several workers have reported that microwave heating can lower the sintering temperature in several materials by several hundreds of degrees and shorten the sintering time. A knowledge of when the critical temperature is reached for the material would be very useful. Some workers[19-21] have observed that the effect is self-limiting, or the material undergos a chemical change and is elevated to a temperature at which it absorbs energy and a stable chain reaction can occur.

Several workers have tried to model this runaway effect. Kenkre et al.[18] have postulated that the system could consist of two species (A and M). A consists of absorbing entities, which absorb microwaves through the Debye mechanism. The M species are the interstitial atoms or vacancies, at low temperatures, which lie in potential wells which bind them. If they obtain enough energy to escape the well, they act like free particles and absorb microwave radiation.

$$\frac{dT}{dt} = P\left[k_A + f(T)k_M\right] - \sigma T^4 \qquad (2.13).$$

Where:

σ is the Boltzmann's constant.
T is temperature
$k_A = n_A c_A$ where n_A is the number of the absorbers of A, and Pc_A is the rate at which each absorbs energy from the microwaves, where P=microwave power.

They have applied this equation to experimental results and have found that the theory provides a good description of the thermal runaway effect.

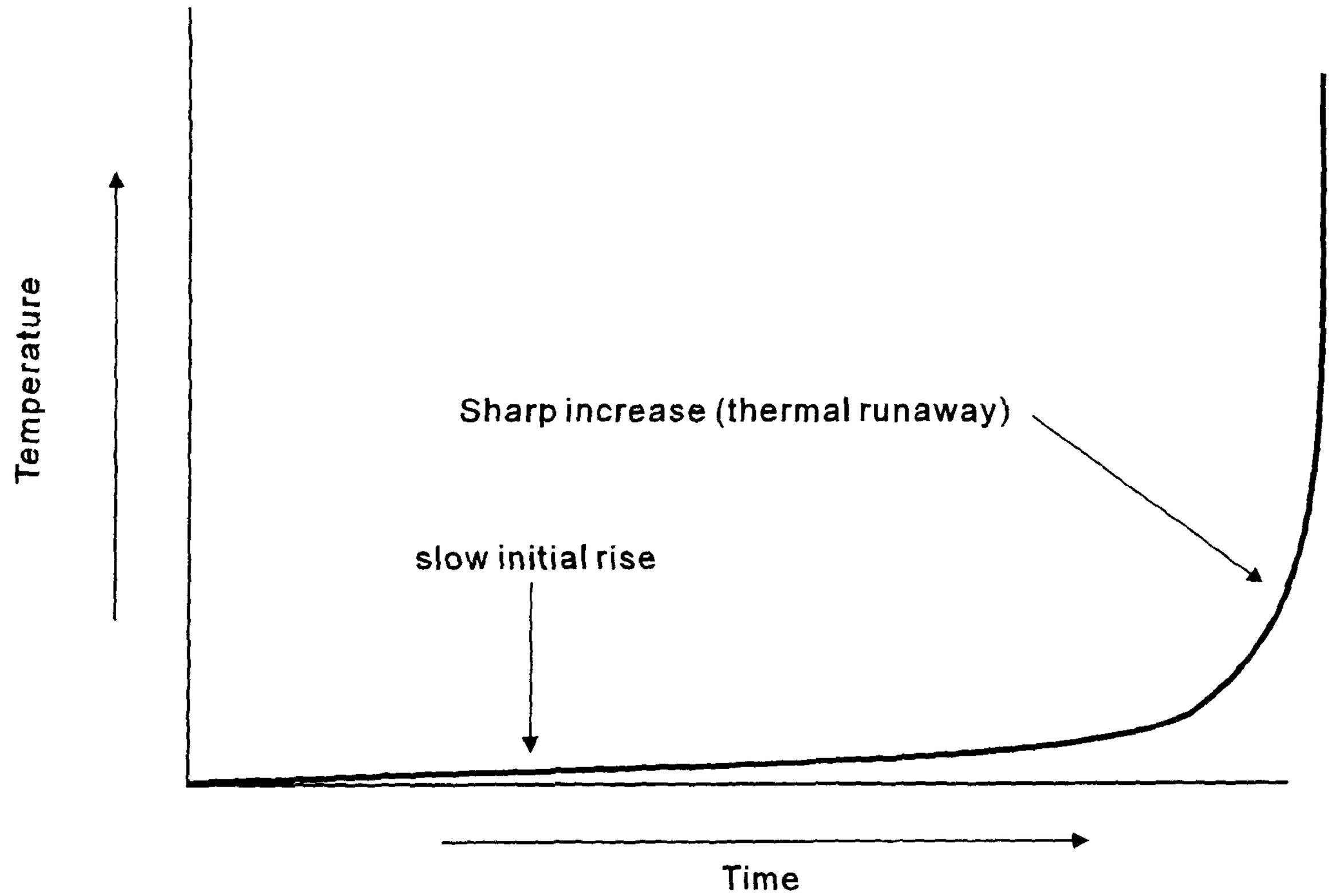

Figure 2.7. The thermal runaway effect under microwave irradiation.

2.1.3. Microwave Equipment.

The two types of microwave equipment detailed in this study are multimode devices and single mode devices. Multimode devices have the advantage that they are relatively inexpensive and are very useful for a variety of chemical applications. The one main disadvantage is that the microwave energy is distributed around the cavity and thus not all the energy is absorbed by the sample. Single mode cavities have the advantage that all the microwave energy can be focused onto a very small volume (e.g. the catalyst itself) but the equipment is more expensive.

2.1.3.1. Multimode cavities.

These are the most widely used devices. The normal domestic microwave oven is of this type. The equipment is relatively simple and the oven can heat a wide variety of materials although heating uniformly is a problem. Figure 2.8 details the essential features of the device. It consists of a microwave generator (magnetron), a section of waveguide and the cavity itself.

2.1.3.2. The magnetron.

Figure 2.9 is a schematic diagram of a fixed tuned magnetron. The magnetron is a thermionic diode with an anode and a directly heated cathode. When the cathode is heated, the emitted electrons are attracted by the anode. The anode is made up of a number of small cavities which act as tuned circuits. The gap across the small cavity acts like a capacitor, the anode is thus a series of circuits which are tuned to oscillate at a specific frequency. When the magnetron oscillates, the electrons release energy (at a certain frequency) to a microwave field which is radiated from an antenna. This type of magnetron is known as a fixed tuned magnetron. In the present work the magnetron operated with an output frequency of 2450 ± 13 MHz. Approximately 1200 W is received by the magnetron, but only 600W is converted to electromagnetic energy. The remaining energy is converted to heat which must be dissipated by cooling.

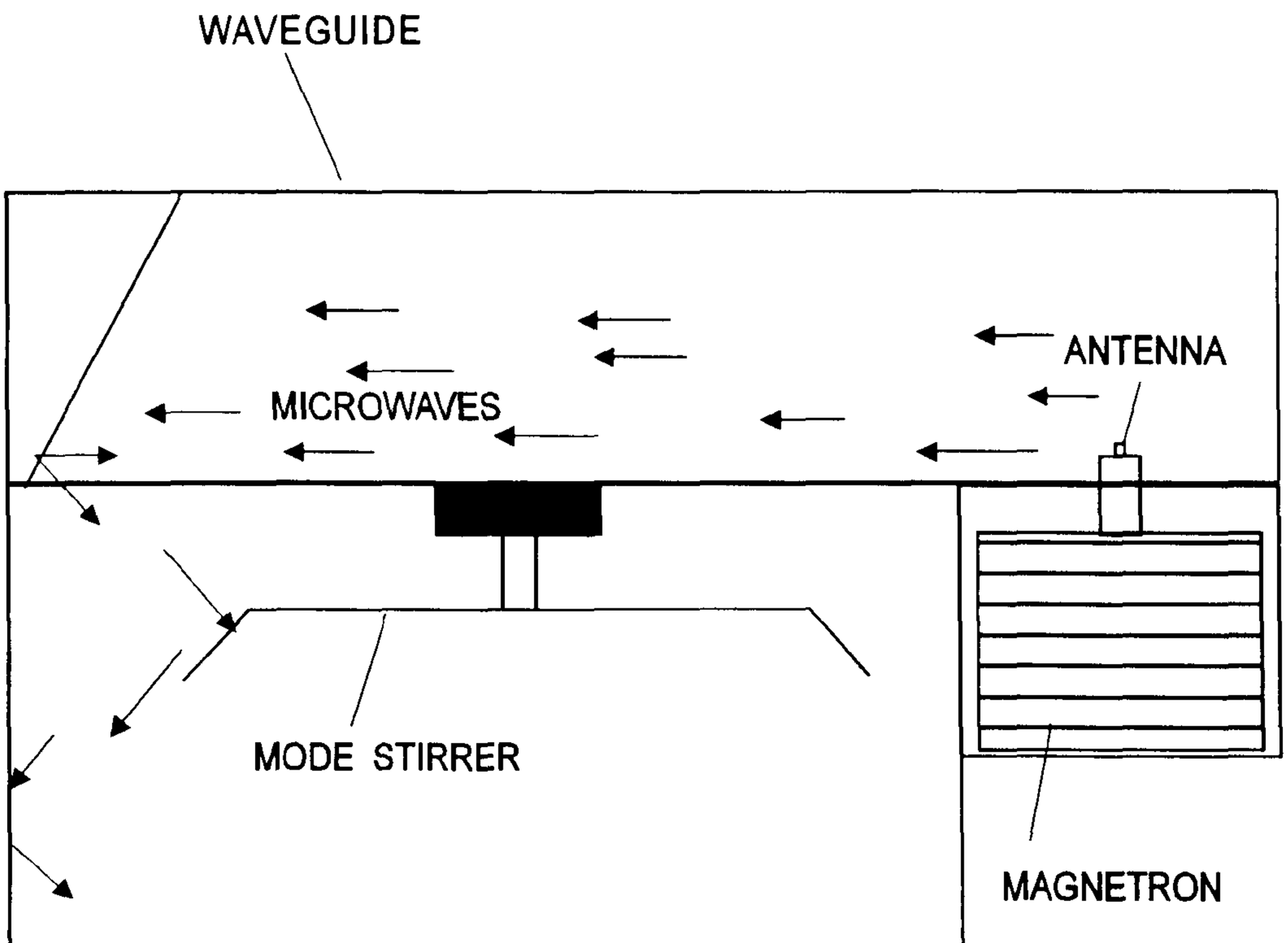

Figure 2.8. Schematic diagram of a domestic microwave oven.

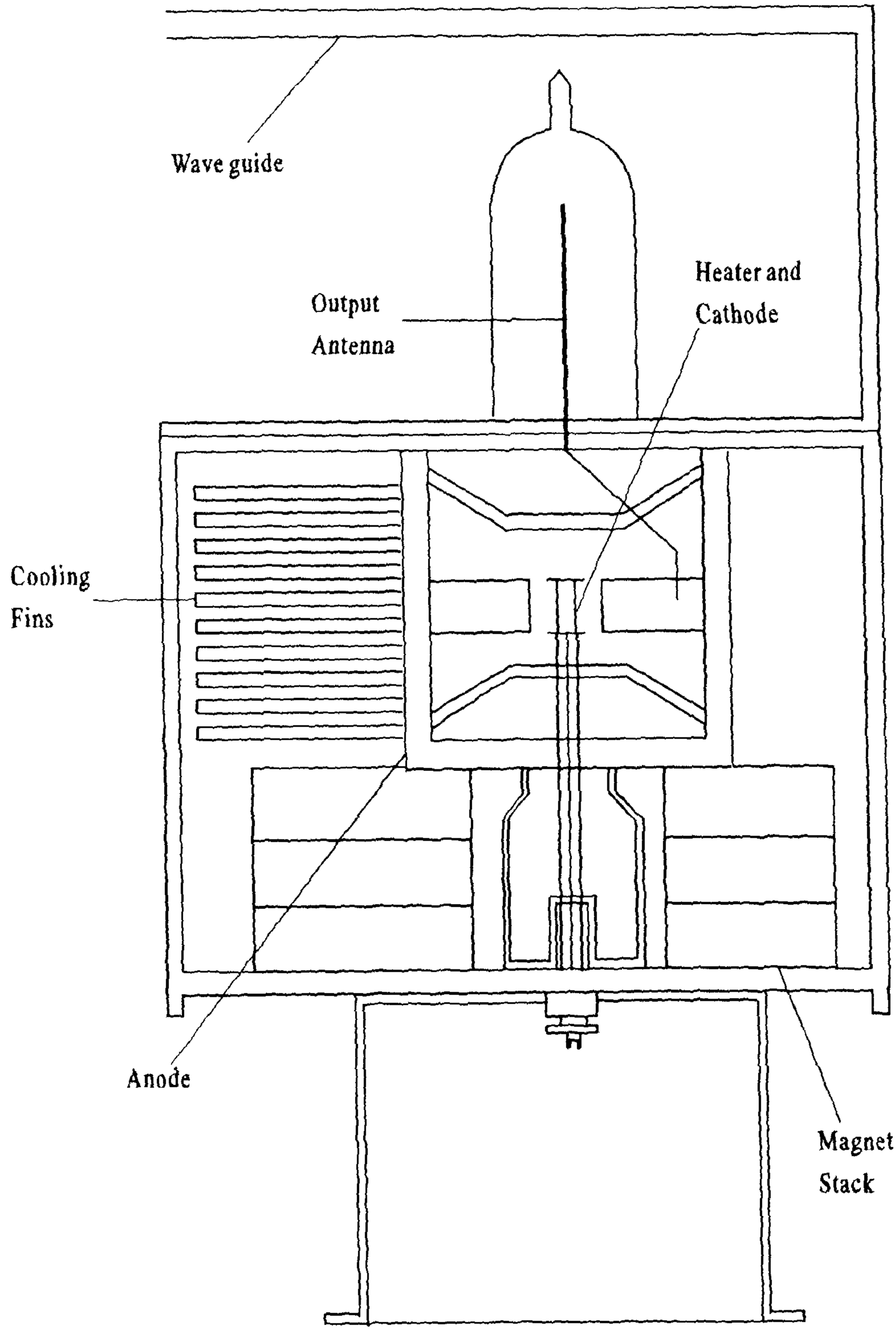

Figure 2.9. Schematic diagram of a fixed tuned magnetron.

2.1.3.3. The waveguide.

The microwave energy produced by the magnetron is introduced to the cavity via a section of waveguide. The waveguide is an open rectangular box made of metal (to reflect the microwaves). The walls reflect the microwaves, and so direct the microwaves into the cavity. The dimensions of the waveguide are critical since the minimum frequency which can be propagated is related to the cross section of the waveguide.

$$c/f = 2d \qquad (2.14).$$

Where:

c is the speed of light
f is the cut-off frequency
d is the larger of the dimensions of the rectangular section of waveguide (for a domestic microwave oven the dimensions are typically 9 cm x 5 cm).

2.1.3.4. The cavity.

The walls of the cavity are also reflective, this increases the absorbance by the sample because the energy is being reflected by the walls and through the sample more frequently. However, if the sample is too small, or its dielectric properties are such that it does not absorb the microwaves very efficiently, the microwave energy can be reflected back into the waveguide and damage the magnetron.

Domestic microwave ovens have a thermistor to protect the magnetron by cutting the power when overheating occurs. Experiments are hence usually performed with a "load" present in the cavity. This "load" usually consists of a suitable volume of water in a vessel. A simple system can be set up where water is fed into and out of the vessel to maintain a constant volume of water. Industrial microwave ovens, which are used for acid dissolution, have a device called a terminal circulator (see figure 2.10). The circulator uses ferrites and a static magnetic field to divert the reflected microwaves into a dummy load where the energy can be dissipated as heat.

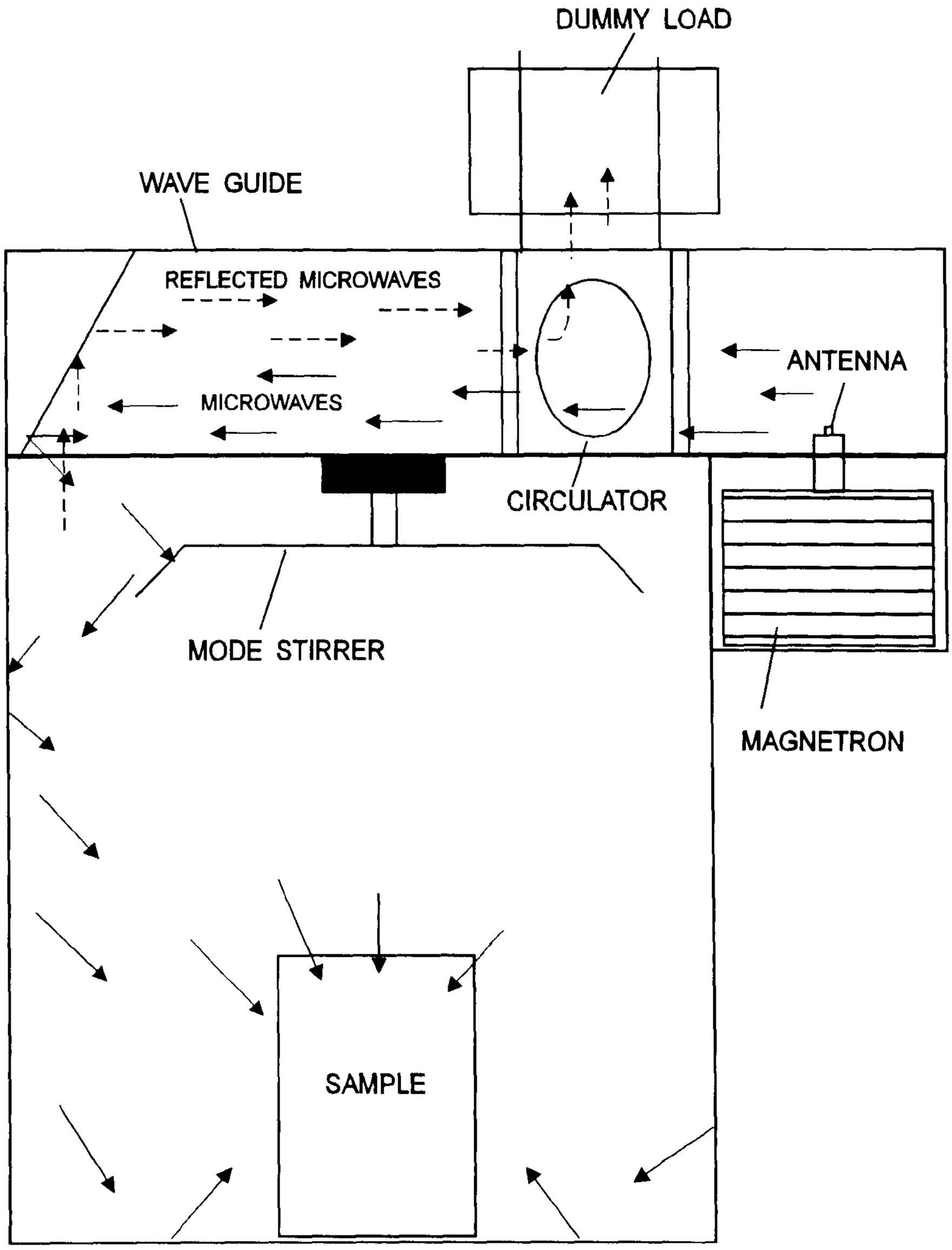

Figure 2.10. Schematic diagram of components of a laboratory microwave oven.

The microwaves entering the cavity are reflected from wall to wall. A pattern within the cavity is thus established, where certain areas receive large amounts of energy while others almost none. To ensure a more even distribution of the microwave field, ovens are equipped with two pieces of apparatus to ensure more uniform heating in the chosen sample.

A mode stirrer can be fitted, this is a blade shaped like a fan, which deflects the energy entering the cavity so a more homogeneous distribution of the energy is obtained. Microwave ovens are also supplied with a turntable so that the sample is being moved between different areas of the cavity.

2.1.3.5. The duty cycle.

In domestic microwave ovens, different power settings are obtained by pulsing the microwave energy. This is done by "cycling" the magnetron to obtain an average power level. The duty cycle is simply the time the magnetron is on divided by the time base. The time base used in domestic microwave ovens is quite long (e.g. of the order of 30 seconds). In this case for a certain power level (e.g. the lowest) the magnetron would be cycled so it was on for 5 seconds and off for 25 seconds. In industrial microwave ovens, this time base is considerably shorter. Typically to obtain 50% power of 600W, the magnetron is on for 0.5 seconds and off for 0.5 seconds.

2.1.3.6. Single mode devices.

The apparatus and experimental details of the single mode device used in the catalytic work in this microwave study will be discussed in more detail later. Simply stated a single mode heater establishes a much higher electric field strength than a multimode device, at a position where the sample can be placed. This can be extremely useful when heating low loss dielectric materials such as polymers and certain ceramic materials. The cavity consists of a metallic enclosure into which a microwave signal is generated. This signal is of a certain electromagnetic field polarisation and will be reflected between preferred directions. The superposition of the incident and reflective waves give rise to a standing wave, the geometry of which can be calculated. This enables the sample to be placed at the position of maximum electric field. However,

since the dielectric properties vary for different samples and also with temperature, for the sample to have the optimum transfer of the electromagnetic energy, the dimensions of the cavity must be continually changed so that the cavity can be made to resonate at the working frequency.

2.1.4. Temperature Measurement.

There is an increasing body of information which refers to the microwave enhancement of reaction rates in chemical reactions[8-9, 27-53]. However, an accurate measurement of the reaction temperature within a microwave field is often neglected, and so interpretation of the results is questionable. Determination of the temperature of a sample in a microwave field is very difficult. Metallic probes such as thermocouples and resistance thermometers are subject to inductive heating and their very presence can distort the microwave field and lead to arcing. Infrared techniques have been employed, but they have a major disadvantage in that the surface temperature is measured preferentially. Optical fibre techniques have the advantage in that they are transparent to microwave radiation and so can give an accurate measurement of the temperature of a sample. However, the cost of the equipment often deters experimental workers who wish to carry out subjective preliminary experiments. To overcome these difficulties several workers have used mathematical modelling for determination of temperature[22]. We have found that a good measurement of sample temperature, in a microwave cavity, can be readily be achieved by the use of a miniature gas thermometer, connected by capillary to an externally mounted pressure transducer.

2.1.4.1. Shielded Thermocouples.

Devices such as thermocouples must be shielded if they are to be used for measurement of temperature in a microwave field[23]. The thermocouple is grounded to dissipate the electrical charge that accumulates at the tip of the probe. Gold plating of the tip and the shielding is recommended to lower the electrical resistance. The device is usually grounded at the wall of the unit. Industrial microwave ovens, such as those constructed by CEM, have used this technique for measuring the rate kinetics of chemical reactions[24-26]. Mingos and Baghurst[27] have used this technique successfully

to study the microwave sintering of alumina and the microwave synthesis of inorganic materials by placing the sample in a crucible which has a hole in the base where the thermocouple can be situated. The temperature is then read and this indication is used in a feedback mechanism so the reaction temperature can be controlled by varying the microwave power. Wilkenciz et al.[28] have used shielded thermocouple techniques when heating high purity minerals such as magnetite and haematite and other inorganic compounds. They have reported that temperatures have been recorded with an error of $\pm$ 2%. For materials which are transparent to microwave energy this error would be greater since the probe itself would be heated.

The use of thermocouples in single mode cavities is not advisable since the electric field generated is of a greater magnitude than in multimode devices. Karmazsin et al.[29] have reported the direct use of a thermocouple in a waveguide. As stated before, the electric and magnetic field in a waveguide can be mathematically modelled as shown in figure 2.11.

In this set-up, if a thermocouple is placed in the Z direction it will receive the maximum amount of the microwave energy. But if it is placed in the X or Y direction it will collect the zero amount of energy. As shown in the diagram the thermocouple is inserted in the wave guide in the X direction.

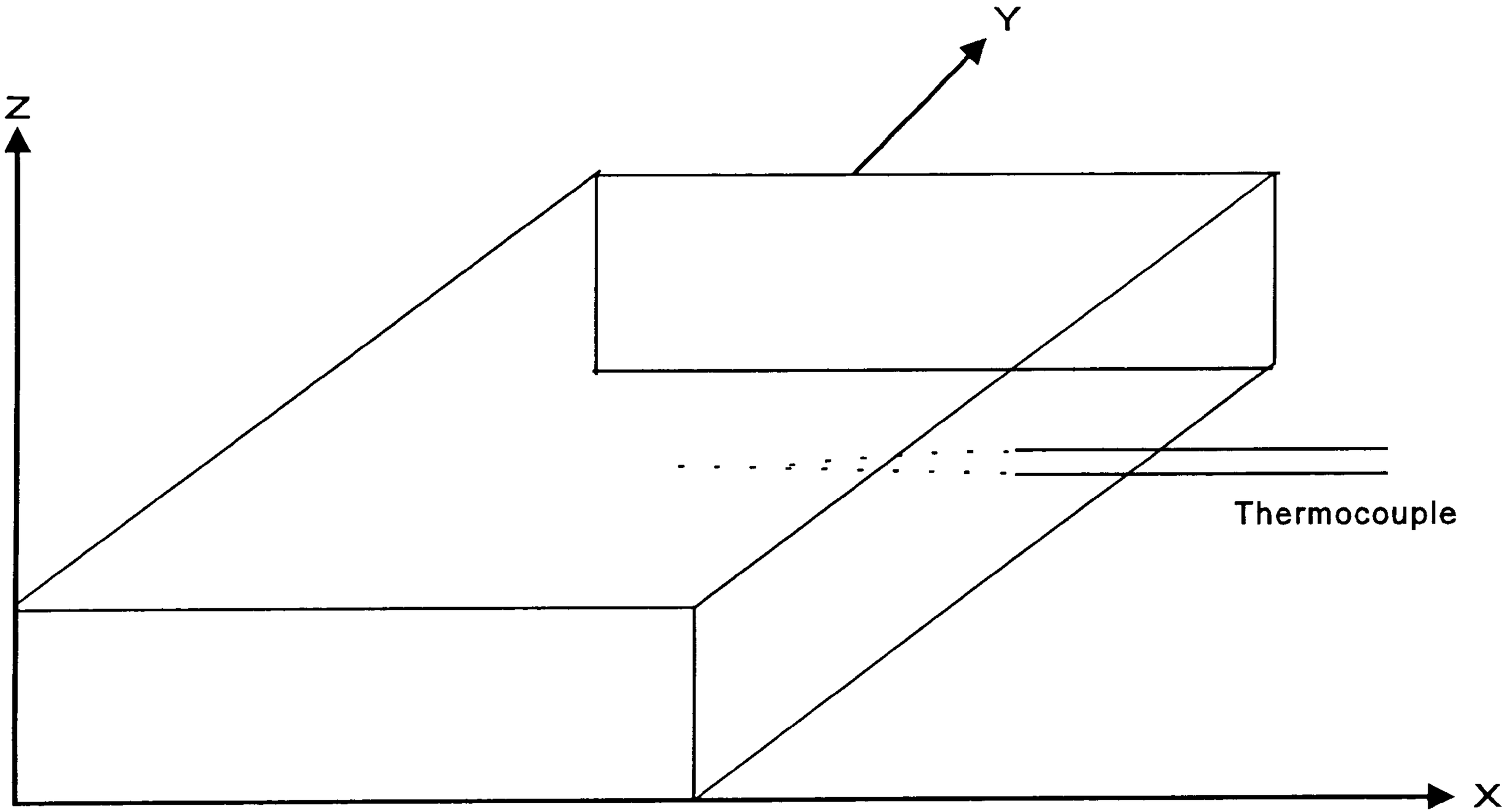

Figure 2.11. Schematic diagram showing direct use of thermocouple in waveguide.

2.1.4.2. Infrared devices.

Infrared pyrometers provide a relatively inexpensive method for measurement of temperature in a microwave field. However, their main disadvantage is that they are a surface sensitive technique. They operate due to the fact that all substances above absolute zero emit radiant energy. The rate of emission per unit area increases with temperature, the Stefan-Boltzmann's equation gives a relationship between the total radiation power, I, emitted from the warm object and temperature, T.

$$I = \sigma T^4 \qquad (2.15).$$

Where σ is the Stefan-Boltzmann's constant. Thus the temperature of a substance can be measured by use of a device that is responsive to radiant energy. For bodies near room temperature, most of the emission is in the long-wavelength infrared.

Non-contact temperature measuring instruments which convert infrared radiation from any object into an electrical signal have been used for measuring surface temperatures of a sample when heated by a microwave field. For the temperature to be measured accurately, there must be a direct line of sight between the detector and the heated area.

Baghurst and Mingos[30] have used an infrared pyrometer for use with their thick-walled glass reaction vessel. They report that a number of transition-metal organometallic and co-ordination compounds have been synthesised with a dramatic reduction in the reaction time. Temperatures of 40-60°C (in excess of the boiling point) at 10 atm have been recorded.

Mincy et al.[31] have developed a microwave oven digestion system which uses an infrared probe to monitor the temperature of the digestion vessel. The output from the probe was used to control the magnetron so that a constant temperature was maintained.

2.1.4.3. Fibre Optic Devices.

As stated earlier, fibre optic devices are ideal for temperature measurement in a microwave field because they are transparent to microwave energy. The operation of the device is based on the principles described in section 2.1.4.2. One type of optical fibre works by the use of a black body cavity which when heated transmits the energy to an optical device via the optical fibre. The signal is then amplified, digitised and converted into an indication of the temperature of the black body.

Fibre optic devices have been successfully used in closed Teflon vessels for acid digestion experiments[32-33]. However the probe can be damaged by exposure to strong oxidising acids and is protected by inserting the probe into a Teflon PTA tube. Several workers[34-36] have used this equipment for temperature measurement during the experiment. Baghurst and Mingos[34] have investigated superheating effects in several solvents using this technology for temperature measurement and have recorded that temperatures in excess of 20°C above the boiling point have been achieved by some solvents. Jow et al.[35] have developed a computer-controlled microwave system incorporating fibre-optic technology to maintain temperature to cure epoxy/amine resins by controlled pulsing. The technique is very reliable and gives an accurate indication of the temperature. Unfortunately the equipment is very expensive and this has resulted in investigation of a cheaper alternative.

2.1.4.4. Gas Thermometry.

This report details an investigation attempting to use the principles of gas thermometry for temperature measurement in a microwave field[37]. The principles of the gas thermometer as a primary thermometer are from the nearly ideal behaviour shown by many gases and the fact that small departures from ideal behaviour are simple functions of density and temperature.

A miniature gas thermometer, connected by a capillary to a pressure transducer mounted externally to the microwave cavity can give a good indication of the temperature of a particular sample. These thermometers have been constructed from silica, which does not interact with microwaves, and thus can form part of silica reaction

vessels and can monitor the temperature within a catalyst bed during reaction in the presence of microwaves.

2.1.5. Chemical Reactions.

The evidence for microwave enhancement of reaction rates in chemical reactions is growing. Mingos and Baghurst[8] have made an extensive review on microwave applications. Abramovitch[38] has recently reviewed the application of microwave energy to organic synthesis. Although the first recorded application of microwave energy in organic synthesis was reported in 1969[39], it was not until the 1980's that workers attempted to synthesise small organic molecules in domestic microwave ovens. Giguere et al.[40] and Gedye et al.[41] made the first significant reports which has since prompted more research in microwave energy for organic synthesis.

Gedye et al.[41] have carried several types of organic reactions and rate enhancements of between five and approximately one thousand were observed when the reactions were carried out in a microwave oven, compared to classical organic chemical reactions. The majority of the reported reactions where rate enhancements have been observed were carried out in sealed polytetrafluoroethylene vessels and, from the information published it is not possible to separate the inevitable rate enhancement caused by the higher temperatures and the resulting autothermal pressures from any intrinsic effect such as specific bond activation by microwaves.

Alloum et al.[42] and Gutierrez et al.[43] have avoided the generation of high pressures in microwave ovens by using reagents adsorbed on alumina or clay. Rate enhancements were still observed. Baghurst et al.[44] have synthesised mixed metal oxides in an alumina crucible in a microwave oven in a fraction of the time taken using conventional heating techniques.

Detailed comparisons between thermal and microwave irradiation have been performed[45-47]. Early suggestions were that microwave radiation influenced reactions in a specific way, for example specific bond activation[48]. More recently there has been some evidence that these rate enhancements observed are, at least to some extent, due to superheating caused by the absorption of microwaves[49-51]. Despite all of these

claims, measured temperatures are seldom quoted. Bose et al.[52-54] have attempted to address the problem of temperature control of reactions in a microwave ovens and assert that the reactions carried out were under conditions without rapid temperature or pressure rise. They claim this was achieved by carrying out the reaction in a flask that had been previously frozen in a block of ice. This claim seemed highly dubious since any material that undergoes dielectric loss will absorb microwave radiation and so become heated.

2.1.5.1. Superheating effects.

Evidence that the rate enhancement of chemical reactions by microwave irradiation is due to superheating has been accumulating[9, 34, 45]. Baghurst and Mingos[34] have performed experiments on organic solvents using fibre optic techniques, and established that in some cases the solvents superheat by 13-26°C above their conventional boiling points at atmospheric pressure. This superheating effect can be explained by conventional boiling theory. When a liquid is heated using conventional heating, the heating rate is dependent on the specific heat capacity (equation 2.16).

$$Q = m\ Cp\ dT \qquad (2.16).$$

If this equation is differentiated with respect to time, the heating rate is a function of the power.

$$\frac{dQ}{dt} = \text{Power} = m\ Cp\left(\frac{dT}{dt}\right) \qquad (2.17).$$

Convective heating is the dominant heat transfer process when a liquid is heated conventionally.

$$\text{Power} = \frac{dQ}{dt} = kA\,dT \qquad (2.18).$$

Where:

A is the contact surface area.
k is the convective heat transfer coefficient
dT is the temperature difference between the liquid and the surface which is heating it.

Therefore the heating rate depends on surface area and the temperature of the surface. In conventional heating nucleate boiling arises from indentations (pits, crevices or scratches) on the surface of the vessel in which bubbles can form. Heat transfer in vigorous nucleate boiling is a result of local convection caused by the rapid growth and

disengagement of vapour bubbles from the surface. Evaporation occurs all around the bubble to the liquid interface, the energy for evaporation is provided by a layer of superheated liquid which surrounds the bubble. Once bubbles have formed and the bubble is released from the cavity, boiling commences. The number of the sites at which the bubbles form is limited by the liquid properties, the surface and the temperature. In normal conventional heating, the reaction vessel itself is directly heated, therefore the walls of the vessel heat the liquid. This means that the walls are hotter than the bulk of the liquid, so the greater temperature achieved in the liquid will be at the walls. Superheated layers will be adjacent to sites where bubble formation and hence nuclei can form. In microwave heating, the liquid itself is heated, the vessel itself is relatively cooler, and so liquid adjacent to the walls of the vessel will be below the temperature of the bulk liquid (figure 2.12). The ability of the liquid to "wet" the surface is important. Organic solvents wet the surface well and this reduces vapour being trapped in the cavities so reducing bubble formation. Water only superheats to 104°C, because it wets the surface poorly, so there are more sites for bubble formation.

Our own investigation into this effect has been to heat solvents under normal conventional methods and by microwave radiation. This work is in collaboration with Dr. Hamilton at ICI Wilton. Temperature measurement has been by use of thermocouples (inserted into the liquid) and gas thermometry. The work has tried to ascertain the degree of superheating as a function of volume and power.

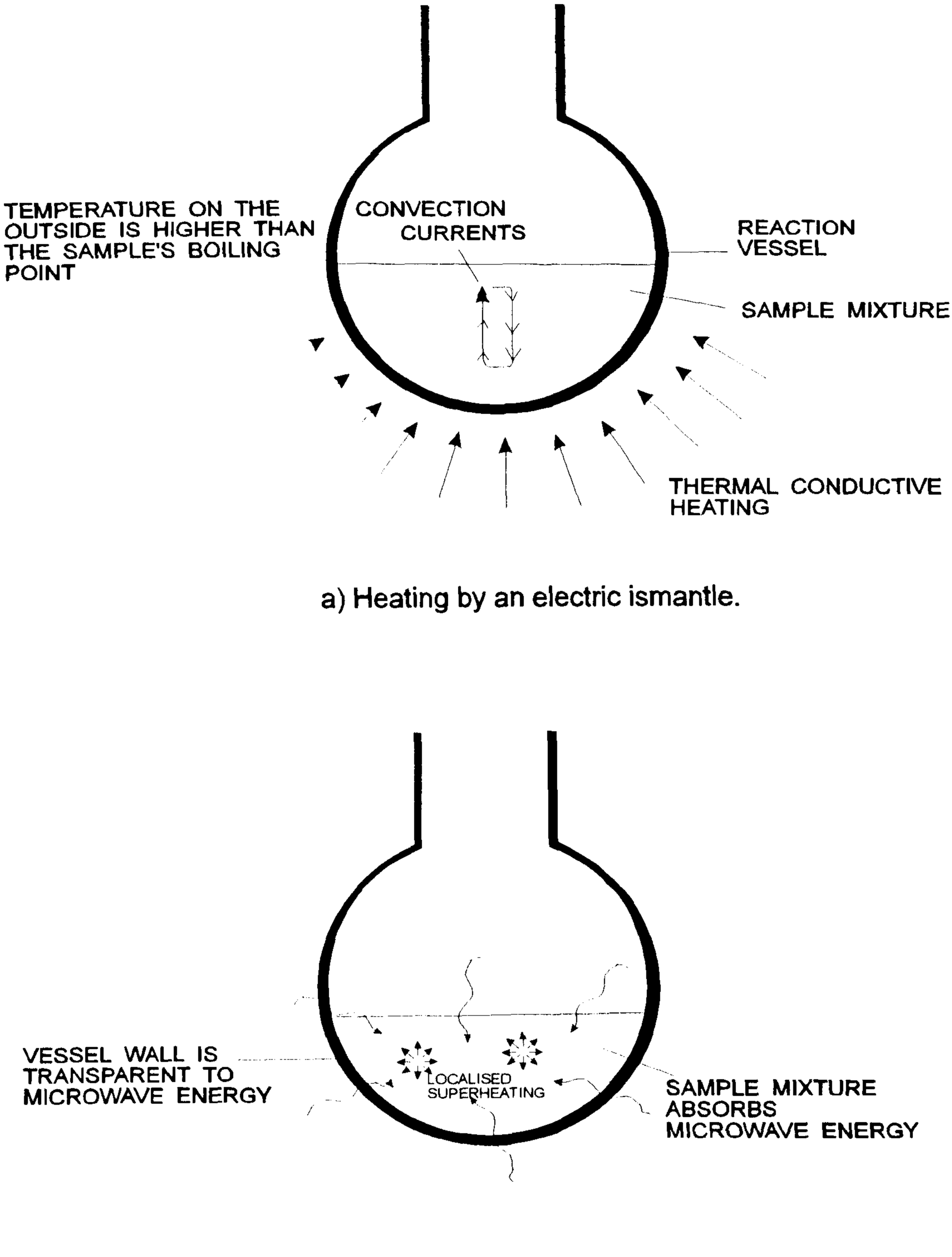

a) Heating by an electric ismantle.

b) Irradiating with microwaves.

Figure 2.12. The processes of conductive and microwave heating.

2.2. Experimental.

2.2.1. Apparatus.

2.2.1.1. The Gas Thermometer.

Initial experiments were made with thermometers which had been constructed from Pyrex. Since the idea seemed feasible, thermometers were then constructed from silica which increased the operational range of temperature measurement. The bulb dimensions are 10 mm in length and 6 mm diameter blown out onto the end of capillary of 0.5 mm internal diameter. This is connected to the pressure transducer using the capillary tubing which has 6.35 mm outside diameter. The pressure transducers used were a SE 21/V (5 psi) model with a low voltage output (mV). The connection to the gas thermometer was made using a standard ¼" Wade fitting with rubber rings for the seal. The other model used was Eurosensor Model 600 with a range of 0-199 kPa and an output of 1-6V. The connection to the gas thermometer was with rubber tubing or a Drallim fitting incorporating a rubber seal.

2.2.1.2. The microwave ovens.

A domestic microwave oven used in this work was a Toshiba Delta-wave model number ER-770E/EW with a maximum power output of 650 W. Eight reduced power levels were achieved by pulsing the full 650 W at preset time intervals. The microwave frequency was 2.45 GHz. The apparatus was equipped with a mode stirrer and a turn-table to ensure even distribution of the energy within the oven. The oven was modified by inserting holes in the top and back of the oven, so that a system was set up which comprised of a reaction vessel situated inside the oven connected to a externally mounted reflux condenser via either a section of polytetrafluoroethylene tubing or a Pyrex connecting tube. Care was taken to sleeve the exit holes from the cavity with chokes which comprised of short lengths of grounded metal tubes. These tubes prevented microwave leakage, but allowed glassware tubing to pass into the oven. The chokes used in the experiments were typically 35mm diameter copper 140mm in length with a 20 mm flange of the bottom. The reaction vessel could also incorporate the gas

thermometer, which was inserted through the hole in the back or top of the oven. If necessary, an adequate load for the microwave power was provided by a continuous flow of water through a coil of polytetrafluoroethylene tubing inside the oven. For the purposes of the experiments the turntable was removed.

The microwave oven was modified to a design by Dr. Hamilton (ICI) so that continuous irradiation could be achieved with variable power (figure 2.13). As supplied by an unmodified oven, the primary winding of the step-up transformer in the oven receives 240V, 4A, 50 Hz a.c. mains voltage via the control circuitry. To modify the output of the magnetron, the potential across the magnetron needed to be varied. To accomplish this the primary winding of the the step-up transformer must receive a variable voltage (by use of a Variac). The control circuitry must feed the primary winding of the Variac and the output from the Variac must feed the primary winding of the step-up transformer

A second domestic microwave oven used in the experiments was a MATSUI 33TC oven with a maximum power output of 700W which was used in collaboration with ICI. The output from the transducer was connected to an IWATSU SS-7606 60 MHz cathode ray oscilloscope and a personal computer with suitable analogue to digital capabilities. A computer programme was devised by Dr. Hamilton (ICI) so that the output from the pressure transducer could be recorded with respect to time.

An industrial microwave oven used in this work was the CEM model MDS 81D which was provided by CEM. This was designed for acid dissolution experiments. The oven was equipped with a terminal circulator so that reflected microwaves were diverted into a ferrite dummy load where the energy was dissipated as heat. This oven provided more control over the power generated by the magnetron, for example 50% power meant that the magnetron was on for 0.5 seconds and off for 0.5 seconds. The oven was modified in a similar fashion to the Toshiba by inserting holes in the top and side of the oven, so that a system was set up which comprised a reaction vessel situated inside the oven connected to a externally mounted reflux condenser via either a section of polytetrafluoroethylene tubing or a Pyrex connecting tube.

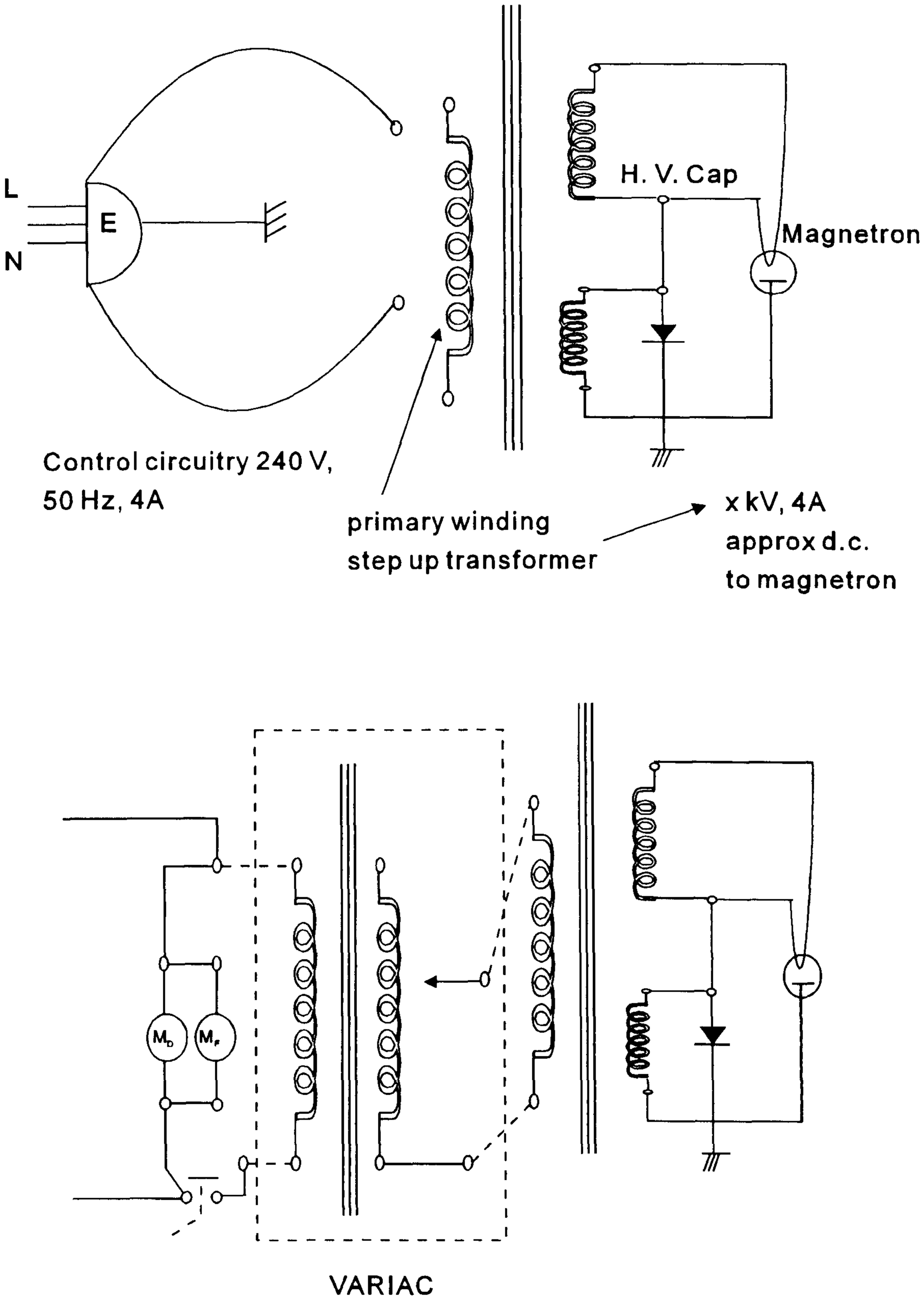

Figure 2.13. Circuit diagram of modification to oven.

2.2.2. Calibration.

2.2.2.1. Calibration of the Gas Thermometer.

The thermometer was calibrated by attaching a thermocouple to the gas thermometer and heating both in a gas chromatography oven, recording the output from the pressure transducer and plotting this against the temperature of the thermocouple.

2.2.2.2. Calibration of the duty cycle.

The duty cycle for separate reduced power setting was recorded for the Toshiba Delta-wave model number ER-770E/EW. This was achieved by using water (500 ml) in a beaker, which was placed in the oven and irradiated at each level. The time was noted when the magnetron was active and how long it was inactive by using the sound of the relay operation.

2.2.2.3. Calibration of the Variac.

Calibration of the power output for different settings of the Variac was performed by placing water (500 ml) in the oven and irradiating for a known length of time and recording the temperature before and after irradiation.

2.2.3. Experiments on heating solvents.

2.2.3.1. Irradiation of N,N-dimethylformamide, toluene and 1,2-dichloroethane.

Glass tubes containing either N,N-dimethylformamide (DMF), toluene and 1,2-dichloroethane (15 ml) were placed in separate tubes which were immersed in water-filled beakers, the water then being frozen into blocks of ice. The beaker was placed in the Toshiba oven with the gas thermometer inserted into the solvent as shown in figure 2.14. The experiments were performed at power level 1; at this setting the radiation is pulsed. Each beaker was placed in the oven and irradiated for 3 minutes as described by Bose[52]. The experiments were then repeated with a longer exposure time of 10 minutes. The final experiments were performed under continuous irradiation and the samples were heated up to their boiling points.

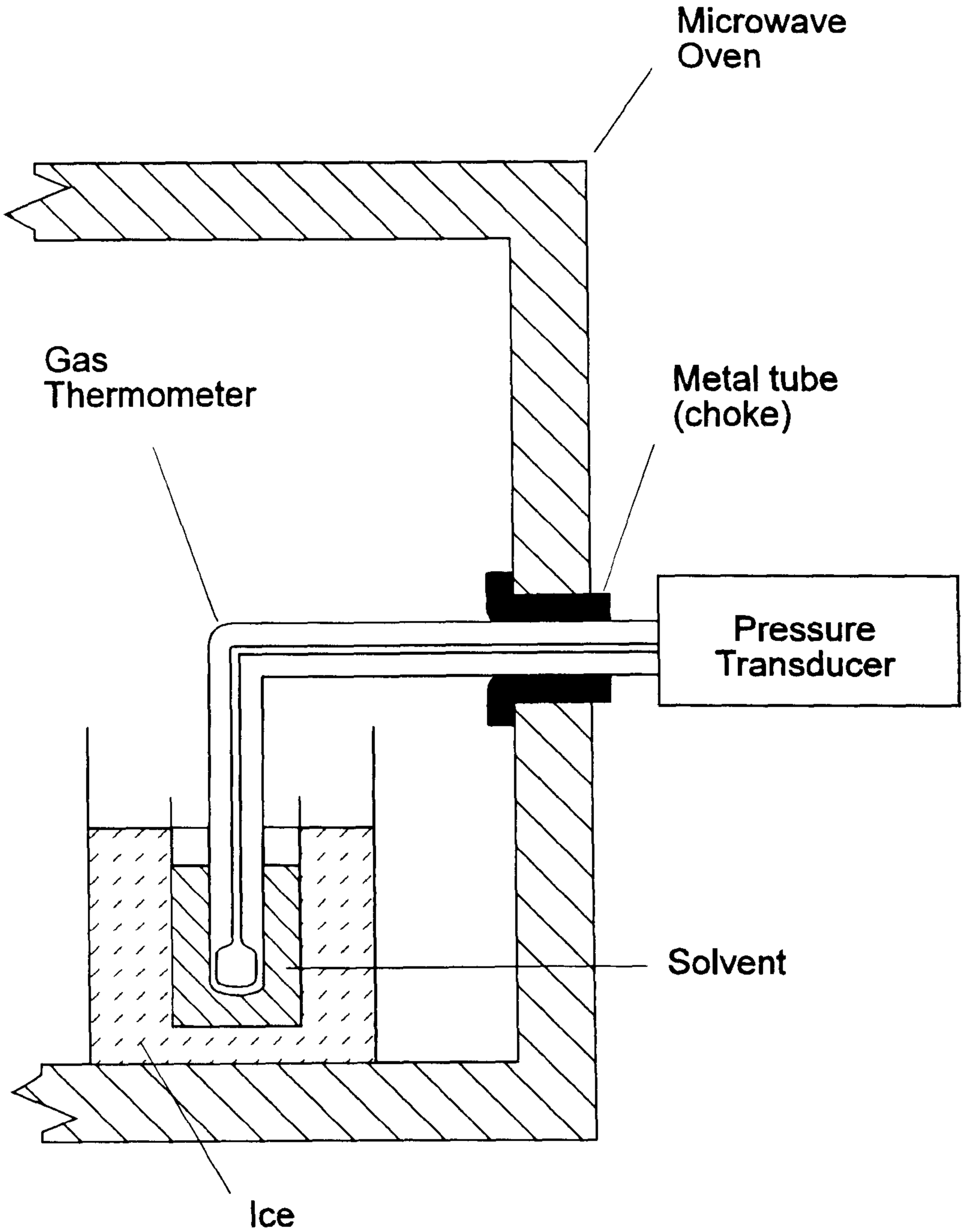

Figure 2.14. Schematic diagram of apparatus with gas thermometer inserted into solvent.

2.2.3.2. Irradiation of solvents.

The apparatus was set up as shown in figure 2.15. A known quantity of liquid was placed in the flask and irradiated under microwave conditions. The output from the pressure transducer was noted. When the signal had reached a maximum (i.e. the liquid was boiling under reflux conditions), the reading was noted. With the experiments using a thermocouple, when the liquid was being boiling under reflux conditions, the power was switched off and the thermocouple was inserted into the liquid.

2.2.3.3. Irradiation of azeotropic mixture.

The apparatus was set up for distillation with a mercury thermometer placed in the stillhead. A solution of ethanol (50 ml) and water (50 ml) was placed in the vessel and irradiated under microwave conditions. The refractive index of the liquid distilled at different temperature (recorded by the thermometer) was analysed using a refractometer. The experiment was repeated under normal thermal conditions.

2.2.3.4. Investigation of superheating effects.

A known quantity of liquid was placed in the flask and irradiated under microwave conditions. The signal from the pressure transducer was recorded by the computer periodically. When the signal had reached a maximum, i.e. the liquid was boiling under reflux conditions, the reading was noted, and the power switched off. An additional quantity of liquid was added to the flask, with care, and the experiment was continued in this way until the flask could not hold any more liquid, so the addition of more liquid was deemed to be unsafe. Experiments were conducted using various solvents under varying conditions of volume and microwave power.

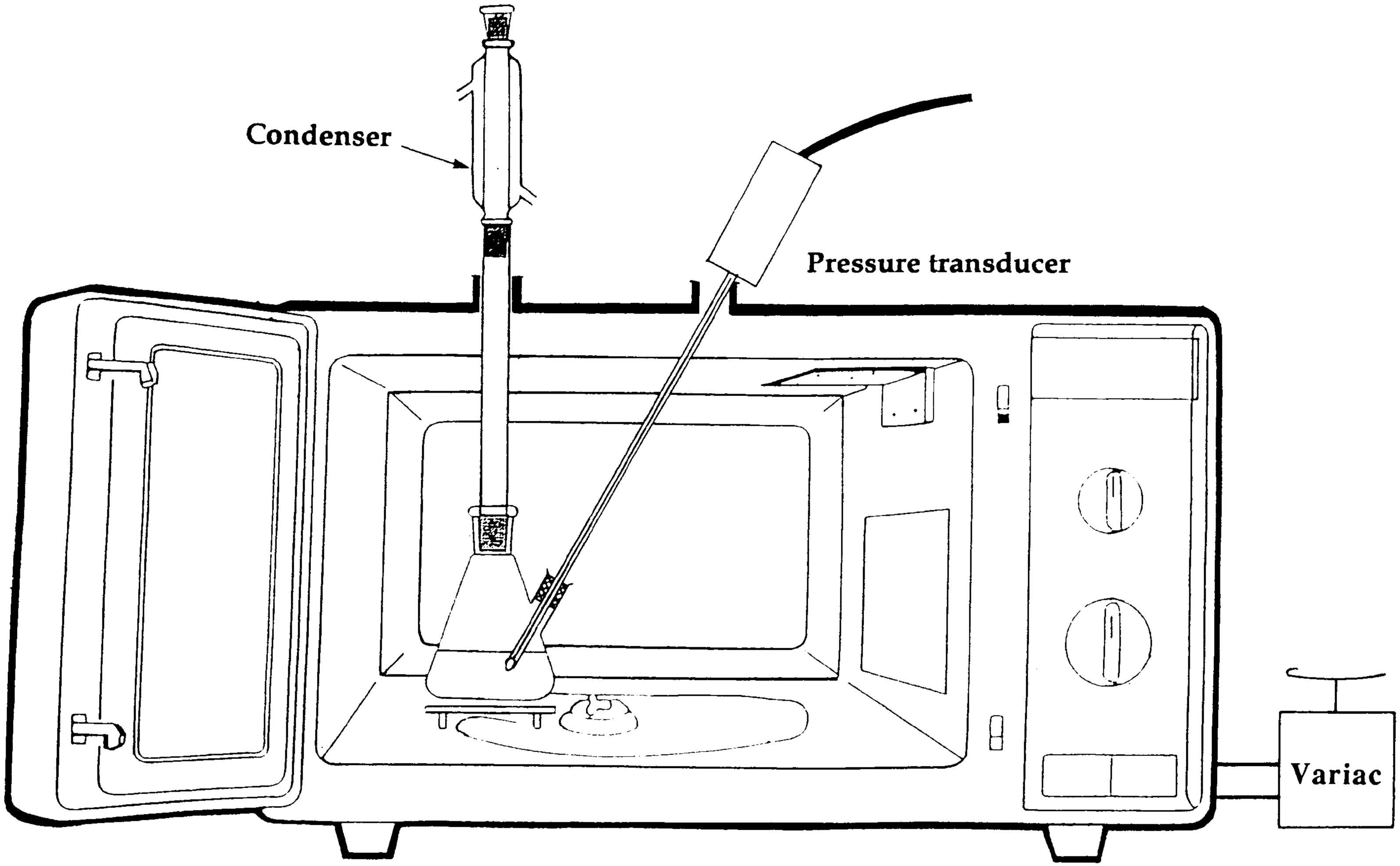

Figure 2.15. Schematic diagram of apparatus for heating solvents under microwave irradiation.

2.3. Results.

2.3.1. Calibration.

2.3.1.1. Calibration of the Gas Thermometer.

The initial calibrations were performed using the SE 21/V model pressure transducer. The reproducibility of the calibrations was poor. This was for a number of reasons; the reference side was exposed to the atmosphere so that changes in atmospheric pressure from day to day affected the reading. The reference side was then connected to a fixed volume in the form of an empty lecture bottle. This improved the calibration, but the reading was not stable and it was realised that the bottle was acting as a thermometer itself. The reference side was then blanked off using a metal rod. The calibrations then showed better reproducibility. It was found that the reproducibility and stability of the gas thermometer were better if the thermometer was not moved or disconnected.

Connection of the thermometer to the smaller, less cumbersome, portable pressure transducer, EuroSensor Model No 600D15P12D5 with a pressure range of 0-15 psi and a output signal range of 1-6 VDC, and calibrating as before proved very successful. The curve is as shown in figure 2.16 and a cubic equation of the form $y=ax^3+bx^2+cx+d$ fits the curve. Accurate temperature measurements were made by calibrating the gas thermometer in ice and water and obtaining the constant d. From the output reading (y), the temperature (x) could be obtained.

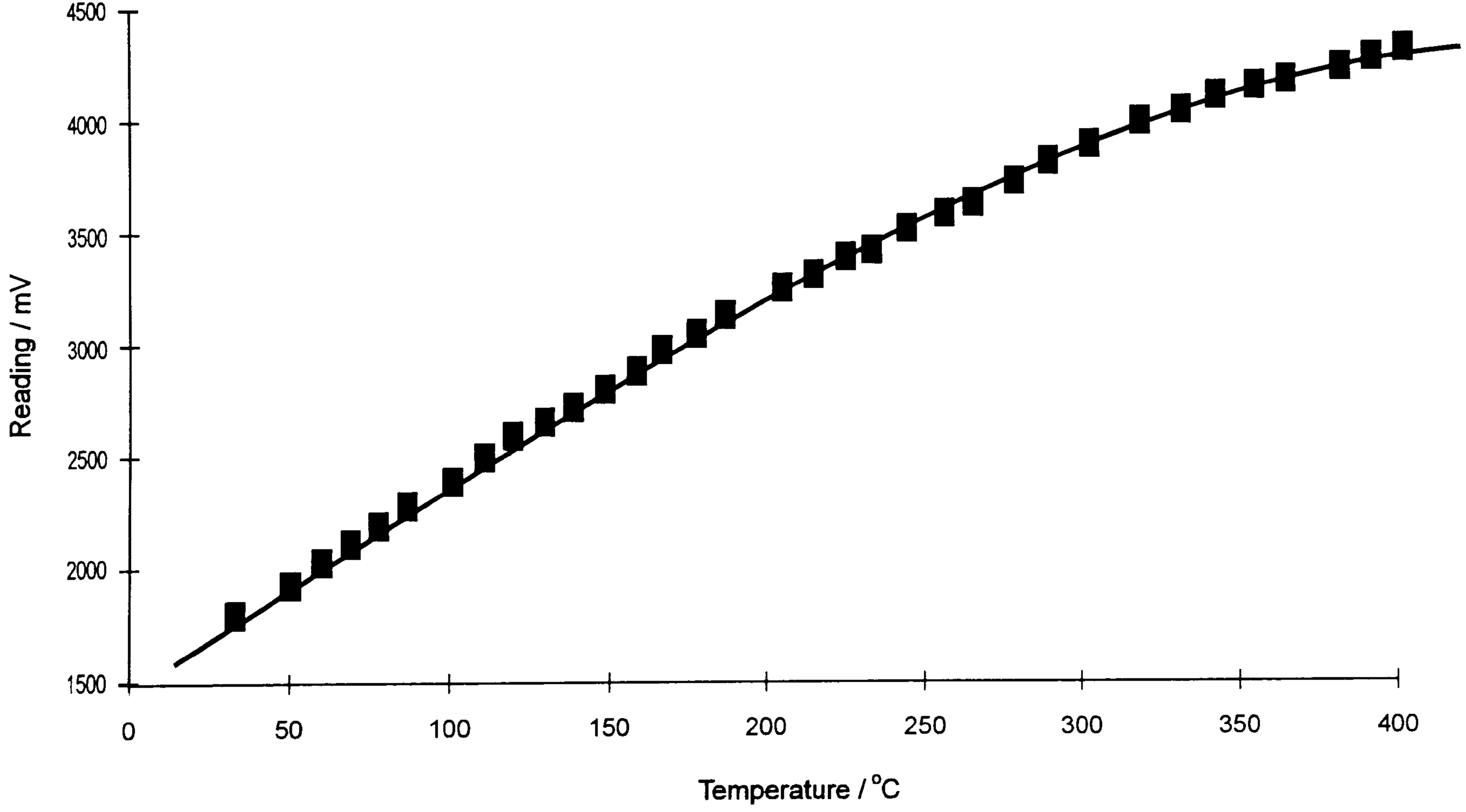

Figure 2.16. Calibration of Gas Thermometer.

2.3.1.2. Variation in the timecycle of the magnetron.

The time on line for the magnetron against reduced power settings is shown in table 2.4.

Table 2.4.
The timecycle of the magnetron for power settings of the Toshiba oven.

Power Setting	Magnetron on / seconds	Magnetron off / seconds
1	5	25
2	8	22
3	10	20
4	14	16
5	15	15
6	18	12
7	21	9
8	24	6
9	continuous	0

2.3.1.3. Calibration of the Variac.

The calibration of the Variac is presented in figure 2.17. Using the following equation the power output can be calculated for each increment of the Variac output.

$$\text{Power / Watts} = \frac{\text{mass} * \text{specfic heat capacity} * \text{change in temperature}}{\text{Time}} \qquad (2.19).$$

As can be seen continuous irradiation of 20 W can be achieved. The problem was that the response was not linear, and there was a substantial jump from 70 W to 490 W as the applied voltage was taken from 89% to 95% of the mains voltage.

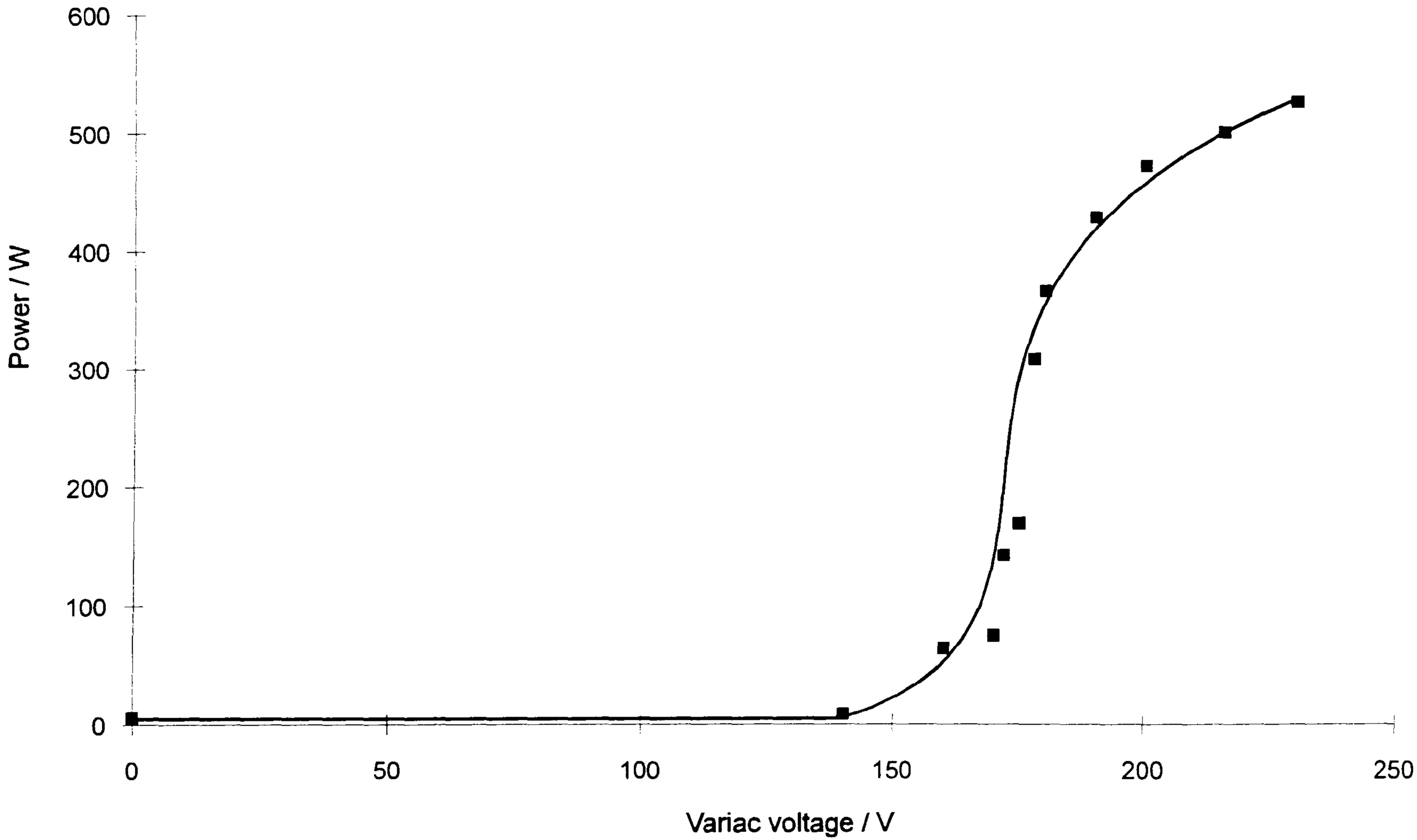

Figure 2.17. Power performance of microwave oven at different Variac voltages.

2.3.2. Results from heating of solvents under microwave irradiation.

2.3.2.1. Irradiation of N,N-dimethylformamide, toluene and 1,2-dichloroethane.

Figure 2.18 shows the trace from a chart recorder connected to the output from the pressure transducer. The spikes correspond to the pulses of power from the microwave source. The results show that all three solvents were heated considerably after a short period of time, even at this low power setting. After 3 minutes the block was removed and it was seen that the ice had only melted around the side of the beaker which contained it. The next experiments again showed that the solvents were heated, but on removal of the beakers the ice had melted around the tubes and at the side of the beaker. A summary of the results is shown in table 2.5.

Table 2.5.
Temperature rise of three solvents when subjected to pulsed microwave radiation at 560 W.

Solvent	Initial temp / °C	Final temp / °C	Radiation time / mins
DMF	-13	10	3
DMF	-13	22	10
toluene	-7	2	3
toluene	-7	10	10
1,2-dichloroethane	-2	14	3
1,2-dichloroethane	0	18	10

2.3.2.2. Irradiation of solvents.

Figure 2.19 shows the results from the experiments using the gas thermometer inserted into the solvent under thermal and microwave conditions. The figure shows the output from a chart recorder which had recorded the signal from the gas thermometer for both the thermal and microwave experiments, the gas thermometer was recording a higher temperature when the solvent was being heated under microwave irradiation than under normal thermal conditions.

Table 2.6 shows the results from the experiments when a thermocouple was inserted into the solvent which had just been boiling under microwave irradiation using the CEM oven. The results show that the polar solvents were attaining a higher temperature than their normal boiling point under microwave radiation.

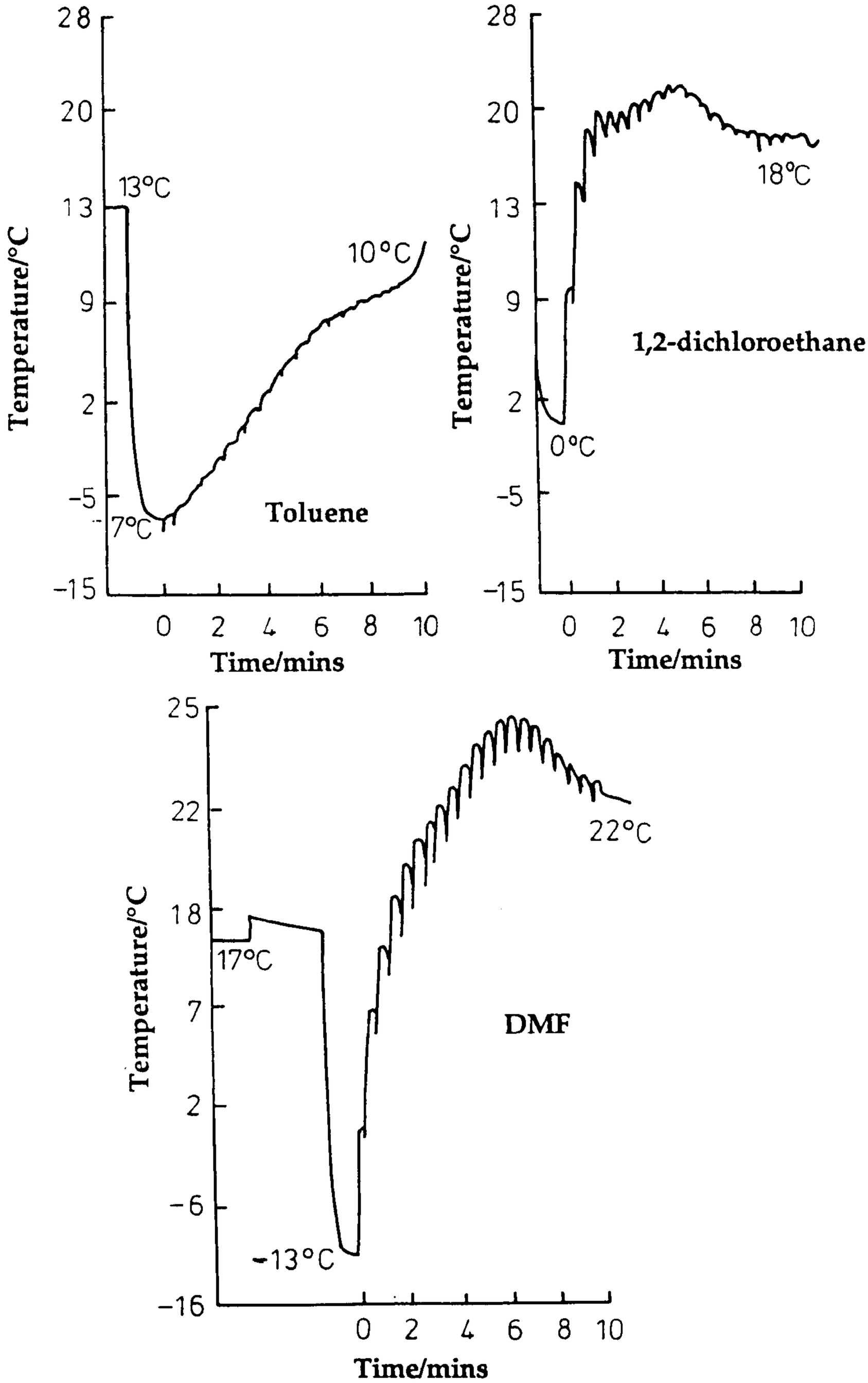

Figure 2.18. Gas thermometer output against time for microwave irradiation of solvents.

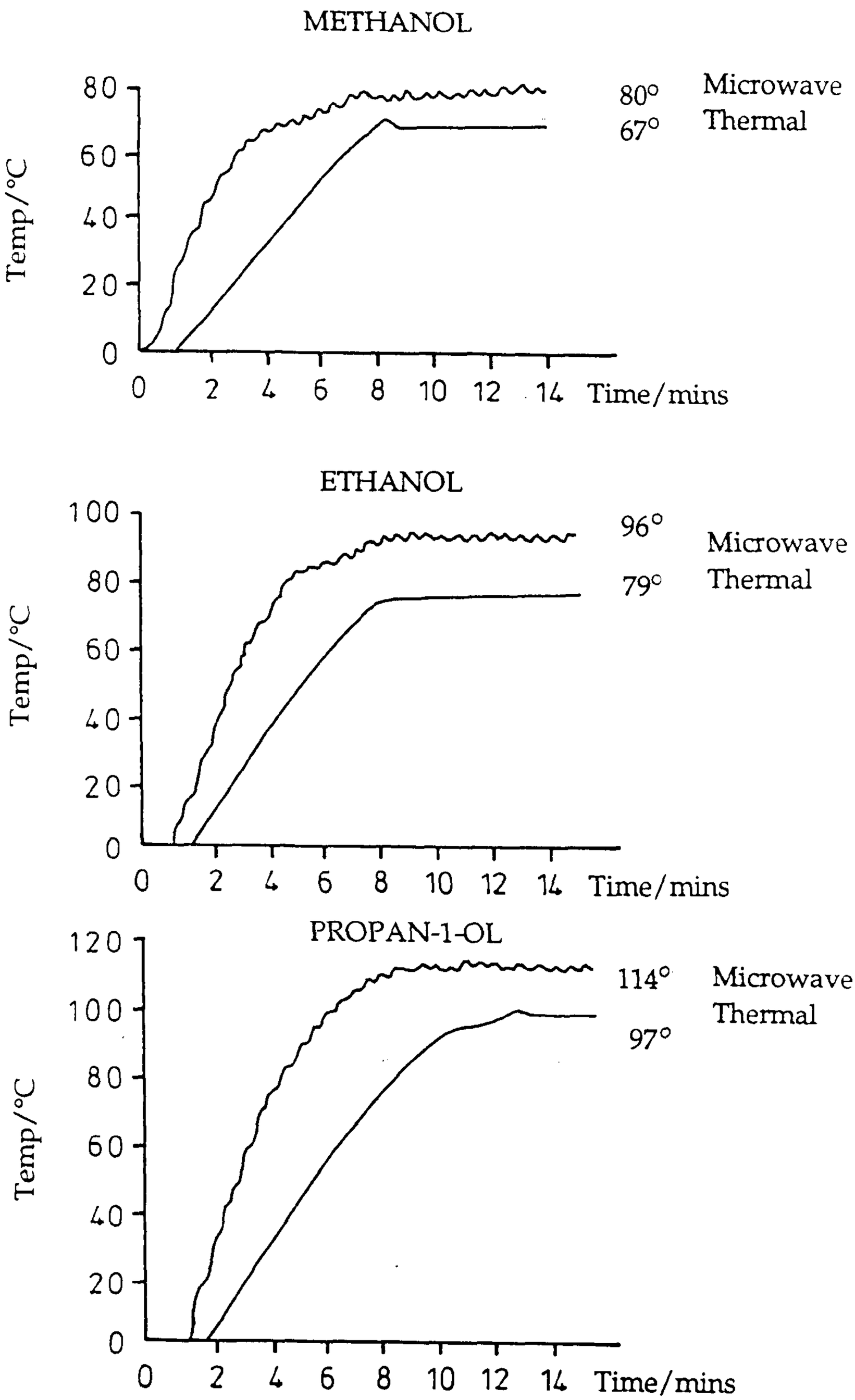

Figure 2.19. Gas thermometer output against time for heating of solvents under thermal and microwave conditions.

Table 2.6.
The temperature achieved by several solvents under varying microwave power.

Solvent	% Power	Boiling Point / °C	Temperature / °C
Water	20	100	103-104
	30		103
	40		103-104
	50		103
Pentanol	30	137	141
	40		140
Methanol	20	65	73
	30		77
	40		77
Ethanol	30	78	83-84
	40		81
	50		82
Propan-2-ol	20	82	89-90
	30		92
	40		93
	50		92
Butan-1-ol	20	117	125
	30		128
	40		128
THF	30	66	74
	40		77
	50		75-76
	60		75
Pentane	20	36	no significant rise
Hexane	30	69	no significant rise

2.3.2.3. Irradiation of azeotrope mixture.

Figure 2.20 presents the results from irradiation of the azeotrope mixture. The figure is a plot of the refractive index against the temperature recorded by the thermometer in the stillhead, for each sample taken. The results show within experimental error there was no difference between the thermal and microwave experiments.

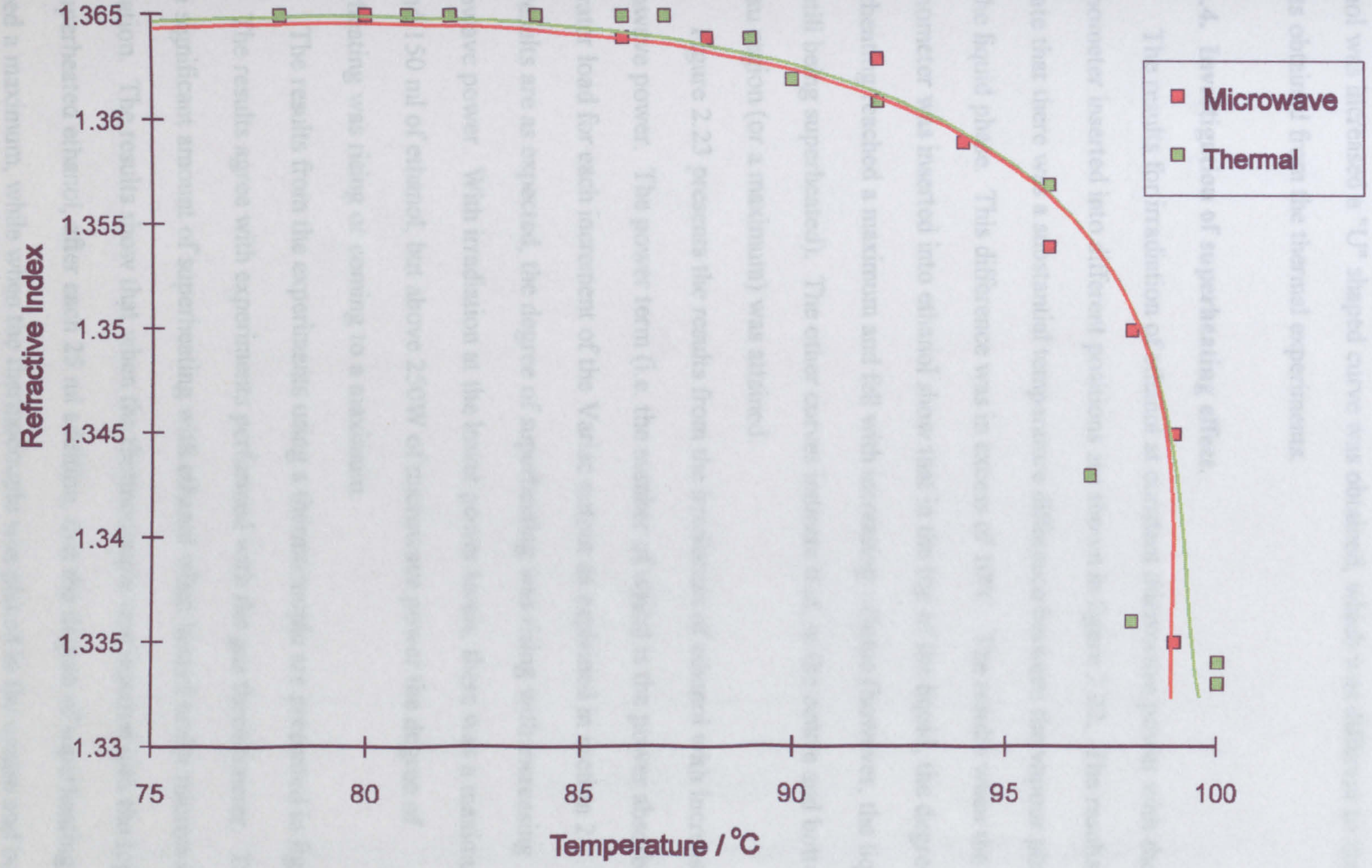

Figure 2.20. Refractive index against temperature recorded by thermometer in stillhead.

Figure 2.21 shows the boiling point composition curves for water and ethanol heated under thermal and microwave conditions with the thermocouple inserted into the liquid after it was boiling under reflux conditions. The boiling point of ethanol heated under microwave irradiation was approximately 100°C, so as the concentration of ethanol was increased a "U" shaped curve was obtained, which was different to the results obtained from the thermal experiments.

2.3.2.4. Investigation of superheating effect.

The results for irradiation of ethanol at constant microwave power with the gas thermometer inserted into different positions are shown in figure 2.22. The results indicate that there was a substantial temperature difference between the vapour phase and the liquid phase. This difference was in excess of 10°C. The results when the gas thermometer was inserted into ethanol show that in the top of the liquid, the degree of superheating reached a maximum and fell with increasing volume (however, the liquid was still being superheated). The other curves indicate that, in the centre and bottom, a plateau region (or a maximum) was attained.

Figure 2.23 presents the results from the irradiation of ethanol with increasing microwave power. The power term (i.e. the number of watts) is the power absorbed by the water load for each increment of the Variac output as explained in section 2.3.1.3. The results are as expected, the degree of superheating was rising with increasing microwave power. With irradiation at the lower power levels, there was a maximum around 150 ml of ethanol, but above 250W of microwave power the degree of superheating was rising or coming to a maximum.

The results from the experiments using a thermocouple are presented in figure 2.24. The results agree with experiments performed with the gas thermometer. There was a significant amount of superheating with ethanol when heated under microwave irradiation. The results show that when the thermocouple was inserted into the top of the superheated ethanol, after each 25 ml addition, that the degree of superheating reached a maximum, while when the thermocouple was placed in the centre and bottom of the flask, the temperature was continuing to either rise or come to a maximum.

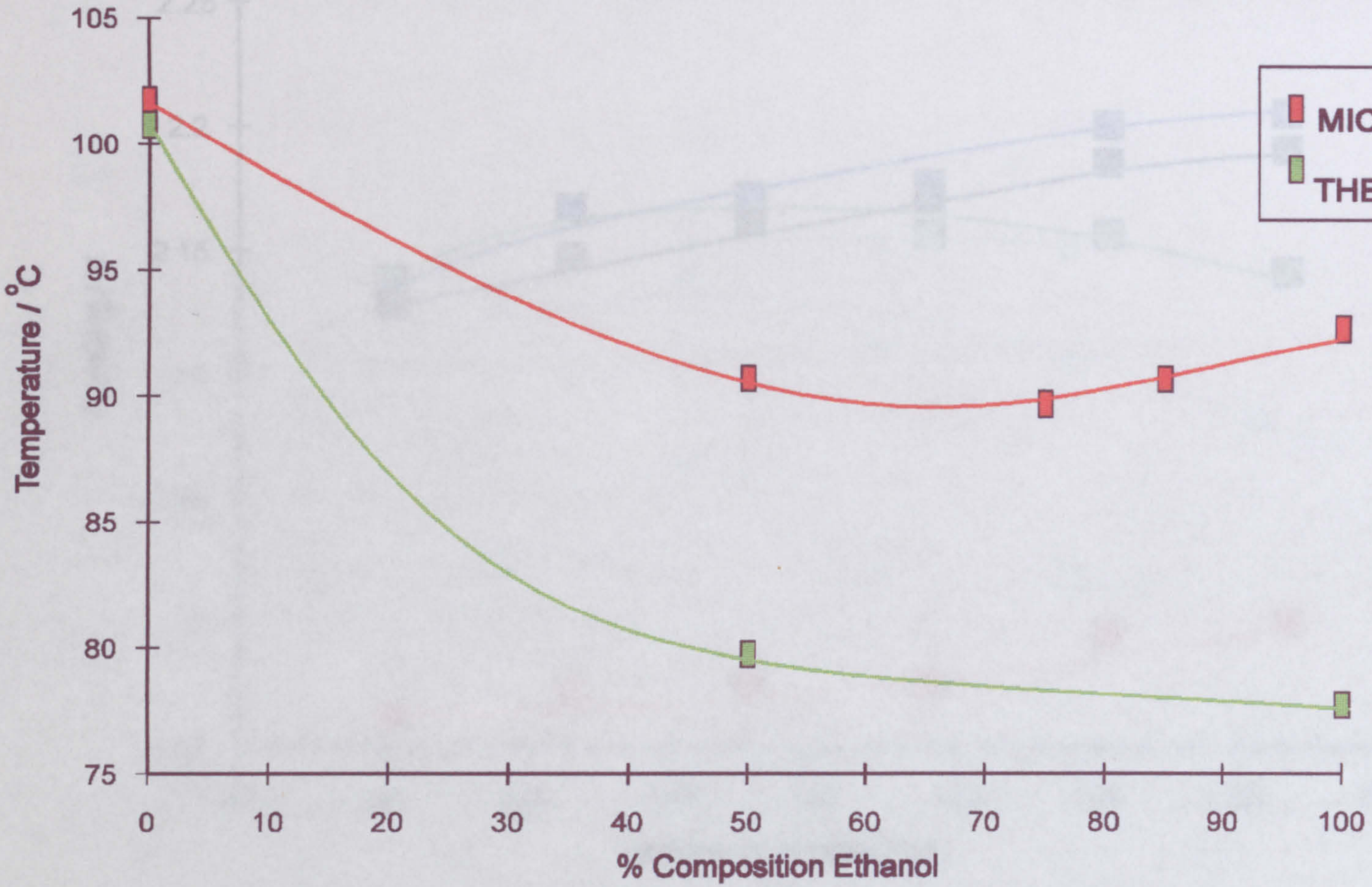

Figure 2.21. Boiling points attained by different mixtures of ethanol and water heated under thermal and microwave conditions.

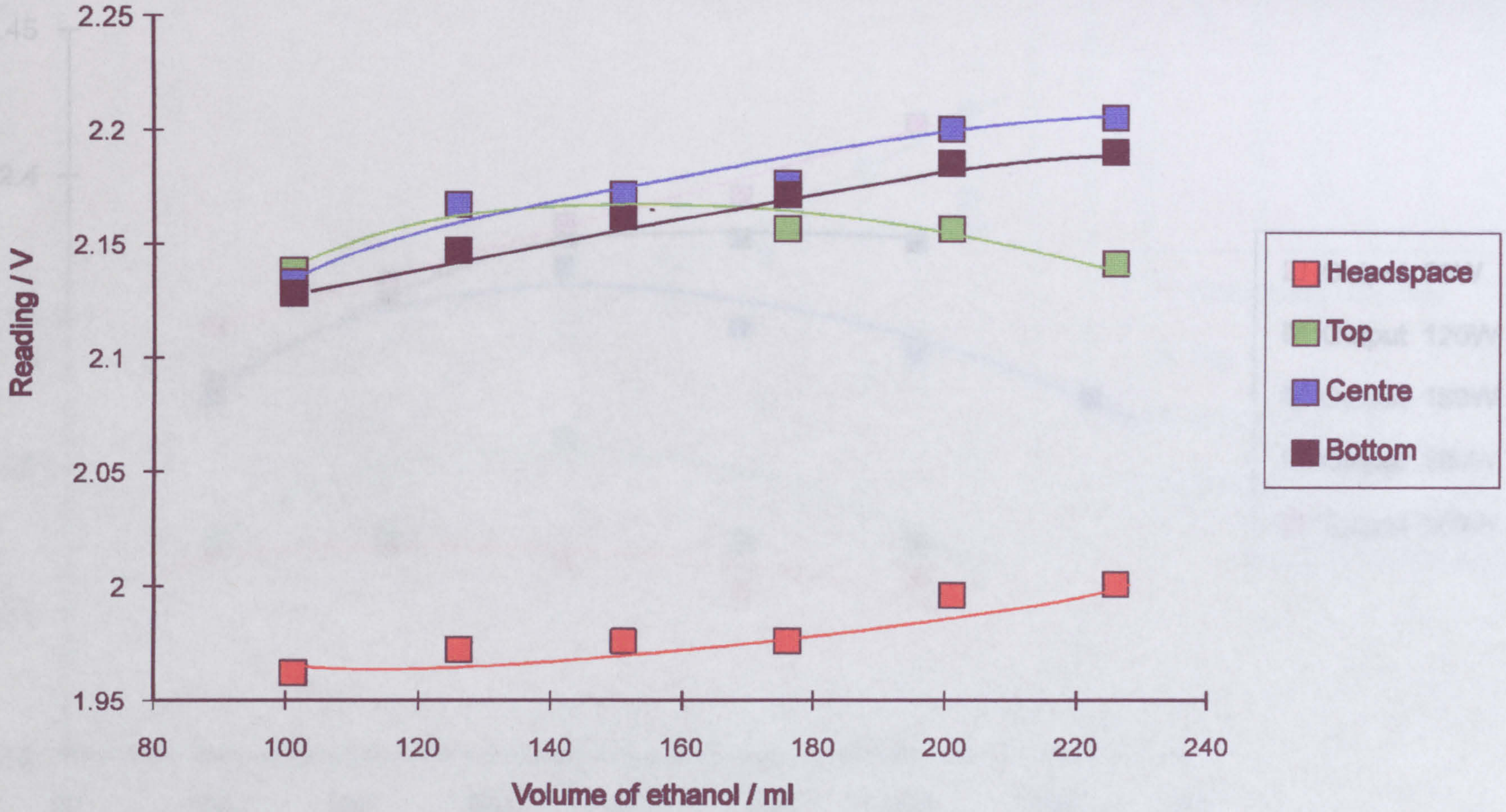

Figure 2.22. Gas thermometer reading against volume of ethanol under microwave irradiation at constant magnetron power output.

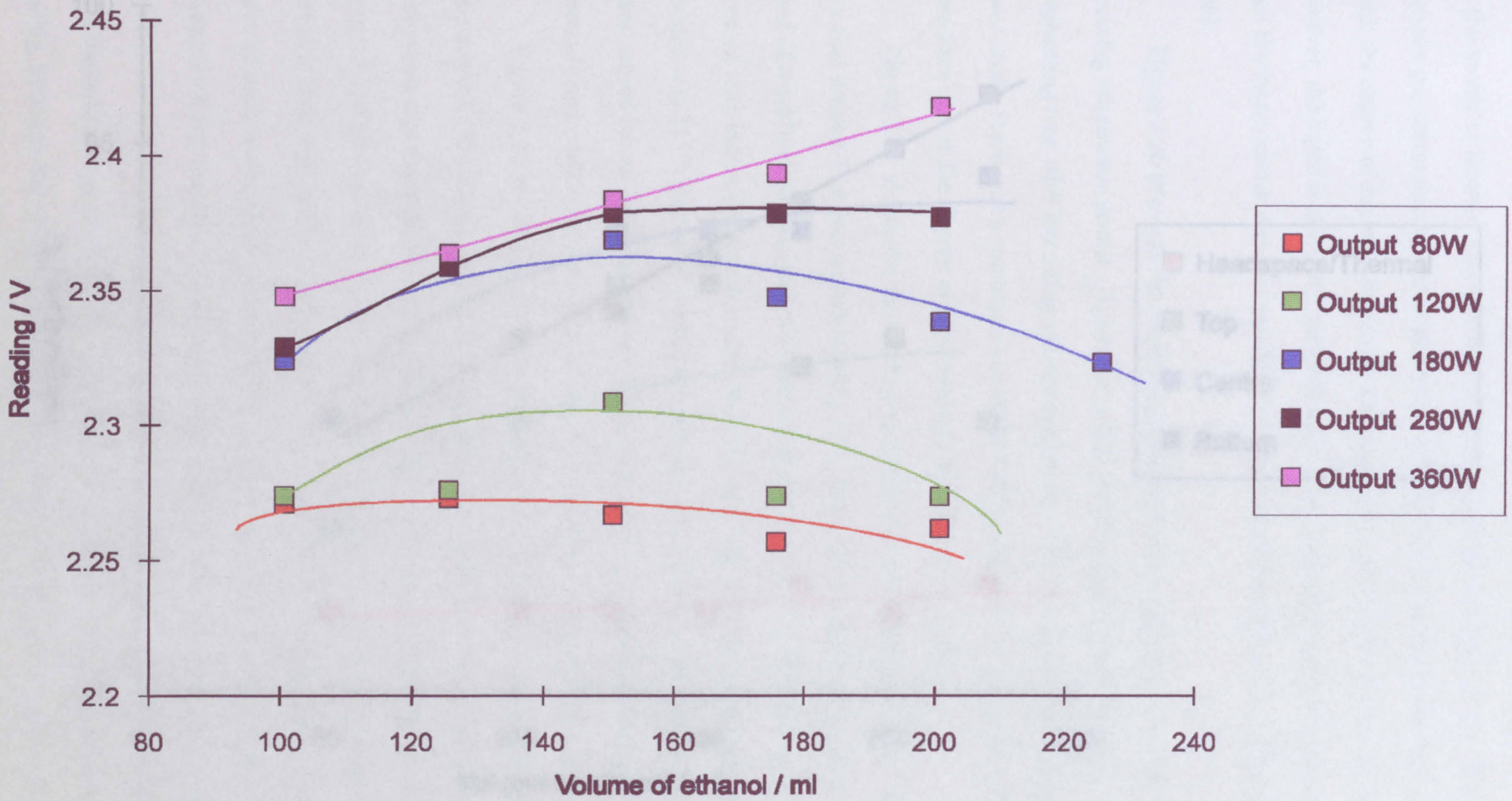

Figure 2.23. Gas thermometer reading against volume of ethanol under microwave irradiation with increasing magnetron power output.

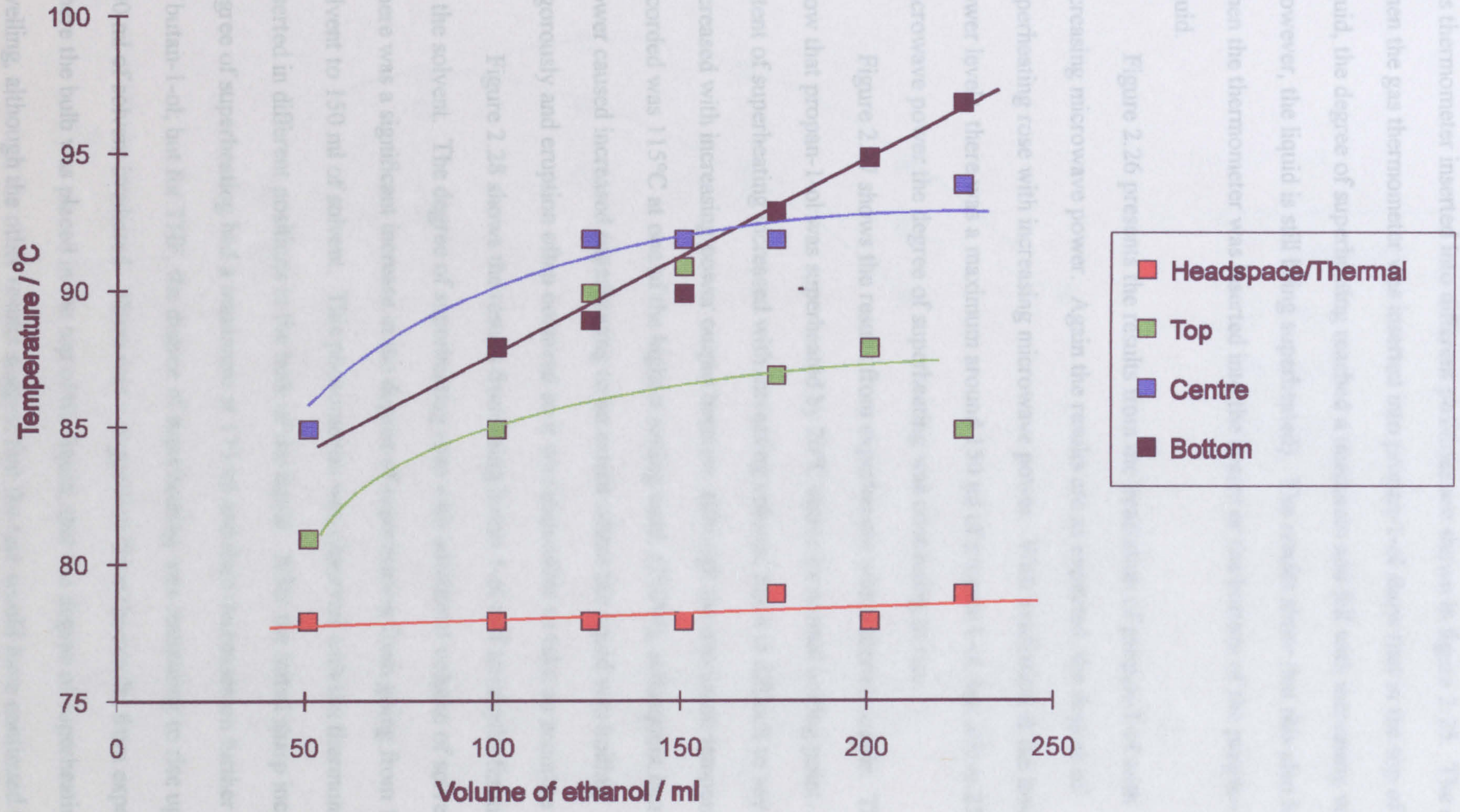

Figure 2.24. Temperature recorded by thermocouple after insertion into ethanol which had been boiling under microwave irradiation.

The results for irradiation of propan-1-ol at constant microwave power with the gas thermometer inserted into different positions are shown in figure 2.25. The results when the gas thermometer was inserted into propan-1-ol show that in the top of the liquid, the degree of superheating reached a maximum and fell with increasing volume (however, the liquid is still being superheated). The results show that this also happened when the thermometer was inserted into the centre or the bottom of the propan-1-ol liquid.

Figure 2.26 presents the results from the irradiation of propan-1-ol with increasing microwave power. Again the results are as expected, the degree of superheating rose with increasing microwave power. With irradiation at the lower power levels, there was a maximum around 150 ml of propan-1-ol, but above 250W of microwave power the degree of superheating was continuing to rise.

Figure 2.27 shows the results from experiments with a thermocouple. The results show that propan-1-ol was superheated by 20°C above its normal boiling point. The extent of superheating increased with increasing volume, but it is difficult to say that it increased with increasing power output because, although the maximum temperature recorded was 115°C at one of the highest setting used, (280W), subsequent increase of power caused increased superheating to an extent where the liquid was boiling vigorously and eruption often occurred so it was impossible to take an accurate reading.

Figure 2.28 shows the results from using butan-1-ol and tetrahydrofuran (THF) as the solvent. The degree of superheating rose with additional volume of solvent. There was a significant increase in the degree of superheating from going from 125 ml of solvent to 150 ml of solvent. This phenomenon was observed with the thermometer inserted in different positions in the bulk of the liquid. After the initial sharp increase, the degree of superheating had a maximum at 175 ml and then decreases on further addition of butan-1-ol; but for THF, the degree of superheating was continuing to rise up to 200 ml of solvent irradiated. There was a suggestion from the results from experiments where the bulb was placed in the top of the liquid, that the degree of superheating was levelling, although the other results suggest that the rate would have continued to increase on further addition of solvent.

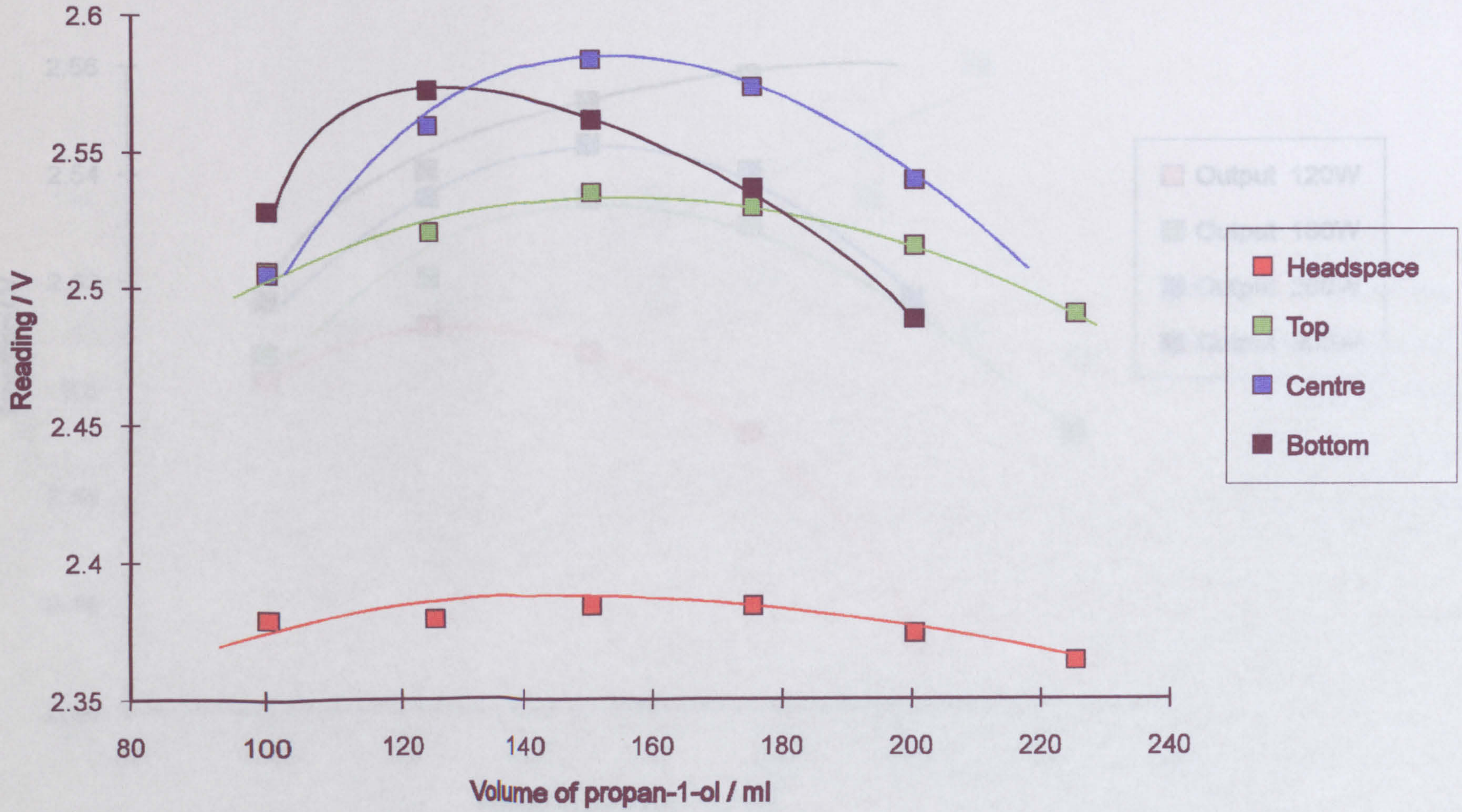

Figure 2.25. Gas thermometer reading against volume of propan-1-ol under microwave irradiation at constant magnetron power output.

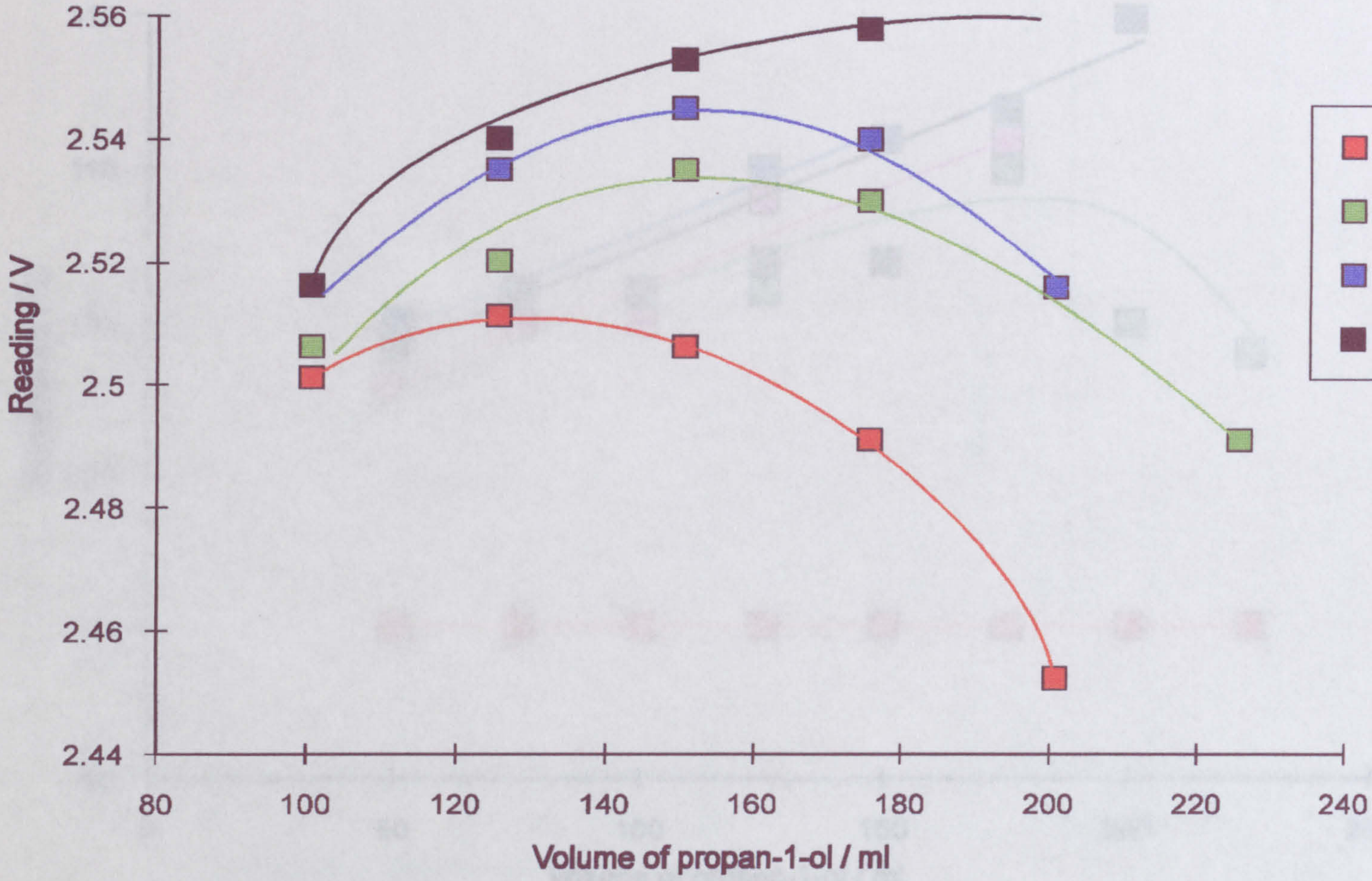

Figure 2.26. Gas thermometer reading against volume of propan-1-ol under microwave irradiation with increasing magnetron power output.

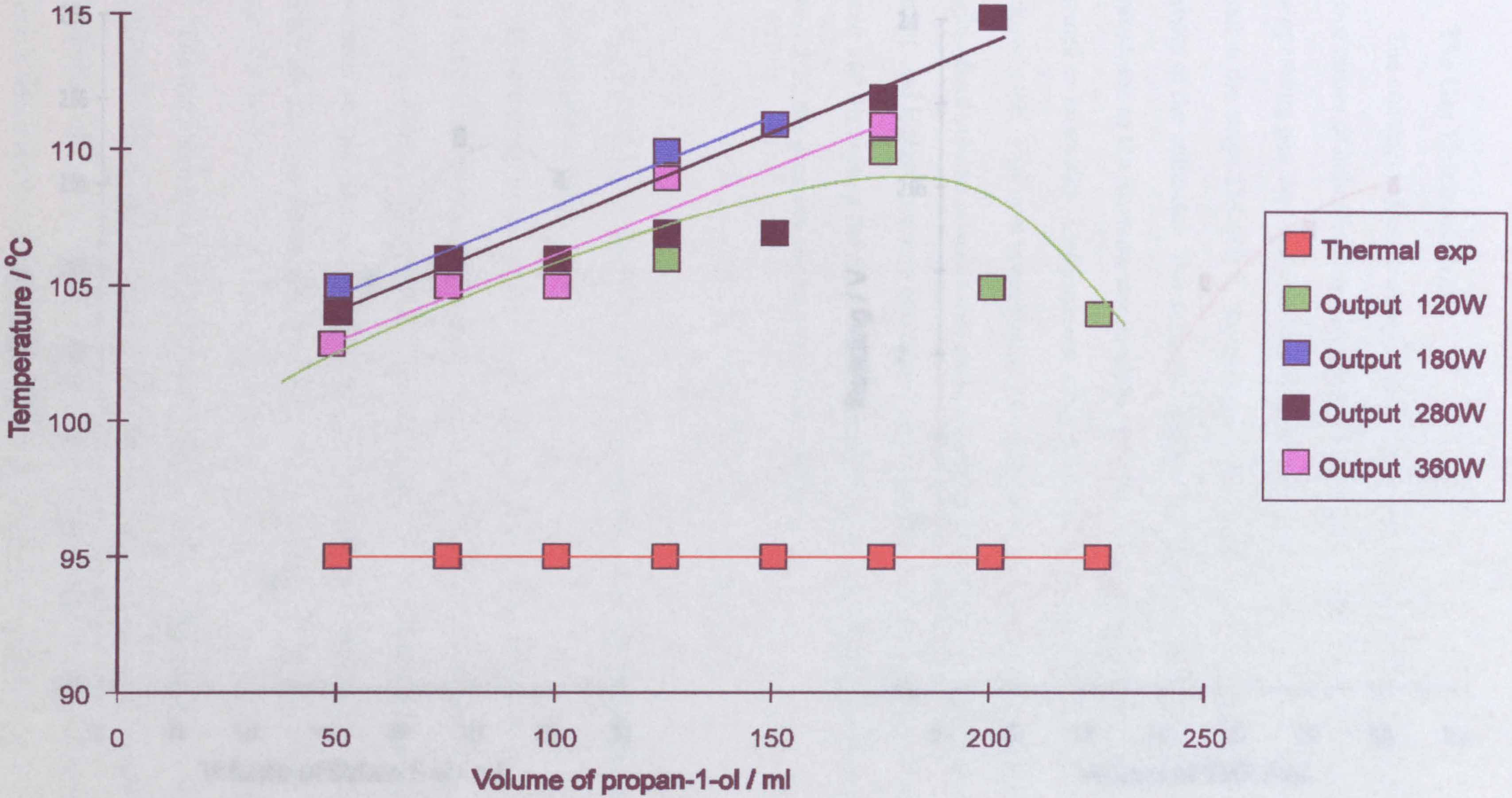

Figure 2.27. Temperature recorded by thermocouple after insertion into propan-1-ol which had been boiling under microwave irradiation.

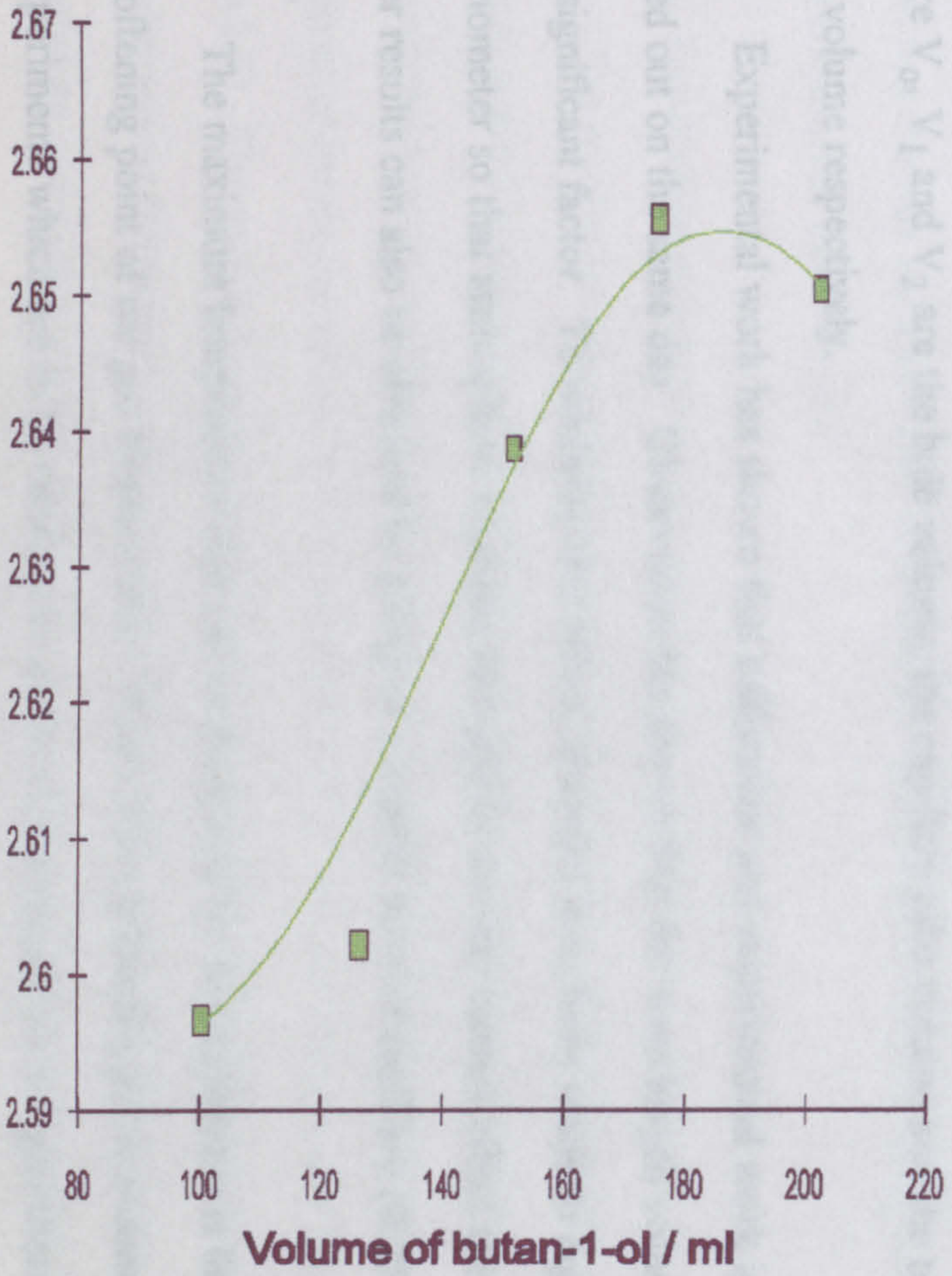

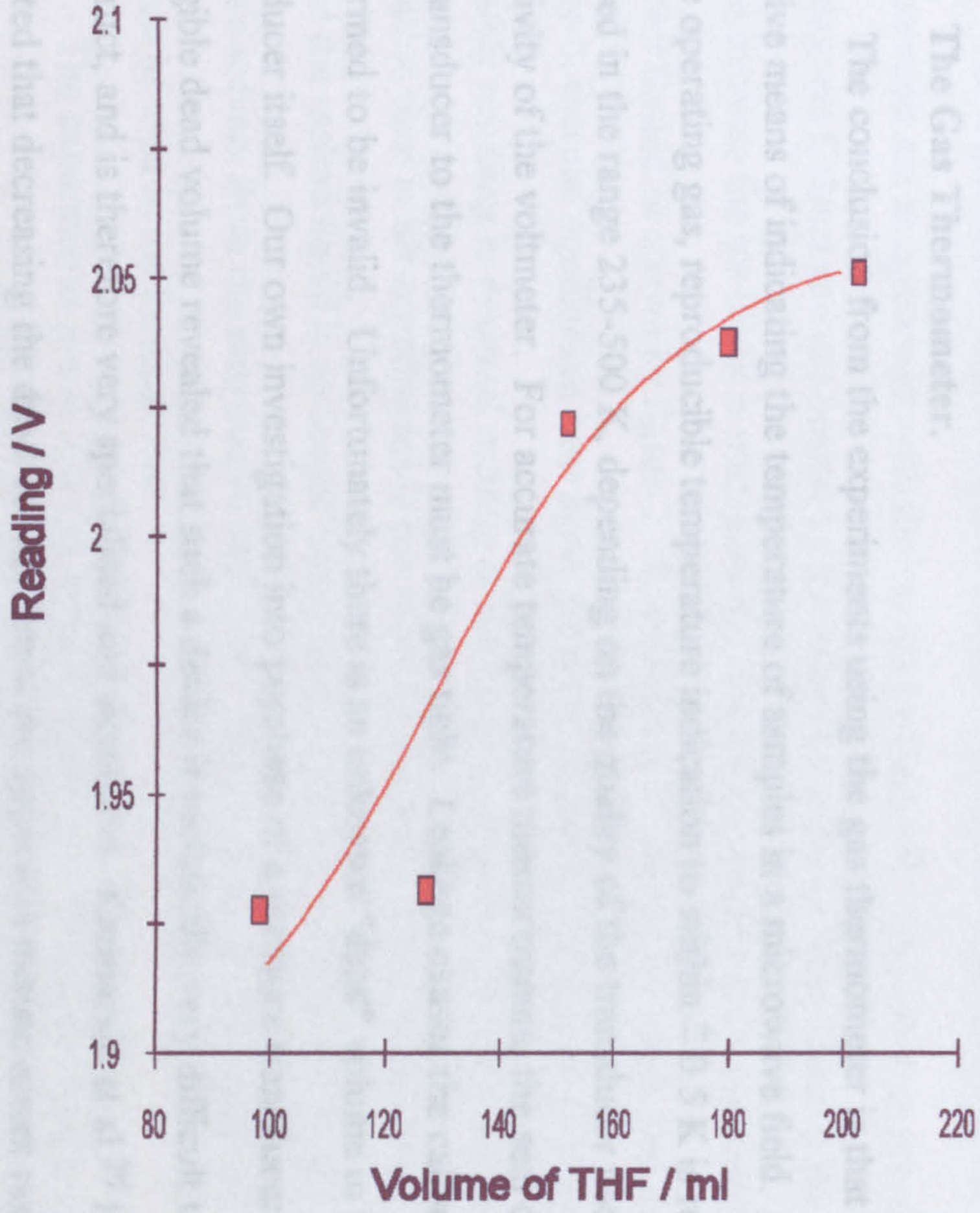

Figure 2.28. Gas thermometer reading against volume of butan-1-ol and THF under microwave irradiation at constant magnetron power output.

2.4. Discussion.

2.4.1. The Gas Thermometer.

The conclusion from the experiments using the gas thermometer is that it is an effective means of indicating the temperature of samples in a microwave field. Using air as the operating gas, reproducible temperature indication to within $\pm$ 0.5 K is readily attained in the range 235-500 K, depending on the quality of the transducer used and the sensitivity of the voltmeter. For accurate temperature measurements, the seal connecting the transducer to the thermometer must be gas tight. Leakage causes the calibration performed to be invalid. Unfortunately there is an unknown "dead" volume in the transducer itself. Our own investigation into purchase of a pressure transducer with a negligible dead volume revealed that such a device is technically very difficult to construct, and is therefore very specialised and expensive. Karmazsin et al.[29] has reported that decreasing the dead volume limits the apparatus measurement range. In equation 2.20 the pressure can be expressed as follows.

$$P = P_o \frac{V_o + V_1 + V_2}{V_o \frac{T_o}{T} + V_1 + V_2} = f(T_1) \qquad (2.20).$$

Where V_o, V_1 and V_2 are the bulb volume, the capillary tube volume and the transducer's dead volume respectively.

Experimental work has shown that calibration and experimental work is best carried out on the same day. Observation has shown that the stem length volume V_1 can be a significant factor. To minimise this effect, attempts have been made to lag the thermometer so that atmospheric changes throughout the day cannot affect the reading. Better results can also be obtained by going to a smaller bore of capillary (0.25 mm) in silica.

The maximum temperature that can be measured by this apparatus is limited to the softening point of the gas thermometer. Pyrex has a softening point around 500°C, so experiments which are to be conducted above this temperature use gas thermometers and vessels which are constructed from silica. The maximum temperature that can be measured is also limited to the pressure transducer's output range.

2.4.2. Irradiation of N,N-dimethylformamide, toluene and 1,2-dichloroethane.

The experiments on microwave radiation on organic solvents using the gas thermometer are in agreement with the results by Gedye[41]. The solvents are not held at zero degrees Celsius and are heated by the microwave field. While there is no melting of the ice because the ice block is transparent to impinging microwaves, the sample is however heated as shown by figure 2.18 and table 2.5. As the ice block and the sample are not in thermal equilibrium heat flows from the relatively hot sample to the ice, thus inevitably resulting in eventual melting of the ice (not observed by Bose as total irradiation time in his experiments is too short (3 minutes)). Once some of the ice has melted the melted liquid is no longer transparent to the microwaves and hence shields the organic solvent from the microwave radiation. This accounts for the observed maxima that can be seen in the heating trace.

The experiments prove that the claim by Bose et al.[52] that the temperature of the reaction can be controlled by placing the reaction vessel in a block of ice is erroneous. Although the ice itself does not absorb microwaves the solvent does as shown in figure 2.18. The synthetic chemistry involved in not questionable, but the claim of temperature control is. The applications of the gas thermometer for indication of temperature have shown that the rate enhancements observed are due to solvent superheating caused by the absorption of microwaves.

2.4.3. Irradiation of solvents.

The results from the experiments using the gas thermometer have shown that the solvents attain a higher temperature under microwave irradiation than under normal conventional heating conditions. The results from inserting the thermocouple into the solvent after irradiation are in good agreement with Neas[9] and Mingos and Baghurst[34] (table 2.7). The readings recorded are lower, but this is probably due to the fact that they were using fibre optic devices, which allowed them constantly to monitor the temperature under microwave conditions. The method of taking temperature by inserting a thermocouple means that several seconds are needed from stopping the microwave power, inserting the thermocouple and recording the temperature.

Table 2.7.
Comparison of temperature attained for different solvents under microwave irradiation.

Solvent	Boiling Point / °C.	Temperature (Neas)[9]	Temperature (Mingos)[34]	Temperature (this work)
Water	100	105	104	104
Methanol	65	84	84	80
Ethanol	78	----	103	97
Propan-2-ol	82	108	100	93
Butan-1-ol	117	138	132	128

2.4.4. Heating of azeotropic mixture under microwave irradiation.

Some of the early results stimulated investigation of the azeotropic mixture of water and ethanol. In the water and ethanol system, the mixture is destablised, relative to the ideal solution. This means that the excess Gibbs function is positive (less favourable to mixing). This is shown in figure 2.29[55].

If we consider figure 2.29, if we start with a liquid of composition a_1 and follow the changes in the vapour, the mixture will boil at a_2 and will have a vapour composition of a'_2. This vapour will condense to give a liquid composition corresponding to a_3. This will give a vapour composition of a'_3 and this will condense to give a_4. As can be seen, the vapour is moving towards equilibrium at b. Thus a azeotropic vapour will emerge. This occurs with ethanol/water which boils unchanged when the water content is 4% and the temperature is 78°C.

Under microwave conditions, it was speculated that we might obtain a different composition in the distillate. Water is not superheated under these conditions because of the surface tension of water. The boiling point composition curve is different under microwave conditions, so we predicted that a new azeotrope will be formed as described schematically in figure 2.30. However, when experiments were conducted under thermal and microwave conditions, the same compositions distilling from the column were obtained (figure 2.20).

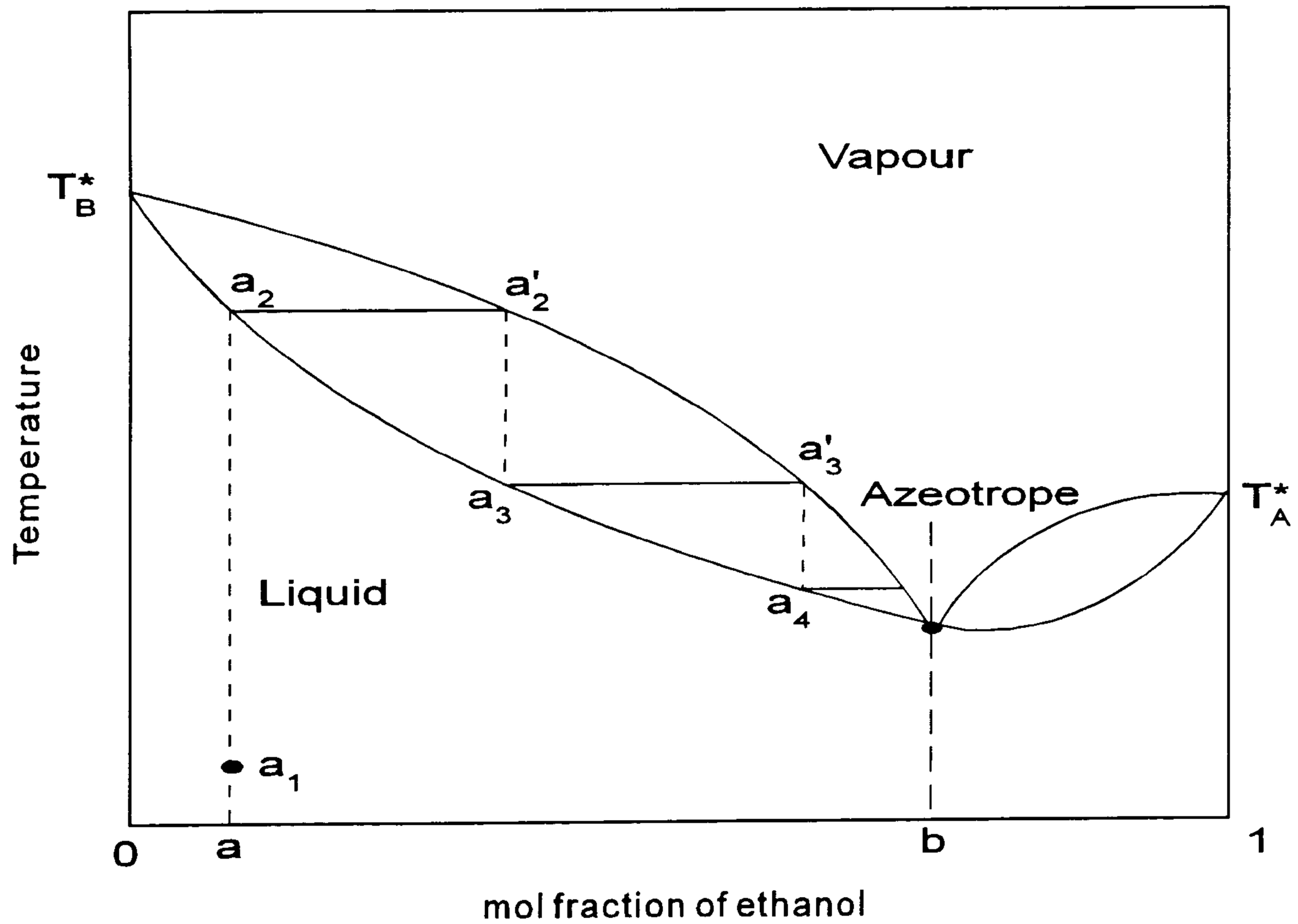

Figure 2.29. A low boiling azeotrope (water:ethanol).

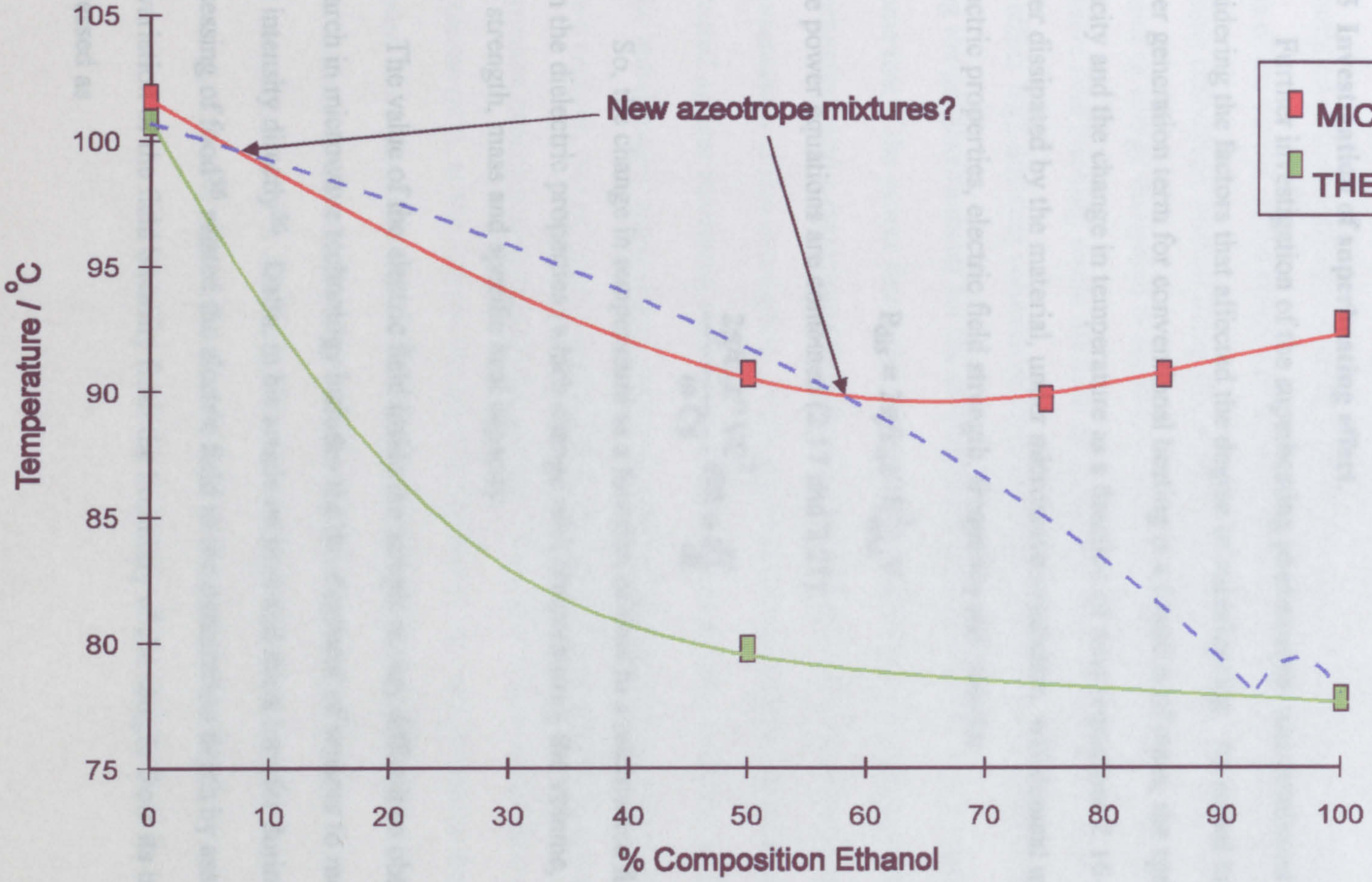

Figure 2.30. Postulated new azeotrope mixyture for ethanol/water.

This is because when the liquid first starts to condense (a'_2 to a_3), as shown in the diagram, the liquid formed will be at the same composition a_3 in both the microwave and thermal experiments. The vapour initially may be boiling at a higher temperature with a different composition, but the changes towards a azeotropic mixture occur in the vapour that rises through the fractionating column. Experiments using higher microwave power outputs show the same results.

2.4.5 Investigation of superheating effect.

Further investigation of the superheating phenomenon was continued by considering the factors that affected the degree of superheating. As stated in 2.1.4.1. the power generation term for conventional heating is a function of mass, the specific heat capacity and the change in temperature as a function of time (equations 2.16-2.18). The power dissipated by the material, under microwave irradiation, will depend upon its dielectric properties, electric field strength, frequency and volume.

$$P_{dis} = 2\pi f \varepsilon_0 \varepsilon'' E^2_{rms} V \qquad (2.21).$$

If the power equations are combined (2.17 and 2.21).

$$\frac{2\pi f \varepsilon_0 \varepsilon'' V E^2_{rms}}{m\ Cp} = \frac{dT}{dt} \qquad (2.22).$$

So, the change in temperature as a function of time in a microwave field depends upon the dielectric properties (which change with temperature), the volume, the electric field strength, mass and specific heat capacity.

The value of the electric field inside the sample is very difficult to obtain. Current research in microwave technology includes the development of sensors to monitor the field intensity directly[56]. Datta, in his article on heat and mass transfer during microwave processing of food[56] related the electric field to the penetration depth by assuming that the variation of the field intensity from the boundary of the sample from its interior is expressed as

$$E = E_0 e^{-\alpha_e x} \qquad (2.23).$$

Where x is the distance inside the sample from the boundary and α_e is related to the dielectric constant by

$$\alpha_c = \frac{1}{2\ Dp} \qquad (2.24).$$

where Dp is the penetration depth.

The extent of superheating must depend on the volume of sample in the cavity. As outlined in the microwave heating section, the microwave energy is reflected by the walls of the cavity. If the volume of the sample is too small, the energy may go through multiple reflections without being absorbed by the sample. Datta[56] has shown how the amount of energy dissipated in the load increases with load volume. This changes the effective field intensity inside the load as its size changes. It was decided to investigate this effect with different volumes of solvent under microwave and thermal conditions, using the gas thermometer for the measurement of temperature. It is reasonable to assume that if the power dissipated increases with volume, so must the extent of superheating, and a maximum would be reached. Figure 2.31 is a schematic representation of this assumption. If the superheated temperature, for a suitable solvent, is plotted against increasing volume, we would expect a curve as shown in figure 2.31. In the initial stages, superheating increases with increasing volume, this is probably due to two reasons, one of which would be that the volume is so small that not all the microwave energy is absorbed by the solvent. The other reason could be a surface area to volume ratio, as the volume increases in the vessel, this would reduce the relative amount of nucleation at the walls. With increasing addition of solvent, the extent of superheating would reduce. This could be due to a lack of power, the load is so large that not all the liquid is absorbing the microwave power. Between these two regions there is a plateau region.

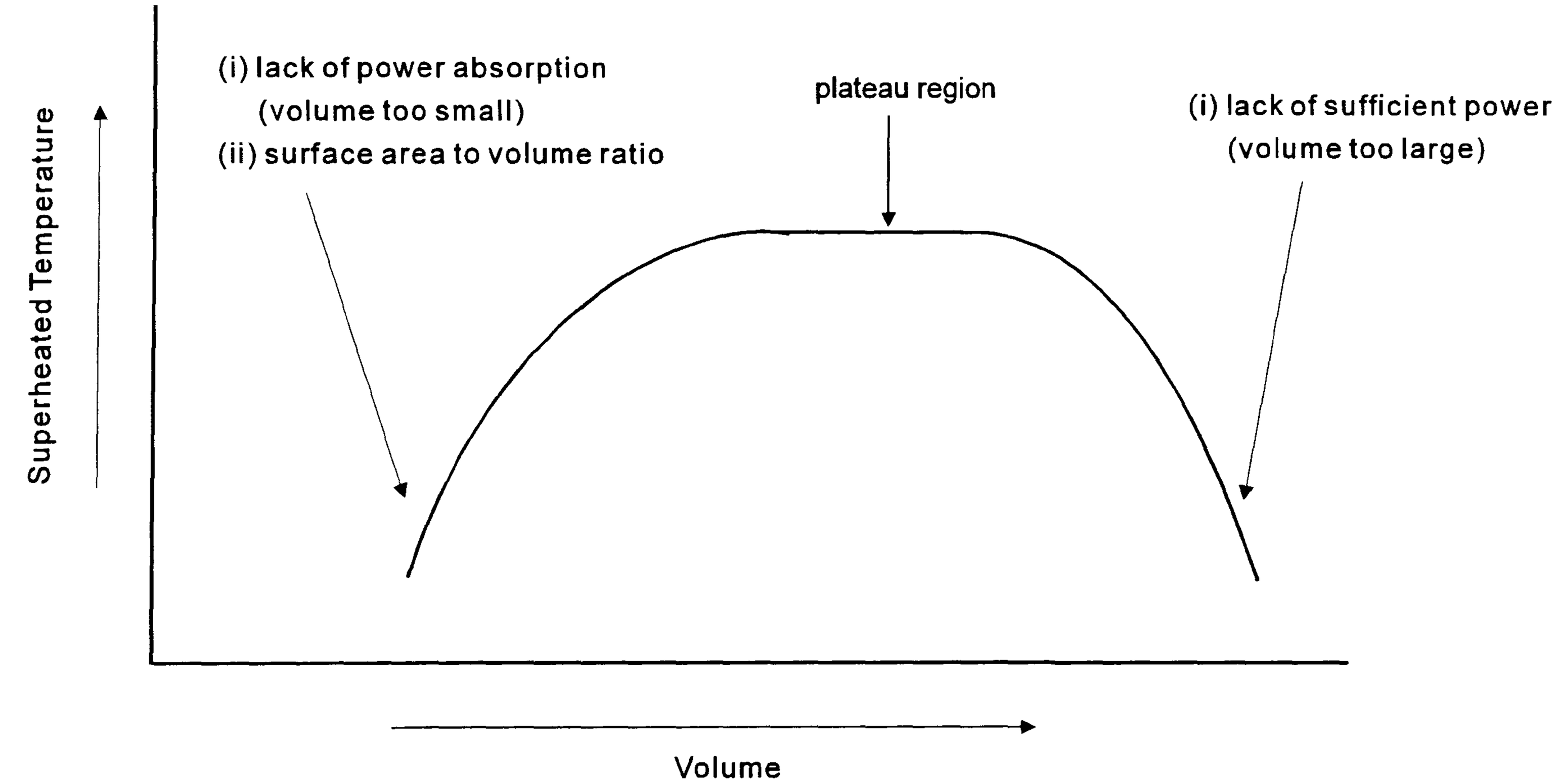

Figure 2.31. Schematic representation of superheating effect with increasing volume.

Another factor could be that the dielectric properties of the solvent change with temperature and so ε" (and hence tan δ) could be significantly reduced at the maxima of the superheating effect. The electric field strength changes with volume so a maximum value for the electric strength could be reached. Since the electric field strength is an important parameter, this increase in superheating should also occur with increasing power, so experiments were conducted to see if this was true.

Table 2.8.
The dielectric properties[8] and calculated penetration depths for the solvents used.

	Frequency		
	3×10^9 Hz	3×10^9 Hz	
Solvent	ε'	ε"	Dp / cm
Ethanol	6.5	1.6	3.1
Propan-1-ol	3.7	2.5	1.5
Butan-1-ol	3.5	1.6	2.3

The penetration depth is an important parameter in microwave heating. Table 2.8 shows the solvents employed and their dielectric properties. The penetration depths were calculated using the above information and equation 2.5. It is interesting how the penetration depth does not follow a trend with the homologous series. Butan-1-ol has a penetration depth between ethanol and propan-1-ol so if penetration depth is an significant factor, then the trend in the results should reflect it. However, it must be emphasised that the penetration depths we calculated using equation 2.5 are rough estimates from the data given on dielectric properties, and temperature has not been taken into account.

As outlined before, superheating occurs in the relative absence of nucleation sites. These sites are usually present on the surface of the vessel. Nucleation will occur at some stage in the microwave experiments and a "bump" will occur. If a new, very clean vessel is used, the number of nucleation sites will be greatly diminished, therefore superheating is more likely to occur. The vessel used in the experiments was not a new vessel. Scratches and indentations are clearly evident on the surface of the vessel, even though the vessel was cleaned thoroughly. It was decided to use this vessel so that superheating under normal thermal conditions would be reduced, so the same vessel was

used for both thermal and microwave experiments. The gas thermometer was also inserted in the liquid in the experiments, thus providing a surface for nucleation. The gas thermometer was not temperature calibrated, instead just the voltage reading was used as a indication of temperature. The higher the reading, the higher temperature that was being produced. Calibration of the thermometer was considered not essential, careful calibration was very time consuming, and this calibration was needed from day to day.

The results from using ethanol as the solvent and placing the gas thermometer in different parts of the liquid agree with the assumption that superheating increases with increasing volume until the plateau is reached as outlined in figure 2.31. Little or no superheating occurs with high surface area to volume ratio containers. The effect increases towards a maximum as the volume increases. But as the volume is increased further, heat is lost from the irradiated area into the central region (i.e. the centre of the bulk solvent does not absorb any microwave radiation at all due to the increased volume). The degree of superheating thus falls off dramatically. The data recorded from the experiments performed on ethanol with the bulb at the top of the liquid show that this maximum is reached quickly and falls with additional volume. The surface of the liquid should be cooler than the bottom or centre because it is losing vapour. The results indicate that the liquid is considerably hotter than the vapour phase, and this effect is not a function of the gas thermometer, as when the bulb was placed in the headspace, it recorded the same reading within experimental conditions.

Superheating was proven using a thermocouple to measure the temperature. Whilst proving that superheating is increasing with volume, the results are inconclusive in that inserting the thermocouple to exactly the same position in the top or centre is not very irreproducible. Time was needed to allow the thermocouple to heat up and record the temperature, and in certain circumstances the introduction of the thermocouple into the superheated liquid causes eruption of the liquid as explained by Buffler and Lindestrom[57]. The liquid boils rapidly and vigorously, erupting up through the condenser, this occurred with higher power levels and higher volumes.

The microwave power could be altered in the experiments by incorporation of a Variac into the circuitry of the microwave oven. The power consumed by a water load

as a function of Variac voltage shows that the output is not linear. Power consumed by the liquid is preferred since power dissipated depends upon the volume and dielectric properties of the liquid used. Varying the Variac voltage alters the intensity of microwave radiation generated. The results show that the degree of superheating is increasing with the applied microwave power. This is because the effective radiation experienced by ethanol increases even though the penetration depth remains constant. The degree of superheating increases with increasing microwave power and does not fall as dramatically with volume.

The experiments using propan-1-ol agree with the hypothesis. Propan-1-ol is definitively being superheated (20°C above its normal boiling point). Superheating increases with increasing volume, but there is an distinct maximum at 150 ml of solvent. This maximum occurs at a lower volume than with using ethanol as the solvent. This is due to the smaller penetration depth for propan-1-ol compared with ethanol (table 2.8). As the volume is increased not all the microwave power is being absorbed by propan-1-ol so the temperature falls. Increasing the microwave power increases the degree of superheating.

When butan-1-ol is used as the solvent, experiments to investigate the influence of power on superheating are too difficult to conduct. Low microwave power is insufficient to heat butan-1-ol so that it is boiling under reflux conditions, while higher power levels cause a too vigorous heating effect. Experiments were conducted at one power level with the bulb inserted in different positions. The results agree with calculated values for penetration depth. Butan-1-ol has a penetration depth that is between ethanol and propan-1-ol. When the gas thermometer is placed at the bottom of the flask, the extent of superheating rises with increasing volume, until a maximum is obtained around 175 ml. With propan-1-ol, the same trend is observed but with a lower volume, and with ethanol, the trend is continued but a larger volume is needed. There is a significant increase in the reading from going from 125 ml of butan-1-ol to 150 ml. This suggests that the sample volume (125 ml) is too small a load for absorption of microwaves.

Tetrahydrafuran is known to superheat in excess of 20°C above its boiling point under microwave irradiation[9, 34]. But there are problems in using varying microwave power. Low power levels result in the solvent not being heated to its boiling point, and higher levels cause a vigorous boiling. The results show that superheating is rising with increased volume; again there is a significant increase in the reading from 125 ml to 150 ml of THF.

2.4.6. Conclusions from this work.

The conclusions from these series of experiments are that the rate enhancements observed, under microwave conditions, by ourselves and other workers could be due to superheating. The parameters that dictate the extent of superheating are the quality of reaction container (e.g. surface of glassware), the surface tension of the solvent used, power, volume and the electric field strength. The extent of superheating is also dependent on the surface area to volume ratio. Experiments have clearly shown that superheating increases with increasing volume, and with increasing power. However, above a certain power output and a certain volume, the liquid can boil vigorously and erupt. Although superheating is shown to increase with microwave power, it is misleading to state that the power levels were constant throughout these studies. It is difficult to measure absolute power dissipation because microwave power dissipation is linearly dependent on the magnitude of ε''. It would be more accurate to state that the power setting, or power emitted by the microwave source is constant throughout the studies.

This information could be extremely useful for synthetic chemists. Optimisation of volume and power output for different solvents could prove extremely valuable because increasing the temperature at which a chemical reaction occurs will increase the rate of reaction. It is however, feasible that reactions under microwave radiation could produce different products when compared to conventional techniques. Since the temperature is increased by microwave radiation, it is possible that this increased temperature could exceed the activation energy required for a new reaction which was not possible at the normal reflux temperature.

2.5. References.

1. Jolly W. L., "The Synthesis and Characterisation of Inorganic Compounds", Prentice Hall, (1970).
2. Debye P., "Polar Molecules", Chemical Catalog, New York, (1929).
3. Frohlich H., "Theory of Dielectrics", 2nd edn., Oxford University Press. London, (1958).
4. Daniel V., "Dielectric Relaxation", Academic Press, New York, (1967).
5. Cole K. S. and Cole R. H., J. Chem. Phys., **9**, 341, (1941).
6. Metaxas A. C. and Meredith R. J., "Industrial Microwave Heating", Peter Peregrinus Ltd., (1983).
7. Neas E. D. and Collins M. J., in "Introduction to Microwave Sample Preparation", H. M. Kingston and L. S. Jassie (Eds.), American Chemical Society, 7, (1988).
8. Mingos D. M. P. and Baghurst D. R., Chem. Soc. Rev., **20**, 1, (1991).
9. Neas E. D., "Basic Theoretical Concepts in Microwave Chemistry", Lecture presented at the first World Congress on Microwave Chemistry, (1992).
10. Boocher C. J. F., "Theory of Electric Polarisation", Elsevier, Amsterdam, (1952).
11. Meakins R. J., Trans. Faraday Soc., **51**, 953, (1955).
12. Smyth C.P., "Dielectric Behavoiur and Structure", McGraw-Hill, New York, (1955).
13. Meakins R. J., Trans. Phys. Soc., **52**, 320, (1956).
14. Von Hippel A. R., "Dielectric Materials and Applications", MIT Press, (1954).
15. Wagner K. W., Arch. Elekrotech, **2**, 371, (1914).
16. Meek T. T., J. Mat. Sci. Lett., **6**, 638, (1987).
17. Huang H. F., J. Microwave Power, **11**, 305, (1976).
18. Kenkre V. M., Skala L., Weiser M. W., and Katz J. D., J. Mat. Sci., **26**, 2483, (1991).
19. Ford J., and Pei D., J. Microwave Power, **2**, 61, (1967).

20. Tinga W. R., "Microwave dielectric constants of metal oxides Part 1", Electromagnetic Energy Reviews, **1**, 2, (1988).

21. Tinga W. R., "Microwave dielectric constants of metal oxides Part 2", Electromagnetic Energy Reviews, **2**, 1, (1989).

22. Turner I., and Jolly P., J. Microwave Power and Electromagnetic Energy, **25**, 211, (1990).

23. Kingston H. M., and Jassie L. B., Anal. Chem., **58**, 2534, (1986).

24. Bacci M., Bini M., Checcucci A., Ignesti A., Millanta L., Rubino N., and Vanni R., Proc. 14th Microwave Power Symp., Monaco, p42, (1979).

25. Bacci M., Bini M., Checcucci A., Ignesti A., Millanta L., Rubino N., and Vanni R., J. Chem. Soc. Faraday Trans., 77, 1503, (1981).

26. Checcucci A., Olmi R., and Vanni R., J. Microwave Power, **20**, 161, (1985).

27. Mingos D. M. P., and Baghurst D. R., J. British Ceramics Trans., **91**, 124, (1992).

28. Walkiewicz J. W., Kazonich G., and McGill S. L., Minerals and Metallurgical Processing, **2**, 39, (1988).

29. Karmazsin E., Barhoumi R., and Satre P. J., J. Thermal Analysis, **29**, 1269, (1984).

30. Baghurst D. R., and Mingos D. M. P., J. Chem. Soc. Dalton Trans., 7, 1151, (1992).

31. Mincy D. W., Williams R. C., Giglio J. J., Graves G. A., and Pacella A. J., Analytica Chica Acta., **264**, 97, (1992).

32. Wickershiem K. A., Proc. SPIE, **713**, 150, (1986).

33. Papoutis D., Photonics Spectra, 5360, March, (1984).

34. Baghurst D. R., and Mingos D. M. P., J. Chem. Soc. Chem. Comm., **9**, 674, (1992).

35. Jow J., Delong J. D., and Hawley M. C., Sample Quarterly., 46, January, (1989).

36. Prosetya H., and Datta A., J. Microwave Power and Electromagnetic Energy, **26**, 4, (1991).

37. Bond G., Moyes R. B., Pollington S. D., and Whan D. A., Meas. Sci. Technol., **2**, 571, (1991).

38. Abramovoitch R. A., Organic Preparations and Procedures Int., **23**, 683, (1991).

39. Vanderhoff J. W., U. S. Patent, No. **3, 432,413,** (1969).

40. Giguere R. J., Bray T. L., and Duncan S. M., Tet. Letts., **27**, 4945, (1986).

41. Gedye R. N., Smith F. E., and Westway K. C., Can. J. Chem., **66**, 17, (1988).

42. Alloum A. B., Labiad B., and Villemin D., J. Chem. Soc. Chem. Comm., **16**, 386, (1989).

43. Gutierrez E., Loupy A., Bram G., and Ruiz-Hitzky E., Tet. Letts., **30**, 945, (1989).

44 Baghurst D. R., Chippindale A. M., and Mingos D. M. P., Nature, **332**, 311, (1988).

45. Pollington S. D., Bond G., Moyes R. B., Whan D. A., Candlin J. P., and Jennings J. R., J. Org. Chem., **56**, 1313, (1991).

46. Jahnagen E. G. E., Lentz R. R., Pesheck P. S., and Holt Sackett P., J. Org. Chem. **55**, 3406, (1990).

47. Raner K. D., Straus C. R., Vyskoc F., and Mokbel L., J. Org. Chem., **58**, 950, (1993).

48. Sun W-C., Guy P.M., Jahngen J. H., Rossomando E. F., and Jahangen G. E., J. Org. Chem., **53**, 4414, (1988).

49. Armstrong, B. F., and Neas, E. D., Separation Sci. and Tech., **25**, 2007, (1990).

50. Gedye R. N., Rank W., and Westaway K. C., Can. J. Chem., **69**, 706, (1991).

51. Bond G., Moyes R. B., Pollington S. D., and Whan D. A., Chemistry and Industry, **18**, 686, (1991).

52. Bose A. K., Manhas M. S., Ghosh K., Raju V. S., Tabei K., and Urbanczyk-Lipkowska Z., Heterocycles, **30**, 741, (1990).

53. Bose A. K., Manhas M. S., Ghosh M., Shah M., Raju V. S., Bari S. S., Newaz S. N., Banik B. K., Chaudhary A. G., and Barakat K. J., J. Org. Chem., **56**, 6968, (1991).

54. Banik B. K., Manhas M. S., Kaluza Z., Barakat K. J., and Bose A. K., Tet Letts., **33**, 3603, (1992).

55. Atkins P. W., "Physical Chemistry", 3rd edition, Oxford University Press, 180, (1986).

56. Datta A., Chemical Engineering Progress, p47, June, (1990).

57. Buffler C. R., and Lindstrom T., Microwave World, **9**, 10, (1988).

Chapter Three.

Toluene Disproportionation.

3.1. Introduction.

3.1.1. BTX Products.

3.1.1.1. Industrial Requirements for BTX.

Benzene, toluene and xylenes (BTX) are important aromatic hydrocarbons in the petrochemical industry. Inoue and Oliver[1] have extensively investigated the role of BTX products in the petrochemical industry and have summarised a large body of work on uses, viability and synthesis of BTX compounds. The major use of these compounds is in the polymer and plastics industry. They are important precursors of many of the polymers used in modern society. However, BTX production in 1985 for Western Europe, the United States and Japan, varied between 60 and 70% of installed capacity. The consequences of this are that, except in third world countries, there is unlikely to be significant capacity addition and because of the excess capacity, the market for aromatic compounds has become very competitive with small profit margins[2].

Before the end of the 1960's the major demand in BTX products was for benzene. Benzene is used to make styrene, cyclohexane and phenols. Styrene is used in rubber, polymers and copolymer plastics. Cyclohexane is used in the production of nylon 6 and nylon 66. Phenol is used in resins and in minor capacities in detergents, dyes, pesticides and in antioxidants. Toluene is mainly used for the production of benzene, however, other uses include explosive, diisocyanates, solvents and in unleaded petrol. Since the late 1960's, there has been increasing demand for polyester products, of which xylenes are used as precursors. Each isomer of xylene is restricted to one major use, orthoxylene is used in resins by being converted to phthalic anhydride, there is little demand for metaxylene except in resins and paraxylene is used in the production of polyester fibres and films by conversion to terephthalic acid.

3.1.1.2. Extraction of BTX compounds.

Aromatic production is mainly derived from petroleum, by pyrolysis gasoline supplemented by catalytic reforming. Recovery of BTX is by liquid extraction or distillation.

3.1.2. Processes used for production of BTX compounds.

Since the 1960's there have been changes in the demand for BTX products. Toluene was produced in surplus, so it was converted to benzene and xylenes. Now, it is in more demand due to its use in high octane unleaded petrol. The demand in the modern industrialised world is to make better use of technology for more flexible production of BTX products. Apart from the disproportionation of toluene, there are two other significant processes for production of BTX compounds, the Xylenes Plus Process, and the Tatoray Process[1,2].

3.1.2.1. The Xylenes Plus Process.

This process has been developed by Sinclair Oil and used by Arco Technology, Inc. a subsidiary of the Atlantic Richfield Company. The process converts toluene and C_9 aromatics to benzene and C_8 aromatics by disproportionation and transalkylation. The catalyst used in this process is a noble metal, which is continually regenerated by use of a moving bed type reactor. Hydrogen is not used as a feedstock, so costs are reduced. Yields of over 95% of the theoretical molar yields are obtained. The yield of C_8 aromatics depends on the mixture of toluene and C_9 aromatics, but typically ranges from 55 to 84 weight percent of fresh feed while benzene ranges from 40 to 10 weight percent.

3.1.2.2. The Tatoray Process.

This process has been developed by Toray. The process requires a hydrogen atmosphere and a hydrogen recycle compressor is required. The gas from the compressor is combined with toluene and C_9 aromatics, which are vapourised and superheated and passed through the catalyst bed. The products are cooled, condensed and reprocessed by BTX fractionation.

3.1.3. Disproportionation of toluene.

Toluene disproportionation is performed on an industrial scale by ICI Chemicals and Polymers Division. The research and development for the process is carried out by the Hydrocarbons Research Group at Wilton. ICI North Tees Works is one of the world's largest with a capacity of 800 000 tonnes per year of aromatic products[3]. The plant has several major processes of which toluene disproportionation is one. The main products are benzene, toluene, xylenes and ethylbenzene and BTX products are converted on site. Benzene is used for making ethylbenzene for styrene plastics, cumene for phenol for thermoplastics, cyclohexane for nylon and nitrobenzene for aniline dyes and polyurethane. Xylenes are used for paraxylene (for polyester) and for solvents. Toluene is used for conversion to benzene, solvents and polyurethane foam. The paraxylene plant is at Wilton, and produces 330 000 tonnes per year of paraxylene which is mostly converted to pure terephthalic acid (PTA).

3.1.3.1. Chemistry.

Disproportionation of toluene is defined as the conversion of two moles of toluene to equimolar amounts of benzene and xylene isomers as shown in scheme 3.1.

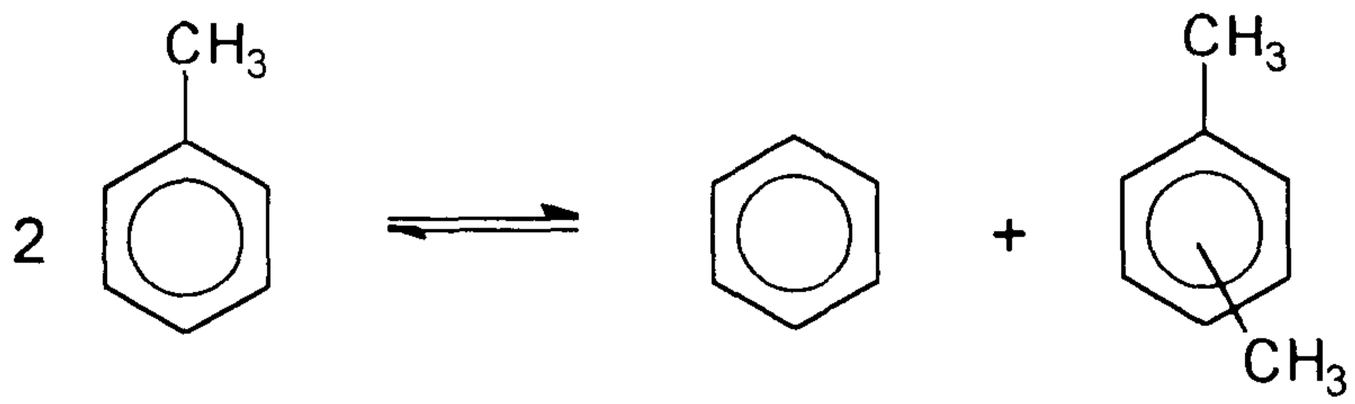

Scheme 3.1.
Disproportionation of toluene to give benzene and xylenes.

The reaction is reversible. Pitzer and Scott[4] have studied equilibrium constants using catalysts of aluminium bromide and anhydrous hydrogen bromide at 50°C. They calculated the equilibrium constant K (equation 3.1) to be in the range 0.15 to 0.22. The equilbrium constant increases with temperature and does not differ significantly between the vapour to liquid state.

$$K_N = \frac{N_{benzene}\, N_{xylene}}{N^2_{toluene}} \qquad (3.1).$$

Where N = mol fraction.

Hastings and Nicholson[5] calculated the theoretical equilibrium concentrations at various temperatures as shown in table 3.1.

Table 3.1.
Equilibrium concentrations of toluene disproportionation (mol%).

Temperature / K	Benzene	Toluene	Xylenes	Trimethyl-benzenes
300	30.0	44.0	22.2	3.6
400	30.2	43.1	22.7	3.8
500	31.2	42.2	22.6	3.7
600	31.5	41.7	22.7	3.8
700	31.9	41.1	22.7	3.9
800	32.0	40.6	23.1	3.9
900	32.3	40.6	22.7	3.9
1000	32.4	40.3	22.8	4.0

Oliver and Inoue[1] have summarised the early work on kinetics studies of the catalysed reaction but there are several conflicting interpretations of the data. One interpretation is that the reaction is surface controlled and can be well represented by the Langmiur-Hinshelwood equation. Physical steps that can be involved on solid catalysts have been found to be insignificant in determining the rate of reaction[6]. The chemical steps involved are

1. Adsorption on the solid surface
2. Chemical reaction on the surface of the catalyst.
3. Desorption of the product from the surface of the catalyst

The rate is also dependent on the partial pressure of toluene and the forward reactions are second order with respect to toluene[6-9]. Other reports have concluded that the forward reaction is first order with respect to toluene[10-11].

3.1.3.2. Mechanism.

The major studies on the mechanism of alkylation reactions catalysed by Friedel-Crafts catalysts were conducted in the 1950's [12-14]. The different types of complexes formed by electrophilic reagents with aromatic hydrocarbons have been classified as π- and σ-complexes. σ-Complexes are more stable and are defined as a complex formed when the acceptor group is linked by a σ-bond to a particular carbon of the aromatic ring, whereas π-complexes are less stable and are defined as complexes having a weak interaction between the electrophilic atom or group and the π-electrons of the aromatic system. The accepted mechanism was first proposed by McCauley and Lien[15] using HF and BF_3.

$$Ar + HF \Leftrightarrow Ar{\bullet}H^+ + F^- \qquad (3.2).$$

$$F^- + BF_3 \Leftrightarrow BF_4 \qquad (3.3).$$

$$Ar + HF + BF_3 \Rightarrow Ar{\bullet}H^+ + BF_4^- \qquad (3.4).$$

The first step in their mechanism is the addition of a proton (from the acid catalyst) to the toluene at the ring carbon atom which holds the alkyl group forming a σ-complex as shown in scheme 3.2.

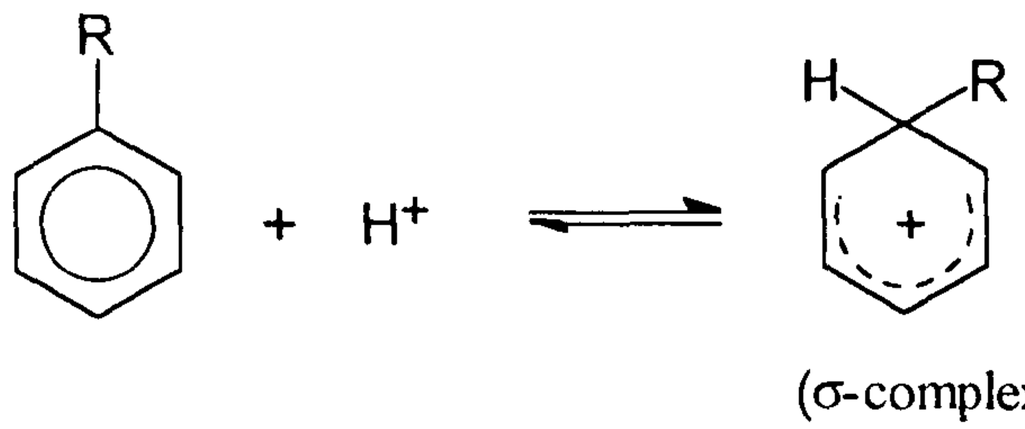

(σ-complex)

Scheme 3.2
Addition of proton to toluene at the ring carbon holding the alkyl group.

The next step in the reaction is the reaction between the σ-complex and a neutral aromatic molecule as shown in scheme 3.3. This mechanism is postulated for disproportionation of toluene at low temperatures. At higher temperatures side reactions occur due to the aromatic cation dissociating into a neutral aromatic and an alkyl carbonium ion. The carbonium ion can then react further by isomerisation, transalkylation, polymerisation and hydride ion abstraction.

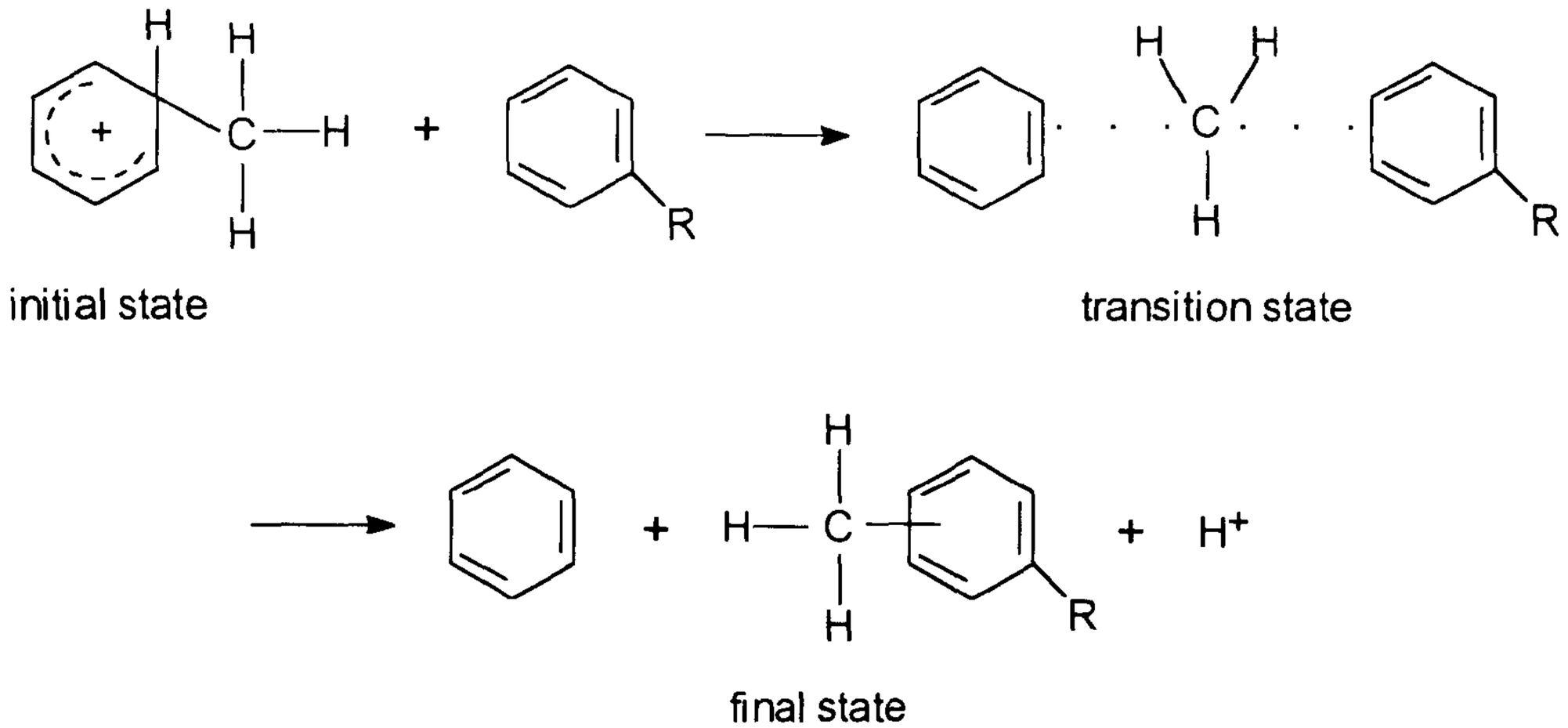

Scheme 3.3.
Reaction between the σ-complex and a neutral aromatic molecule (toluene).

3.1.3.3. Catalysts used for toluene disproportionation.

Research on toluene disproportionation catalysis to produce xylenes has been extensive. The catalyst types used for these reactions can be grouped into three categories, namely Friedel Crafts[4, 12-17], silica-alumina[18-19] and zeolite types[20-24]. A summary of research on these catalysts with the various conditions employed has been conducted by Inoue and Oliver[1].

In general zeolites are shown to be the superior catalysts. Amorphous acid catalysts show a low selectivity for disproportionation and are less active. Yashima et al.[25] observed that toluene is converted in high yield to benzene and xylenes over hydrogen mordenite. However, hydrogen mordenite fouled rapidly and activity disappeared after a few hours on stream. The relatively new zeolite type ZSM-5 has been found to be an excellent catalyst for toluene disproportionation[26-28]. However, mordenite is still an important industrial catalyst since it can convert the bulky trimethylbenzenes to xylenes[29-31]. A mechanism for toluene disproportionation over zeolite catalyst has been proposed by Kaeding et al.[26] based on the mechanism proposed by McCauley and Lien[15] (scheme 3.4).

This mechanism is based on the fact that zeolite catalysts, which are effective for alkylation or transalkylation, contain strong protonic acid sites. The proton from the acid form of the zeolite, H^+Zeol^- attacks toluene at the carbon atom holding the alkyl group. This has the effect of weakening the carbon methyl bond and thus transferring it

to a second toluene molecule. This reaction occurs within the zeolite pores so, due to steric hindrance, the para- position is most likely to be attacked. Transfer of a proton from the protonated xylene back to the zeolite regenerates the acid site. The mechanism is consistent with the accumulation of information developed from studies of Friedel-Crafts catalysts, the acidic properties of zeolites and the product distribution from the reaction.

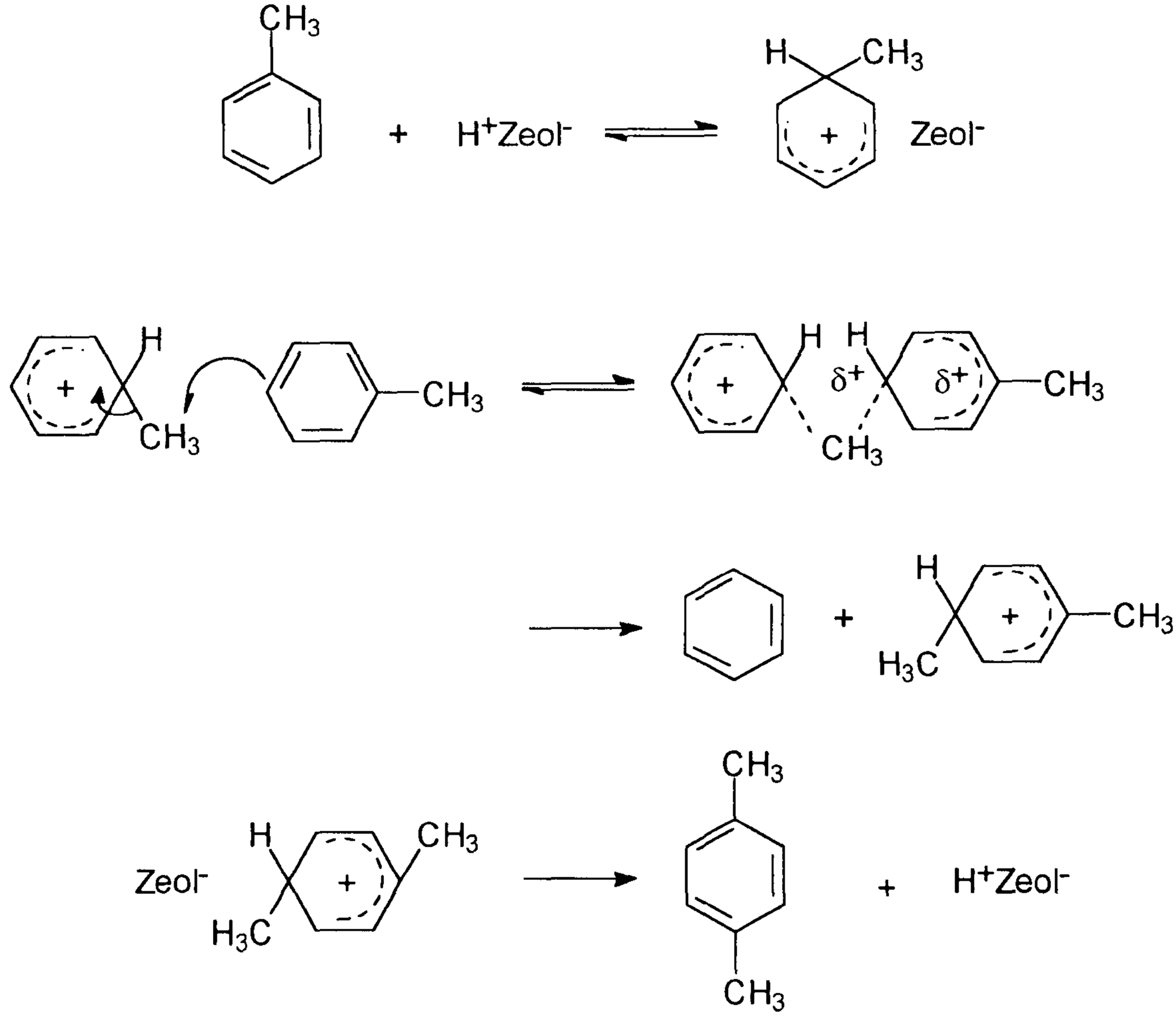

Scheme 3.4.
Mechanism for toluene disproportionation over a zeolite catalyst[26].

Benzene and paraxylene are produced, but isomerisation of paraxylene occurs to give the mixture of the three xylenes.

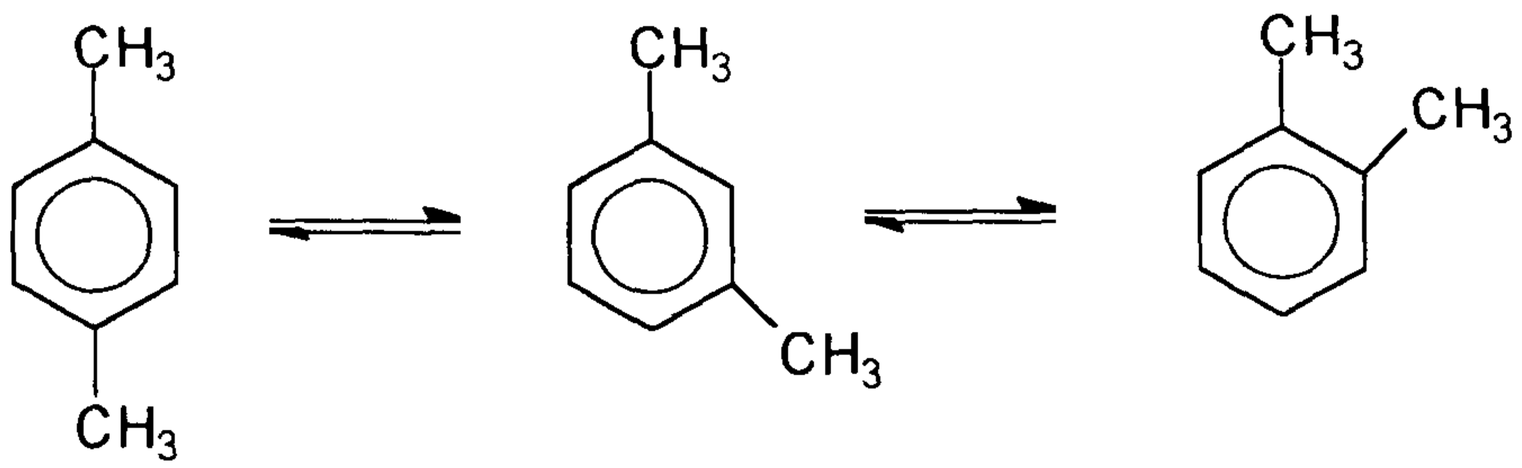

paraxylene metaxylene orthoxylene

Scheme 3.5.
Isomerisation of xylenes.

3.1.3.4. Production of Paraxylene.

In the disproportionation of toluene, the products are benzene and a mixture of xylenes; the equilibrium distribution of the isomers is 22% orthoxylene, 54% metaxylene and 24% paraxylene according to Allen and Yats[32].

The isomer paraxylene is the required product to make 1,4-benzenedicarboxylic (terephthalic) acid. The terephthalic acid is produced mainly by the liquid phase oxidation of paraxylene in ethanoic acid with a cobalt/manganese catalyst. Most companies convert the almost insoluble, high-melting point diacid to the dimethyl ester for purification.

The Hercules-Witten process is shown in scheme 3.6.

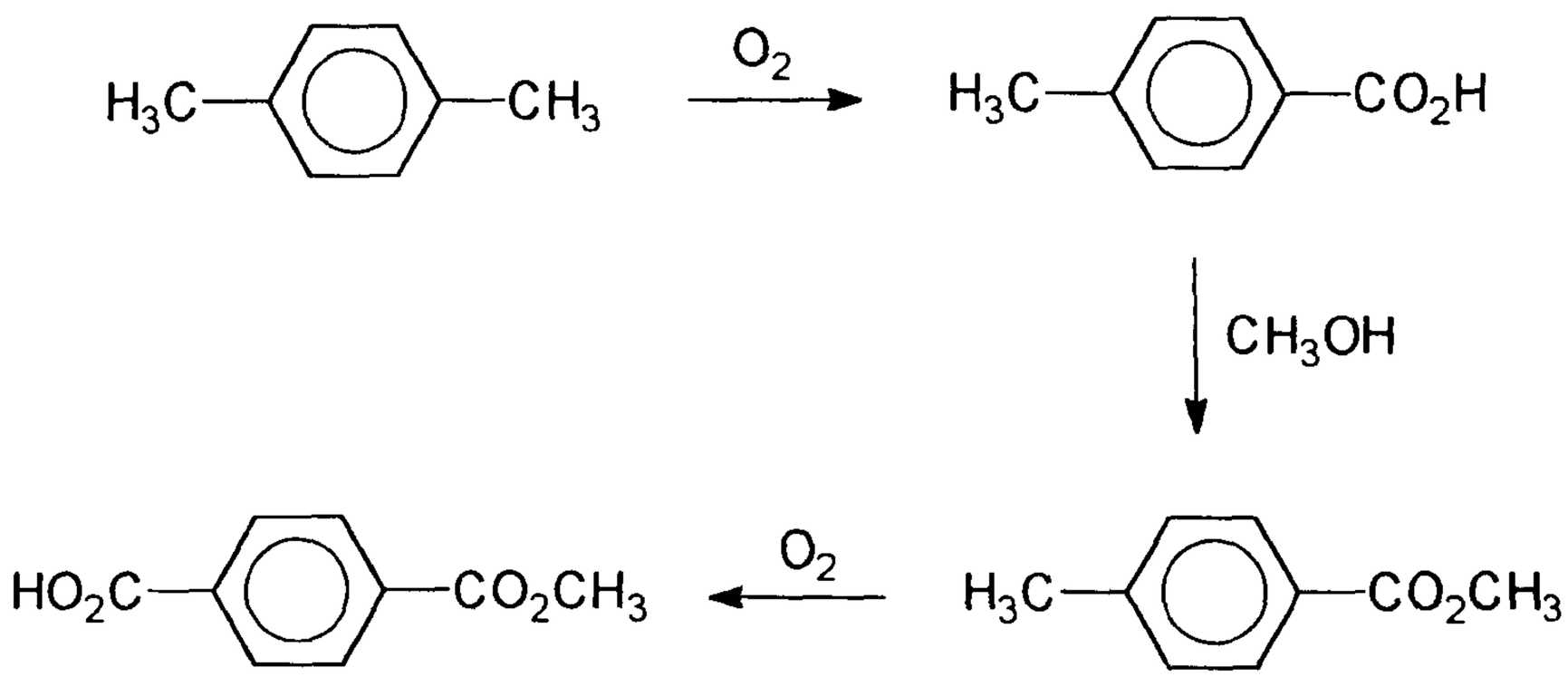

Scheme 3.6.
The Hercules-Witten process.

In this process paraxylene is oxidised without a solvent to 4-methylbenzoic (p-toluic) acid, which is esterified before further oxidation as shown in scheme 3.6. The final esterification again gives dimethyl terephthalate for purification. The major end use of pure terephthalic acid (PTA) is the production of polyesters for which ICI was one of the pioneers[33]. PTA capacity at Wilton has been regularly expanded and paraxylene quality has been upgraded to 99.8%. 80% of ICI 's PTA is exported, half of which is outside Europe, particularly to the Far East. The production of paraxylene yields 330 000 tonnes per year, most of which is converted to pure terephthalic acid (PTA) on site. The two PTA plants have a combined capacity of around 500 000 tonnes per year.

3.1.3.5. Current research in disproportionation of toluene.

Current research in toluene disproportionation studies is to develop catalysts and processes which are highly selective to paraxylene, have constant activity and longer lifetime for the catalyst. Kinetic studies on disproportionation of toluene by solid acid catalysts[34], hydrogen mordenite[7,9] and ZSM-5[10] have been carried out. The conclusion from these studies has revealed that hydrocarbon reactions occur on Bronsted acid sites. Strong acid sites are active for toluene disproportionation. There is also evidence from Yashima et al.[22] that these are responsible for paraxylene selectivity although a mechanism has not been proposed. Bhat[35] contradicts this proposal in his pulse microreactor studies he has concluded that paraxylene selectivity is due to shape selective inhibition. A mathematical study on paraxylene has been performed by Wei[36], who has concluded that selectivity to paraxylene increases with decreasing conversion.

This has led to the development of Mobil's (STDP) "Selective Toluene Disproportionation" process[37-40]. Kaeding et al.[26] and Meshram[40] have investigated toluene disproportionation over ZSM-5 zeolites which were modified with phosphorus, boron or magnesium. They propose that incorporation of these elements into the zeolite framework reduces the dimensions of pore openings and channels sufficiently to favour formation and outward diffusion of paraxylene. However, this results in lower conversion. There have been patents relating to disproportionation which deal principally with changes in catalyst formulation. The objective of the process is high

selectivity to paraxylene. A recent report[41] has details of a selective toluene disproportionation process, based on Mobil's ZSM-5, which is in operation at Enichem Anic's refinery in Gelta, Italy. The temperature used was 455°C, with a hydrogen to hydrocarbon ratio of 3:1. The catalyst used was modified ZSM-5. The optimum toluene conversion was 30% with a selectivity to paraxylene of 82% (% paraxylene in total xylenes). Paraxylene selectivity was shown to increase with increasing temperature and decreasing conversion of toluene. The process was run for 500 days, whereupon the catalyst was regenerated and then ran for 100 days to confirm that regeneration was successful.

Research on mordenite catalysts for disproportionation of toluene has been conducted on mordenites which have been modified. Aluminium deficient mordenites have been prepared and have been shown to be more active than the parent mordenite[42]. Incorporation of modifiers such as nickel into the mordenite has been observed to increase activity[43-44]. Manoiu et al.[45] have studied disproportionation of toluene, diluted by different amounts of metaxylene, for the purpose of determining if disproportionation can be carried out with the simultaneous isomerisation of metaxylene.

Ugina et al.[46] and Beltrame et al.[47] have investigated the effects of crystal size, silicon-to-aluminium ratio and activation methods. The conclusions from their work were that, although paraxylene formation was slightly favoured by increasing the crystal size, the selectivity was not enhanced. Increasing the aluminium content enhanced the activity of the catalyst but the selectivity to disproportionation was decreased. The explanation given is that increasing the aluminium content leads to the formation of superacid sites which promote dealkylation of toluene.

The effect of the carrier gas on the reaction has also been studied[6,48-49]. These studies have shown that the degree of conversion is in the order $Ar>N_2>He>H_2$, but the lifetime of the catalyst is enhanced by hydrogen. The effect of poisoning catalysts with such substances as sulphur or CFCs has also been studied[44, 50-51],and in some cases this poisoning led to greatly enhanced lifetimes compared with the untreated catalyst.

3.1.4. The nature of this study.

Disproportionation of toluene was the reaction chosen for this study for the comparison of microwave irradiation with normal thermal heating. It was hoped that microwave irradiation would have a beneficial effect on the reaction, increasing paraxylene enhancement whilst maintaining a high conversion. A detailed careful comparison, between thermal and microwave effects, was required so a reactor and an analysis system was designed and constructed for this purpose. The catalysts chosen for the study were mordenite and ZSM-5. The first experiment was to heat mordenite under microwave irradiation in a domestic microwave oven. The temperature attained was only 240°C even under full power (650 W), so all future microwave experiments were carried out using the single mode cavity device.

The chemicals used were HZSM-5 (BDH) and hydrogen mordenite (BDH and Strem Chemicals). No modification of the catalysts was carried out. The toluene used was analytical grade also obtained from BDH chemicals. The hydrogen used was high purity hydrogen obtained from Energas Industrial Gases.

3.2. Experimental.

3.2.1. Apparatus.

3.2.1.1. The reactor.

One of the primary considerations when designing the reactor was that the same reactor should be usable in both a conventionally heated and in a microwave irradiated environment. This is because subtle changes in rate and product distribution can arise from changing the reactor design. The programme of work required careful comparisons to be made between thermally and microwave activated reactions, hence the need to use the same reactor in both sets of experiments.

A schematic diagram of the reactor is shown in figure 3.1. The reactor was constructed from silica. The reactant stream, comprising toluene vapour in a carrier gas, entered via the upper arm of the reactor, passed through the catalyst bed, and the products exited the reactor via the second arm into a gas chromatograph.

The temperature of the catalyst bed was monitored in three ways, either by the use of a thermocouple or by using a gas thermometer with its bulb in the centre of the reactor or by infrared pyrometry. The gas thermometer was calibrated against the thermocouple reading when the reactor was placed within a conventional furnace. During microwave irradiation, where the use of a thermocouple is not possible, the gas thermometer or an infra-red pyrometer was used to record the temperature of the catalyst bed.

3.2.1.2. Low pressure equipment for toluene disproportionation.

Figure 3.2 shows the apparatus used for the disproportionation of toluene under atmospheric pressure conditions. The reactor was heated by either, a conventional furnace controlled by a Gulton West MC30/3A device, or within a microwave single mode cavity. A "bubbler" containing toluene in a bath of ice and water saturated the carrier gas with toluene vapour and supplied toluene at a vapour pressure of 7.1 torr in a carrier gas stream.

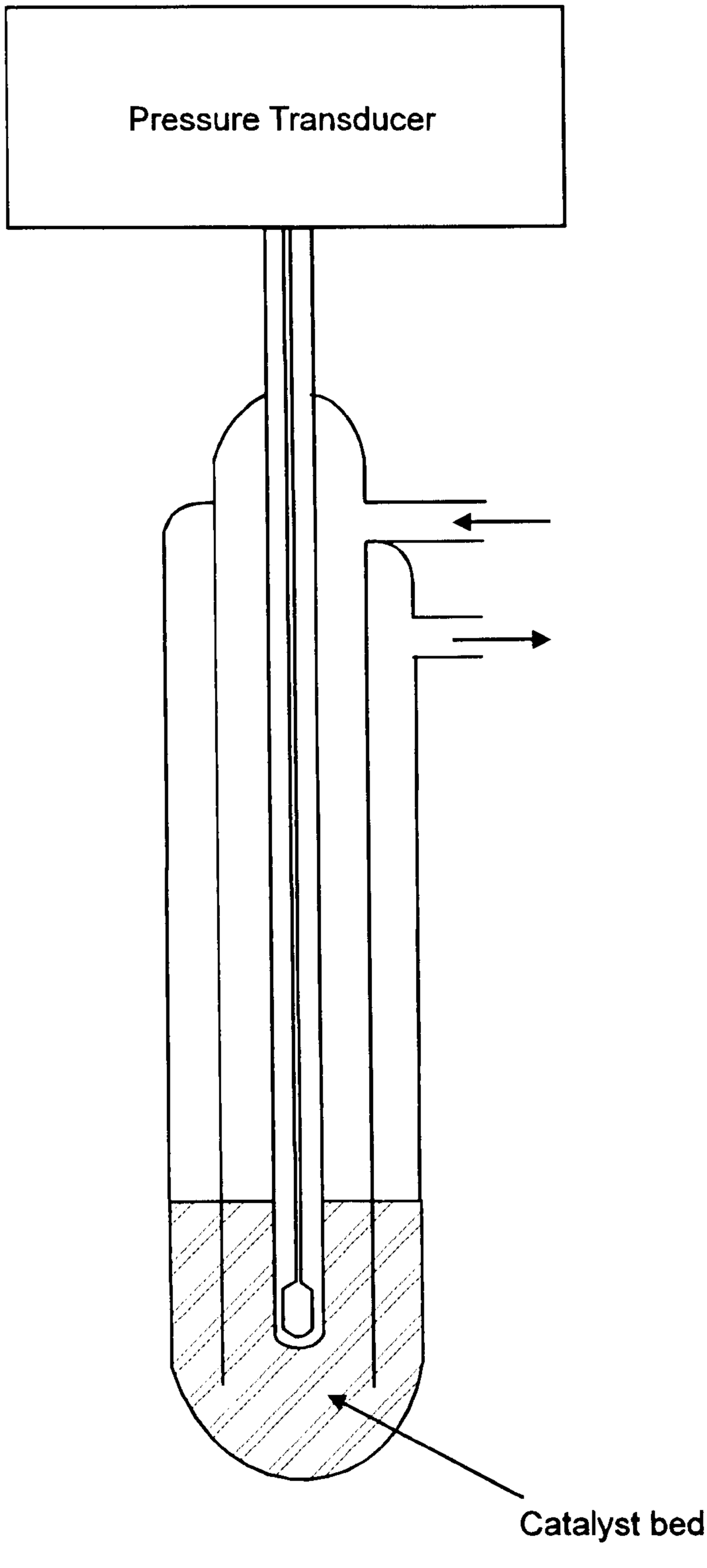

Figure 3.1. Schematic diagram of reactor.

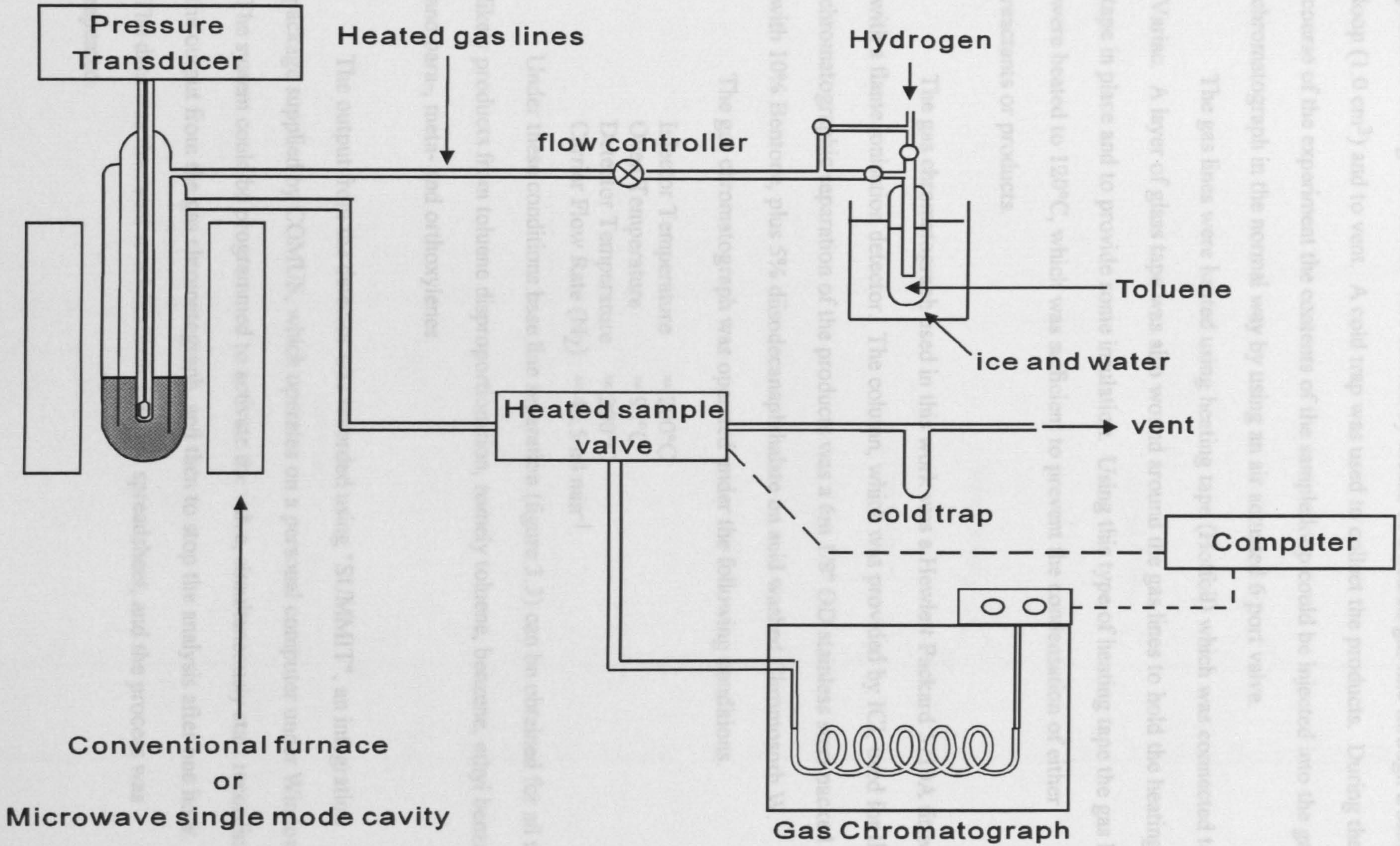

Figure 3.2. Schematic diagram of analysis system for disproportionation of toluene.

The flow rate through the catalyst bed was varied by means of a flow controller. The products exiting the reactor were carried by means of a heated gas line through a sample loop (1.0 cm^3) and to vent. A cold trap was used to collect the products. During the course of the experiment the contents of the sample loop could be injected into the gas chromatograph in the normal way by using an air actuated 6 port valve.

The gas lines were heated using heating tape (Hotfoil) which was connected to a Variac. A layer of glass tape was also wound around the gas lines to hold the heating tape in place and to provide some insulation. Using this type of heating tape the gas lines were heated to 120°C, which was sufficient to prevent the condensation of either reactants or products.

The gas chromatograph used in this work was a Hewlett Packard 5710A fitted with a flame ionisation detector. The column, which was provided by ICI, used for the chromatographic separation of the products was a 6m 1/8" OD stainless steel packed with 10% Bentone, plus 5% diisodecanaphthalate on acid washed Chromosorb W.

The gas chromatograph was operated under the following conditions.

Injector Temperature	= 200°C
Oven Temperature	= 95°C
Detector Temperature	= 200°C
Carrier Flow Rate (N_2)	= 42.5 ml min^{-1}.

Under these conditions base line separation (figure 3.3) can be obtained for all the likely products from toluene disproportionation, namely toluene, benzene, ethyl benzene and para-, meta- and orthoxylenes.

The output from the detector was recorded using "SUMMIT", an integration package supplied by COMUS, which operates on a personal computer under Windows. The system could be programmed to activate the valve, simultaneously start recording the output from the gas chromatograph, and then to stop the analysis after one hour. The data was then sent to a Microsoft EXCEL spreadsheet, and the process was repeated.

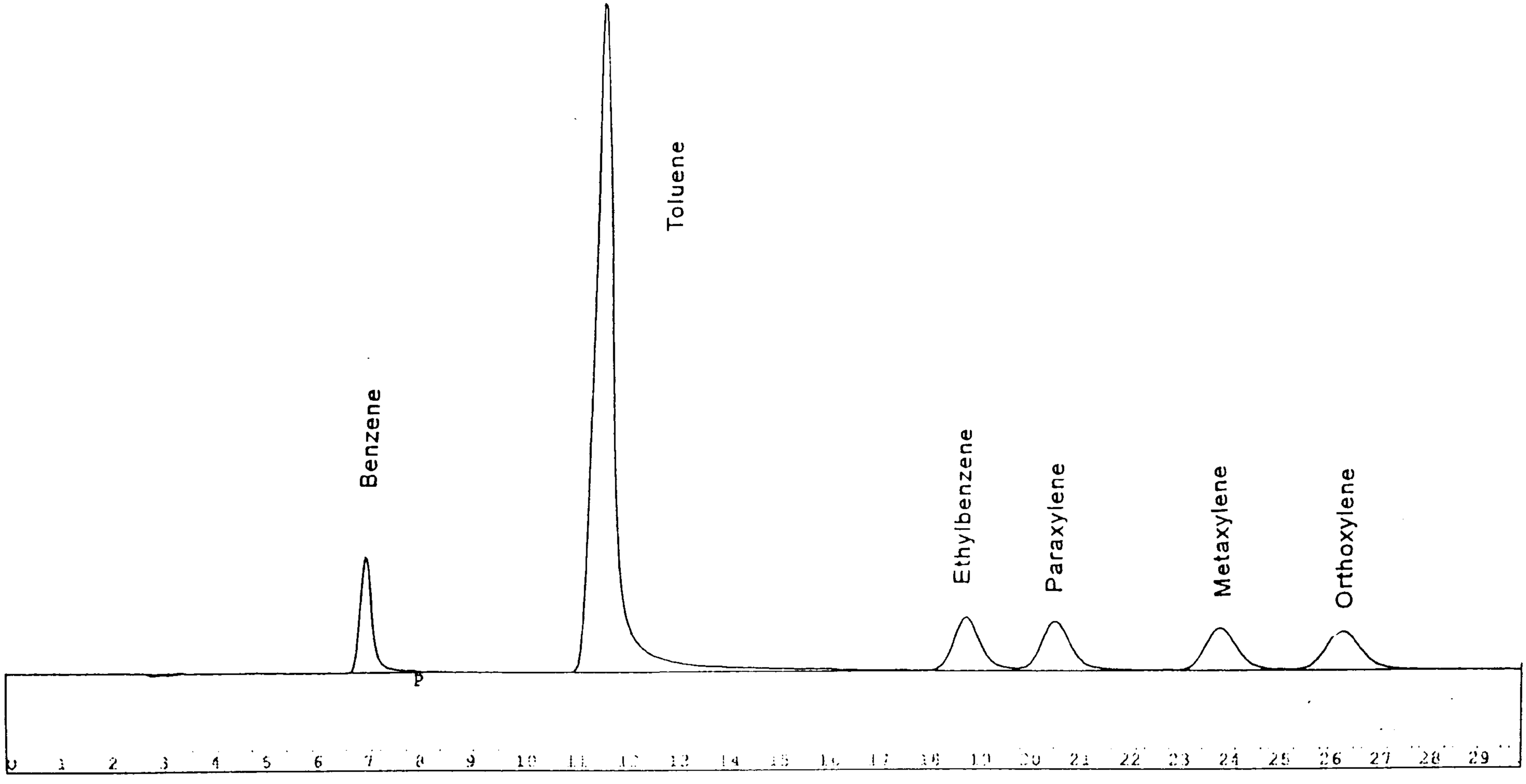

Figure 3.3. Typical Chromatographic trace from SUMMIT for injection of standard.

The products isolated from the cold trap were analysed by mass spectrometry. The instrument used for this was a Finnigan MAT 1020 gas chromatograph/mass spectrometer (GC/MS).

3.2.1.3. Microwave apparatus.

The apparatus used to heat the sample under microwave radiation was a single-mode cavity constructed by Microwave Heating Ltd. The microwave frequency employed was 2.45 GHz. This cavity (figure 3.4) consisted of five main units. These were a control unit which was capable of continuously varying the microwave power, a microwave generator (magnetron 2.45 GHz, maximum power 750 W), a section of wave-guide into which the reactor was placed, a means of monitoring the temperature while the sample was being irradiated, and a personal computer with suitable analogue to digital capabilities.

The wave-guide can itself be considered as five separate sections (figure 3.5). Microwaves produced by the magnetron entered the launch section and then the test section through the circulator. The function of the circulator was to direct the microwaves through 120°. This caused microwaves exiting the launch section to be directed into the test section, and microwaves that were reflected, having been not absorbed by the sample, to be turned through a further 120° into a water load. This prevented reflected microwaves re-entering the launch section where they would cause overheating and eventual failure of the magnetron. The function of the contactless double plunge tuner was to reflect the microwaves efficiently, thus establishing a standing wave with the maximum in the E field at the point at which the sample was mounted in the test section. Tuning of the cavity was achieved by varying the position of the double plunge tuner, by way of a screw thread mechanism, until a maximum signal was obtained from a tuning probe.

The reactor with the sample under investigation was mounted in the test section. The temperature of the sample could be monitored either by the gas thermometer or by observation of the sample with an infra-red pyrometer through the observation port.

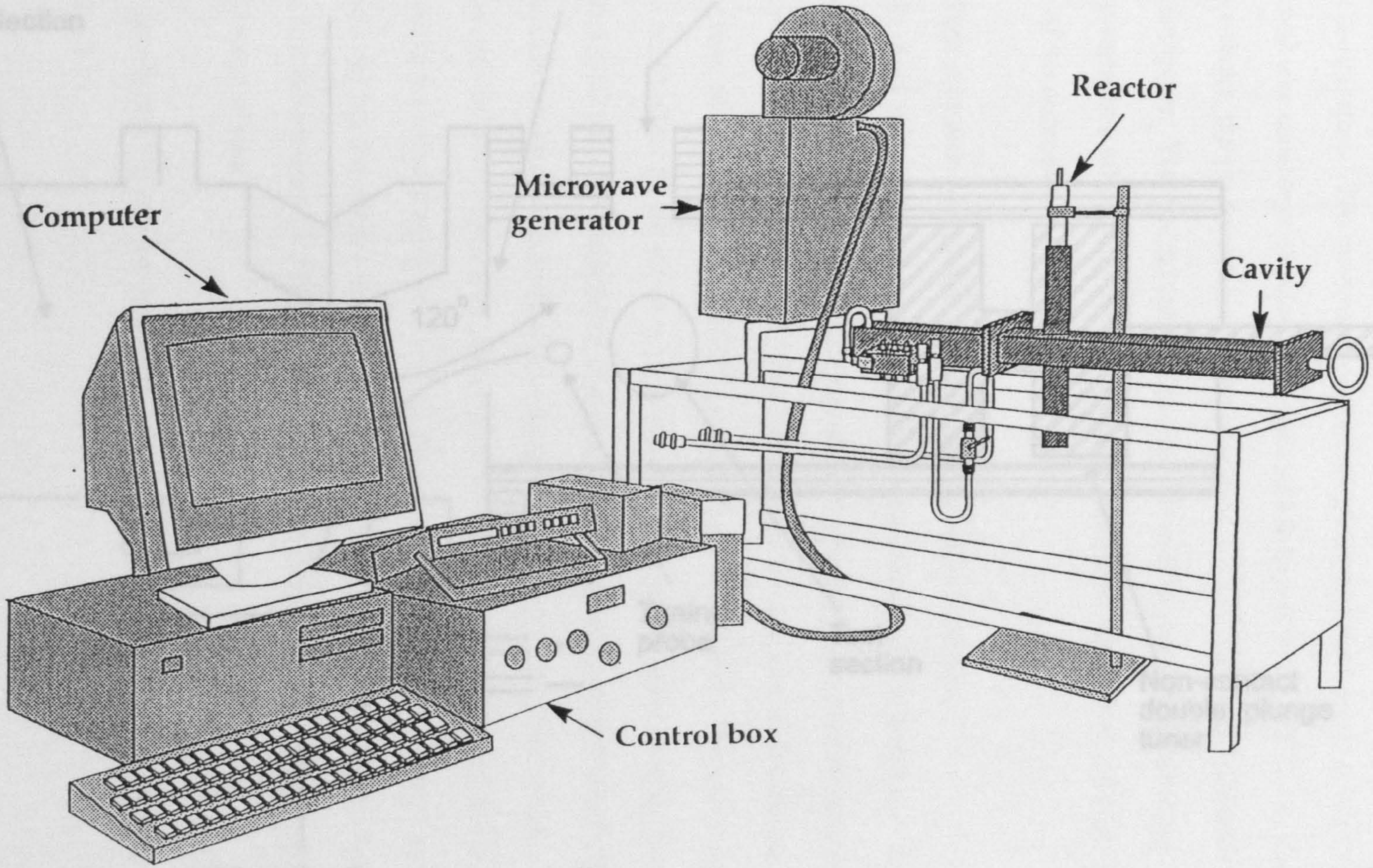

Figure 3.4. Schematic diagram of microwave single mode cavity.

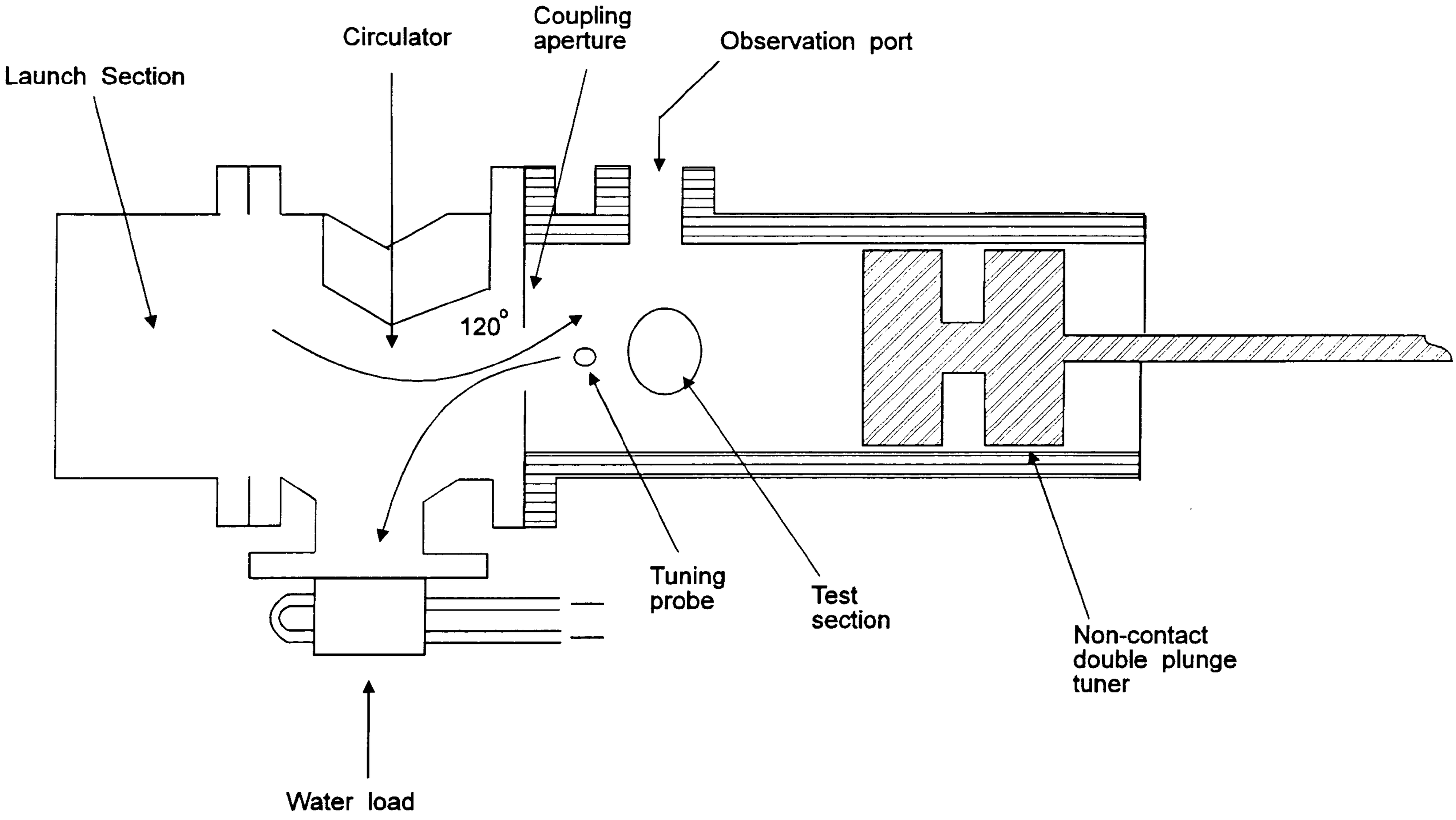

Figure 3.5. Plan view of wave guide section of apparatus.

The use of gas thermometry for the measurement of temperature within a microwave field has been dealt with in more detail in Chapter 2. The majority of the results presented here have made use of an infra-red pyrometer (Tasco THI-302DX) to measure the sample temperature. The pyrometer responded to infrared radiation over the range 8 - 12 μm and was capable of measuring temperature in the range 0 - 500°C. In this temperature range, the pyrometer yielded an output of 0 - 5 V which was digitised and fed to the computer. The desired temperature for the reaction was attained using a computer programme which read the voltage produced by the pyrometer and adjusted the power of the microwave radiation accordingly.

3.2.2.4. High pressure equipment for toluene disproportionation.

This study was carried at in the Hydrocarbons Laboratory at ICI Wilton. Figure 3.6 shows the apparatus used for the analysis of the disproportionation of toluene under high pressure conditions. The reactor (steel tubular reactor) was placed in a furnace with a vaporiser unit, at a temperature of 195°C, placed above the reactor. The gas supply to the reactor could either be air at low pressure, nitrogen at low pressure or hydrogen at high pressure (300 psi). Liquid toluene was pumped from a bottle using a Gilson HPLC pump at various rates to the vaporiser unit where it was vaporised and then passed through the reactor with the relevant carrier gas. The flow rate over the catalyst bed was varied by using the toluene pump rate and the flow controllers of the carrier gas supply. The products exiting the reactor were carried by means of a heated gas line into an oven, which was at a temperature of 200°C to prevent condensation of products, through a sample valve and to vent.

The gas chromatograph and column conditions were the same as described in section 3.2.1.2.

The output from the detector was recorded by "MULTICHROM" an computer package, which is used by ICI, which is networked to several PC's. The gas chromatography system receives a signal from MULTICHROM which activates the valve and starts the analysis and this cycle is repeated every hour.

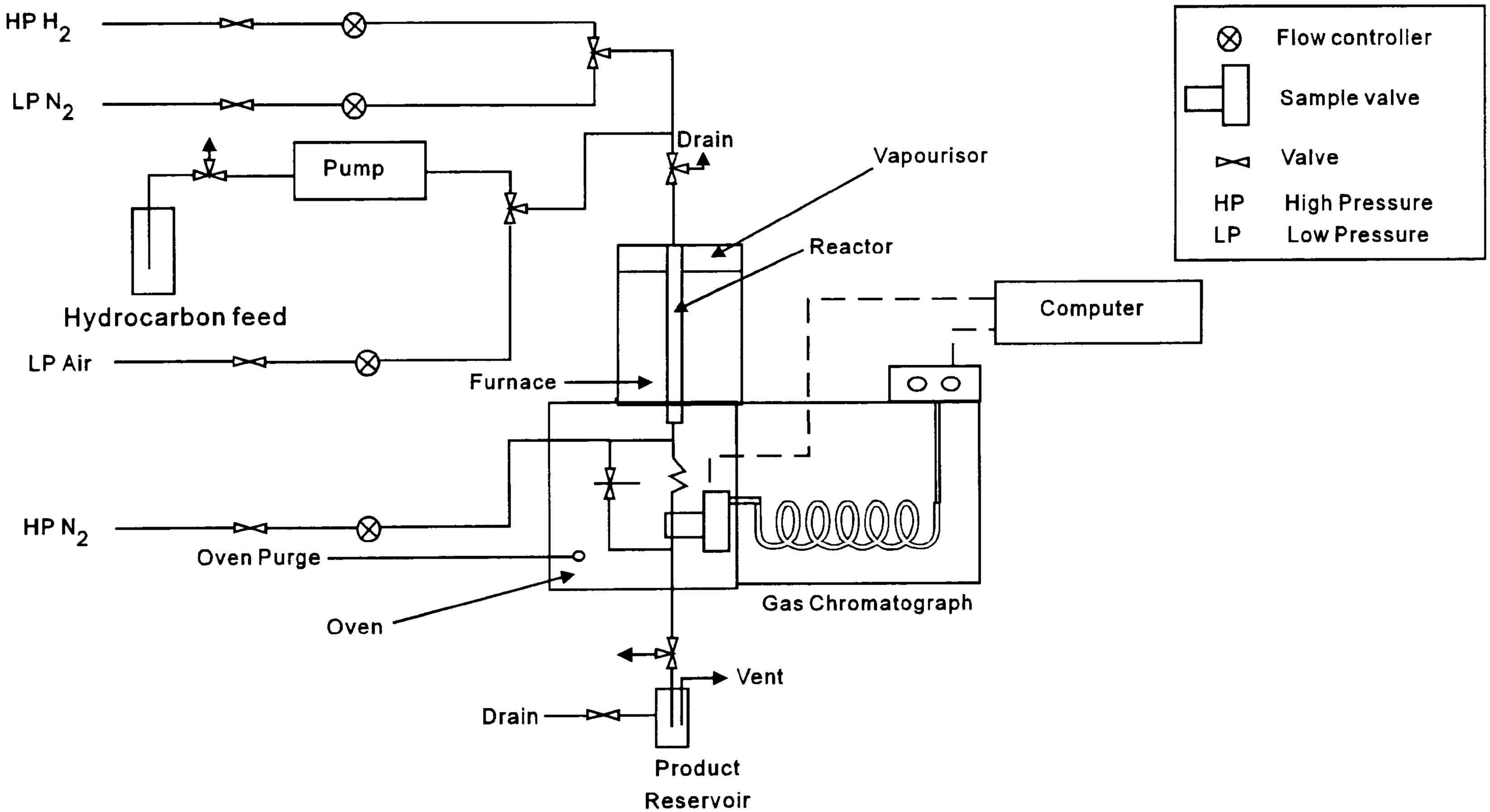

Figure 3.6. Schematic diagram of high pressure equipment for disproportionation of toluene.

3.2.2. Calibration.

3.2.2.1 Calibration of response factors for toluene disproportionation.

Several calibration standards were made up and analysed. The standards were made by weighing 10g of toluene and adding weighed amounts of the other components. Standard 1 contained 10g of toluene and 1g of each of the other components, standard 2 contained 10g of toluene and 1.1g of the each of the other components and standard 3 contained 10g of toluene and 1.3g of each of the other components. 0.2 microlitres of each standard was injected into the injector port of the gas chromatograph. The response factors were calculated using the SUMMIT calibration facility where toluene was used as the internal reference peak.

3.2.3. Experiments on disproportionation of toluene.

Table 3.2 is a summary of the data obtained from Merck (BDH), and Strem Chemicals about the catalysts which were used in this study.

Table 3.2.
Information on catalysts obtained from suppliers.

	BDH Zeolite Hydrogen form of ZSM-5	BDH Zeolite Hydrogen form of mordenite	Strem Zeolite Hydrogen form of mordenite
Nominal Particle size	2 mm spheres	2 mm spheres	1/16" pellets
Surface area	300 m^2g^{-1}	350 m^2g^{-1}	450 m^2g^{-1}
Average bulk Density	0.72 gml^{-1}	0.68 gml^{-1}	0.59 gml^{-1}
Pore Volume	0.48 gml^{-1}	0.53 gml^{-1}	not supplied
Pore diameter	not supplied	not supplied	8-9Å
Silica/Aluminium	50	20	10
Sodium Content	0.03%	0.03%	not supplied
Potassium Content	0.01%	0.02%	not supplied
Sulphate content	0.01%	0.04%	not supplied
Water content	not supplied	not supplied	11%

3.2.3.1. Thermal experiments under atmospheric pressure conditions.

The same procedure was observed for each experiment. The catalyst (3.3g) was loaded into the reactor and activated overnight under flowing nitrogen at 450°C. The carrier gas was changed to pure hydrogen for 1 hour, then the temperature was altered to the reaction temperature. A continuous stream of toluene in pure hydrogen was passed through the catalyst and the conversion was measured at hourly intervals. The lifetime of the catalyst was studied at various temperatures.

3.2.3.2. Experiments under microwave conditions.

The catalyst was activated overnight under flowing nitrogen (42.5 ml min^{-1}) under normal thermal conditions at 450°C. Then hydrogen was allowed to flow through the catalyst for 1 hour at 450°C under thermal conditions. The reactor was then transferred to the single mode cavity and the catalyst was brought up to reaction temperature under microwave conditions. Toluene in hydrogen was then passed through the catalyst and analysis was commenced. At the end of the day the toluene was taken off-line, the microwave power was turned off, and the catalyst left overnight under flowing hydrogen at room temperature. At the start of the next day the catalyst was brought up to reaction temperature under microwave conditions and toluene brought on-line and analysis recommenced.

3.2.3.3. Thermal experiments under high pressure conditions.

The same procedure was observed for each experiment. The catalyst (1.0g) was loaded into the reactor and activated overnight at 500°C under air (15 psi). Nitrogen (10 psi) was passed over the catalyst while the temperature was reduced. Hydrogen (300 psi) (100 ml min^{-1}) was passed over the catalyst for one hour. Liquid toluene was pumped into the system at 15 ml h^{-1} for 5 minutes, then the pump rate was reduced to 6.6 ml h^{-1}. When hydrocarbon vapour was observed from the vent line, the toluene pump rate and the hydrogen flow rate were altered to the conditions required for that particular experiment.

Experiments were conducted to study the lifetime of the catalyst under various hydrogen to hydrocarbon ratios and various temperatures.

3.3. Results.

3.3.1. Calibration.

The response factor for each component was calculated by SUMMIT as follows. Toluene was used as the reference peak.

$$RF_j * \frac{Area_j * Con_{rf}}{Area_{rf}} = Con_j \qquad (3.5).$$

Where:
RF_j is the response factor for component j.
Con_j is the amount of component in calibration mix.
$Area_j$ is the area of peak j.
Con_{rf} is the amount of reference component in calibration.
$Area_{rf}$ is the area of reference peak.

Table 3.3 shows the results from the calibration standards. The integration calculations were performed using these factors.

Table 3.3.
Retention time and response factor for each product from toluene disproportionation.

Component	Retention time / min	Response factor
Cracked products	2:07	----
Benzene	7:35	0.92
Toluene	12:16	1.0000
Ethylbenzene	19:42	0.88
Paraxylene	21:28	0.90
Metaxylene	24:49	0.83
Orthoxylene	27:18	0.80

3.3.2. Results from experiments on toluene disproportionation.

3.3.2.1. Thermal experiments under atmospheric pressure conditions.

Figure 3.7 presents the results of the initial experiments with hydrogen mordenite (Strem Chemicals) using an injection method. This was the trace from a 5 microlitres injection of toluene. The trace shows that reaction had taken place but chromatographic resolution had been lost, therefore all subsequent experiments were performed using a continuous flow of toluene. Figure 3.8 shows a typical chromatograph output trace from SUMMIT for toluene disproportionation.

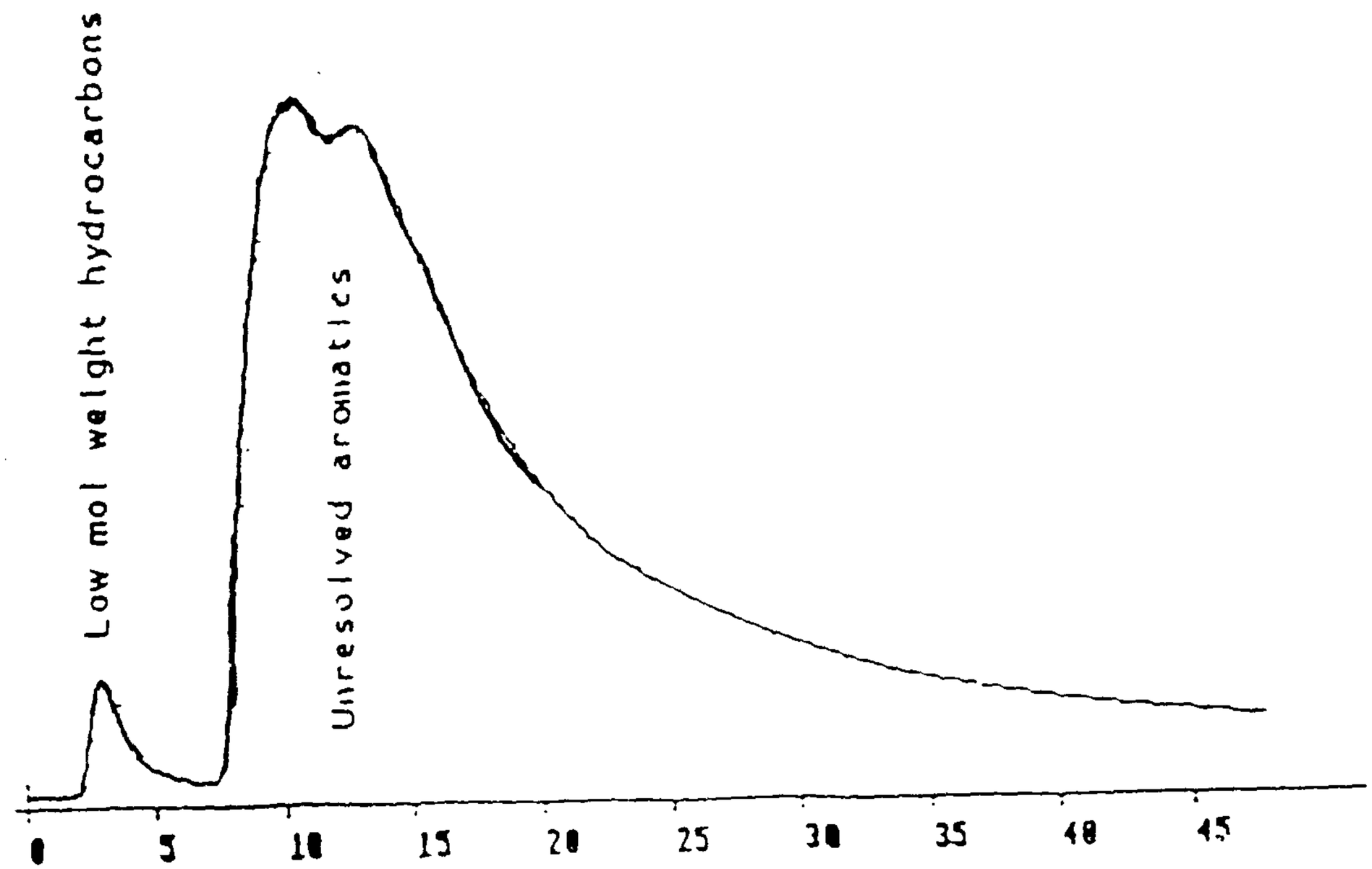

Figure 3.7. Chromatographic trace from injection of toluene over catalyst.

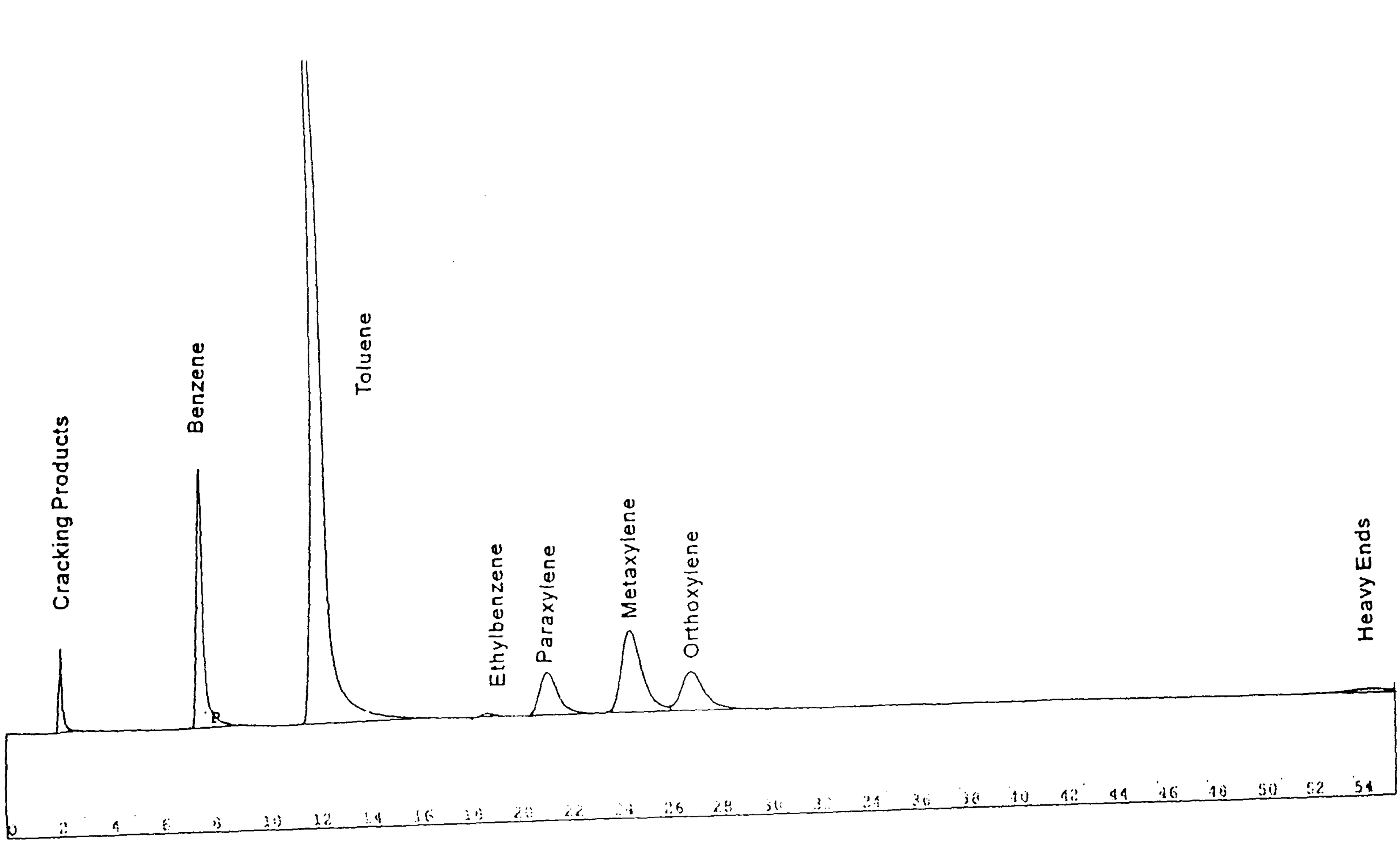

Figure 3.8. Typical chromatographic trace from SUMMIT for toluene disproportionation.

The results from the experiments performed on hydrogen mordenite (Strem Chemicals) using different ratios of N_2:H_2 as a carrier gas are shown in figure 3.9. The diagram is a plot of toluene conversion over hydrogen mordenite with respect to time using toluene at a vapour pressure of 7.1 torr in different carrier gases and at a temperature of 350°C. Initially, conversion of toluene was approximately 40% but, as the experiment continued, the conversion started to fall. After approximately 20 hours the conversion was relatively stable. When the concentration of hydrogen was raised the conversion also raised. Experiments using pure hydrogen increase the lifetime of the catalyst even though the initial conversion is low. When the catalyst was discharged from the reactor, after each experiment, the colour of the pellets was black.

Figure 3.10 presents the results of the experiments using pure hydrogen as the carrier gas at different temperatures. The same effect is observed, initially the conversion was high (65%), but as the experiment continued, the conversion fell to below 30%. Increasing the temperature increased the conversion and the lifetime of the catalyst up to a temperature of 425°C. Experiments performed at 450°C show that although, the initial conversion was comparable to experiments carried out at 425°C, the conversion more quickly fell. Therefore the optimum conversion was at a temperature of 425°C

The molar ratio of toluene to hydrogen is calculated below.

$$\frac{7.1}{760} * 42.5 = 0.397 \text{ ml of toluene gas per minute.} \quad (3.6).$$

$$= 23.82 \text{ ml of toluene gas per hour}$$

$$\frac{23.82}{22414} = 1.062*10^{-3} \text{ moles of toluene per hour.} \quad (3.7).$$

$$\frac{42.5 * 752.9}{760} = 42.1 \text{ ml of hydrogen gas per minute.} \quad (3.8).$$

$$\frac{42.1 * 60}{22414} = 0.1127 \text{ moles of hydrogen per hour.} \quad (3.9).$$

$$\frac{0.11277}{1.0625 * 10^{-3}} = 106.1 \text{ moles of hydrogen to 1 mole of toluene.} \quad (3.10).$$

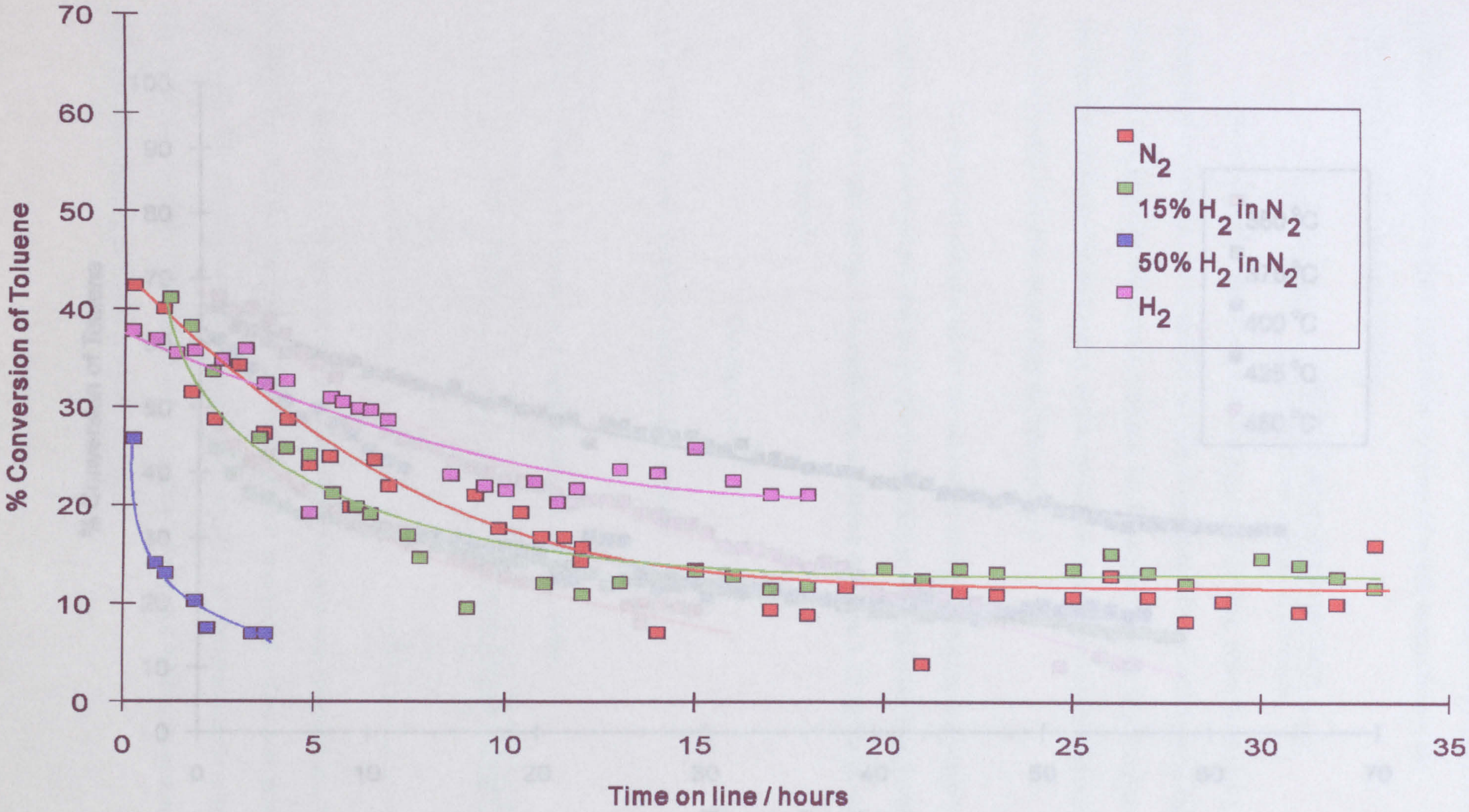

Figure 3.9. Conversion of toluene at 350°C over hydrogen mordenite (Strem Chemicals) under various conditions.

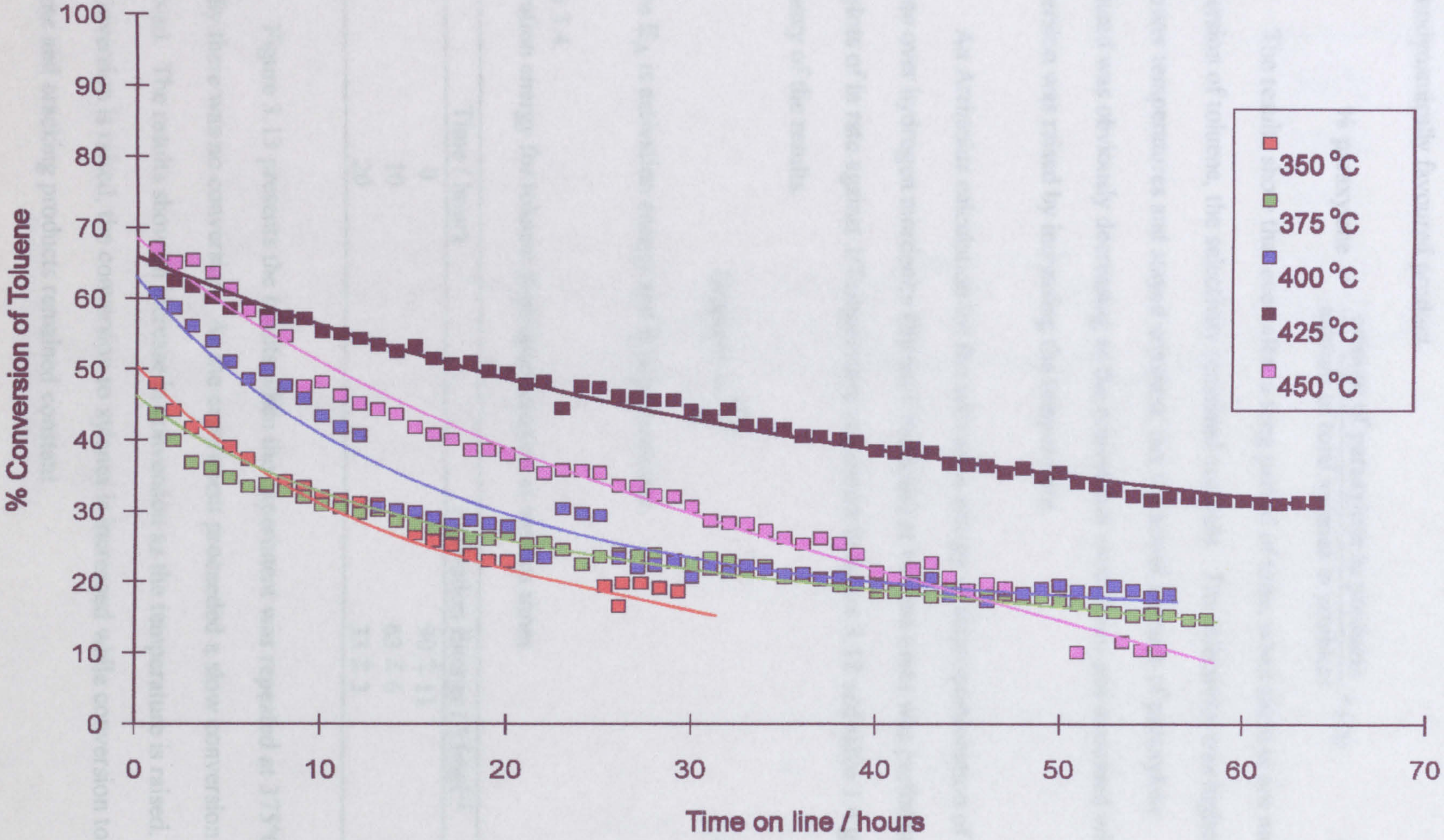

Figure 3.10. Toluene conversion over hydrogen mordenite (Strem Chemicals) at different temperatures.

Figure 3.11 shows the selectivity to paraxylene. The selectivity calculation was performed by only considering the three xylenes; of which metaxylene is the thermodynamically favoured product.

$$\% \text{ paraxylene} = \frac{\text{amount of paraxylene in products}}{\text{amount of total xylenes in products}} * 100 \qquad (3.11).$$

The results show that even after a long period of time, when there is not much conversion of toluene, the selectivity remained constant. The selectivity was higher at the lower temperatures and stayed constant, but the actual amount of paraxylene produced was obviously decreasing as the conversion went down and increased when the conversion was raised by increasing the temperature.

An Arrhenius calculation for the activation energy of disproportionation of toluene over hydrogen mordenite (Strem Chemicals) at various times was performed. The plots of ln rate against 1/Temperature are shown in figure 3.12 and table 3.4 gives a summary of the results.

$$\text{Gradient} = \frac{-E_A}{R} \qquad (3.12).$$

Where E_A is activation energy and R is gas constant.

Table 3.4.
Activation energy for toluene disproportionation at various times.

Time / hours	Activation Energy / $kJmol^{-1}$
0	90 ± 11
10	63 ± 6
20	33 ± 3

Figure 3.13 presents the results when the experiment was repeated at 375°C. Initially there was no conversion. As the experiment proceeded a slow conversion was observed. The results show an increase in conversion as the temperature is raised. As the conversion is raised, the conversion to xylenes is increased while conversion to benzene and cracking products remained constant.

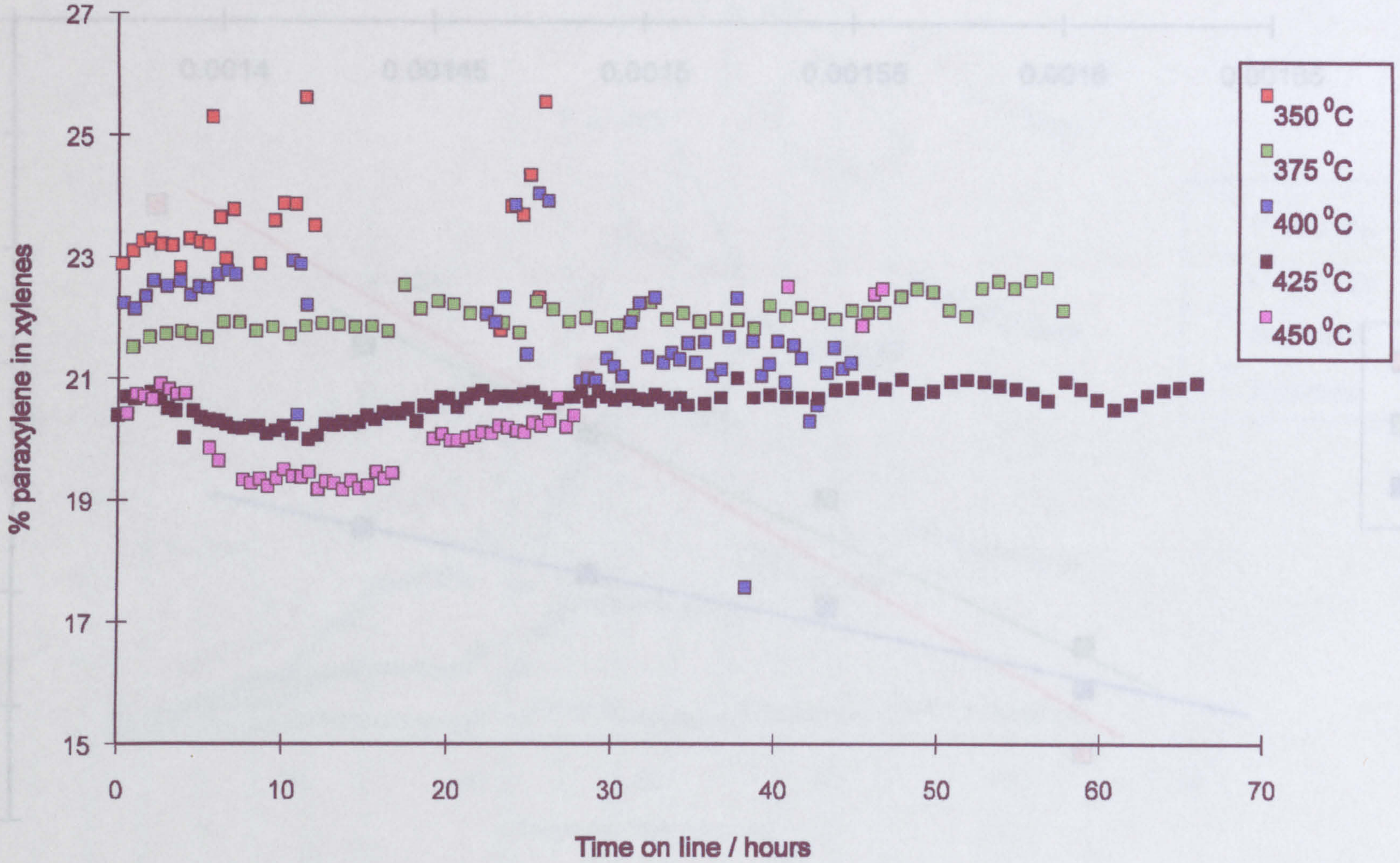

Figure 3.11. Selectivity to paraxylene over hydrogen mordenite (Strem Chemicals) at different temperatures.

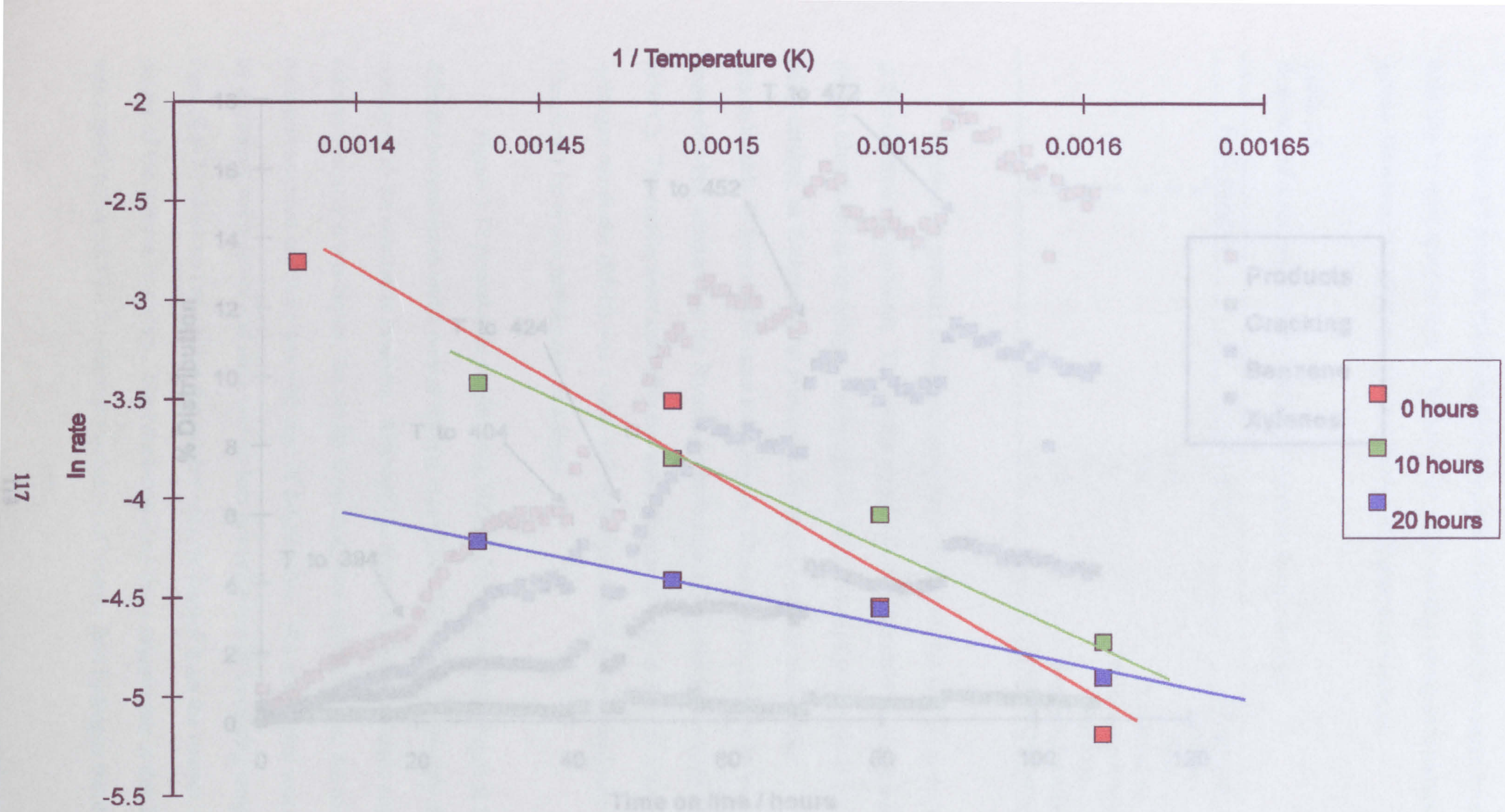

Figure 3.12. Arrhenius plot for toluene disproportionation over hydrogen mordenite (Strem Chemicals) at different times.

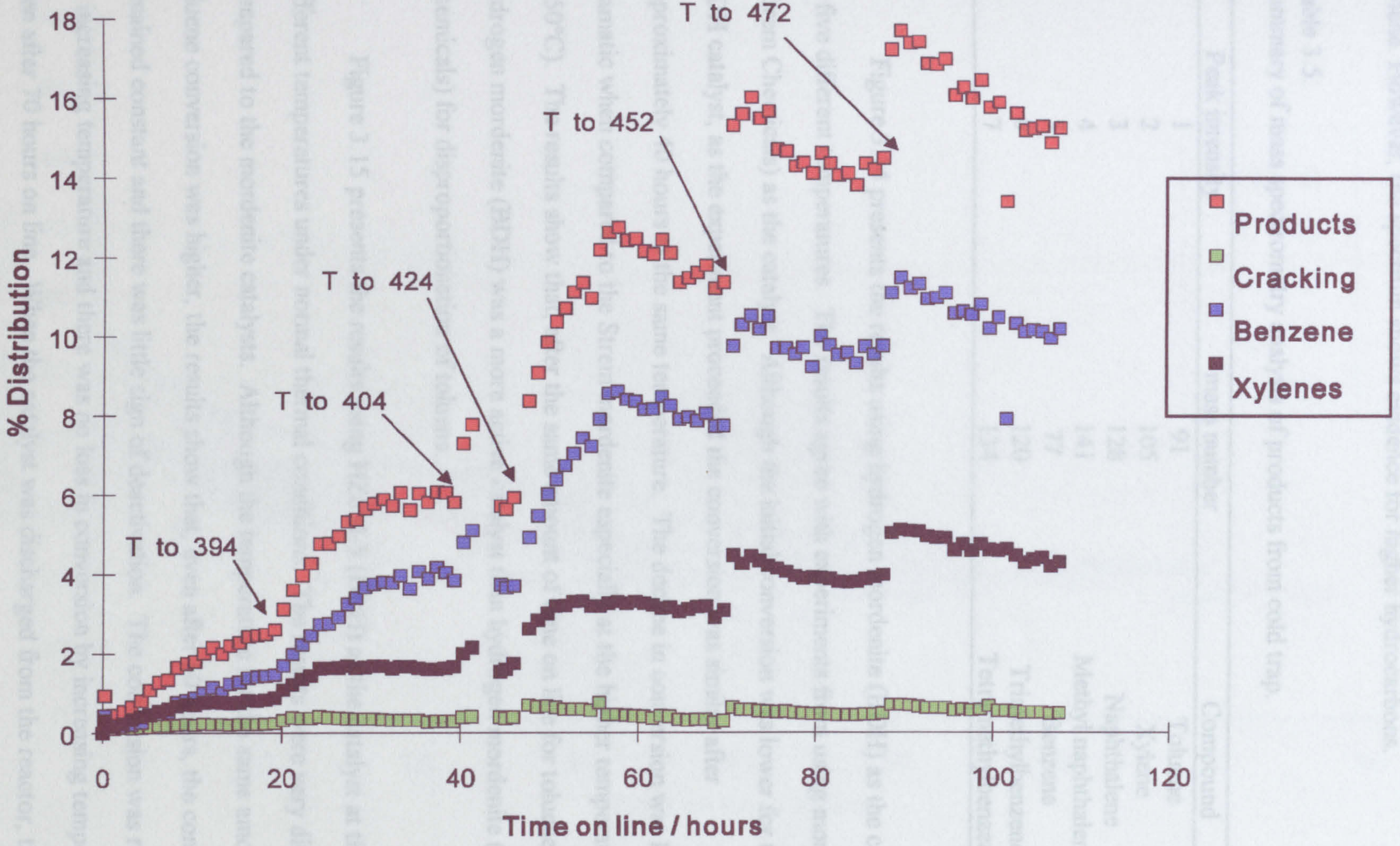

Figure 3.13. Disproportionation of toluene over hydrogen mordenite (Strem Chemicals) at 375°C.

Table 3.5 presents the results of the analysis of the products isolated from the cold trap by mass spectrometry. Toluene is the major product along with benzene and xylene. However, the spectrum shows evidence for higher hydrocarbons.

Table 3.5.
Summary of mass spectrometry analysis of products from cold trap.

Peak intensity	mass number	Compound
1	91	Toluene
2	105	Xylene
3	128	Naphthalene
4	141	Methyl naphthalene
5	77	Benzene
6	120	Trimethylbenzene
7	134	Tetramethylbenzene

Figure 3.14 presents the results using hydrogen mordenite (BDH) as the catalyst at five different temperatures. The results agree with experiments from using mordenite (Strem Chemicals) as the catalyst. Although the initial conversion was lower for the BDH catalyst, as the experiment proceeded the conversion was similar after approximately 40 hours at the same temperature. The decline in conversion was less dramatic when compared to the Strem mordenite especially at the higher temperatures (450°C). The results show that, after the same amount of time on line for toluene, hydrogen mordenite (BDH) was a more active catalyst than hydrogen mordenite (Strem Chemicals) for disproportionation of toluene.

Figure 3.15 presents the results using HZSM-5 (BDH) as the catalyst at three different temperatures under normal thermal conditions. The results were very different compared to the mordenite catalysts. Although the temperature for the same amount of toluene conversion was higher, the results show that, even after 60 hours, the conversion remained constant and there was little sign of deactivation. The conversion was raised by increasing temperature and there was no loss in conversion by increasing temperature even after 70 hours on line. When the catalyst was discharged from the reactor, the colour of the spheres was black. The conclusion from these experiments is that HZSM-5 was a more active catalyst for disproportionation of toluene than hydrogen mordenite.

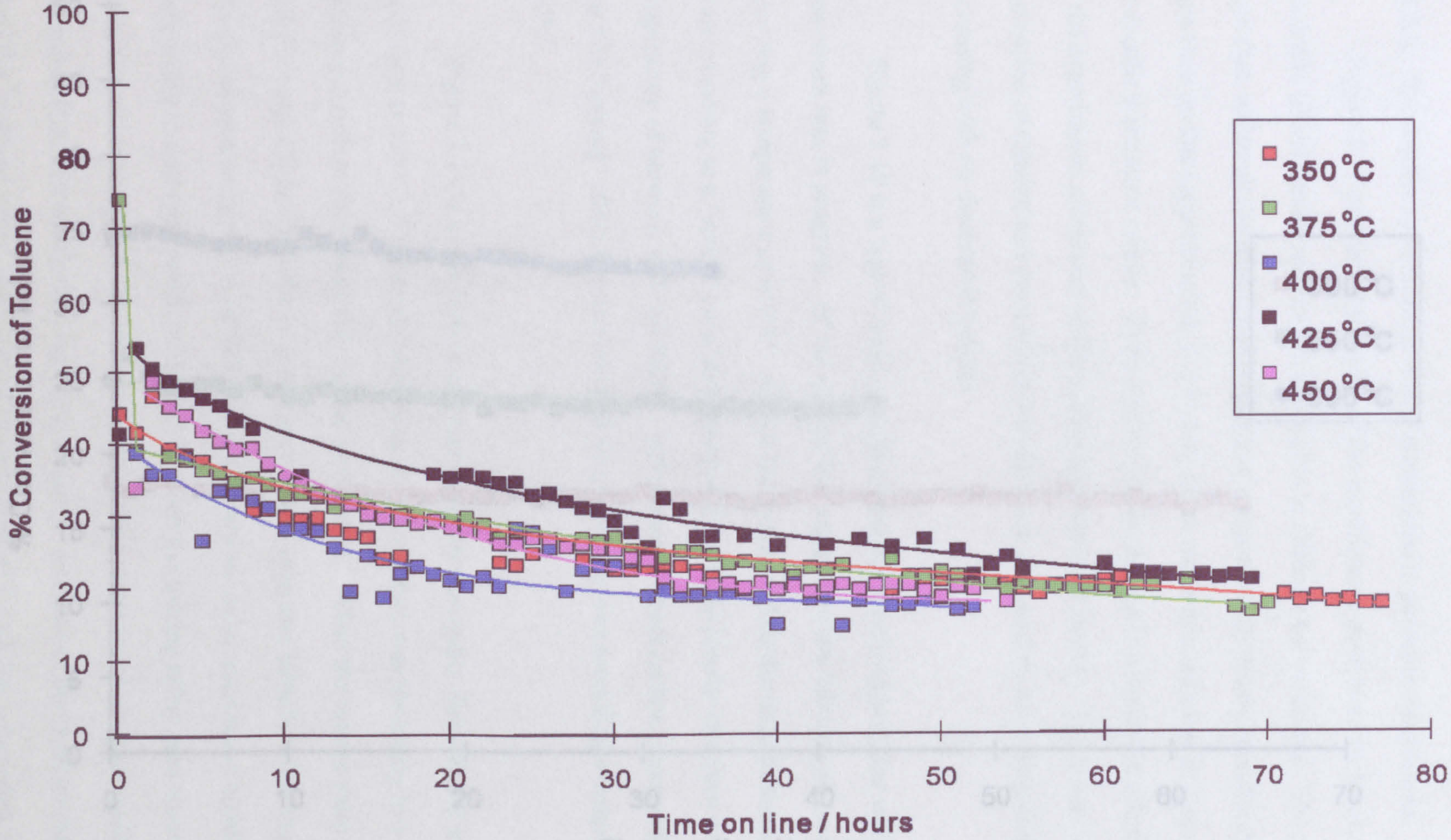

Figure 3.14. Conversion of toluene over hydrogen mordenite (BDH) at different temperatures.

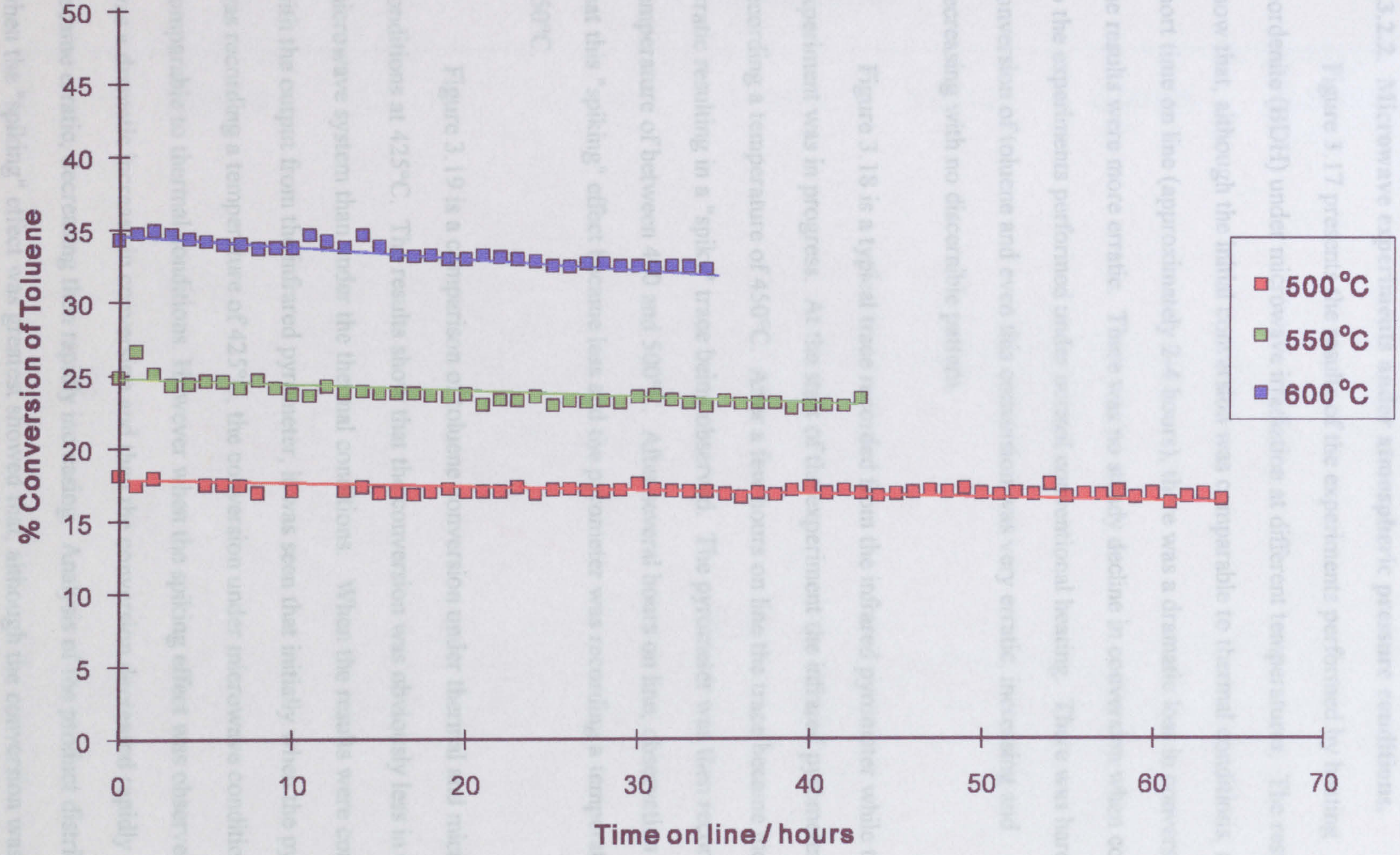

Figure 3.15. Conversion to toluene at different temperatures over HZSM-5 (BDH).

From these results an Arrhenius plot was performed (figure 3.16) giving an activation energy of 50 ± 3 kJmol^{-1}.

3.3.2.2. Microwave experiments under atmospheric pressure conditions.

Figure 3.17 presents the results of the experiments performed by heating mordenite (BDH) under microwave irradiation at different temperatures. The results show that, although the initial conversion was comparable to thermal conditions, after a short time on line (approximately 2-4 hours), there was a dramatic loss in conversion and the results were more erratic. There was no steady decline in conversion when compared to the experiments performed under normal conventional heating. There was hardly any conversion of toluene and even this conversion was very erratic, increasing and decreasing with no discernible pattern.

Figure 3.18 is a typical trace recorded from the infrared pyrometer while the experiment was in progress. At the start of the experiment the infrared pyrometer was recording a temperature of 450°C. After a few hours on line the trace became more erratic resulting in a "spiky" trace being observed. The pyrometer was then recording a temperature of between 400 and 500°C. After several hours on line, observation showed that this "spiking" effect became less and the pyrometer was recording a temperature of 450°C.

Figure 3.19 is a comparison of toluene conversion under thermal and microwave conditions at 425°C. The results show that the conversion was obviously less in the microwave system than under the thermal conditions. When the results were compared with the output from the infrared pyrometer, it was seen that initially when the pyrometer was recording a temperature of 425°C, the conversion under microwave conditions was comparable to thermal conditions. However when the spiking effect was observed there was a dramatic increase in conversion and then the conversion decreased rapidly and became erratic, decreasing then rapidly increasing. Analysis of the product distribution when the "spiking" effect was greatest showed that, although the conversion was increased, the major products were benzene and cracking products.

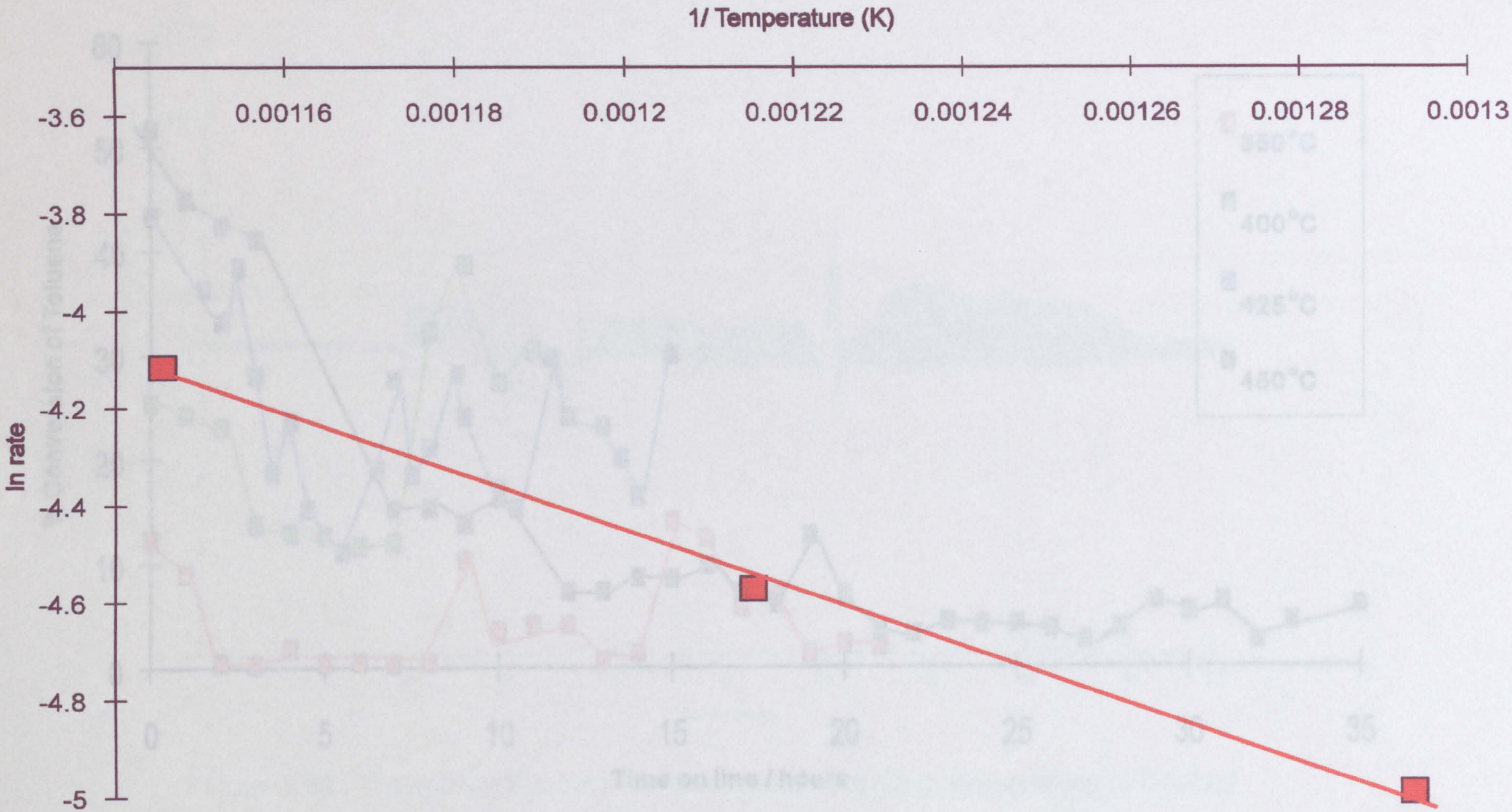

Figure 3.16. Arrhenius plot for toluene disproportionation over HZSM-5 (BDH).

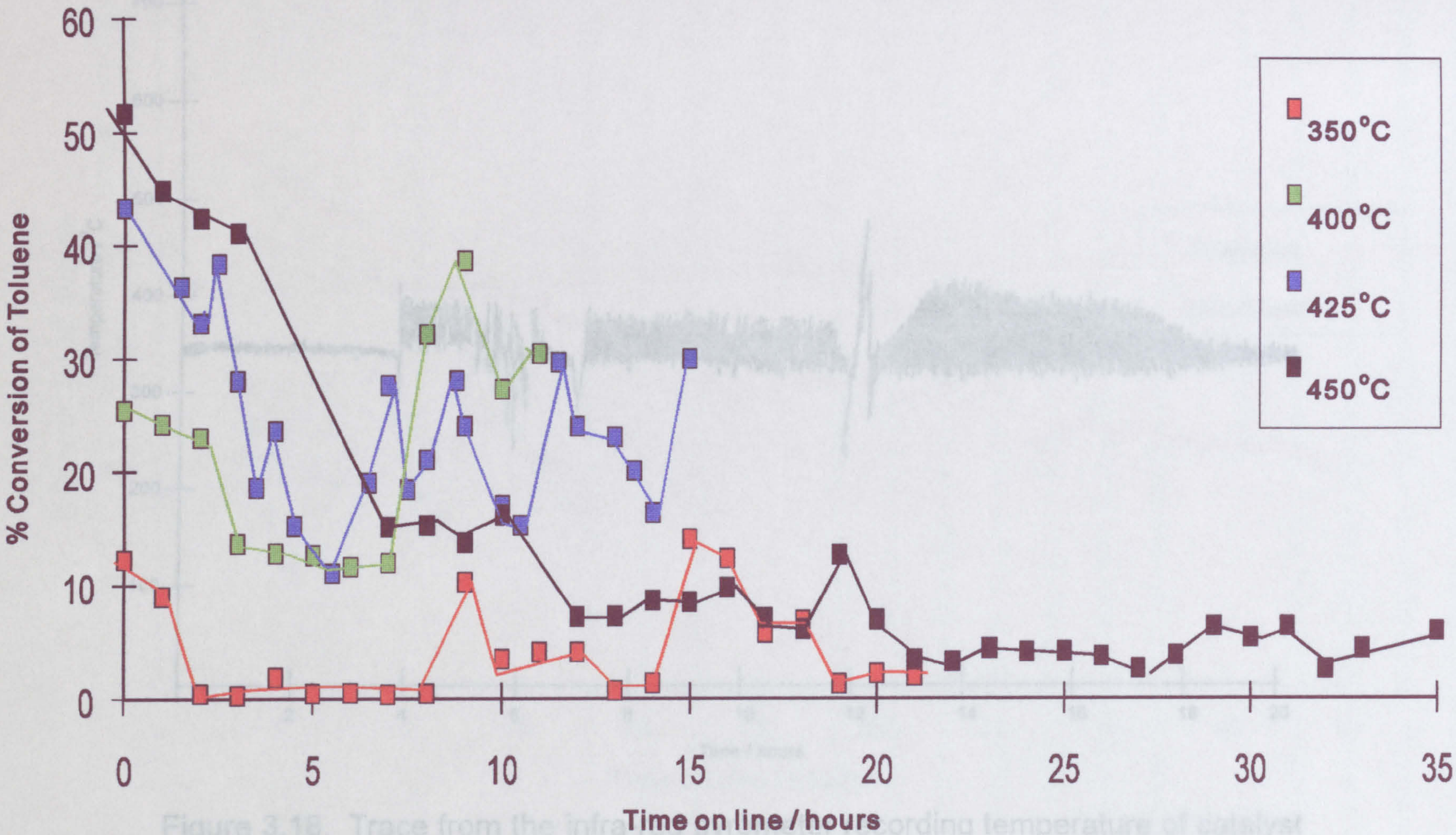

Figure 3.17. Conversion of toluene over hydrogen mordenite (BDH) under microwave conditions.

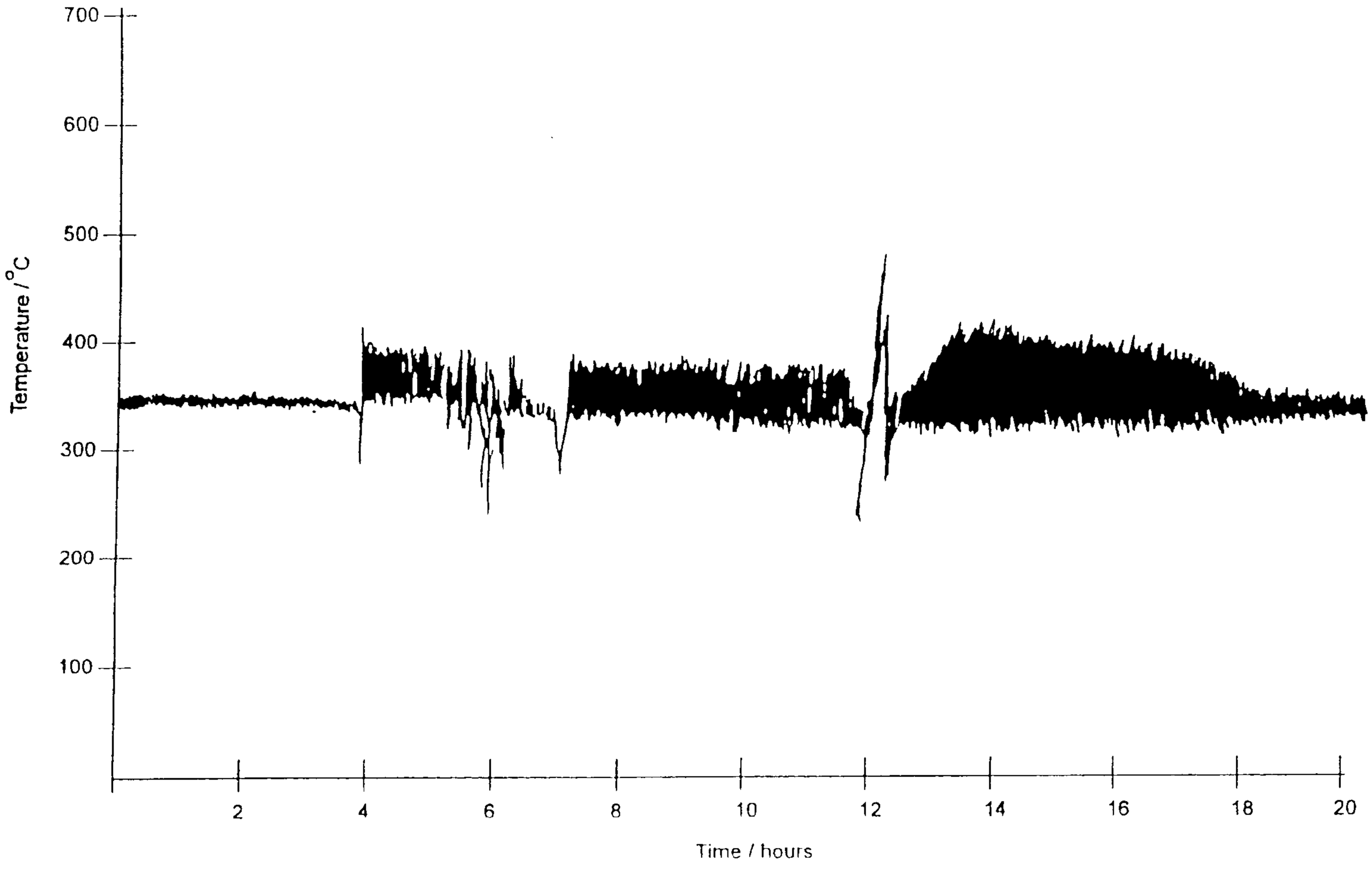

Figure 3.18. Trace from the infra-red pyrometer recording temperature of catalyst under microwave irradiation.

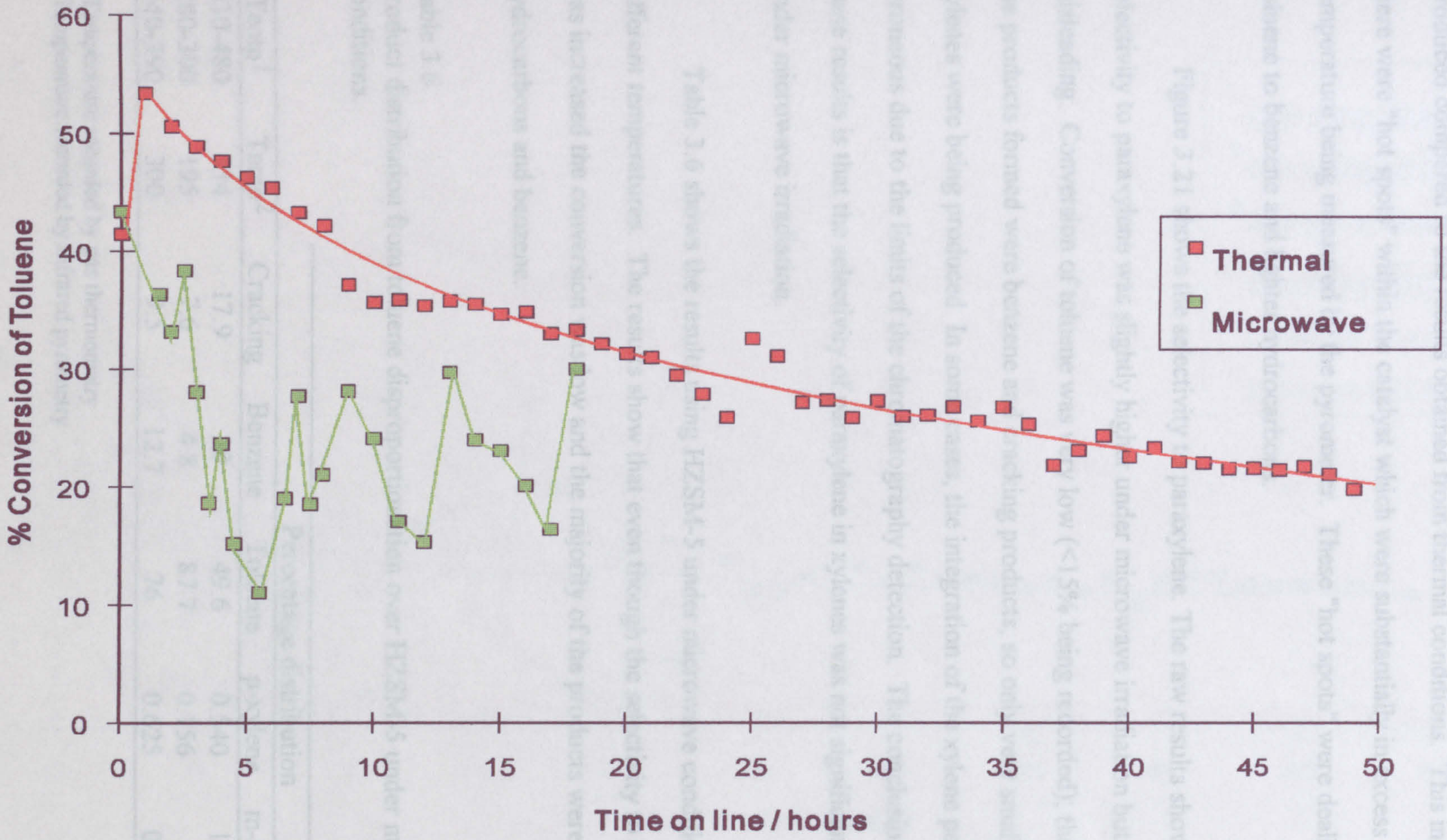

Figure 3.19. Conversion of toluene over hydrogen mordenite (BDH) under thermal and microwave conditions at 425°C.

Figure 3.20 shows the comparison of cracking, benzene and xylenes under both thermal and microwave conditions at 425°C. The results show that microwave conditions resulted in more cracking and benzene (benzene to xylene ratio >1) being produced compared to the results obtained from thermal conditions. This indicated that there were "hot spots" within the catalyst which were substantially in excess of the bulk temperature being measured by the pyrometer. These "hot spots" were dealkylating toluene to benzene and lighter hydrocarbons.

Figure 3.21 shows the selectivity to paraxylene. The raw results show that the selectivity to paraxylene was slightly higher under microwave irradiation but this was misleading. Conversion of toluene was very low (<15% being recorded); the majority of the products formed were benzene and cracking products, so only very small amounts of xylenes were being produced In some cases, the integration of the xylene peaks was erroneous due to the limits of the chromatography detection. The conclusions from these results is that the selectivity of paraxylene in xylenes was not significantly enhanced under microwave irradiation.

Table 3.6 shows the results using HZSM-5 under microwave conditions at 3 different temperatures. The results show that even though the selectivity to paraxylene was increased the conversion was low and the majority of the products were light hydrocarbons and benzene.

Table 3.6.
Product distribution from toluene disproportionation over HZSM-5 under microwave conditions.

		Percentage distribution					
Temp[1]	Temp[2]	Cracking	Benzene	Toluene	p-xylene	m-xylene	o-xylene
430-480	334	17.9	30	49.6	0.540	1.253	0.641
280-300	195	7.6	4.8	87.7	0.156	0	0
340-390	300	9.5	12.7	76	0.625	0.737	0.372

[1] Temperature recorded by gas thermometry
[2] Temperature recorded by infrared pyrometry

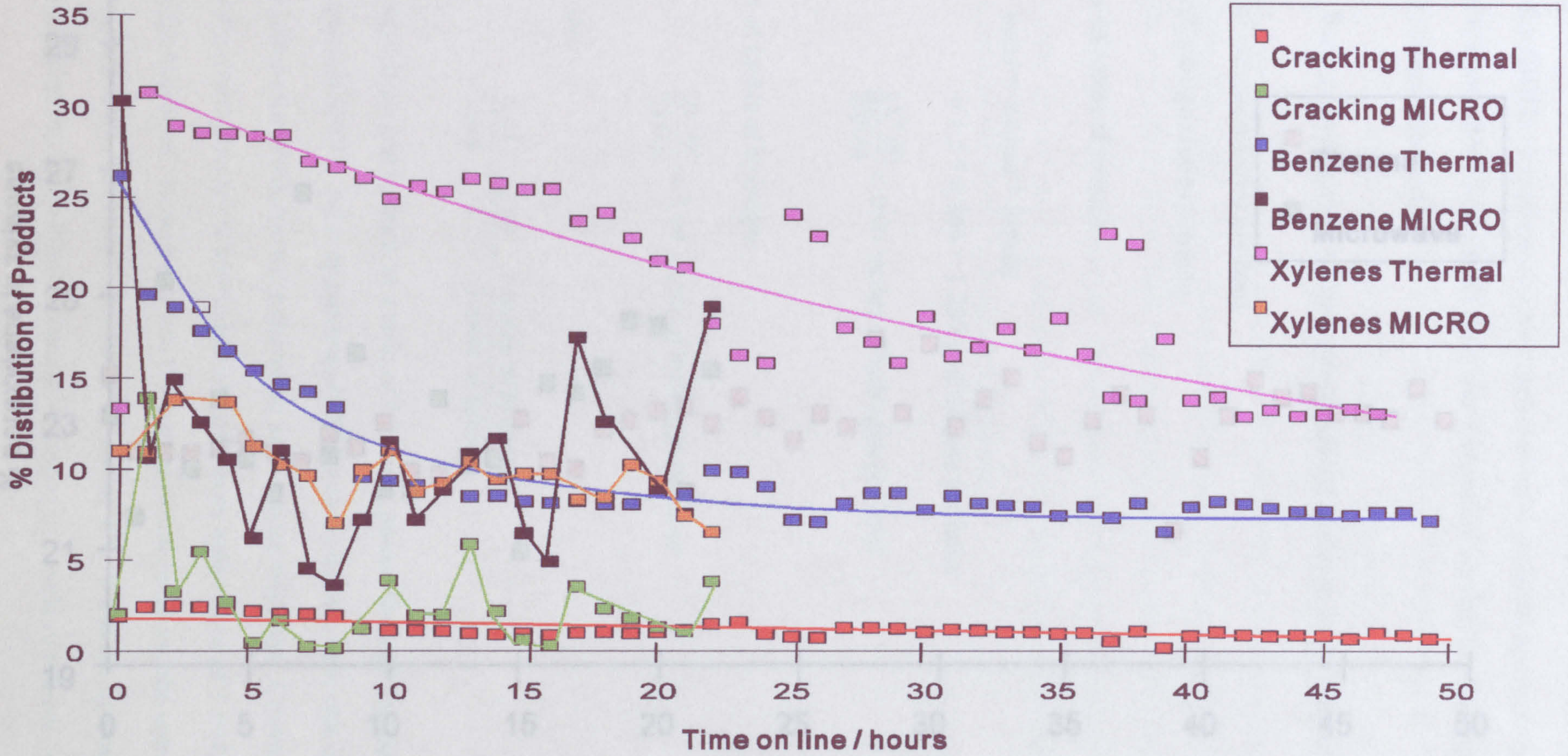

Figure 3.20. Distribution of Products from disproportionation of toluene over hydrogen mordenite (BDH) under thermal and microwave conditions at 425 °C.

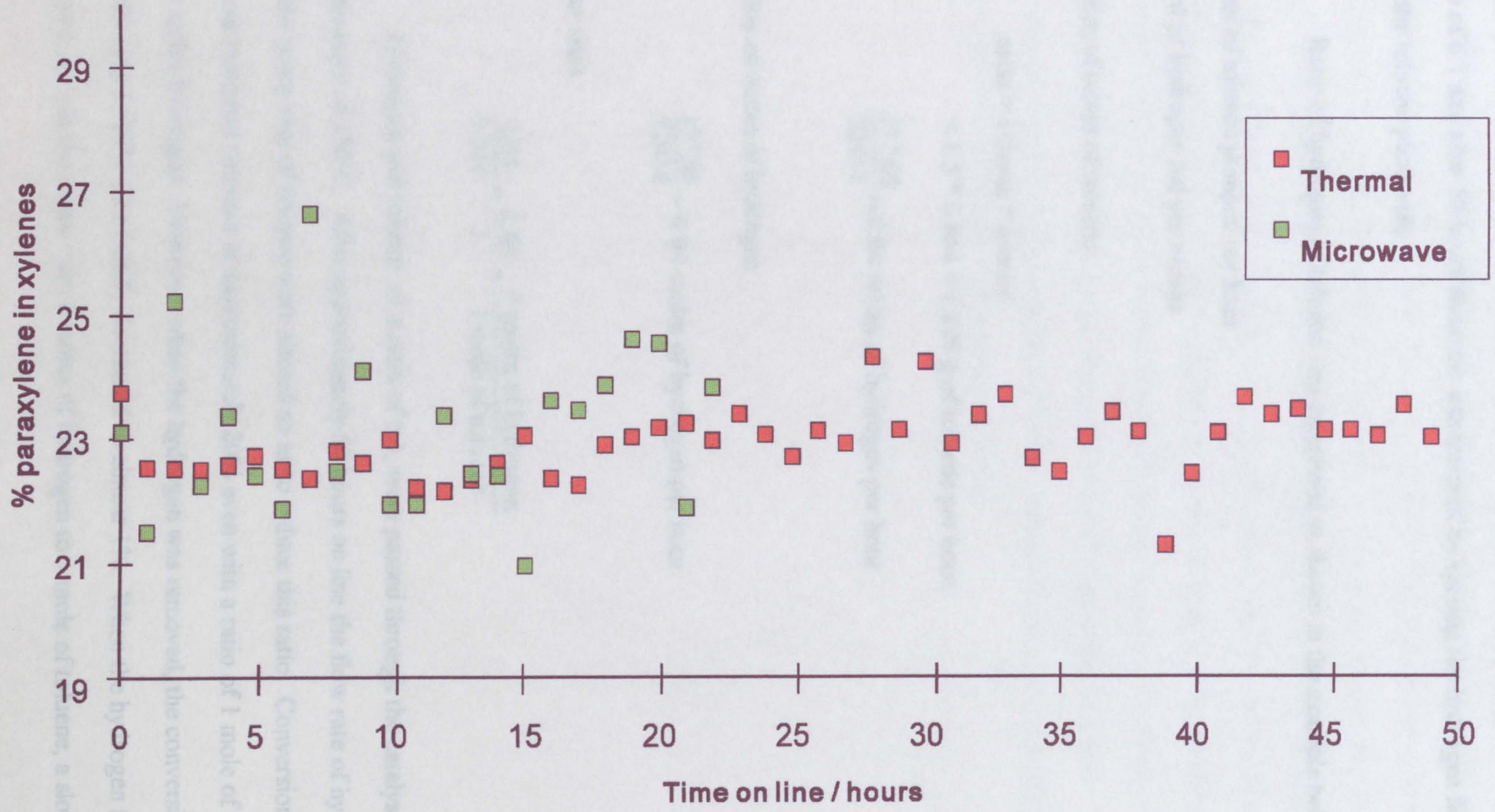

Figure 3.21. Selectivity to paraxylene from disproportionation of toluene over hydrogen mordenite (BDH) under thermal and microwave conditions at 425 °C.

3.3.2.3. Thermal experiments at high pressure.

Figure 3.22 presents the results of an extended experiment on hydrogen mordenite (BDH). Experiments were conducted using an initial hydrogen to toluene ratio of 6:1 and after 50 hours this ratio was lowered by varying the hydrogen flowrate and the toluene pump rate.

Ratio of hydrogen of toluene was calculated as shown in the example below.

1.5 ml of toluene pumped per hour.

15 ml of hydrogen fed per minute.

number of moles of toluene

mass = volume * density

= 1.5 * 0.866 = 1.299 g of toluene per hour. (3.13).

$$\frac{15*60}{22414} = 0.04 \text{ moles of hydrogen per hour} \qquad (3.14).$$

number of moles of hydrogen

$$\frac{15*60}{22414} = 0.04 \text{ moles of hydrogen per hour} \qquad (3.15).$$

Molar ratio

$$\frac{0.04}{0.014} = \frac{2.86}{1} = \frac{3 \text{ moles of hydrogen}}{1 \text{ mole of toluene}} \qquad (3.16).$$

Hydrogen and toluene, at a ratio of 6:1, were passed through the catalyst bed at a temperature of 350°C. After approximately 50 hours on line the flow rate of hydrogen and the pump rate of toluene were altered so as to reduce this ratio. Conversion of toluene remained constant at approximately 20% even with a ratio of 1 mole of toluene to ¾ moles hydrogen. However, when the hydrogen was removed, the conversion initially rose to 26% then rapidly decreased to almost 1%. When the hydrogen flow was returned, as was the molar ratio 6 moles of hydrogen to 1 mole of toluene, a slow rise in

toluene conversion was observed. An increase in temperature to 375°C further increased conversion.

Figure 3.23 presents the results when a similar experiment was performed using hydrogen mordenite (Strem Chemicals) as the catalyst. Hydrogen and toluene were passed over the catalyst at a ratio of 6:1 at 415°C. The experiment was allowed to run for 100 hours and the conversion was constant at 20%. The pump rate of toluene and the flow rate of hydrogen were adjusted so that the molar ratio was decreased to 3:1 and conversion fell to 15%. After several hours there was no change in the conditions so the hydrogen is removed. Again there was an dramatic loss in conversion which was restored by replacing the hydrogen. However previous experiments at lower temperatures showed that a temperature >400°C was needed to restore conversion to the same amount as before the hydrogen was removed.

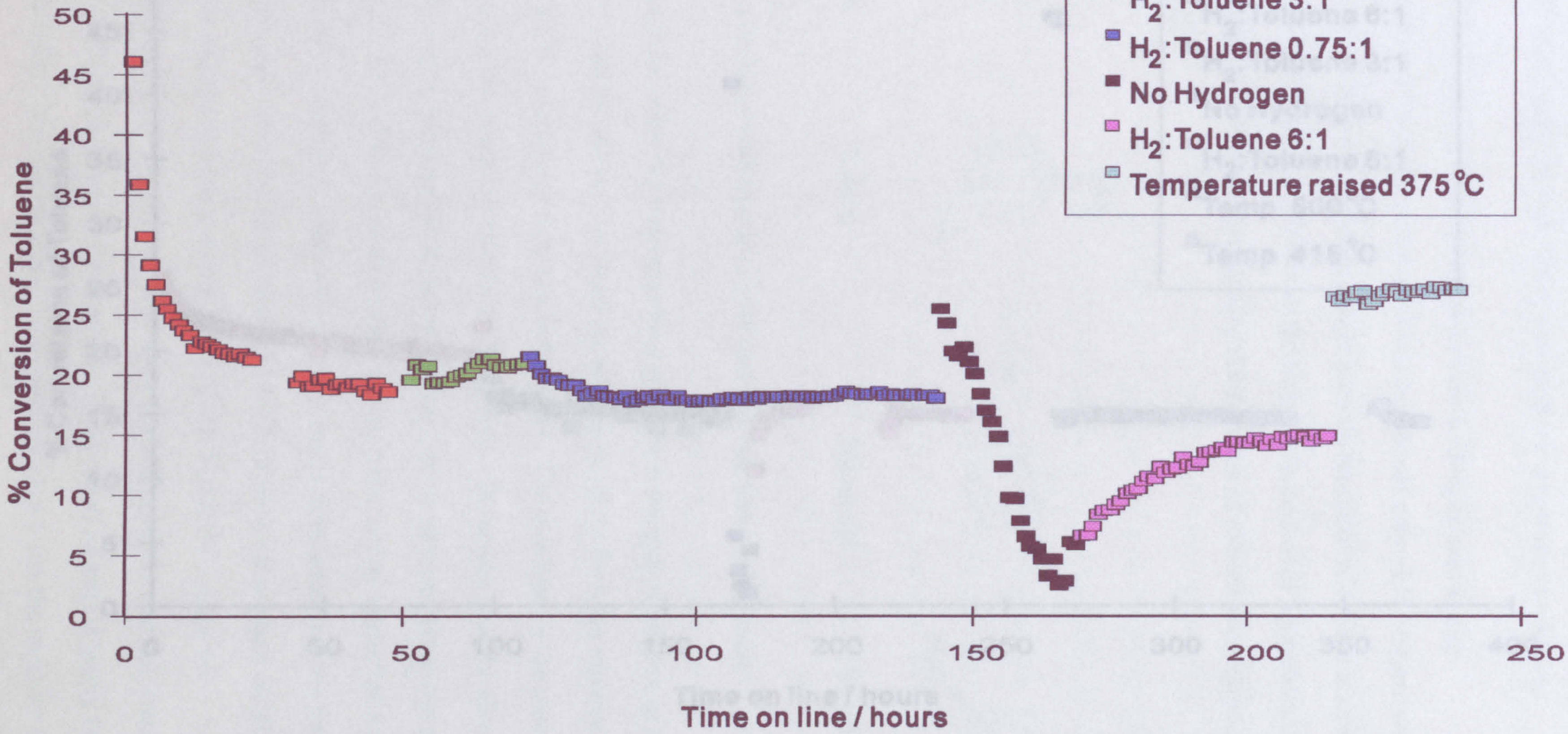

Figure 3.22. Conversion of toluene over hydrogen mordenite (BDH) under various conditions at 350°C.

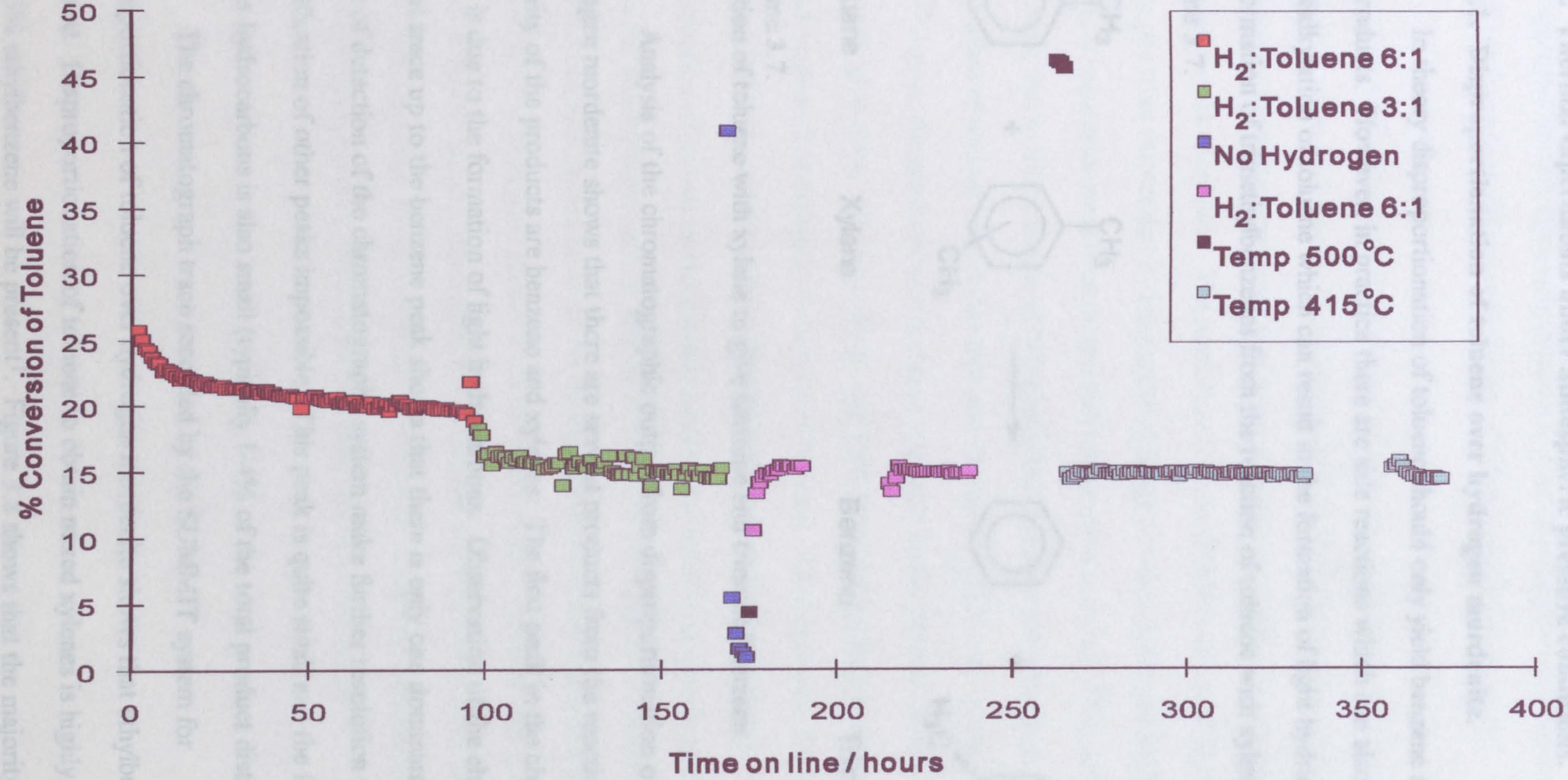

Figure 3.23. Conversion of toluene over hydrogen mordenite (Strem Chemicals) under various conditions at 415°C.

3.4. Discussion.

3.4.1. Thermal experiments under atmospheric pressure conditions.

3.4.1.1. Disproportionation of toluene over hydrogen mordenite.

In theory disproportionation of toluene should only yield benzene and xylenes as the products. However, in practice there are side reactions which can also occur, such as the dealkylation of toluene which can result in the formation of light hydrocarbons and the formation of trimethylbenzenes from the reaction of toluene with xylene as shown in scheme 3.7.

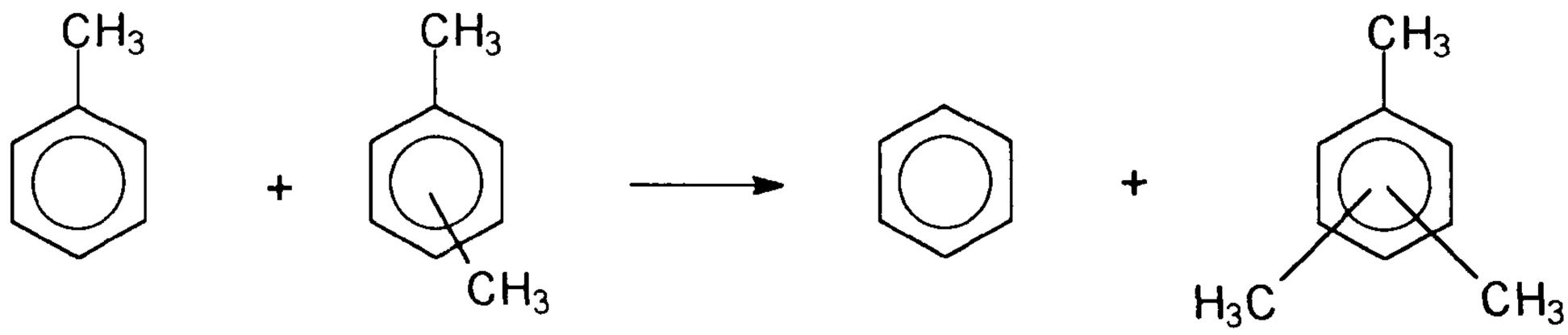

Toluene Xylene Benzene Trimethylbenzene

Scheme 3.7.
Reaction of toluene with xylene to give benzene and trimethylbenzene.

Analysis of the chromatographic output from disproportionation of toluene over hydrogen mordenite shows that there are several products from the reaction. The majority of the products are benzene and xylenes. The first peak in the chromatograph trace is due to the formation of light hydrocarbons. Observation of the chromatographic output trace up to the benzene peak shows that there is only one dominant peak. The limits of detection of the chromatography system make further resolution and identification of other peaks impossible. This peak is quite small and the formation of lighter hydrocarbons is also small (typically 1-4% of the total product distribution).

The chromatograph trace recorded by the SUMMIT system for disproportionation of toluene over hydrogen mordenite shows that ethylbenzene is hardly detected. Disproportionation of toluene to obtain mixed xylenes is highly desirable, as only 3% ethylbenzene will be present[1]. Figure 3.8 shows that the majority of the

products have appeared after 30 minutes of analysis time. However, there is a broad peak, which is just detectable, at 55 minutes. This peak is due to the formation of "heavy ends" typically tri- and tetramethylbenzenes. Each analysis therefore took 60 minutes so that all products from disproportionation of toluene could be analysed.

The results for disproportionation of toluene over hydrogen mordenite (Strem Chemicals) agree with reports in the literature[7,9,42,43,52]. Hydrogen mordenite shows high activity for disproportionation of toluene, however, activity is reduced after several hours on stream of toluene. The experiments using different ratios of N_2:H_2 as the carrier gas have shown that by using pure hydrogen as the carrier gas the lifetime of the catalyst is improved, even though the initial conversion is lower. This can be explained by the fact that in the presence of hydrogen, two reactions are occurring. The first is the dealkylation of toluene to give benzene and methane as products. However, as Bhasker et al.[10] report, the production of methane is usually higher because of the side reaction of toluene to give coke, which combines with hydrogen to give the excess methane. The second reaction is the disproportionation of toluene. After each run, the catalyst was discharged and the colour of the pellets had changed from grey to black. This is due to the formation of carbon on the catalyst surface and within the pore structure. Changing the carrier gas from nitrogen to hydrogen increases the lifetime of the catalyst because hydrogen reduces carbon build-up on the catalyst surface and within the pore structure. Carbonium ions have been shown to be the intermediates for reactions such as coking and disproportionation[7]. Hydrogen mordenite has been shown to have very strong acid sites which have been found to activate hydrogen to reduce the concentration of carbonium ion species on the catalyst and minimise coke formation[53].

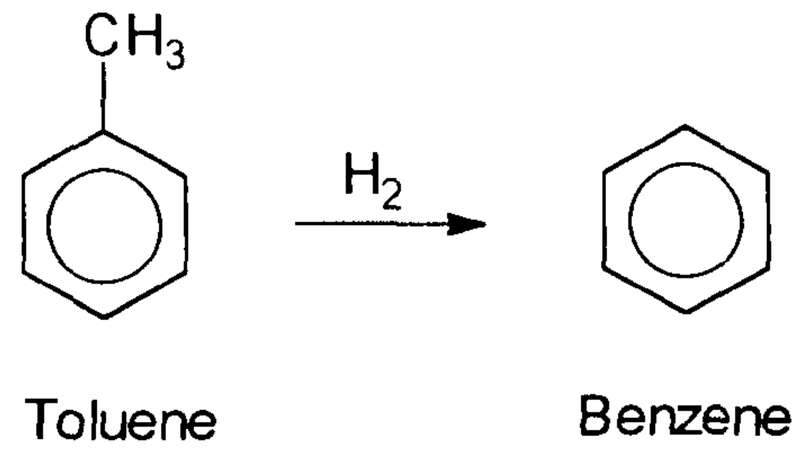

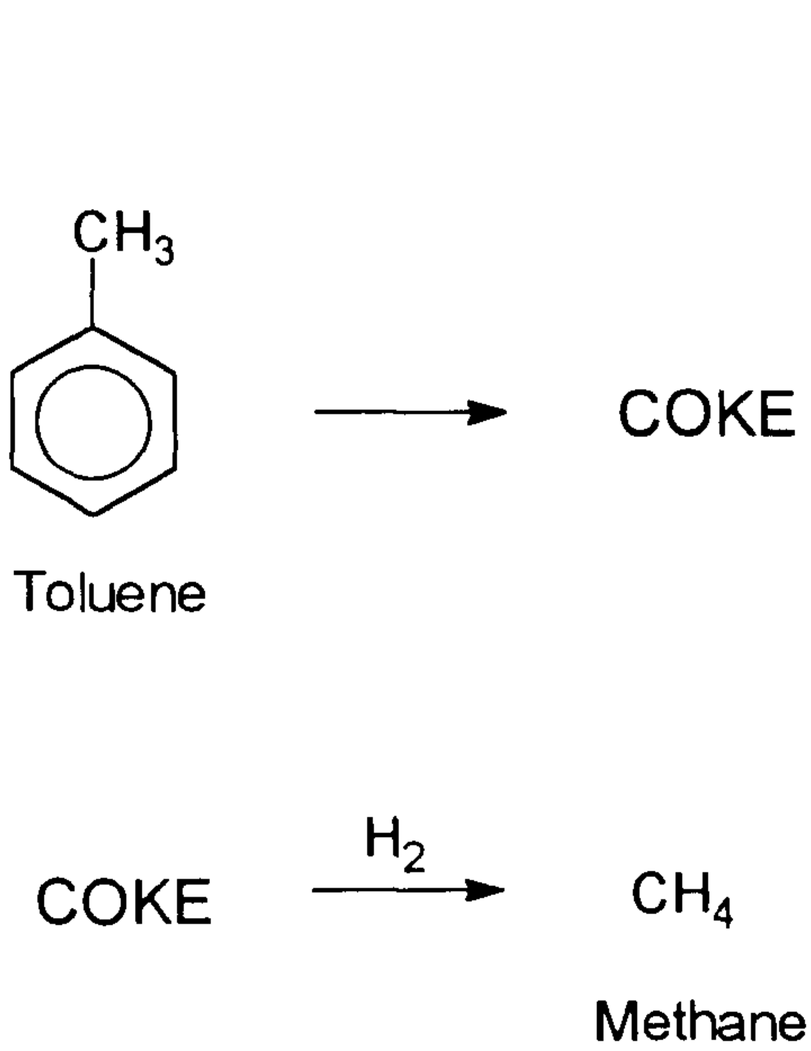

Scheme 3.8.
Reaction of toluene to form coke and reaction of coke with hydrogen to form methane.

The results for disproportionation of toluene over hydrogen mordenite (Strem Chemicals) at first appear to differ from the literature. The thermodynamic equilibrium value for disproportionation of toluene is ≈60% (table 3.1)[5]. The ICI toluene disproportionation plant at North Tees works operates at 49% conversion. The results from the Strem mordenite seem to indicate that the thermodynamic conversion is being exceeded (>65%). At the beginning of the experiment the activation energy was 90 kJ mol^{-1} which differs from the literature value of approximately 60 kJ mol^{-1} [9-10, 29]. However, although the toluene conversion initially was in excess of 60%, analysis of the distribution of products under these conditions showed that there was an excess of cracking products and benzene during the first few hours of toluene on stream. This seems to indicate that there is a dealkylating reaction occurring simultaneously with the disproportionation reaction. Observation of the benzene to xylene ratio shows that after a few hours on line the ratio was approximately 1.1 to 1. At this point the conversion of

toluene had decreased corresponding to the expected thermodynamic value and the activation energy was found to be 63 kJ mol^{-1}.

The results agree with the literature that conversion of toluene increases with increasing temperature[42]. The optimum temperature for conversion of toluene over mordenite (Stem Chemicals) was 425°C. At this temperature the conversion was high and declined more slowly than the experiments performed at lower temperatures. Experiments conducted at 450°C show that although the conversion was initially comparable to the experiments at 425°C, the conversion more quickly declined. Bharati et al.[7] on their studies on hydrogen mordenite, assumed that the coke formation was parallel with the main disproportionation reaction and formulated a relation between the constants of the deactivation rate equation and temperature which showed that the deactivation rate is more sensitive to temperature compared with the main reaction. They calculated that the activation energy for deactivation of the catalyst was 20 kJ mol^{-1} which suggests that the deactivation is rapid. Above 450°C, there is competition between the disproportionation reaction and the dealkylation reaction[43].

In the disproportionation of toluene a mixture of the three xylene isomers is produced, the equilibrium distribution of the isomers is 22% orthoxylene, 54% metaxylene and 24% paraxylene according to Allen and Yats[32]. In the thermal experiments, conducted on hydrogen mordenite (Strem Chemicals and BDH), the selectivity to paraxylene did not exceed the thermodynamic equilibrium.

The experiments on disproportionation of toluene using hydrogen mordenite have been carried out on two different types of mordenite as supplied by the distributors (BDH and Strem Chemicals). The differences are detailed in table 3.2. Toluene conversion is initially higher on the Strem mordenite however, after 40 hours on line, the conversion is approximately the same for both catalysts. The rate of deactivation is less dramatic in the BDH catalyst compared to the Strem. This is more apparent at the higher temperatures. Conversion declines at a faster rate for the Strem catalyst which is run at a temperature of 450°C compared to the BDH catalyst. The major difference between the mordenite samples is the silicon to aluminium ratio. The BDH mordenite has

a Si/Al ratio of 20 while the Strem mordenite has a Si/Al ratio of 10. The Strem mordenite contains more aluminium than the BDH mordenite. Experiments using catalysts with lower Si/Al ratios have shown that the conversion is significantly higher using these catalysts[7, 46-47]. However, analysis of the product distribution show that with these higher conversions the benzene to xylene ratio is >1 indicating that side reactions such as dealkylation of toluene is also taking place. Dealkylation reactions have been shown to take place on high strength Bronsted acidic sites[35, 40]. Increasing the aluminium content of the catalyst is believed to lead to an increase in acidity due to the formation of superacid sites. This is due to extra lattice aluminium species which increase with increasing concentration of aluminium. Coking is also known to take place on high strength Bronsted acid sites[54], so the results obtained from the thermal experiments performed on the mordenite catalysts agree with literature results. Experiments using aluminium deficient mordenites[42] on such reactions as cracking of cumene, hydrocracking, hydroisomerisation of cyclohexane and n-pentane, cracking of hexane and toluene disproportionation have shown that the rate of decline of catalytic activity has been much lower than when compared to the parent mordenite. The explanation for this improvement could be due to the dealumination of mordenite which decreases the resistance to diffusion, therefore the rate of desorption of the products responsible for coke formation is higher. Bierenbaum et al.[55] have explained that the activity of aluminium deficient mordenite is higher than parent mordenite because of the location of the active sites in the mordenite. In the aluminium-deficient mordenites the alumina tetrahedra are further apart when compared to the parent mordenite. Protons are associated with these tetrahedra so the active sites are more dispersed. Therefore, the concentration of active sites near pore mouths is greater in the parent mordenite, thus providing a lower energy path for reaction (and deactivation). This means that the pores are more likely to be blocked in the parent mordenite and hence it is deactivated more quickly than the aluminium deficient mordenite.

3.4.1.2. Disproportionation of toluene over HZSM-5.

The experiments from disproportionation of toluene over HZSM-5 (BDH) have shown that the catalyst is quite different to the mordenite catalyst. The conversion is much lower (17% at 500°C, 24% at 550°C and 33% at 600°C) but this conversion is maintained even after 70 hours on line while experiments on the mordenite catalyst have shown that the conversion is reduced drastically after the same amount of time (to 20%). However, when the catalyst was discharged from the reactor after each experiment, the colour of the spheres was black. The activation energy calculated was 50 kJ mol^{-1} which is lower than some calculated values from toluene disproportionation[6-7] on ZSM-5 but agrees with other calculated values[11].

These results agree with experiments in the literature[26]. Conversion increases with increasing temperature, however, the mole ratio of benzene to xylene also increases with temperature due to dealkylation of toluene. The other minor reaction is the transalkylation reaction to give trimethylbenzene. This is only observed in trace amounts. The selectivity to paraxylene was always at the thermodynamic equilibrium value of 24%.

The reason why no decline was seen in the conversion of toluene in the experiments on disproportionation of toluene over HZSM-5 compared to the mordenite catalysts is the absence of coking within the pore structure of the ZSM-5 catalyst. The channel system in mordenite is essentially two dimensional with elliptical 12 ring apertures, whereas ZSM-5 has two types of channels, with ten ring apertures. One channel system is sinusoidal and has a circular cross section (5.4 x 5.6 Å). The other channel system has elliptical openings (2.2 x 5.8 Å), which are straight and perpendicular to the other channel system. Thus, ZSM-5 has a smaller pore size than mordenite and other larger pore size zeolites as indicated in table 3.7.

Table 3.7.
Pore diameters in zeolites[56].

No of tetrahedra in ring	Maximum free diameter (Å)	Example
6	2.8	
8	4.3	Erionite, A
10	6.3	ZSM-5, Ferrierite
12	8.0	L, Y, Mordenite
18	15	Not yet observed

Typical hydrocarbon dimensions: Benzene = 5.7 x 2.2 Å; n-hexane = 3.5 x 4.2 Å.

Although disproportionation of toluene over ZSM-5 has side reactions occurring, such as dealkylation of toluene and cracking of toluene to give coke[10], the formation of coke is not as drastic in ZSM-5 than in large pore zeolites such as mordenite, because the pores are too small for the formation of the coke precursors. Dejaifve et al.[57] have found that coke forms on the outer the surface of ZSM-5, not within the pore structure, whereas in mordenite, most of the coke is formed within the pores (figure 3.24).

An intensive study of the formation of carbonaeous products (coke) in zeolites have been performed[57-64]. Rollman et al.[58-61] have shown that the most important stage in the formation of coke in large pore zeolite is alkylation of aromatics. The alkyl aromatics cyclise or condense into fused ring polycyclics which will dehydrogenate to coke. Magnoux et al.[65] have investigated the formation of coke during transformation of toluene on HZSM-5 and have reported that the rate of formation and nature of the coke products depends on the temperature. At low temperature (120°C) coke molecules result from condensation, while at high temperature (450°C) alkylation, cyclisation and hydrogen transfer reactions are involved; the rate of coke formation is greater at higher temperature. They have proposed a mechanism of the formation of alkylpyrenes at high temperatures.

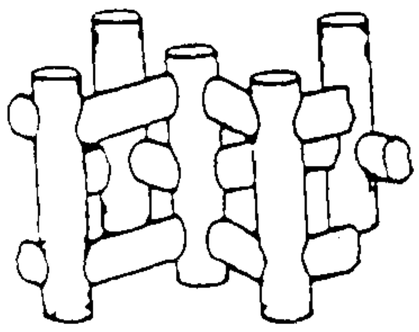

(a)

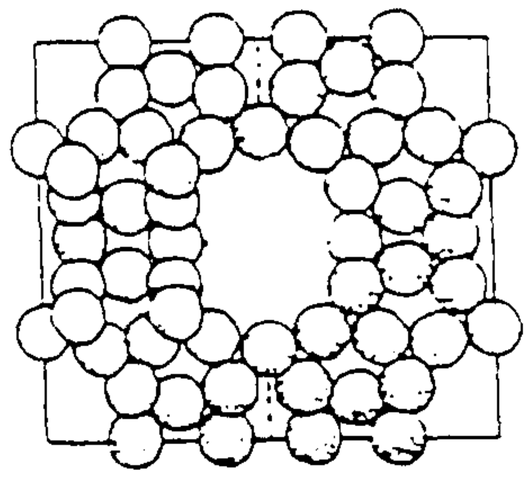

(b)

Structure of (a) ZSM-5 (b) mordenite

A. Pentasil zeolites

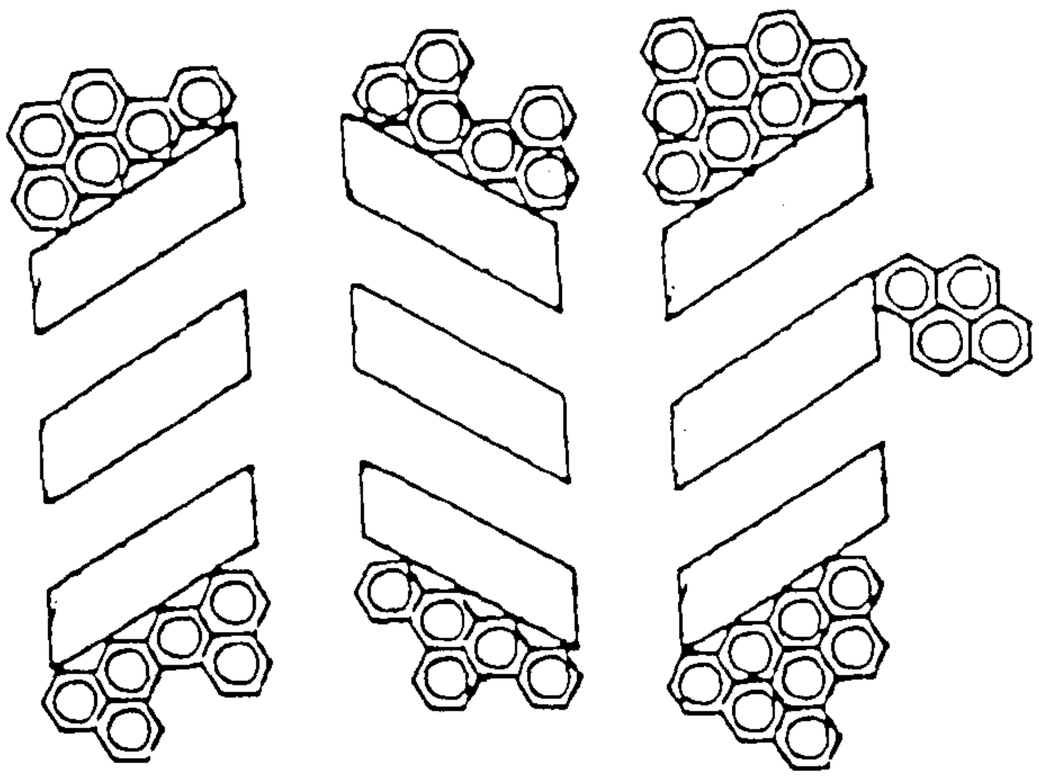

B. Mordenite (and other large pore zeolites).

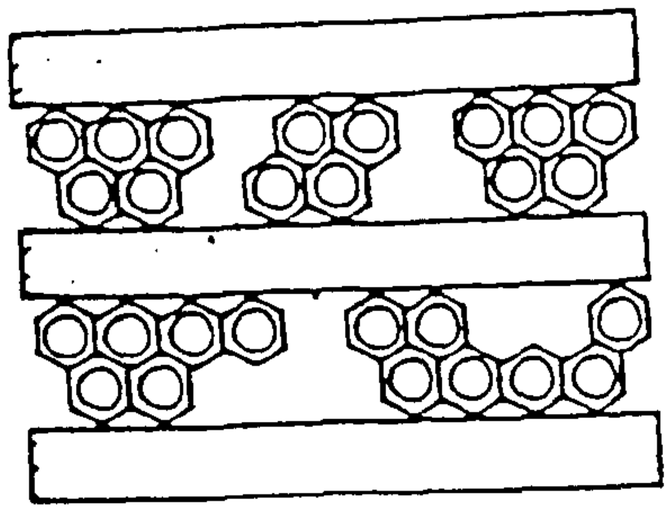

Figure 3.24. Coke formation in zeolites.

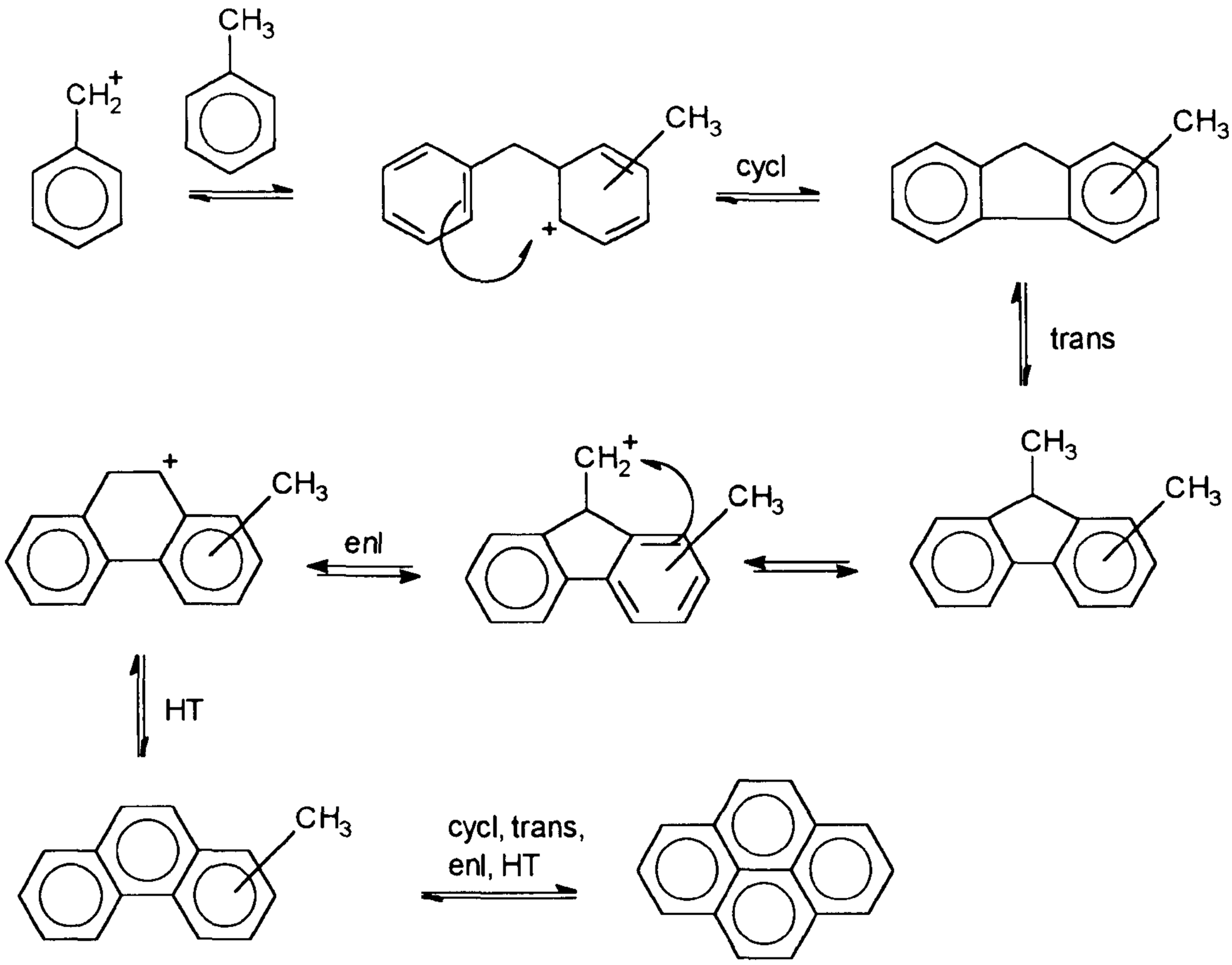

cycl: cyclisation
trans: transalkylation
enl: enlargement of ring
HT: hydrogen transfer

Scheme 3.9.
Mechanism for coke formation during transformation of toluene[65].

The selectivity to paraxylene was always at its thermodynamic equilibrium value of 24% over HZSM-5; this is in agreement with the literature [26, 39-40, 66]. Enhancement of selectivity to paraxylene over ZSM-5 has been obtained by modification of the zeolite. The relative rate of isomerisation of xylenes is 1000 times greater than disproportionation of toluene[66]. Benzene diffuses out of the pores rapidly while the xylenes isomerise rapidly within the pore structure. Paraxylene diffuses more rapidly than meta- or orthoxylene so further isomerisation of ortho- and metaxylene to paraxylene occurs before they escape the pore system. Enhancement of paraxylene can be obtained by introducing steric effects in the pore structure by incorporation of modifiers. This further reduces the diffusion of meta- and orthoxylene, which undergo isomerisation to produce paraxylene.

3.4.2. Microwave experiments under atmospheric pressure conditions.

3.4.2.1. Disproportionation of toluene over hydrogen mordenite.

The experiments for disproportionation of toluene over hydrogen mordenite under microwave irradiation have been disappointing. Conversion of toluene is very erratic and is less as compared to experiments carried out under normal thermal conditions. The majority of the product under microwave conditions is benzene and lighter hydrocarbons. There is only a very small amount of xylenes in the product distribution.

However, observation of the product distribution shows that the initial conversion is comparable to experiments carried out under thermal conditions, especially at the higher temperatures (400, 425 and 450°C). The decline in conversion is at first gradual for the first few hours on line, and then a dramatic loss in conversion is observed and the conversion is very erratic. This implies that after a few hours the interaction of the microwaves with the catalyst is different to the start of the experiment; this is confirmed with observation of the interaction of microwaves with the catalyst. At the start of the experiment the catalyst is activated overnight under flowing nitrogen at 450°C under normal thermal conditions. The reactor is transferred to the single mode cavity and heated under microwave irradiation to the reaction temperature. This is very difficult; heating hydrogen mordenite to temperatures above 200°C under microwave irradiation is very time consuming. The experiments are performed in the single mode cavity since heating mordenite, in the hydrogen form, above 300°C in a microwave oven proved very difficult (as observed by Whittington and Milestone[67]). The dielectric properties of the mordenite are such that it will only absorb microwave energy efficiently when the temperature is above 200°C. Above 200°C heating the catalyst to reaction temperature is relatively easy in the single mode cavity, however, care must be taken so that a thermal runaway does not occur (see section 2.1.2.8.).

When the catalyst is heated to reaction temperature, toluene in hydrogen is passed through the catalyst and reaction commences. As outlined earlier, one of the side reactions of the disproportionation of toluene is the formation of coke within the pore

structure and on the surface of the catalyst. Thus, a carbon laydown on the catalyst commences which leads to deactivation. However, carbon is an excellent absorber of microwave irradiation [68-71], so after a few hours on line, the amount of carbon on the surface of the catalyst is enough to interact with the microwave radiation. The carbon gets hot, thus raising the temperature of the catalyst. Observation indicates that microwaves are being adsorbed by the carbon and the carbon is being burnt off as methane (carrier gas is hydrogen). Temperature measurement under these conditions is a problem. As the carbon gets hot, the infrared pyrometer fails to record accurately the temperature of the catalyst. Observation of the catalyst under these conditions shows that the catalyst is glowing (temperature >500°C). Figure 3.25 is a graph of light emission against wavelength for blackbody radiation spectra. The peak for 773 K has its maximum at 3.5μm while the pyrometer has a range from 8 to 12μm so when the sample is glowing, the pyrometer fails to read the temperature correctly and records that the temperature of the catalyst has dropped (due to radiation emission in the visible part of the spectrum). The computer controls the microwave power by analysing the signal from the pyrometer and adjusting the power accordingly. However, the pyrometer responds very quickly to changes in temperature so the program was modified to drop the power if a temperature in excess of 460°C. When this happens the catalyst's temperature decreases until the power is restored to keep the catalyst at the required temperature. This results in the temperature of the catalyst, (as read by the infrared pyrometer) oscillating around a fixed temperature, resulting in the spiky trace, being observed. The results are very erratic under these conditions because the conversion of toluene depends on the temperature of the catalyst when the contents of the sample are injected into the gas chromatograph.

However, the conversion is always lower than the corresponding thermal experiment. The distribution of products, under these conditions, shows that the majority of the products are benzene and methane indicating that the temperature of the catalyst is significantly higher than that measured by the infra-red pyrometer. After several hours under these conditions, the oscillation decreases, where the pyrometer is recording the temperature accurately.

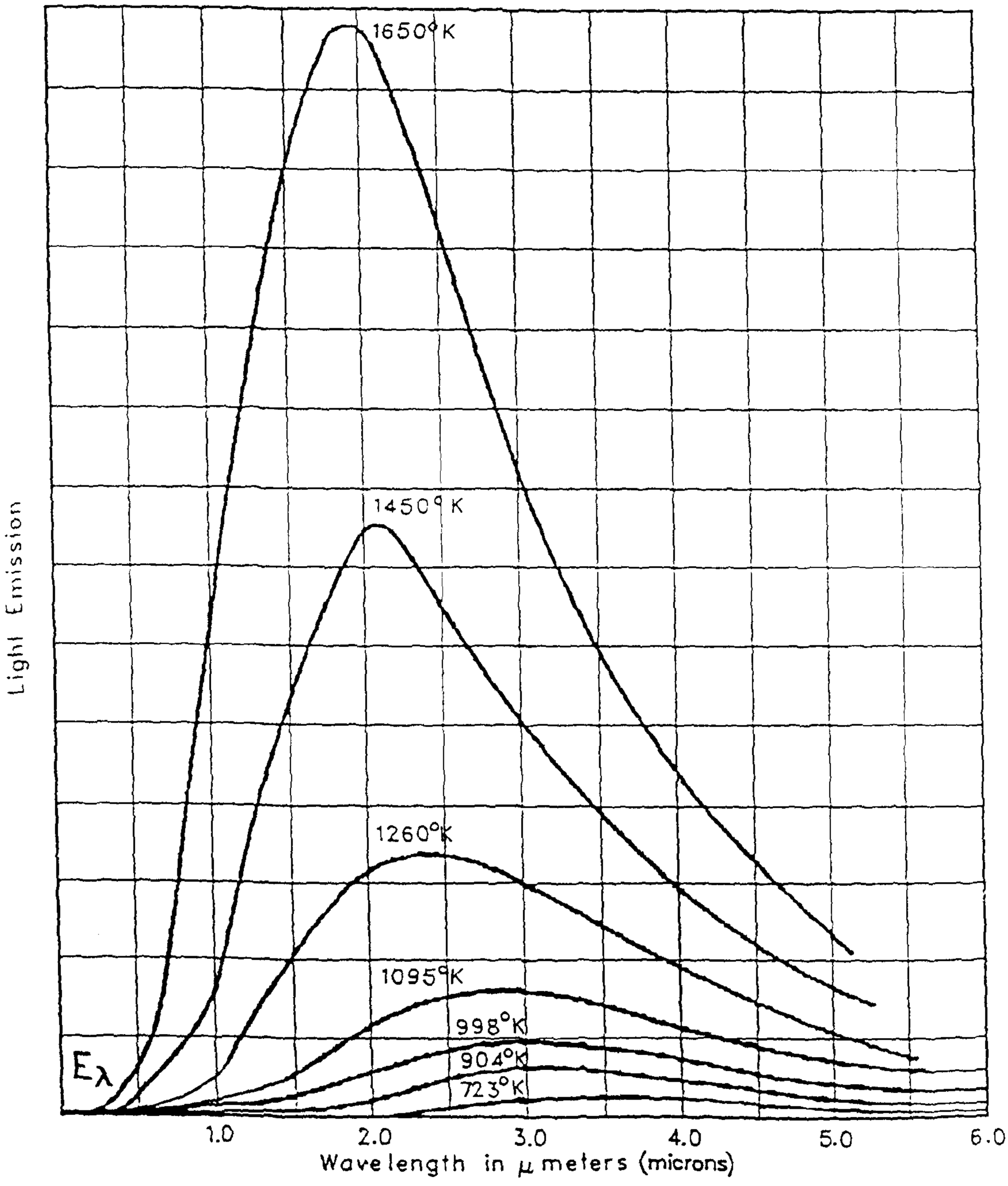

Figure 3.25. Black body radiation.

This indicates that carbon has been burnt off the surface of the catalyst. However, further analysis shows that conversion is very low, and after a few hours the spiky trace is again observed, indicating that the carbon laydown had increased.

At the end of the day, the flow of toluene and the microwave power is switched off and the catalyst is allowed to cool to room temperature under hydrogen. At the start of the next day there is relatively little problem heating the sample to reaction which means that the dielectric properties of the catalyst had altered from the start of the experiment. Observation of the catalyst sample when the reactor is removed from the single mode cavity showed that some of the spheres had fused together and that in some cases there was distortion of the reactor, indicating that a very high temperature had been attained. Thermal experiments were performed using the same conditions for experiments under microwave irradiation to see if there was any deactivation in the catalyst by allowing it to cool to room temperature. The results are shown in figure 3.26 and show that the conversion is not affected by having the catalyst at room temperature overnight under flowing nitrogen.

3.4.2.2. Disproportionation of toluene over HZSM-5.

Because the infrared pyrometer is failing to read the temperature of the catalyst when a significant amount of carbon laydown produces a rapid rise in temperature, experiments were performed using the gas thermometer. The temperature is read by both devices and the results (table 3.6) show that there was a significant difference in temperature recorded by each device. There is an enhancement in selectivity to paraxylene, but as the amount of xylenes is very small (majority of products being benzene and methane) there are problems in detecting the formation of xylenes. However, the temperature recorded by the gas thermometer was erroneous as the experiment proceeded because when the thermometer was recalibrated there was a significant drop in the signal indicating that there was a leak in the gas thermometer system. Therefore the temperature of the catalyst was substantially in excess of the measured temperature by both devices and dealkylation of toluene was occurring.

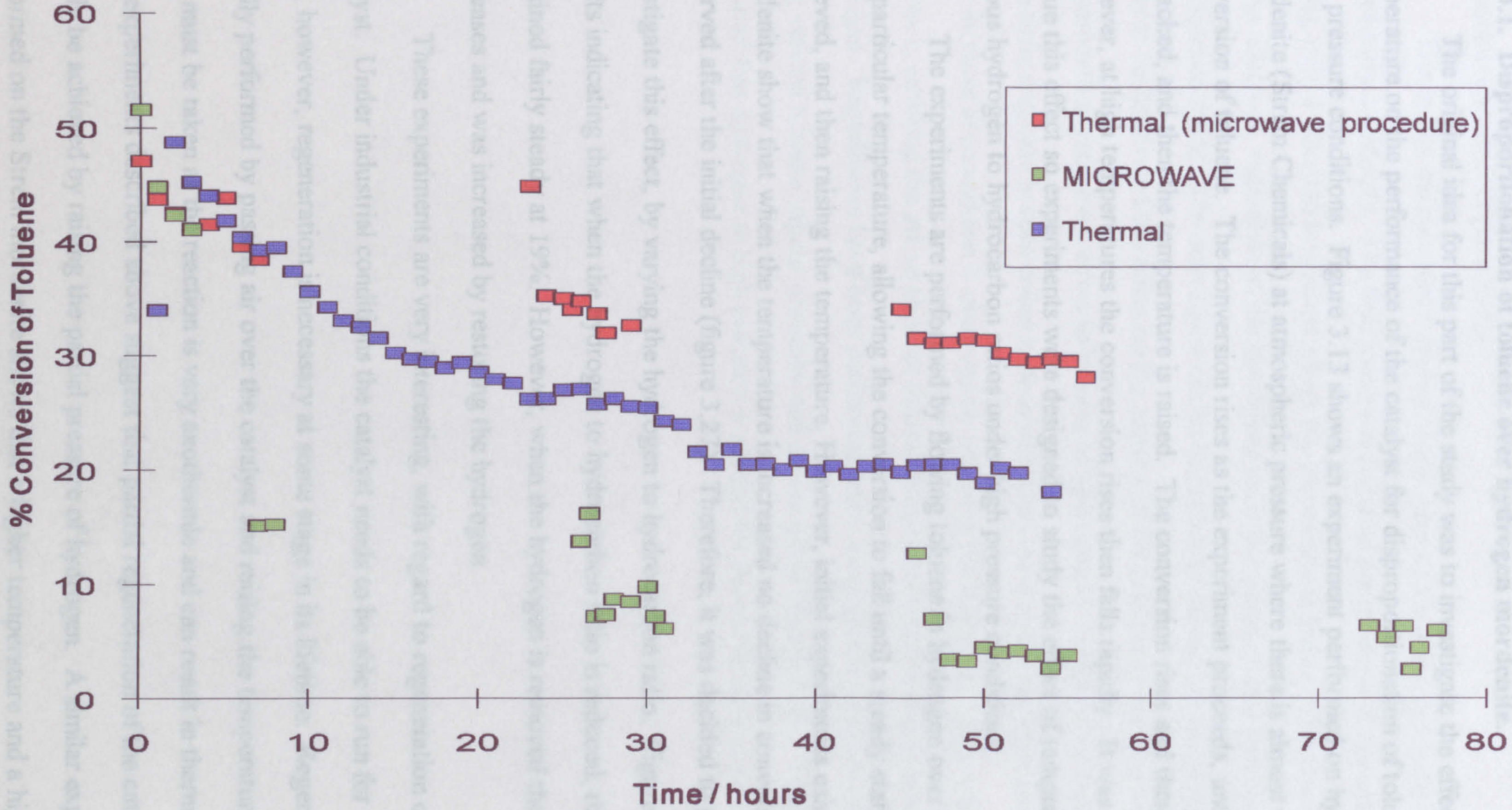

Figure 3.26. Toluene Disproportionation over hydrogen mordenite (BDH) under different conditions at 450°C.

3.4.3. Thermal experiments under high pressure conditions.

3.4.3.1. Disproportionation of toluene over hydrogen mordenite.

The original idea for this part of the study was to investigate the effect of temperature on the performance of the catalyst for disproportionation of toluene under high pressure conditions. Figure 3.13 shows an experiment performed on hydrogen mordenite (Strem Chemicals) at atmospheric pressure where there is almost no conversion of toluene. The conversion rises as the experiment proceeds, until a plateau is reached, and then the temperature is raised. The conversion rises and then levels off, however, at high temperatures the conversion rises then falls rapidly. It was decided to pursue this effect so experiments were designed to study the effect of temperature under various hydrogen to hydrocarbon ratios under high pressure conditions.

The experiments are performed by flowing toluene in hydrogen over the catalyst at a particular temperature, allowing the conversion to fall until a steady state was achieved, and then raising the temperature. However, initial experiments using BDH mordenite show that when the temperature is increased no decline in conversion is observed after the initial decline (figure 3.27). Therefore, it was decided to proceed to investigate this effect, by varying the hydrogen to hydrocarbon ratio. Figure 3.22 shows results indicating that when the hydrogen to hydrocarbon ratio is reduced, the conversion remained fairly steady at 19%. However, when the hydrogen is removed the conversion decreases and was increased by restoring the hydrogen.

These experiments are very interesting, with regard to regeneration of the catalyst. Under industrial conditions the catalyst needs to be able to run for a very long time, however, regeneration is necessary at some stage in its lifetime. Regeneration is usually performed by passing air over the catalyst and raising the temperature. Extreme care must be taken as the reaction is very exothermic and can result in thermal runaway. The experiments described above suggest that partial regeneration of the catalyst could simply be achieved by raising the partial pressure of hydrogen. A similar experiment performed on the Strem mordenite shows that a higher temperature and a higher hydrogen to hydrocarbon ratio are necessary for this to occur (415°C). This meant that

the Strem mordenite is less active than the BDH mordenite. This is agreement with previous results. Deactivation of the catalyst is due to coking and it occurs more rapidly on more acidic zeolites (low Si/Al).

The results indicate that there are two processes for disproportionation of toluene on hydrogen mordenite. The first process is an initial deactivation of the catalyst due to coking, until a situation is reached where the conversion is stable. This deactivation is always observed, regardless of the conditions used (temperature and hydrogen to hydrocarbon ratio). The conversion can be increased by raising the temperature. There seems to be relatively little effect on the activity of the catalyst by varying the hydrogen to hydrocarbon ratio even down to ¾ mole of hydrogen to 1 mole of toluene. However, a dramatic decrease in conversion is observed when there is no hydrogen present. A slow increase in conversion is observed by restoring the hydrogen. This indicates that toluene is covering the active sites for toluene disproportionation and is removed by hydrogen. Experiments have been performed under atmospheric pressure conditions, using various toluene vapour pressures and carrier gases (figure 3.28). They have indicated that hydrogen at high pressure is needed for the conversion to be restored.

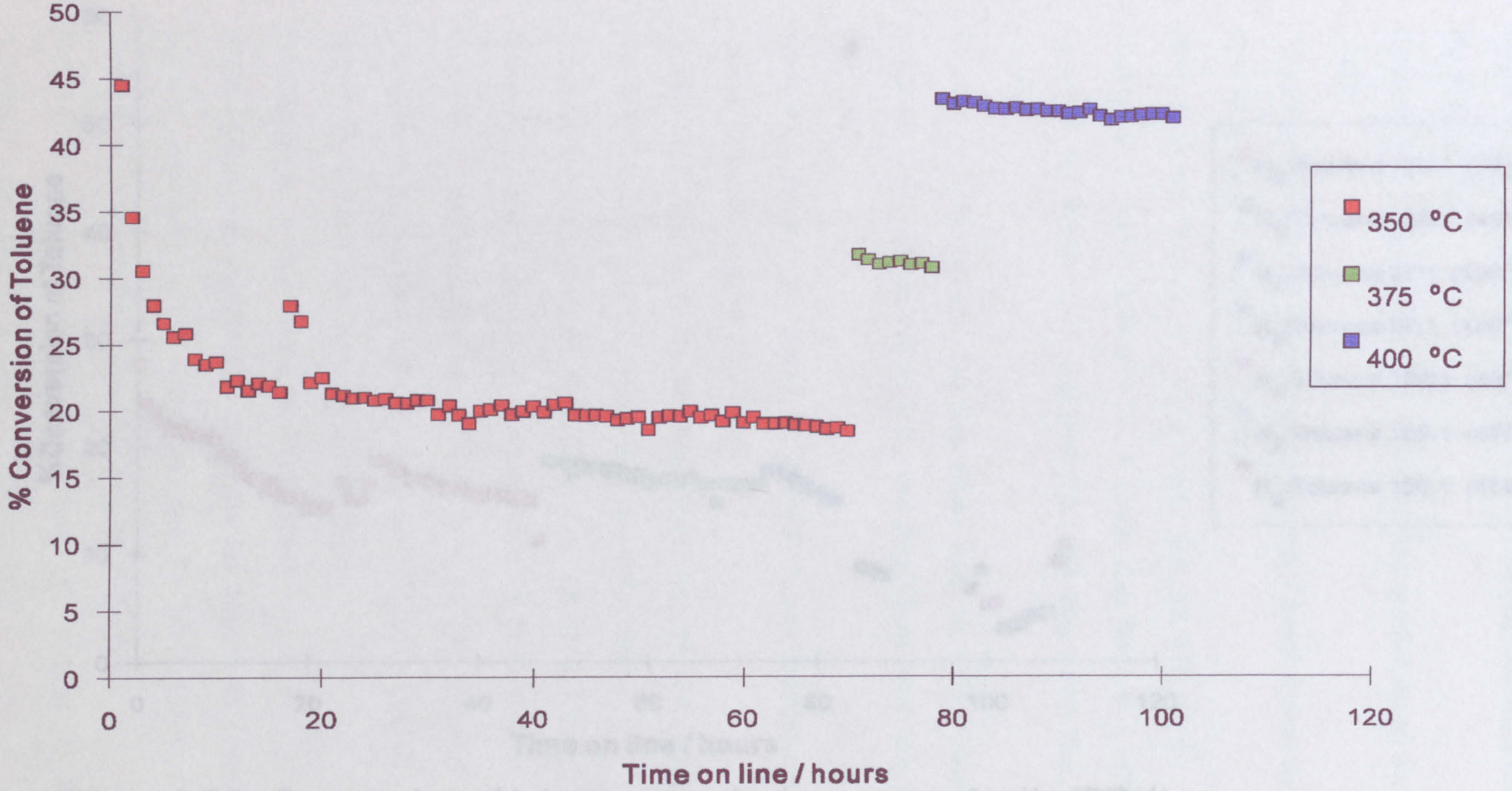

Figure 3.27. Conversion of toluene over hydrogen mordenite (BDH) at high pressure with a hydrogen to hydrocarbon ratio of 6:1.

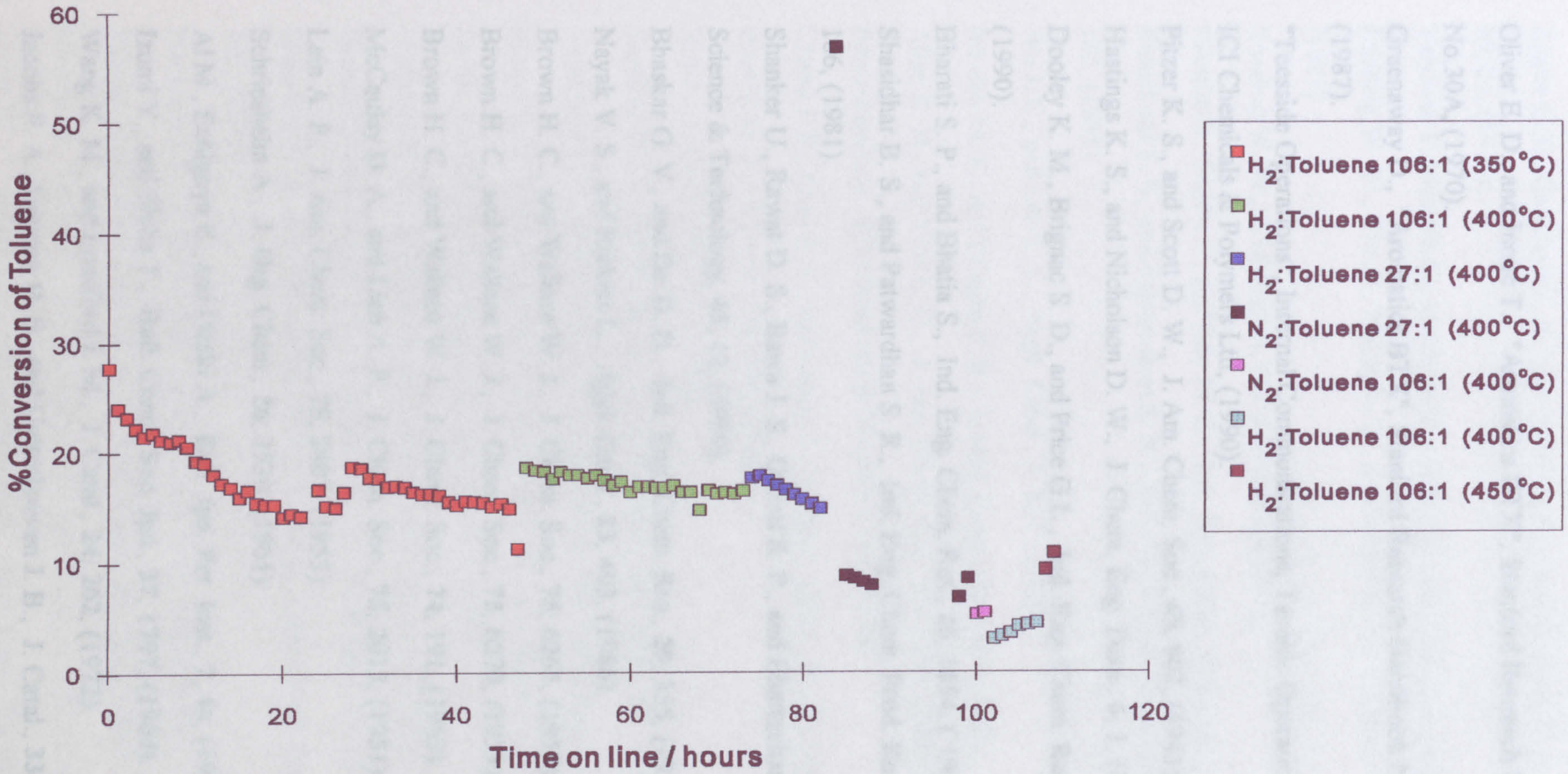

Figure 3.28. Conversion of toluene over hydrogen mordenite (BDH) at atmospheric pressure under various conditions.

3.5. References.

1. Oliver E. D., and Inoue T., "Aromatics BTX", Stanford Research Handbook No.30A, (1970).
2. Greenaway D., "Aromatics BTX", Stanford Research Handbook No.182, (1987).
3. "Teesside Operations", Internal Communications, Teeside Operations, ICI Chemicals & Polymers Ltd, (1990).
4. Pitzer K. S., and Scott D. W., J. Am. Chem. Soc., **65**, 803, (1943).
5. Hastings K. S., and Nicholson D. W., J. Chem. Eng. Data., **6**, 1, (1961).
6. Dooley K. M., Brignac S. D., and Price G.L., Ind. Eng. Chem. Res., **29**, 789, (1990).
7. Bharati S. P., and Bhatia S., Ind. Eng. Chem. Res., **26**, 1854, (1987).
8. Shasidhar B. S., and Patwardhan S. R., Ind. Eng. Chem. Prod. Res. Div., **20**, 106, (1981).
9. Shanker U., Rawat D. S., Bawa J. S., Dabral R. P., and Bhattacharya K. K., Science & Technology, **43**, 12, (1990).
10. Bhaskar G. V., and Do D. D., Ind. Eng. Chem. Res., **29**, 355, (1990).
11. Nayak V. S., and Riekert L., Appl. Catal., **23**, 403, (1986).
12. Brown H. C., and Wallace W. J., J. Chem. Soc., **75**, 6265, (1953).
13. Brown H. C., and Wallace W. J., J. Chem. Soc., **75**, 6279, (1953).
14. Brown H. C., and Wallace W. J., J. Chem. Soc., **74**, 191, (1953).
15. McCaulay D. A., and Lien A. P., J. Chem. Soc., **75**, 2013, (1951).
16. Lein A. P., J. Am. Chem. Soc., **75**, 2407, (1953).
17. Schrieshelm A., J. Org. Chem., **26**, 3530, (1961).
18. Al M., Echlgoya E., and Ozaki A., Bull. Jpn. Pet. Inst., **7**, 46, (1965).
19. Izumi Y., and Shiba T., Bull. Chem. Soc. Jpn., **37**, 1797, (1964).
20. Wang K. M., and Lunsford J. M., J. Catal., **24**, 262, (1972).
21. Jacobs P. A., Leeman H. E., and Uytterhoeven J. B., J. Catal., **33**, 31, (1974).
22. Yashima T., and Hara N., J. Catal., **27**, 329, (1972).

23. Venuto P. B., and Landis P. S., Adv. Catal., **18**, 259, (1965).

24. Aneke L. E., Gerritsen L. A., van den Berg P.J., and de Jong W. A., J. Catal., **59**, 26, (1979).

25. Yashima T.,Moslehi H., and Hara N., Bull. Jpn. Pet. Inst., **12**, 106, (1970).

26. Kaeding W. W., Chu C., Young L. S., and Butter S. A., J. Catal., **69**, 392, (1981).

27. Kaeding W. W., U.S. Patent, No. **4,016,219**, (1977).

28. Mantha R., Bhatia S., and Rao M. S., Ind. Eng. Chem. Res., **30**, 281, (1991).

29. Bhavikatti S. S., and Patwardhan S. R., Ind. Eng. Chem. Prod. Res. Div., **20**, 102, (1981).

30. Wu J. C., and Leu L. J., Appl. Catal., 7, 283, (1983).

31. Ribeiro M. F., and Ribeiro F. R., J. Mol. Catal., **39**, 269, (1987).

32. Allen R. H., and Yats L. D., J. Am. Chem. Soc., **83**, 2799, (1961).

33. Petrochemicals, ICI Chemicals & Polymers Ltd, (1990).

34. Chang J. R., Sheu F. C., and Cheng J. C., Appl. Catal., **33**, 39, (1987).

35. Bhat S. G. T., J. Catal., **75**, 196, (1982).

36. Wei J., J. Catal., **76**, 433, (1982).

37. Kaeding W. W., and Butter S. A., U.S. Patent, No. **3,911,041**. (1975).

38. Kaeding W. W., and Young L. S., U.S. Patent, No. **4,034,053**, (1977).

39. Meisel S. L., McCullough J. P., Lechthaler C. H., and Weisz P. B., Leo. Friend Symp. Am. Chem. Soc. Mtg., Chicago, IL, 74, (1977).

40. Meshram N. R., J. Chem Technol, Biotechnol., **37**, 111, (1987).

41. Gorra F., Breckenridge L.L., and Sailor R. A., Oil & Gas, Oct 12, 60, (1992).

42. Shasidhar B. S., and Patwardhan S. R., Ind. Eng. Chem. Prod. Res. Div., **20**, 102, (1981).

43. Narayanan S., J. Chem. Soc. Farad. Trans., I, **75**, 434, (1979).

44. Ribeiro M. F., and Ribeiro F. R., J. Mol. Catal., **35**, 227, (1986).

45. Manoiu D., Namba S., and Yashima T., Appl. Catal., **1**, 383, (1981).

46. Ugina M. A., Sotelo J. L., and Serrano D. P., Appl. Catal., **76**,183, (1991).

47. Beltrame P., Beltrame P. L., Carniti P., Zuretti G., Leofanti G., Moretti E., and Padovan M., Zeolites, 7, 418, (1987).

48. Schulz-Ekloff G. and Jaeger N. I., Appl. Catal., **33**, 73, (1987).

49. Beltrame P., Beltrame P. L., Carniti P., Forni L., and Zuretti G., Zeolites, **5**, 400, (1985).

50. Yashima T., Sato K., Hayasaka T., and Hara N., J. Catal., **26**, 303, (1972).

51. Kodama H., and Okazaki S., J. Catal., **132**, 512, (1991).

52. Couglan B., and Narayanan S., Chemistry & Industry, 765, (1977).

53. Streitwieser A., and Reif L., J. Am. Chem. Soc., **92**, 3831, (1964).

54. Meshram N. R., Hedge S. G., Kulkarni K., and Ratnasamy P., Appl. Catal., **8**, 359, (1983).

55. Bierenbaum H. S., Partridge R. D., and Weiss A. H., Adv. Chem. Ser., **121**, 605, (1973).

56. Csicsery S. M., Zeolites, **4**, 202, (1984).

57. Dejaifve P., Auroux A., Gravelle P. C., Vedrine J. C., Gabelica Z., Derouane E. G., J. Catal., **70**, 123, (1981).

58. Walsh D. E., and Rollmann L. D., J. Catal., **56**, 195, (1979).

59. Rollmann L. D., J. Catal., **43**, 113, (1977).

60. Walsh D. E., Rollmann L. D., J. Catal., **56**, 139, (1979).

61. Rollmann L. D., Walsh D. E., J. Catal., **56**, 195, (1979).

62. Meinhold R. H., and Bibby D. M., Zeolites, **10**, 146, (1990).

63. Novakova J., and Dolejek Z., Zeolites, **10**, 189, (1990).

64. Nelson P. H., Bibby D. M., and Kaiser A. B., Zeolites, **11**, 337, (1991).

65. Magnoux P., Machado F., and Guisnet M., Proc. 10th Intern. Congr. Catal. Budapest 1992, Part A, p435, Elsevier, Amsterdam.

66. Young L. B., Butter S. A., and Kaeding W. W., J. Catal., **138**, 343, (1992).

67. Whittington B. I., and Milestone N. B., Zeolites, **12**, 815, (1992).

68. Shanley A., Chem. Busin., 43, July August, (1990).

69. Heathcote M., Plastics & Rubber Weekly, 189, 24 July (1989).

70. Zerger R. P., McMahm K. C., Seltzer M. D., Michel R. G., and Suib S. L., J. Catal., **99**, 498, (1986).

71. Bamwenda G., Moore E., and Wan J. K. S., Res. Chem. Interm., **17**, 243, (1992).

Chapter Four.

Toluene Alkylation.

4.1. Introduction.

4.1.1. Microwaves in catalytic reactions.

The basis of this study was to investigate the effect of microwaves on catalytic reactions. It is possible to activate specifically the actual catalytic sites by microwaves and the support matrix should be unaffected[1-9]. This is based on the premise that surface hydroxyl groups will absorb microwaves whereas bulk oxides, in general do not. This hypothesis may be used to affect reactions where both the bulk of the catalyst, the reactants and the products are transparent to microwaves. The reaction chosen for the initial study was the disproportionation of toluene using zeolite catalysts in their hydrogen form. However, the microwave experiments on toluene disproportionation have proved disappointing due to the carbon laydown which absorbs microwaves. It was decided to modify the reaction by the addition of a microwave absorbing reagent, methanol (this could be necessary to "regenerate" the OH groups of the surface of the zeolite). In reactions over catalysts such as SiO_2, Al_2O_3 or zeolites, the OH surface bond is activated by microwaves as a result of its intrinsic dipole moment. If the reaction proceeds via a carbonium ion mechanism (disproportionation of toluene, methylation of toluene), a very large dipole will result. The influence of microwaves on alkylation of toluene with methanol over zeolite catalysts was hoped to be large. It was decided to carry out the next stage of the research by investigating the alkylation of toluene with methanol under thermal and microwave conditions. It was imperative to solve the problem of temperature measurement, so gas thermometry was also employed as a means of measuring the temperature. It was desirable to minimise modification of the equipment, so the initial experiments were performed with an excess of methanol. Results of later experiments necissitated modification of equipment so that alkylation of toluene could be investigated with an excess of toluene.

4.1.2. Alkylation of toluene with methanol.

Of the three isomers of xylenes, the demand for the para-isomer is the greatest. However, in commercial operations such as the disproportionation of toluene, it is usually obtained in a mixture of the three isomers (thermodynamic equilibrium 25% paraxylene, 50% metaxylene, 25% orthoxylene) and thus presents problems in separating the para- isomer from the other isomers and reaction by-products[10-11]. Further production of paraxylene can be obtained by isomerisation of xylenes. Research has been directed at producing paraxylene in excess of its thermodynamic equilibrium value, this has lead to Mobil STDP process (Selective Toluene Disproportionation Process). Paraxylene can also be selectively obtained by alkylation of toluene; alkylation of aromatic hydrocarbons with alcohols was first studied in the late 1800's. However, alkylation of toluene has not been used commercially because the method is not economically viable[10]. Alkylating reagents have included methyl halide, methanol, methyl sulphate, methyl carbonate and methanal. Alkylation using methanal has resulted in a high yield of paraxylene, however, side reactions such as hydrocracking occur. Methanol is the most likely alkylating reagent and has lead to studies using a pilot plant.

4.1.2.1. Industrial Process utilising alkylation of toluene by methanol.

A pilot plant process for alkylation of toluene with methanol to produce xylene has been carried out by Celler and Zyczynnski[10]. The catalyst consisted of 66.3% $H_4P_2O_7$, 29.4% active carbon and 4.3% SiO_2 and was used at a temperature of 360-370°C at a pressure of 34 atmospheres[10]. The toluene to methanol ratio was 2 to 1, (theoretical conversion of toluene is 50%). However, the conversion was very small (12%) and the selectivity to xylenes was lower than the theoretical value. Corrosion of carbon, stainless steel and the acid-resistant ceramic lining was observed in the reactor. The process could not even support the cost of the materials so the study was terminated. However, research is still continuing on alkylation of toluene with methanol investigating conversion and selectivity effects using various catalysts.

4.1.2.2. Chemistry of the reaction.

In the alkylation of toluene with methanol, substitution of the methyl group into toluene is para/ortho orientation and the first stage products are supposed to be para- and ortho isomers (scheme 4.1).

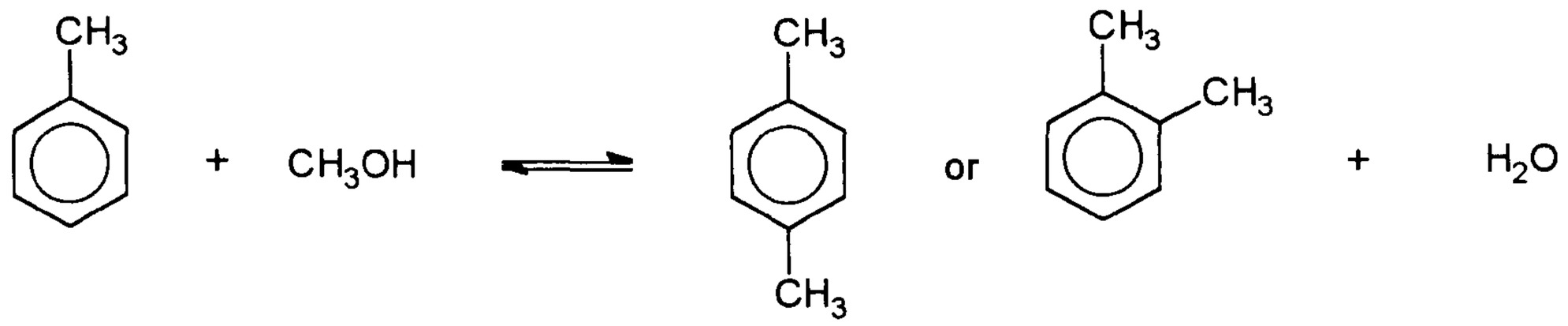

Scheme 4.1.
Alkylation of toluene with methanol to produce para- or orthoxylene and water.

But isomerisation occurs successively or almost simultaneously on acidic catalysts, so a product distribution which corresponds closely to thermodynamic equilibrium (paraxylene 25%, metaxylene 50%, orthoxylene 25%) is achieved

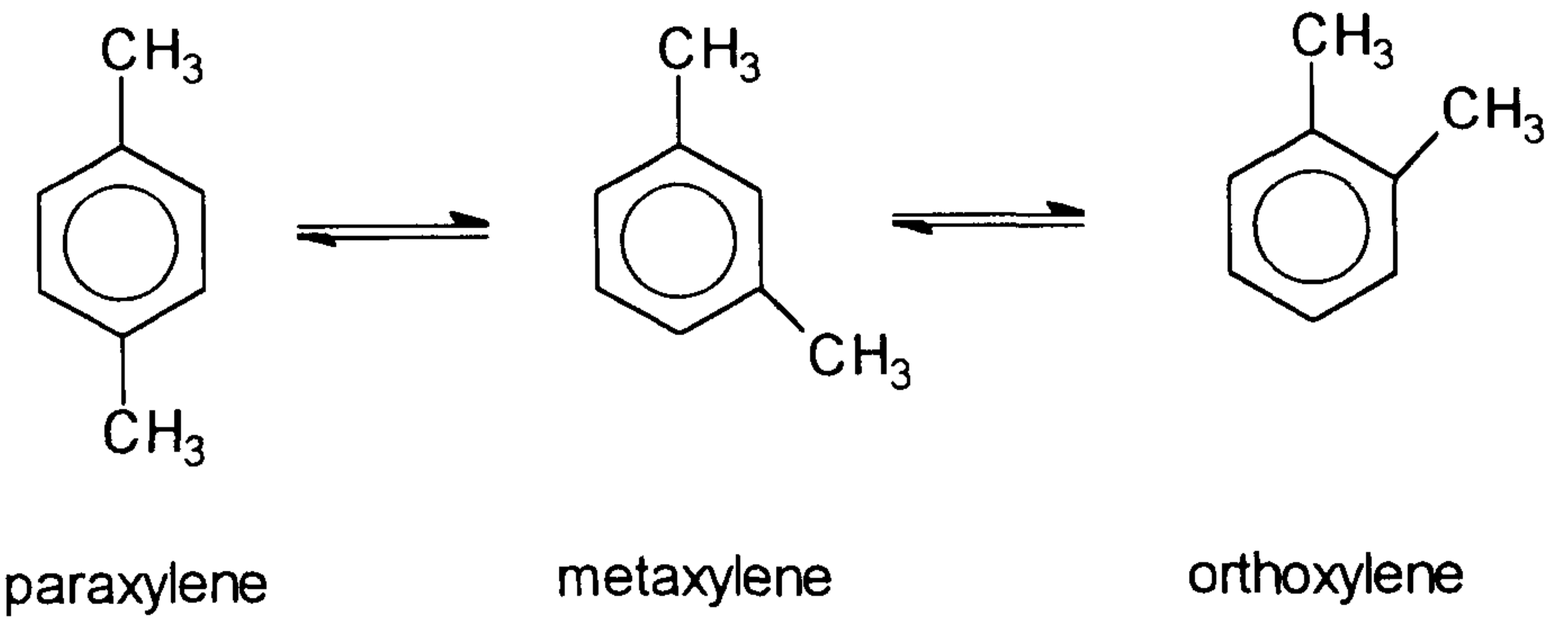

Scheme 4.2.
Isomerisation of xylenes.

There are other side reactions such as dealkylation/disproportionation of toluene, dehydration of methanol, alkylation of xylenes and coke formation. Isomerisation of xylenes has been calculated to be 100 times faster than alkylation of toluene with methanol, which in turn has been calculated to be 10 times faster than toluene disproportionation[14-15]. The Langmuir-Hinshelwood-Hougan-Watson model with dual-site mechanism has been proposed[16-17]. It is believed that for alkylation, both methanol

and toluene will have to move to adjacent sites, while isomerisation can take place on the same site where xylenes are formed[18].

4.1.2.3. Mechanism.

As stated in section 3.1.3.2. the major studies of alkylation reactions catalysed by Friedel-Crafts catalysts were conducted in the 1950's. The different types of complexes formed have been classified as π- and σ-complexes. Several mechanisms have been proposed for alkylation of toluene with methanol with various catalysts[10]. When aluminium chloride is used, the reaction proceeds through the formation of an alkyl halide.

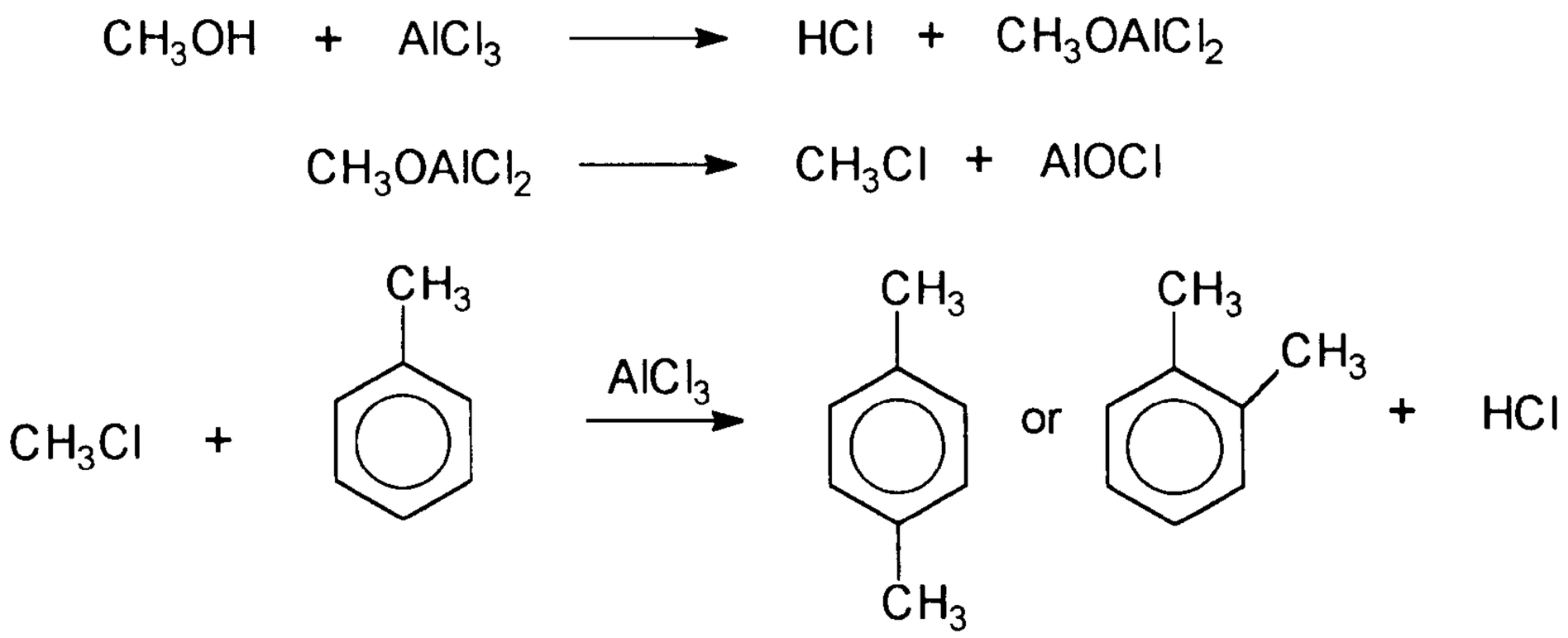

Scheme 4.3.
Mechanism for alkylation of toluene with methanol using Friedel-Craft catalysts[10].

4.1.2.4. Catalysts used for alkylation of toluene.

Research on alkylation of toluene to produce xylenes has been extensive. The catalyst types employed have been Friedel-Crafts, silica-alumina and zeolite types. A summary on the initial research on these catalysts has been conducted by Inoue and Oliver[10].

Alkylation using Friedel-Crafts catalysts presents many difficulties such as the use of special apparatus (corrosion resistant materials), extremely pure starting materials and high pressures[12]. Venuto et al.[19-20] first suggested the possible use of zeolite catalysts for alkylation of aromatic hydrocarbons in the 1960's. Yashima and co-workers[21-22] conducted studies on the alkylation of toluene over zeolite Y in various cationic and decationic forms. Their observations were that selectivity to paraxylene was 46-50% of

the xylene mixture, which exceeded the thermodynamic equilibrium value. When using Mn-Y as a catalyst 50% of the xylene isomers distribution was paraxylene[22]. However, no details were given of the conversion of toluene and methanol or other reaction products. Much attention has been given to alkylation of toluene over ZSM-5 type catalysts. Studies on ZSM-5 [23-25] have revealed that selectivity to paraxylene can be quite high. At low temperatures, (250°C) orthoxylene is the predominantly favoured isomer. However, the selectivity to paraxylene increases with temperature, so at higher temperatures (>400°C) it is the predominantly favoured isomer. This was attributed to the fact at low temperatures, the inner surface of the zeolite pore could not be used efficiently, because the reactants and products needed a higher temperature to go into and out of the narrow pore of ZSM-5. A mechanism for alkylation of toluene with methanol over zeolite catalyst was proposed by Kaeding et al.[25].

In the first stage of the reaction protonation of methanol to form an oxonium ion is proposed. The next stage is the transfer of the methyl group to the aromatic ring and transfer of a proton back to the catalytic site. Alkylation of toluene is believed to be predominant at the para- position due to steric hindrance. However, subsequent isomerisation of paraxylene occurs.

However, most of the studies on zeolite catalyst have shown that conversion of toluene is quite low and deactivation of the catalyst due to coking is a major problem [26-27]. Kinetic studies on alkylation of toluene with methanol using both mordenite and ZSM-5 have revealed that the rate of deactivation is faster when using mordenite and large port zeolites[16, 26-28].

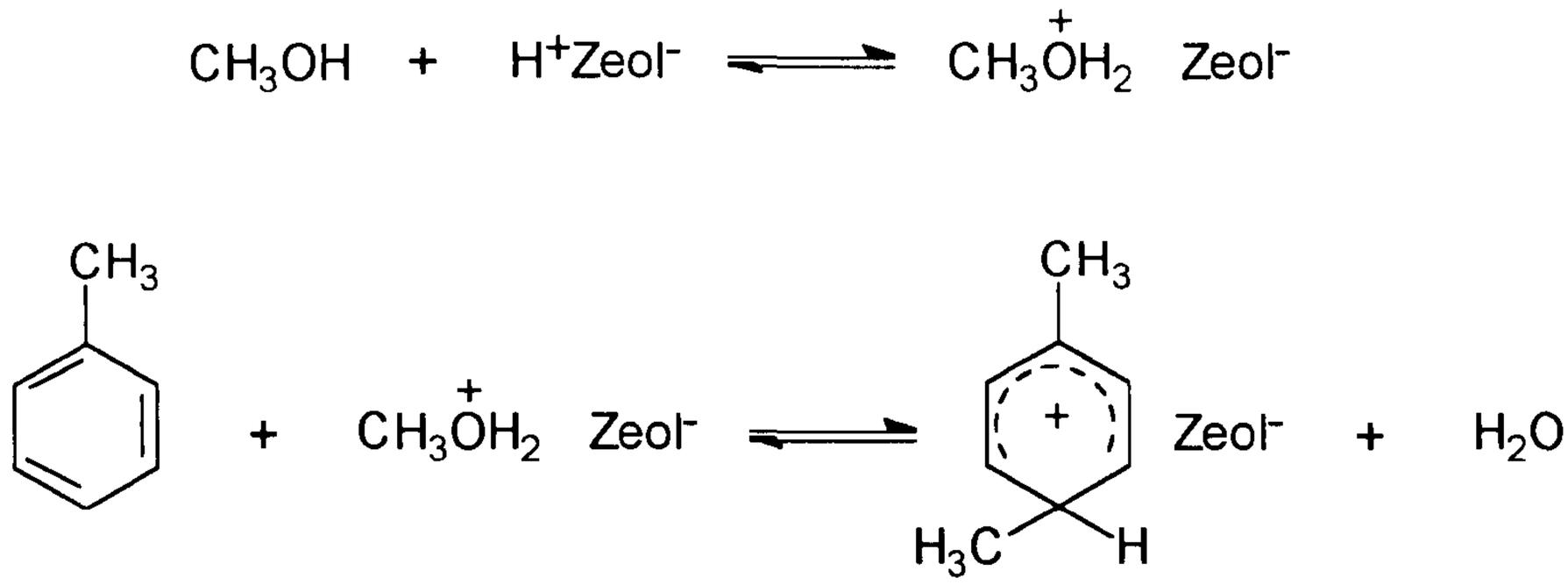

Scheme 4.4.
Mechanism for alkylation of toluene with methanol over a zeolite catalyst[25].

4.1.2.5. Research into alkylation of toluene with methanol.

Research into alkylation of toluene with methanol has been to develop systems where substitution of the methyl group can be either into the benzene ring or the methyl side chain. The substitution into the ring produces xylenes and occurs over acidic catalysts[14, 21, 22, 24, 25], while substitution into the side chain of toluene by methanol to produce ethylbenzene and styrene occurs on catalysts having basic sites[29-34].

Research into alkylation of toluene with methanol to produce xylenes is to develop catalysts which are highly selective to paraxylene, have constant activity and have longer lifetimes. Kinetic studies on alkylation of toluene with methanol have been conducted on solid acid catalysts[10], various forms of zeolite Y[35], HZSM-8[17], and HZSM-5[16]. The conclusion from these studies is that strong Bronsted acid sites are active for the ring alkylation of toluene by methanol.

Much attention has been focused on ZSM-5 catalysts since the initial reports by Chen et al.[23] and Yashima et al.[24]. Studied have been performed on alkylation of toluene by methanol on ZSM-5 modified by incorporation of elements such as boron and phosphorus into the zeolite[14, 24, 36]. Although activity for conversion was reduced,

there was an enhancement in selectivity to paraxylene. They attribute this result to the impregnating reagent being uniformly distributed within the pore structure of ZSM-5, reducing the effective pore structure. Formation of the para- isomer would then be favoured due to steric hindrance and isomerisation of the para- isomer would be reduced. Chen et al.[37] observed that paraxylene selectivity was enhanced using large crystal HZSM-5, while on small crystal HZSM-5, the selectivity to paraxylene was at its thermodynamic equilibrium value of 24%. Small crystal samples have a large external surface so it was concluded that isomerisation of the paraxylene took place on the external surface of the zeolite (with large crystals the isomerisation reaction was suppressed). Lee et al.[38] have studied the effect of modifying ZSM-5 with a silicalite shell and found that although activity is reduced, selectivity towards paraxylene is enhanced. Wei[39] has conducted a mathematical treatment of enhanced paraxylene selectivity in zeolites and has considered the alkylation of toluene by methanol. He has concluded that selectivity to paraxylene would be enhanced with increasing temperature and decreasing conversion.

Reactions using different catalysts has been studied. Nishi et al.[33] has performed experiments using microporous heteropoly oxometalates and have observed enhanced paraxylene selectivity at low temperatures (200-250°C). Blanco et al.[34] have conducted research on alkylation using $AlPO_4$, $AlPO_4$-Al_2O_3, $AlPO_4$-TiO_2, and $AlPO_4$-ZnO_2 catalysts and have found that they are highly active but not para- selective. The effect of poisoning mordenite with CFC's has been studied[40]. The poisoning led to greater conversion and longer lifetimes when compared to the untreated catalyst.

4.1.2.6. The nature for this study.

Experiments were performed using low and high concentrations of methanol. The chemicals used were HZSM-5 (BDH) and hydrogen mordenite (BDH and Strem Chemicals). No modification of the catalysts was carried out. The toluene and methanol used were analytical grade obtained from BDH chemicals. The hydrogen used was the same as that used for the disproportionation experiments.

4.2. Experimental.

4.2.1. Apparatus.

4.2.1.1. The reactor.

The same design of reactor was used as detailed in section 3.2.1.1.

4.2.1.2. Thermal apparatus for alkylation of toluene with methanol using a high molar ratio of methanol.

The apparatus used was the same as that for toluene disproportionation except that the "bubbler" contained toluene (20 cm^3) and methanol (20 cm^3) as shown in figure 4.1. Under these conditions, the saturated carrier gas (hydrogen) supplied toluene and methanol to the catalyst at a molar ratio of 1 mole of toluene to 4 moles of methanol. As shown in figure 4.2 base line separation could be obtained for all the likely products from toluene alkylation with methanol, namely toluene, methanol, benzene, ethyl benzene and para-, meta- and orthoxylenes. The methanol peak had a long tail, which resulted in a large response factor. The column used was the same as described in section 3.2.1.2, which is designed for separation of aromatic products and not for resolution of alcohols.

4.2.1.3. Microwave apparatus.

The microwave apparatus was as described in section 3.2.1.3.

4.2.1.4. Thermal apparatus for alkylation of toluene with methanol using a high molar ratio of toluene.

The apparatus was modified as shown in figure 4.3 so that a "bubbler" containing toluene at room temperature supplied toluene at a vapour pressure of 26.9 torr in a hydrogen carrier gas. A second "bubbler" containing methanol in a bath of ice and water supplied methanol at a vapour pressure of 28.4 torr. A ratio of 3 moles of toluene to 1 mole of methanol was measured by feeding methanol and toluene through a blank reactor and analysing in the normal way. The flow controllers were varied until the SUMMIT system recorded a ratio of 3 moles of toluene to 1 mole of methanol.

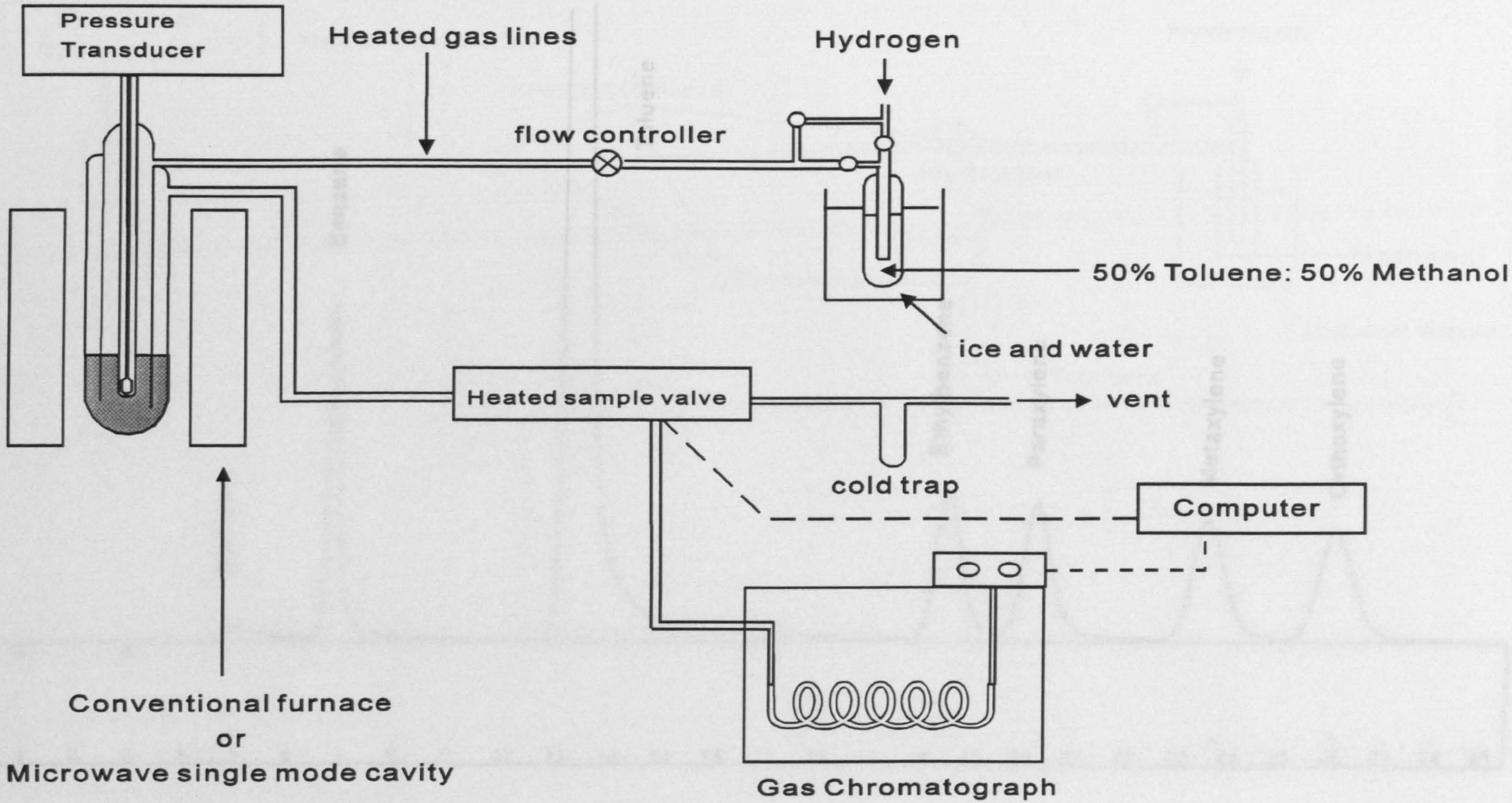

Figure 4.1. Schematic diagram of analysis system for alkylation of toluene by methanol. (Methanol in excess).

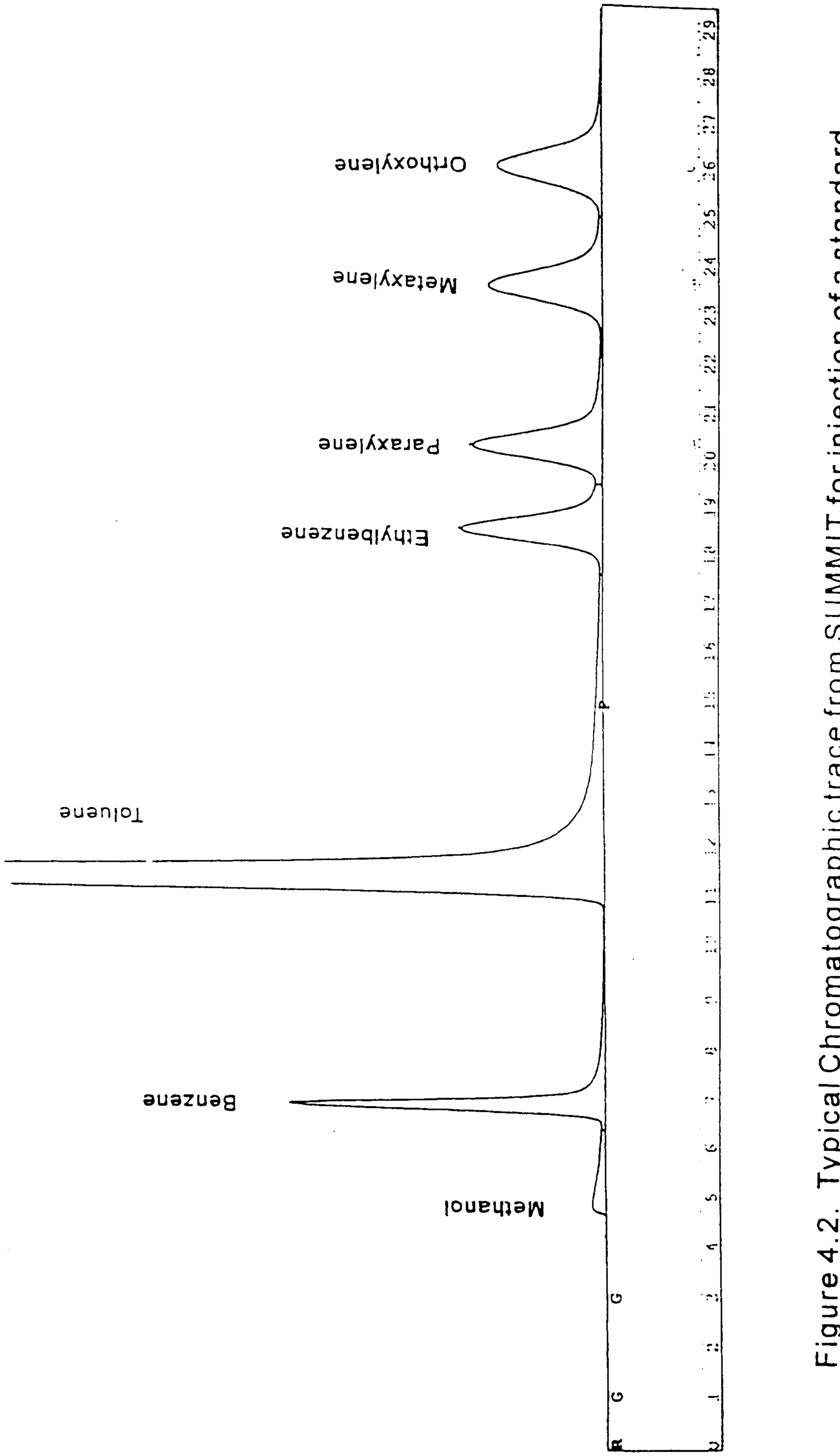

Figure 4.2. Typical Chromatographic trace from SUMMIT for injection of a standard.

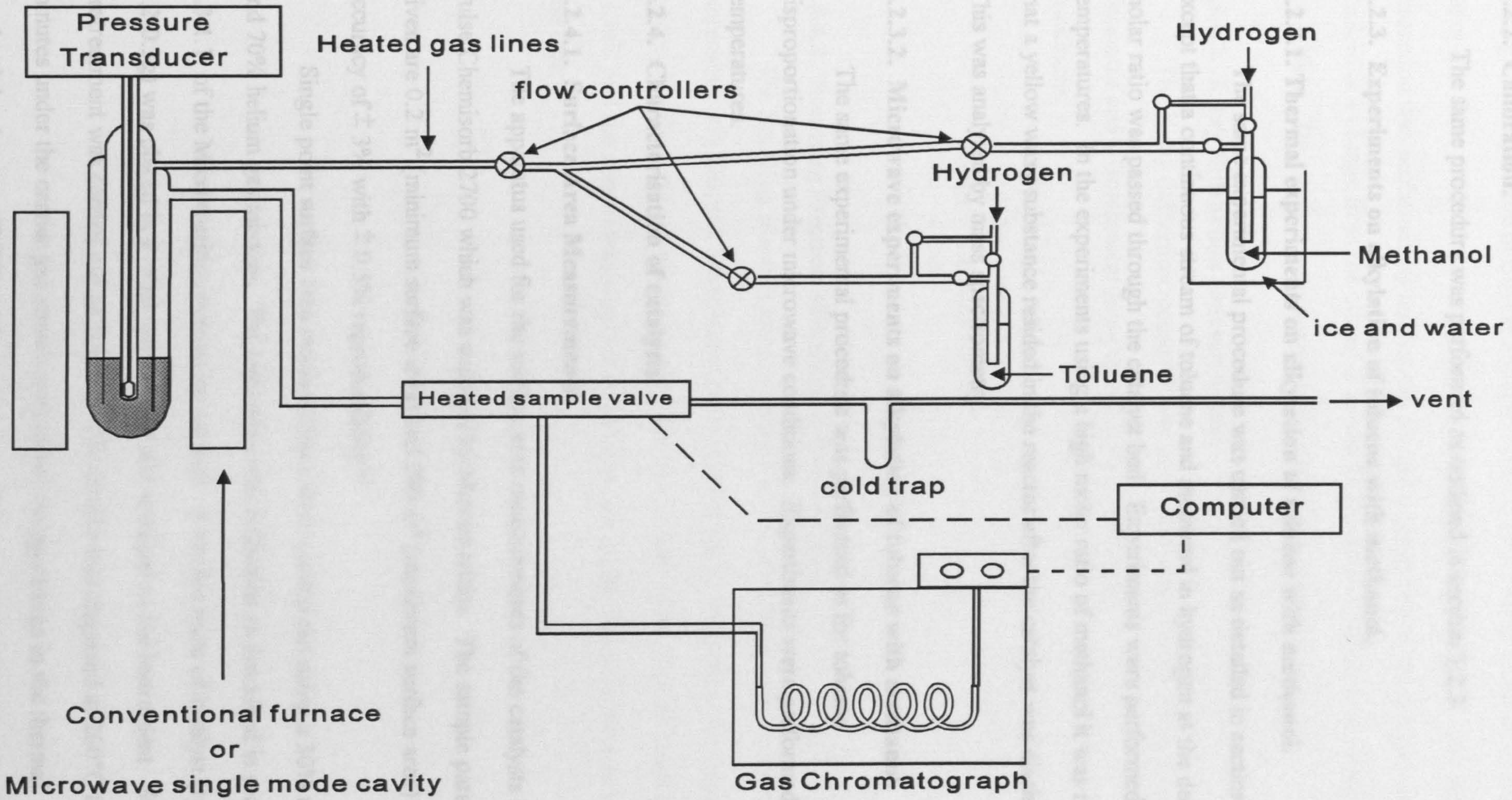

Figure 4.3. Schematic diagram of analysis system for alkylation of toluene by methanol. (Toluene in excess).

4.2.2. Calibration.

The same procedure was performed as outlined in section 3.2.2.

4.2.3. Experiments on alkylation of toluene with methanol.

4.2.3.1. Thermal experiments on alkylation of toluene with methanol.

The same experimental procedure was carried out as detailed in section 3.2.3.1. except that a continuous stream of toluene and methanol in hydrogen at the desired molar ratio was passed through the catalyst bed. Experiments were performed at various temperatures. In the experiments using a high molar ratio of methanol it was noticed that a yellow waxy substance resided in the reactor after the catalyst was discharged. This was analysed by mass spectrometry.

4.2.3.2. Microwave experiments on alkylation of toluene with methanol.

The same experimental procedure was performed as for toluene disproportionation under microwave conditions. Experiments were performed at various temperatures.

4.2.4. Characterisation of catalysts.

4.2.4.1. Surface Area Measurements.

The apparatus used for the surface area measurements of the catalysts was the Pulse Chemisorb 2700 which was supplied by Micromeritics. The sample parameters given are 0.2 m^2 (minimum surface area) and 280 m^2 (maximum surface area) with an accuracy of $\pm$ 3% with $\pm$ 0.5% reproducibility[41].

Single point surface area measurements were carried out using a 30% nitrogen and 70% helium gas mixture. The apparatus was calibrated as described in section 3.3.1.1. of the Micromeritics instruction manual. A known mass of catalyst (typically 0.2-0.3g) was placed in a clean sample tube and attached to the instrument. Sample pretreatment was carried out as follows. The sample was degassed at 260°C for 30 minutes under the carrier gas stream until there was no change in the thermal conductivity detector (TCD) of the instrument. Nitrogen adsorption was performed by

placing the sample tube in a liquid nitrogen bath (-195°C) which resulted in a change in the output from the TCD due to adsorption of nitrogen by the catalyst. Nitrogen desorption was performed by heating the sample to room temperature which again resulted in a change from the output from the TCD due to desorption of nitrogen from the surface. The catalyst was then heated to 260°C and reweighed.

4.2.4.2. X-ray Diffraction Measurements.

The X-ray diffraction measurements were carried out on a Phillips X-ray Generator and a Goniometer using the following conditions:

Conditions:

Cu Kα 40 kV, 30 mA
0.5° 2θ/min; 2°-65°
Range = 1 x 10e3 C.P.S.
T.C. = 4 sec
λ = 1.5418Å.

4.2.4.3. Scanning Electron Microscopy Measurement.

The Scanning Electron Microscopy (SEM) measurements were carried out on a Stereoscan 360 Electron Microscope (Leica-Cambridge). Secondary electrons were collected to form the morphology on the catalyst surface. The electron beam energy was 15 keV and the sample was prepared by sticking the catalyst on a metal plate to form a thin layer.

4.3. Results.

4.3.1. Calibration

Table 4.1 shows the results from the calibration standards. The response factors were calculated by the SUMMIT system as shown in 3.3.1. Toluene was used as the reference peak. The integration calculations were performed using the factors in the table.

Table 4.1.
Retention time and response factor for each product from alkylation of toluene with methanol.

Component	Retention time / min	Response factor
Cracked products	1:35	-----
Methanol	4:20	11.019
Benzene	6:16	0.851
Toluene	10:24	1.0000
Ethylbenzene	16:50	1.16
Paraxylene	18:28	1.03
Metaxylene	24:27	1.18
Orthoxylene	23:38	1.16

4.3.2. Results from experiments on alkylation of toluene with methanol.

4.3.2.1. Thermal experiments using a molar ratio of 1 mole of toluene to 4 moles of methanol.

A typical chromatograph output trace from alkylation of toluene with methanol over a mordenite (BDH) catalyst using a molar ratio of 1 mole of toluene to 4 moles of methanol is shown in figure 4.4. The trace shows no evidence for methanol in the products, so it was supposed that the methanol was completely converted. The figure shows that there was quite a substantial amount of cracking products and the majority products from alkylation of toluene by methanol under these conditions was the formation of light hydrocarbons. Figure 4.5 shows in more detail the cracking products obtained from toluene alkylation and how the distribution of the products vary. The peaks are not fully resolved since the column used was designed for aromatic products.

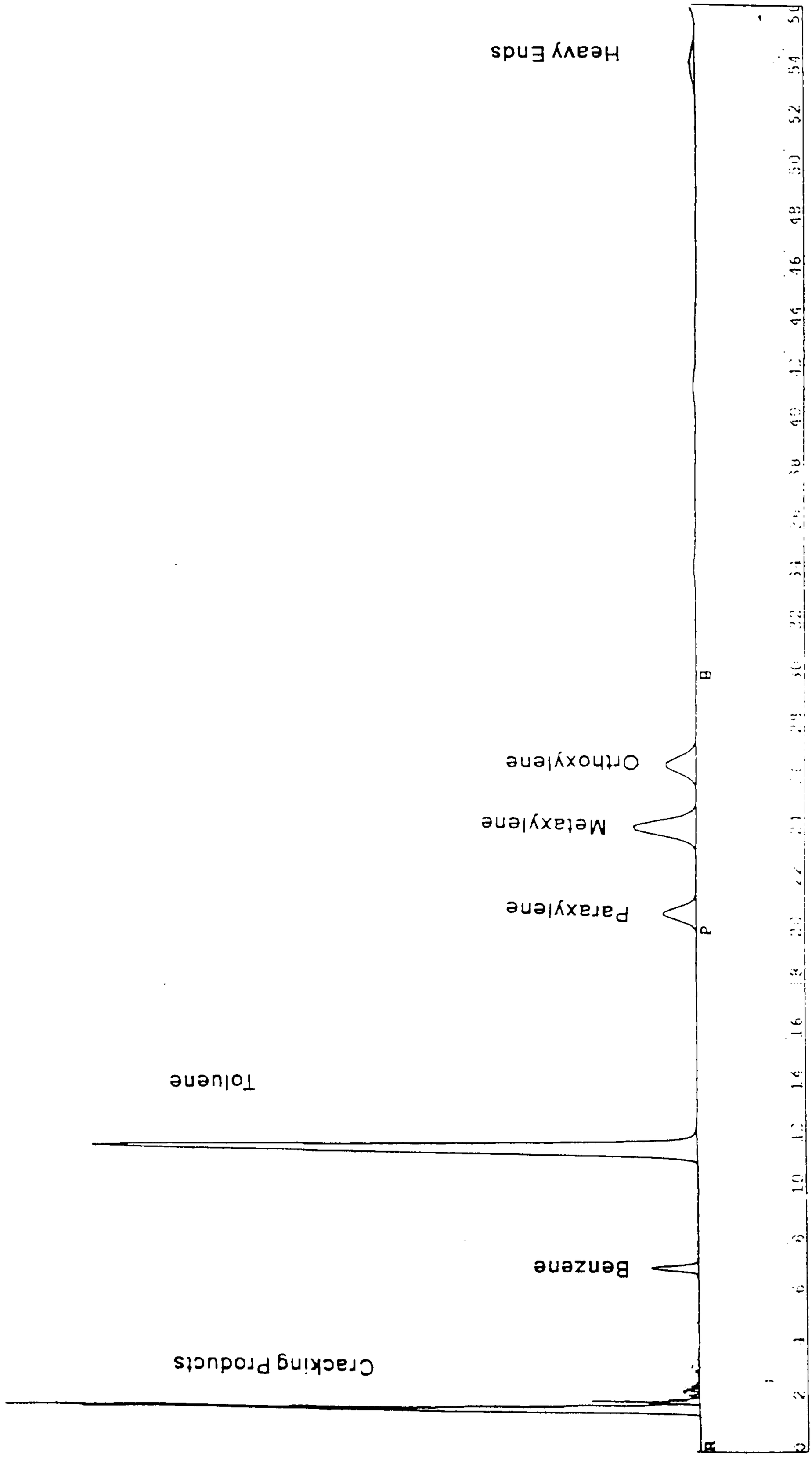

Figure 4.4. Typical Chromatographic trace from SUMMIT for alkylation of toluene with methanol. (Toluene:Methanol ratio 1:4).

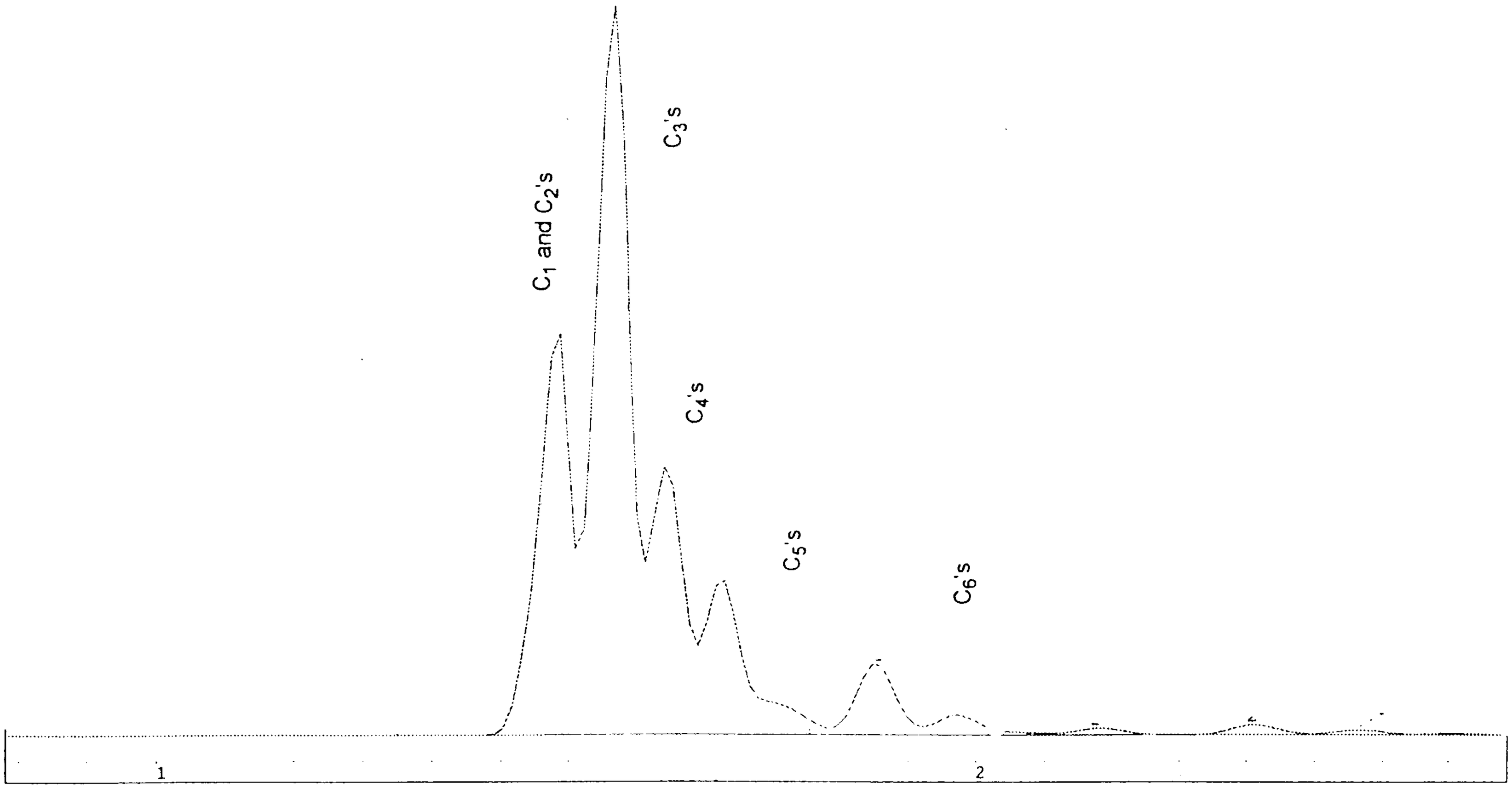

Figure 4.5. Cracking pattern from alkylation of toluene with methanol. (Toluene:Methanol 1:4).

The distribution of the cracking products from toluene alkylation is not of great importance since the objective was xylene formation; suffice it to say that the distribution is mainly C_1, C_2 and C_3 hydrocarbons, with small amounts of C_4, C_5 and aliphatic C_6 hydrocarbons.

Figure 4.6 presents the results from using hydrogen mordenite (BDH) as the catalyst at five different temperatures under normal thermal conditions. The results show that conversion to products was initially quite high at 60-70%, but as the experiment proceeded the conversion rapidly fell. As the temperature was increased the lifetime of the mordenite catalyst decreased. The optimum temperature for alkylation of toluene with methanol over hydrogen mordenite (BDH) was at 350°C. When the catalyst was discharged from the reactor after each experiment, the colour of the spheres was black.

The molar ratio of toluene to methanol was calculated as shown in equation 4.1.

Vapour pressure of toluene at 273K is 7.1 torr.

Vapour pressure of methanol at 273K is 28.4 torr.

$$\frac{7.1}{28.4} = \frac{1 \text{ mole of toluene}}{4 \text{ moles of methanol}} \qquad (4.1).$$

Table 4.2 shows how the selectivity to paraxylene varied with time. The results show that initially the selectivity was comparable to the expected equilibrium value of 24%. But the selectivity decreased with time. Observation of the chromatographic output trace under these conditions showed that there was an increase in selectivity to orthoxylene, although at that stage of the experiment the actual amount of orthoxylene being produced had declined because the conversion had decreased. The most rapid decrease was shown by the catalysts which were run at the lower temperatures of 350 and 375°C.

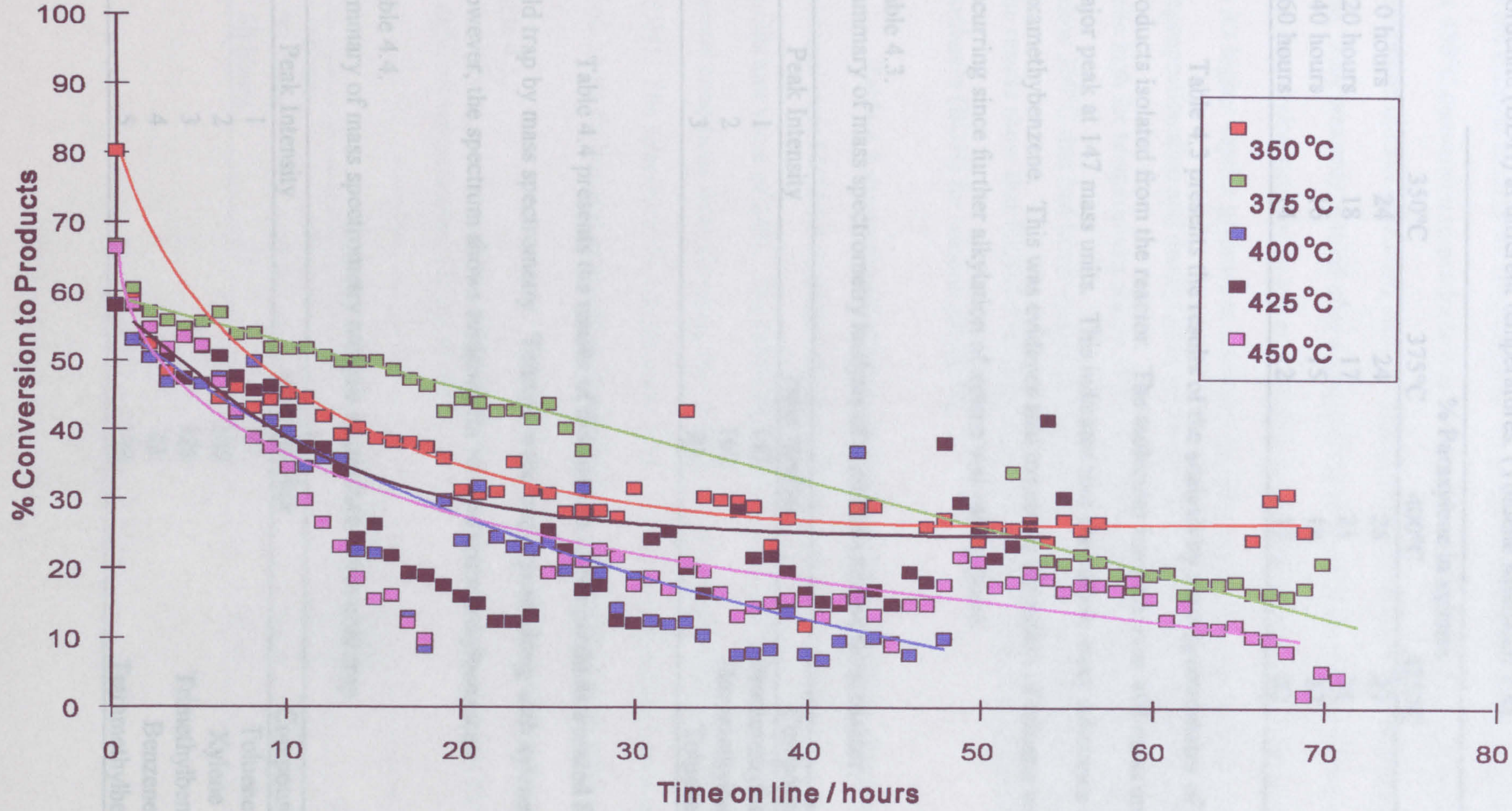

Figure 4.6. Conversion to products from alkylation of toluene with methanol over hydrogen mordenite (BDH) at different temperatures. (Toluene:Methanol 1:4).

Table 4.2.
Selectivity to paraxylene from alkylation of toluene with methanol over hydrogen mordenite (BDH) at different temperatures. (Toluene:Methanol 1:4).

	% Paraxylene in xylenes				
	350°C	375°C	400°C	425°C	450°C
0 hours	24	24	25	23	24
20 hours	18	17	21	21	22
40 hours	16	15	18	22	21
60 hours	14	12	17	22	22

Table 4.3 presents the results of the analysis by mass spectrometry of the products isolated from the reactor. The molecular ion peak is at 162 mass units with a major peak at 147 mass units. This indicates that the yellow waxy substance is hexamethybenzene. This was evidence that excessive alkylation of toluene was occurring since further alkylation of xylene was taking place.

Table 4.3.
Summary of mass spectrometry analysis of products isolated from reactor.

Peak Intensity	mass number	Compound
1	147	Pentamethylbenzene
2	162	Hexamethylbenzene
3	91	Toluene

Table 4.4 presents the results of the analysis of the products isolated from the cold trap by mass spectrometry. Toluene is the major peak along with xylenes. However, the spectrum shows evidence for tri- and tetramethylbenzenes.

Table 4.4.
Summary of mass spectrometry analysis of products from cold trap.

Peak Intensity	mass number	Compound
1	91	Toluene
2	105	Xylene
3	120	Trimethylbenzene
4	78	Benzene
5	134	Tetramethylbenzene

Figure 4.7 presents the results from alkylation of toluene using HZSM-5 (BDH) as the catalyst at different temperatures. Conversion to products rose with temperature. At 450°C conversion to products was 80% and even after 50 hours on line the conversion did not drastically reduce. The diagram shows that conversion appeared to rise. This was only noticed after a long period of time (50 hours), and it was realised that conversion was due to lower methanol concentrations (methanol being used up due to it's higher vapour pressure at ice/water temperature), allowing the selectivity to disproportionation and dealkylation reactions to increase. Conversion to products was quite high for temperatures above 350°C and it was only experiments at temperatures below 350°C that had lower conversions that decreased as the experiment proceeded. The results show that HZSM-5 (BDH) was a more active catalyst than hydrogen mordenite (BDH) for toluene alkylation.

Table 4.5 shows the selectivity to paraxylene from alkylation of toluene with methanol over HZSM-5 (BDH) with time. The selectivity was higher than the expected equilibrium value of 24%. The selectivity to paraxylene had increased significantly under thermal conditions from changing the catalyst from mordenite (BDH) to HZSM-5 (BDH). The selectivity did not decrease as the experiment proceeded even after a period of 60 hours on line and appeared to be stable at 31-33% paraxylene in xylenes.

Table 4.5.
Selectivity to paraxylene from alkylation of toluene with methanol over HZSM-5 (BDH) at different temperatures. (Toluene:Methanol 1:4).

	% Paraxylene in xylenes			
	350°C	375°C	400°C	450°C
0 hours	32.6	32.8	31.9	32.8
20 hours	32.4	32.1	31.8	32.6
40 hours	32	31.9	31.6	33.1

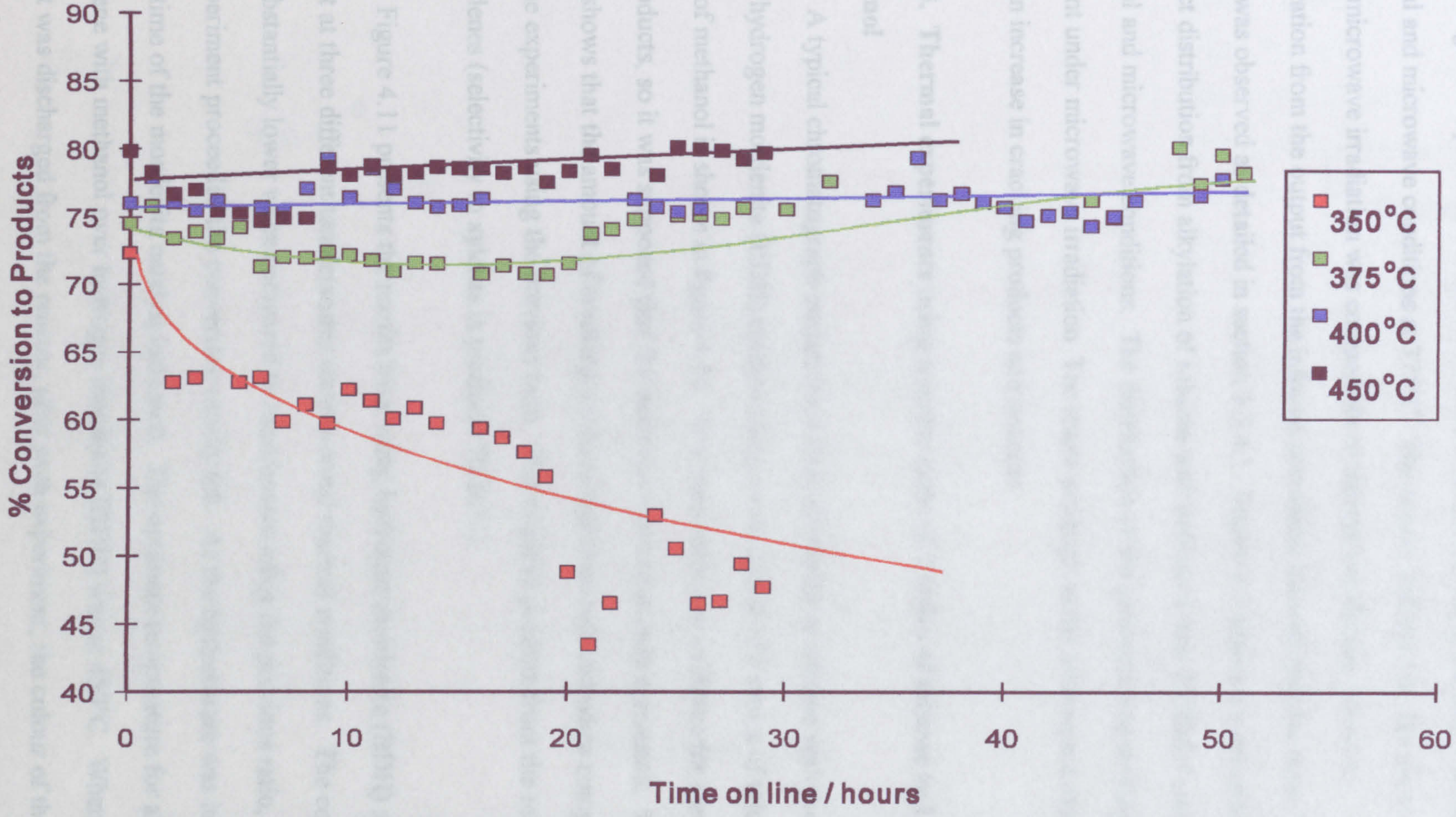

Figure 4.7. Conversion to products from alkylation of toluene with methanol over HZSM-5 (BDH) at different temperatures. (Toluene:Methanol 1:4).

4.3.2.2. Microwave experiments using a molar ratio of 1 mole of toluene to 4 moles of methanol.

Figure 4.8 presents the results of toluene alkylation using HZSM-5 (BDH) under thermal and microwave conditions at 375°C. The results indicate that the conversion under microwave irradiation was comparable to thermal conditions, however, observation from the output from the infrared pyrometer showed that the same "spiky" effect was observed as detailed in section 3.3.4.1. Figure 4.9 shows a comparison of the product distribution from alkylation of toluene with methanol over HZSM-5 under thermal and microwave conditions. The distribution of the products was strikingly different under microwave irradiation The major products under microwave irradiation were an increase in cracking products and benzene.

4.3.2.3. Thermal experiments using a molar ratio of 3 moles of toluene to 1 mole of methanol

A typical chromatograph output trace from alkylation of toluene with methanol over a hydrogen mordenite (BDH) catalyst using a molar ratio of 3 moles of toluene to 1 moles of methanol is shown in figure 4.10. The trace shows no evidence for methanol in the products, so it was supposed that the methanol was completely converted. The figure shows that the amount of cracking products had been reduced when compared with the experiments using the previous ratio. The majority product from the reaction was xylenes (selectivity to xylenes in products 70-80%).

Figure 4.11 presents the results from using hydrogen mordenite (BDH) as the catalyst at three different temperatures under normal thermal conditions. The conversion was substantially lower when compared to experiments using the previous ratio, and as the experiment proceeded the conversion rapidly fell. As the temperature was increased the lifetime of the mordenite catalyst increased. The optimum temperature for alkylation of toluene with methanol over hydrogen mordenite (BDH) was at 450°C. When the catalyst was discharged from the reactor, after each experiment, the colour of the spheres was black.

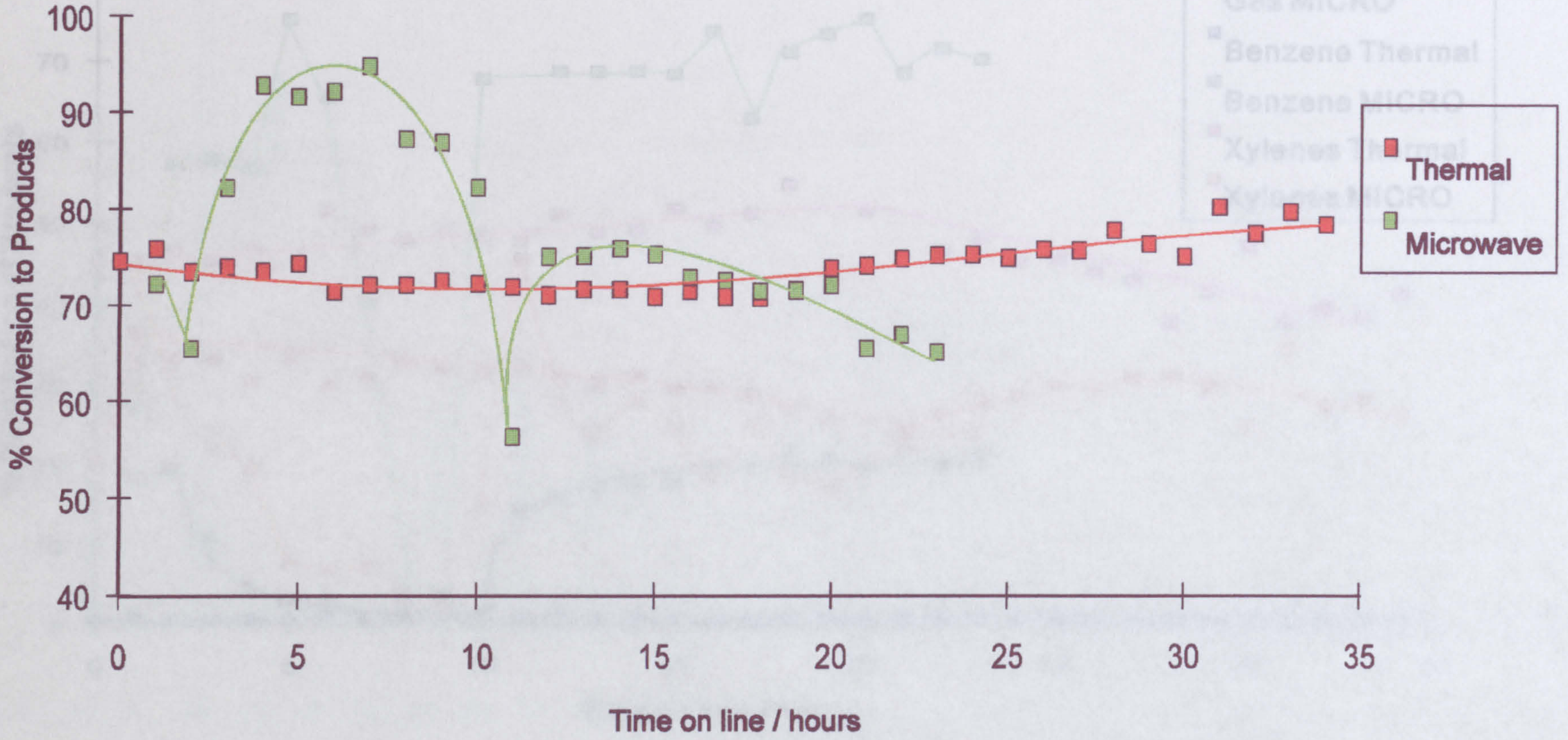

Figure 4.8. Conversion to products from alkylation of toluene with methanol over HZSM-5 (BDH) under thermal and microwave conditions at 375 °C. (Toluene:Methanol 1:4).

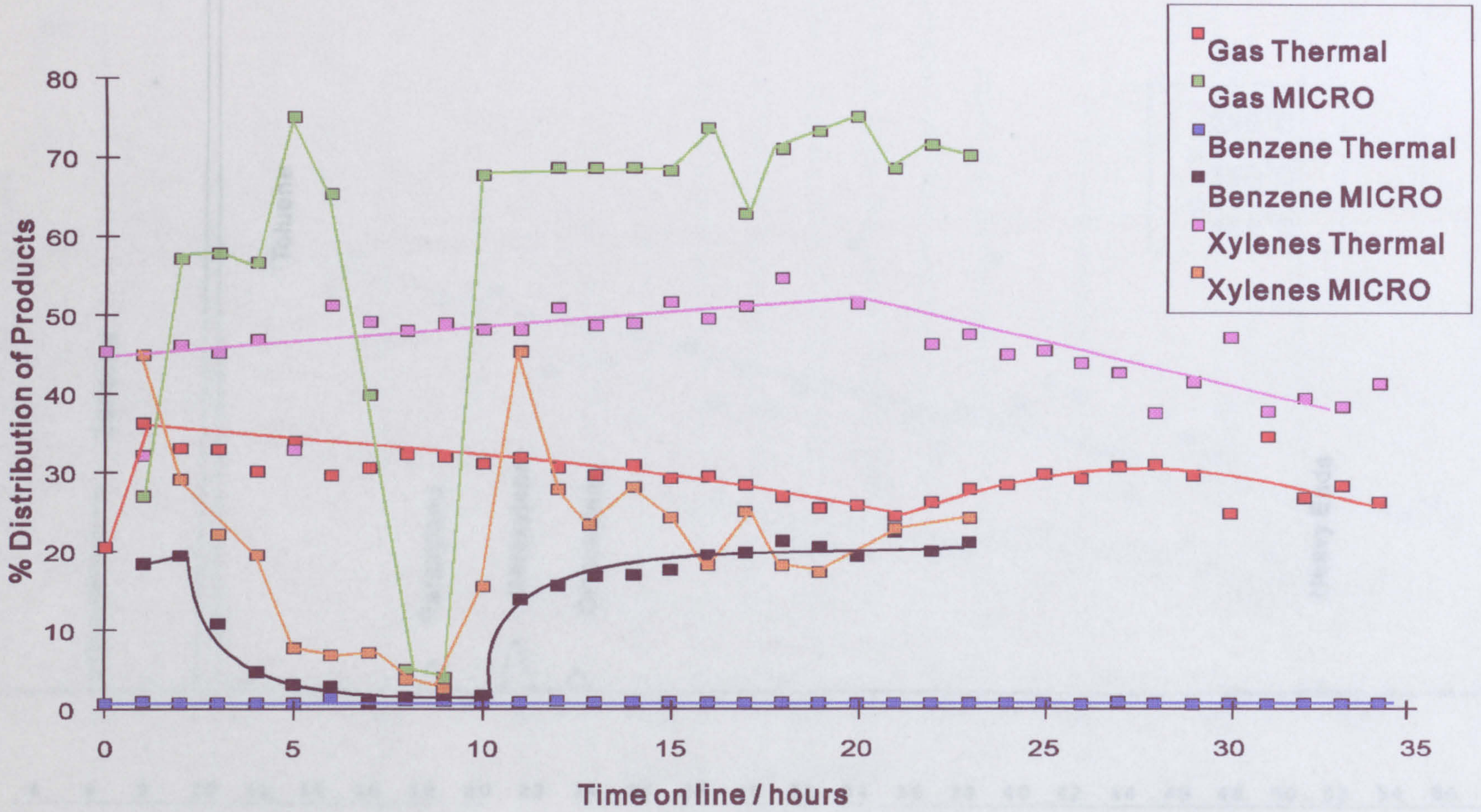

Figure 4.9. Product distribution from alkylation of toluene with methanol over HZSM-5 (BDH) under thermal and microwave conditions at 375 °C. (Toluene:Methanol 1:4).

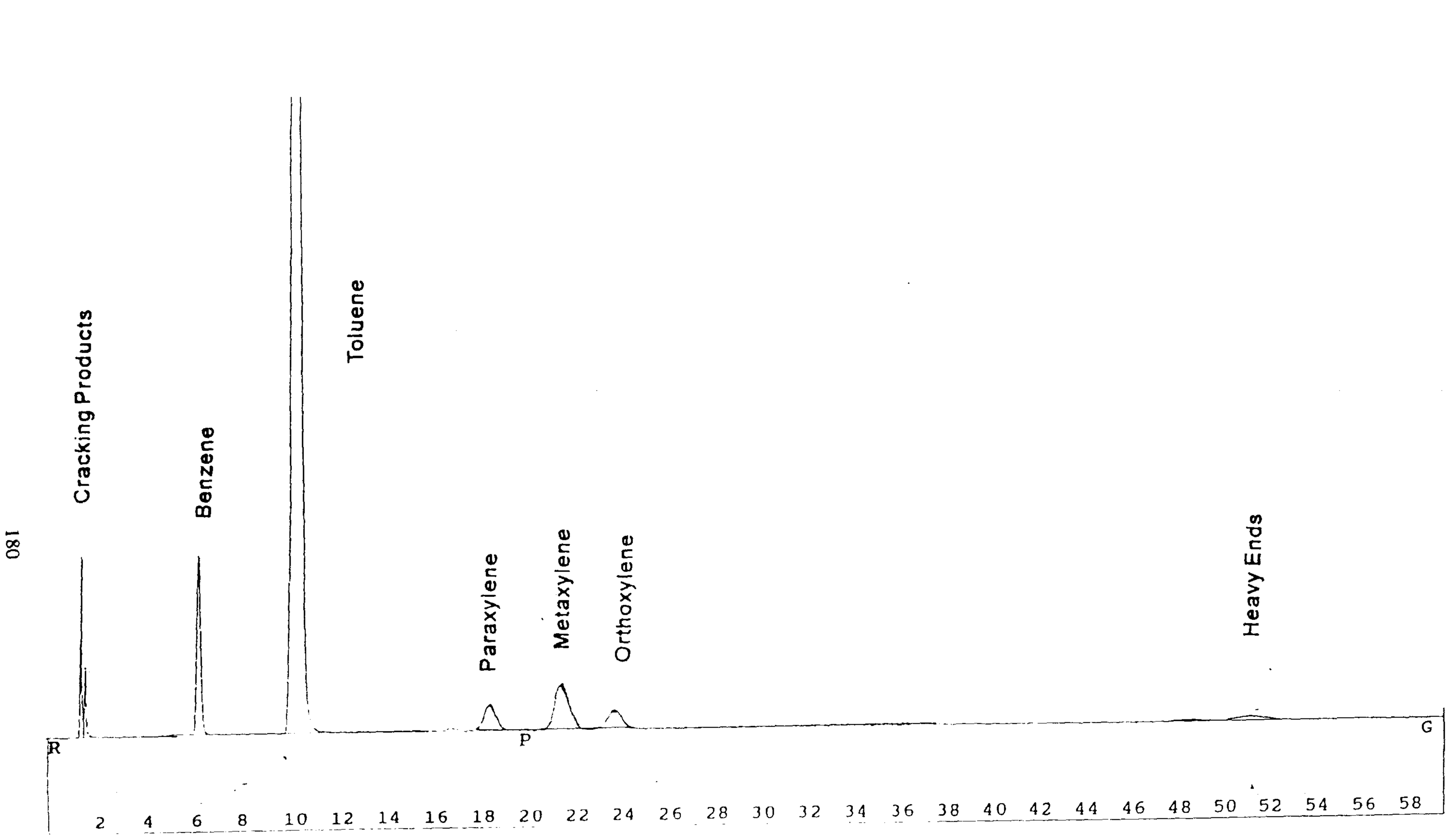

Figure 4.10. Typical Chromatographic trace from SUMMIT for alkylation of toluene with methanol. (Toluene:Methanol ratio 3:1).

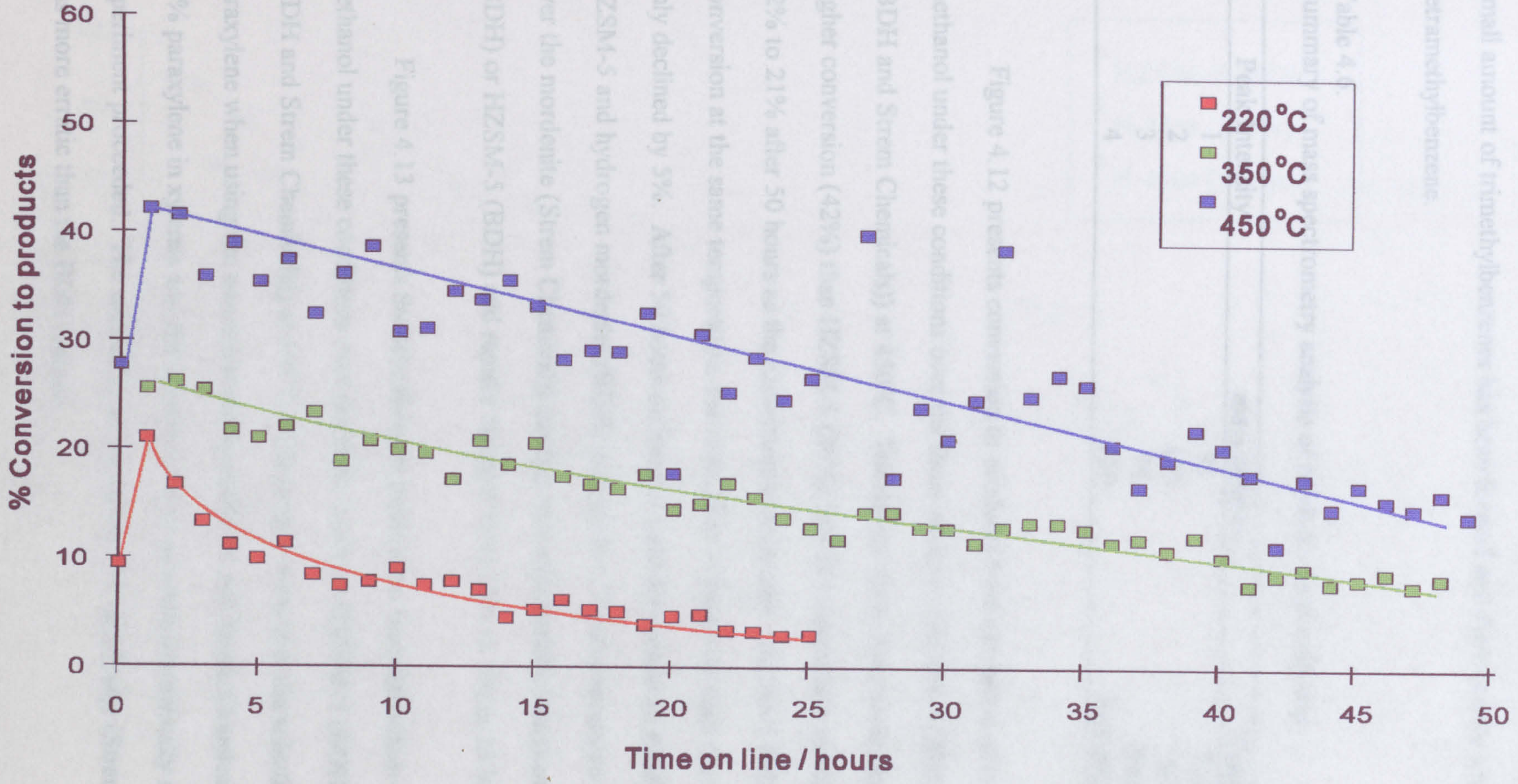

Figure 4.11. Conversion to products from alkylation of toluene with methanol over hydrogen mordenite (BDH) at different temperatures. (Toluene:Methanol 3:1).

Table 4.6 presents the results of the analysis of the products isolated from the cold trap by mass spectrometry. Toluene is the major peak along with xylenes. Only a small amount of trimethylbenzenes has been formed and there is only a trace amount of tetramethylbenzene.

Table 4.6.
Summary of mass spectrometry analysis of products from cold trap.

Peak Intensity	mass number	Compound
1	91	Toluene
2	105	Xylene
3	78	Benzene
4	120	Trimethylbenzene

Figure 4.12 presents conversion to products from alkylation of toluene with methanol under these conditions over the three catalysts (HZSM-5 (BDH) and mordenite (BDH and Strem Chemicals)) at 450°C. The results show that mordenite (BDH) had a higher conversion (42%) than HZSM-5 (26%), but this conversion steadily declined from 42% to 21% after 50 hours as the experiments proceeded. HZSM-5 (BDH) had a lower conversion at the same temperature, but even after 50 hours on lines the conversion had only declined by 5%. After 50 hours on line the total conversion to products for both HZSM-5 and hydrogen mordenite (BDH) was similar. Total conversion to products over the mordenite (Strem Chemicals) catalyst was substantially less than the mordenite (BDH) or HZSM-5 (BDH) and rapidly decayed from 15% to 5% in 25 hours online.

Figure 4.13 presents the selectivity to paraxylene from alkylation of toluene with methanol under these conditions over the three catalysts (HZSM-5 (BDH) and mordenite (BDH and Strem Chemicals)) at 450°C. The results show that the selectivity to paraxylene when using the mordenite catalysts (BDH and Strem Chemicals) was stable at 25% paraxylene in xylenes and did not decrease or increase dramatically as the experiment proceeded. The selectivity to paraxylene for mordenite (Strem Chemicals) was more erratic than the BDH catalyst.

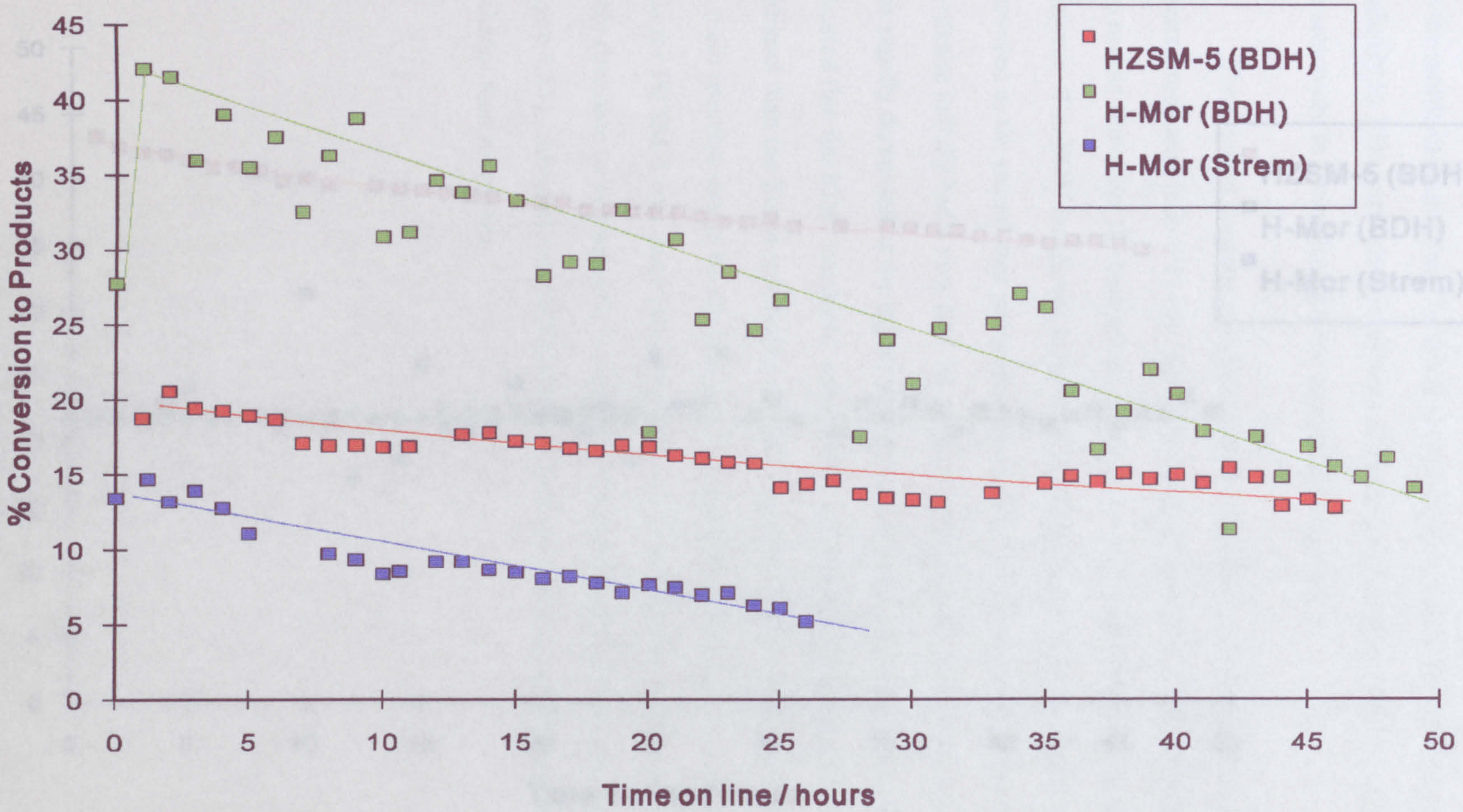

Figure 4.12. Conversion to products from alkylation of toluene with methanol over different catalysts at 450 °C. (Toluene:Methanol 3:1).

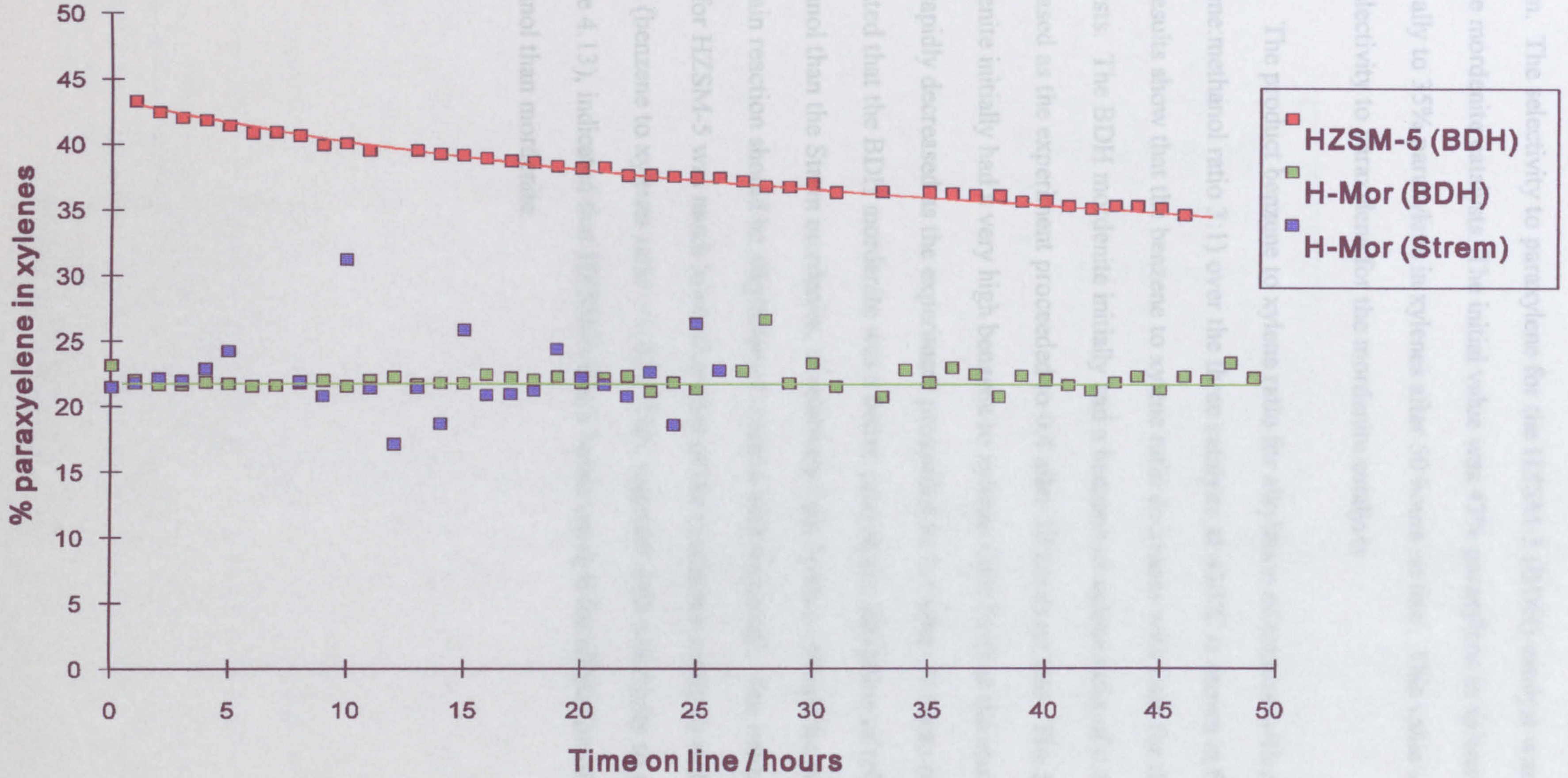

Figure 4.13. Selectivity to paraxylene from alkylation of toluene with methanol over different catalysts at 450 °C. (Toluene:Methanol 3:1).

However, total conversion to products was very low for this catalyst and it was possible that the chromatographic resolution was impaired due to limits of detection for the system. The selectivity to paraxylene for the HZSM-5 (BDH) catalyst was higher than for the mordenite catalysts. The initial value was 43% paraxylene in xylenes and declined gradually to 35% paraxylene in xylenes after 50 hours on line. This value is greater than the selectivity to paraxylene for the mordenite catalysts.

The product benzene to xylene ratio for alkylation of toluene with methanol (toluene:methanol ratio 3:1) over the three catalysts at 450°C is shown in figure 4.14. The results show that the benzene to xylene ratio decreases with time for the mordenite catalysts. The BDH mordenite initially had a benzene to xylene ratio of 0.8 which decreased as the experiment proceeded to 0.4 after 30 hours on line. The Strem mordenite initially had a very high benzene to xylenes ratio (1.9) at the start of the run. This rapidly decreased as the experiment proceeded to 0.4 after 30 hours on line. This indicated that the BDH mordenite was a better catalyst for alkylation of toluene with methanol than the Strem mordenite, as relatively little benzene should be present because the main reaction should be alkylation of toluene with methanol. The benzene to xylene ratio for HZSM-5 was much lower than that of the mordenite catalysts and was very stable (benzene to xylenes ratio = 0.01). This, together with selectivity to paraxylene (figure 4.13), indicated that HZSM-5 was a better catalyst for alkylation of toluene with methanol than mordenite.

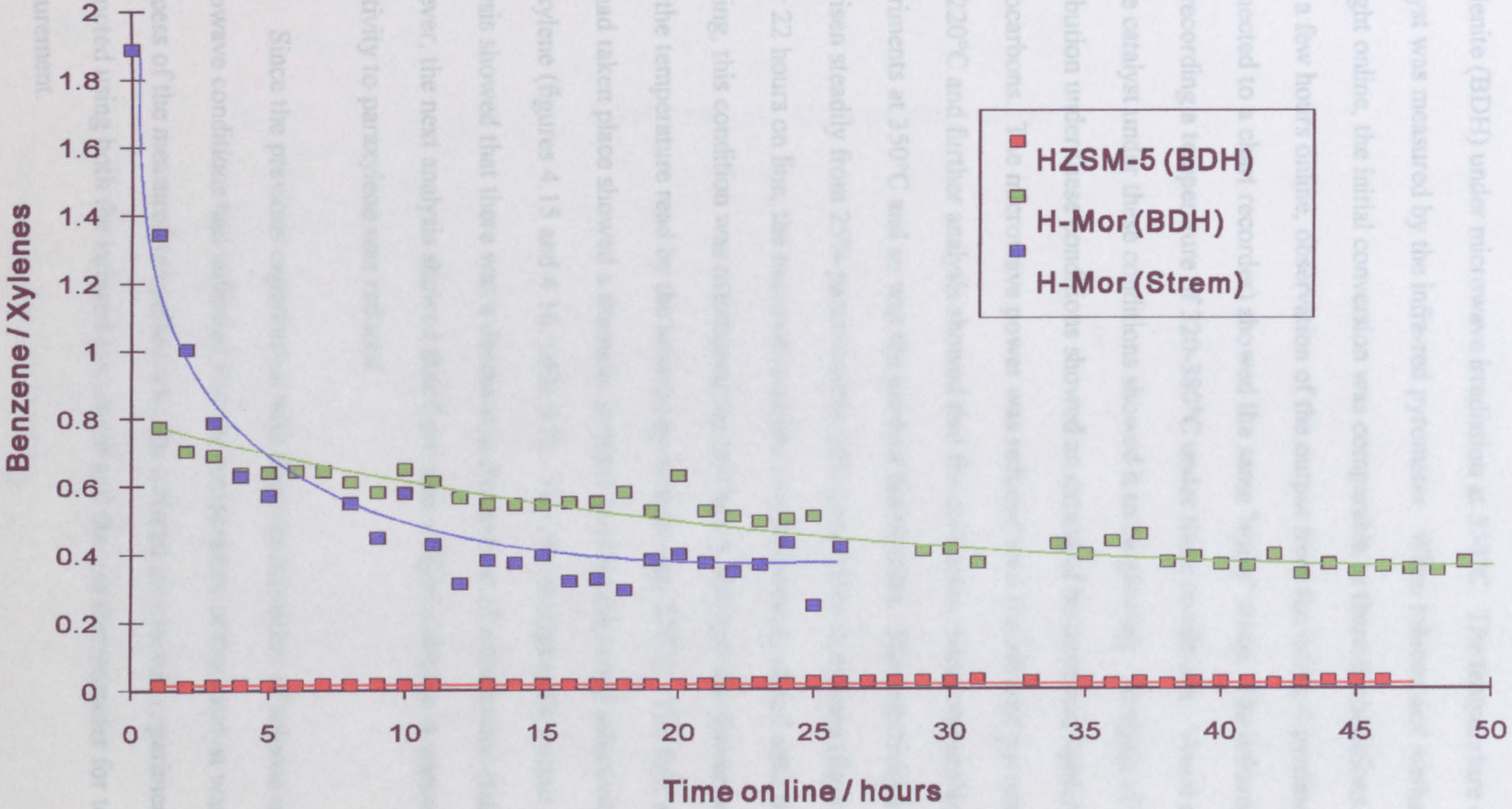

Figure 4.14. Benzene to xylenes ratio from alkylation of toluene with methanol over different catalysts at 450 °C. (Toluene:Methanol 3:1).

4.3.2.4. Microwave experiments using a molar ratio of 3 moles of toluene to 1 mole of methanol.

Figure 4.15 presents the results from alkylation of toluene with methanol over mordenite (BDH) under microwave irradiation at 350°C. The temperature of the catalyst was measured by the infra-red pyrometer. When toluene and methanol were brought online, the initial conversion was comparable to thermal conditions. However, after a few hours online, observation of the output from the infrared pyrometer (connected to a chart recorder) showed the same "spiky" trace. The infrared pyrometer was recording a temperature of 320-380°C under these conditions. Visual observation of the catalyst under these conditions showed it to be glowing. Analysis of the product distribution under these conditions showed an excess of benzene and lighter hydrocarbons. The microwave power was reduced until the infrared pyrometer read 214-220°C and further analysis showed that the conversion was comparable to thermal experiments at 350°C and so was the product distribution. The selectivity to paraxylene had risen steadily from 25% paraxylene to 30% paraxylene in xylenes (figure 4.16). After 22 hours on line, the microwave power was deliberately raised until the sample was glowing, this condition was maintained for two hours and then the power was reduced until the temperature read by the infrared pyrometer was 220°C. The first analysis after this had taken place showed a dramatic increase in conversion and selectivity to paraxylene (figures 4.15 and 4.16, table 4.7). The chromatographic output of this analysis showed that there was a decrease in the amount of orthoxylene (table 4.7), however, the next analysis showed that there was a slight decrease in conversion and the selectivity to paraxylene was reduced.

Since the previous experiments with disproportionation of toluene under microwave conditions had indicated that the temperature of the catalyst was substantially in excess of the measured temperature by the infrared pyrometer, experiments were conducted using both the infrared pyrometer and the gas thermometer for temperature measurement.

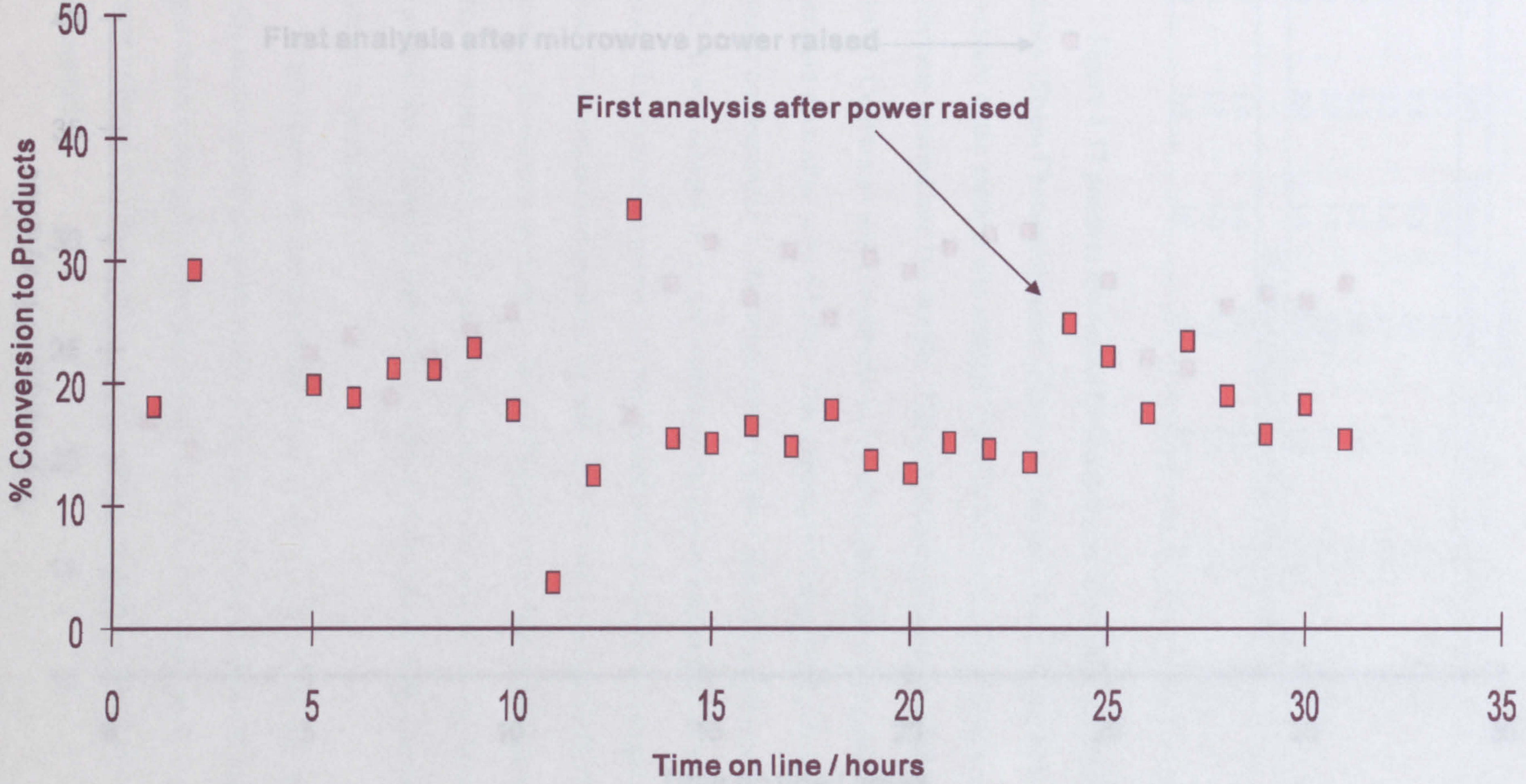

Figure 4.15. Conversion to products from alkylation of toluene over hydrogen mordenite (BDH) under microwave conditions. (Toluene:Methanol 3:1).

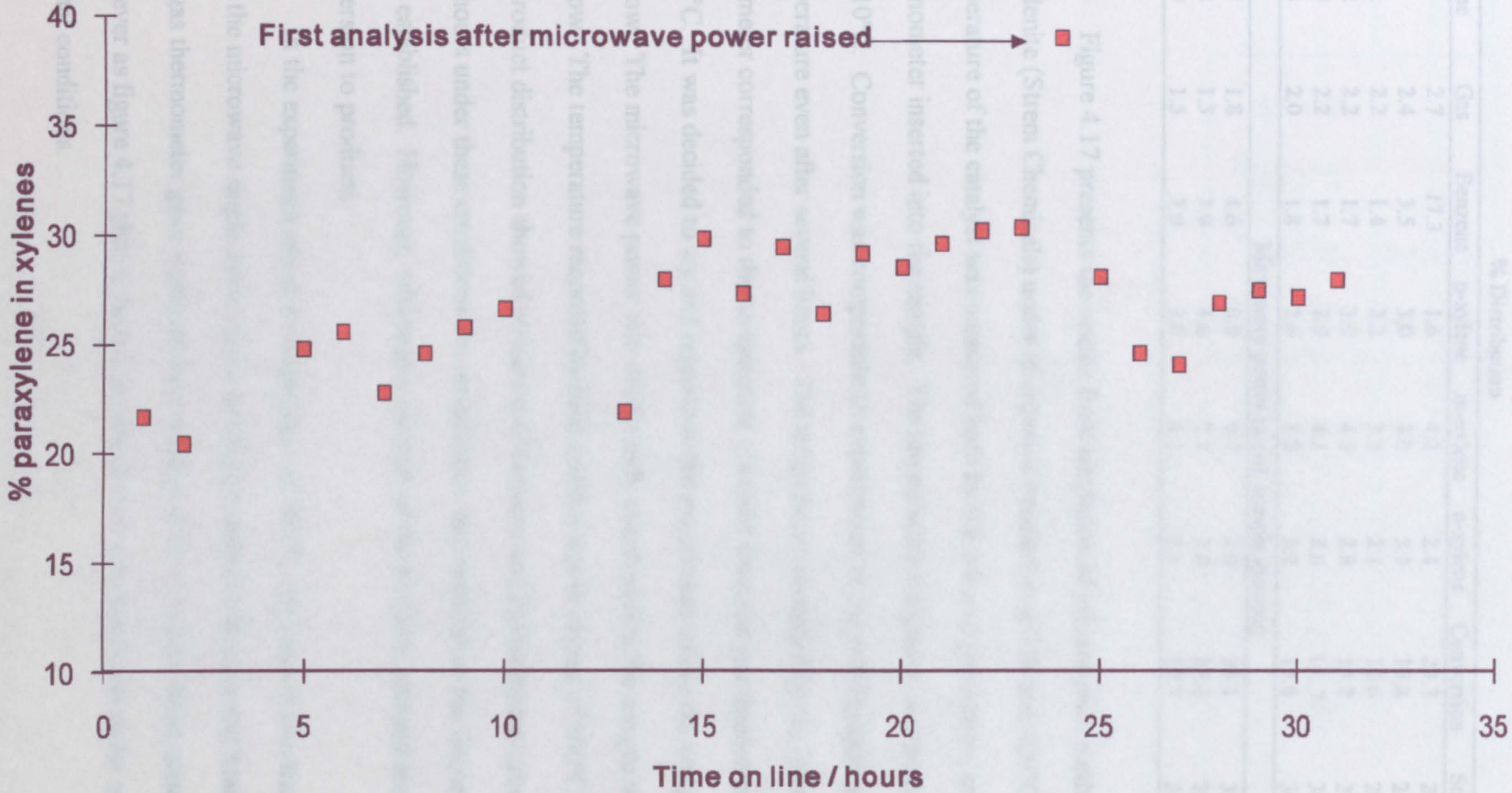

Figure 4.16. Selectivity to paraxylene from alkylation of toluene with methanol over hydrogen mordenite (BDH) under microwave conditions. (Toluene:Methanol 3:1).

Table 4.7.
Alkylation of toluene with methanol over a BDH mordenite catalyst under microwave conditions.

	% Distribution							
Time	Gas	Benzene	p-xylene	m-xylene	o-xylene	Conversion	Sel px	B/X
2	2.7	17.3	1.6	4.2	2.1	29.3	20.5	2.2
5	2.4	3.5	3.0	3.0	3.1	19.8	24.8	0.29
21	2.2	1.4	2.2	3.3	2.1	12.6	28.6	0.18
22	2.2	1.7	3.0	4.3	2.8	15.2	29.7	0.17
23	2.2	1.7	2.9	4.1	2.6	14..7	30.3	0.18
24	2.0	1.8	2.6	3.8	2.1	13.6	30.4	0.2
Microwave power raised, sample glowing								
27	1.8	4.6	6.9	9.7	1.0	25.1	39.2	0.26
28	1.3	3.9	4.6	7.7	3.8	22.3	28.2	0.23
29	1.5	3.0	3.0	6.1	3.1	17.7	24.7	0.24

Figure 4.17 presents the results from alkylation of toluene with methanol over mordenite (Strem Chemicals) under microwave irradiation at 350 and 400°C. The temperature of the catalyst was measured both by the infrared pyrometer, and by the gas thermometer inserted into the sample. The temperature difference was nominally $\pm$ 5-10°C. Conversion was comparable to experiments at the corresponding thermal temperature even after several hours. The temperature recorded by the infrared pyrometer corresponded to the temperature obtained from the gas thermometer to $\pm$ 15°C. It was decided to try and reproduce the experiment where the sample was made to glow. The microwave power was deliberately raised so that the sample was observed to glow. The temperature recorded by both devices was in excess of 500°C. Analysis of the product distribution showed an excess of benzene and lighter hydrocarbons. After two hours under these conditions the temperature was reduced so the former conditions were established. However, subsequent analysis of the products showed almost no conversion to products.

In the experiment run at a temperature of 400°C, the reactor was transferred from the microwave single mode cavity to the conventional furnace and heated to 400°C. The gas thermometer gave a temperature reading of 425°C under these conditions. However as figure 4.17 shows there was almost no conversion even under normal thermal conditions.

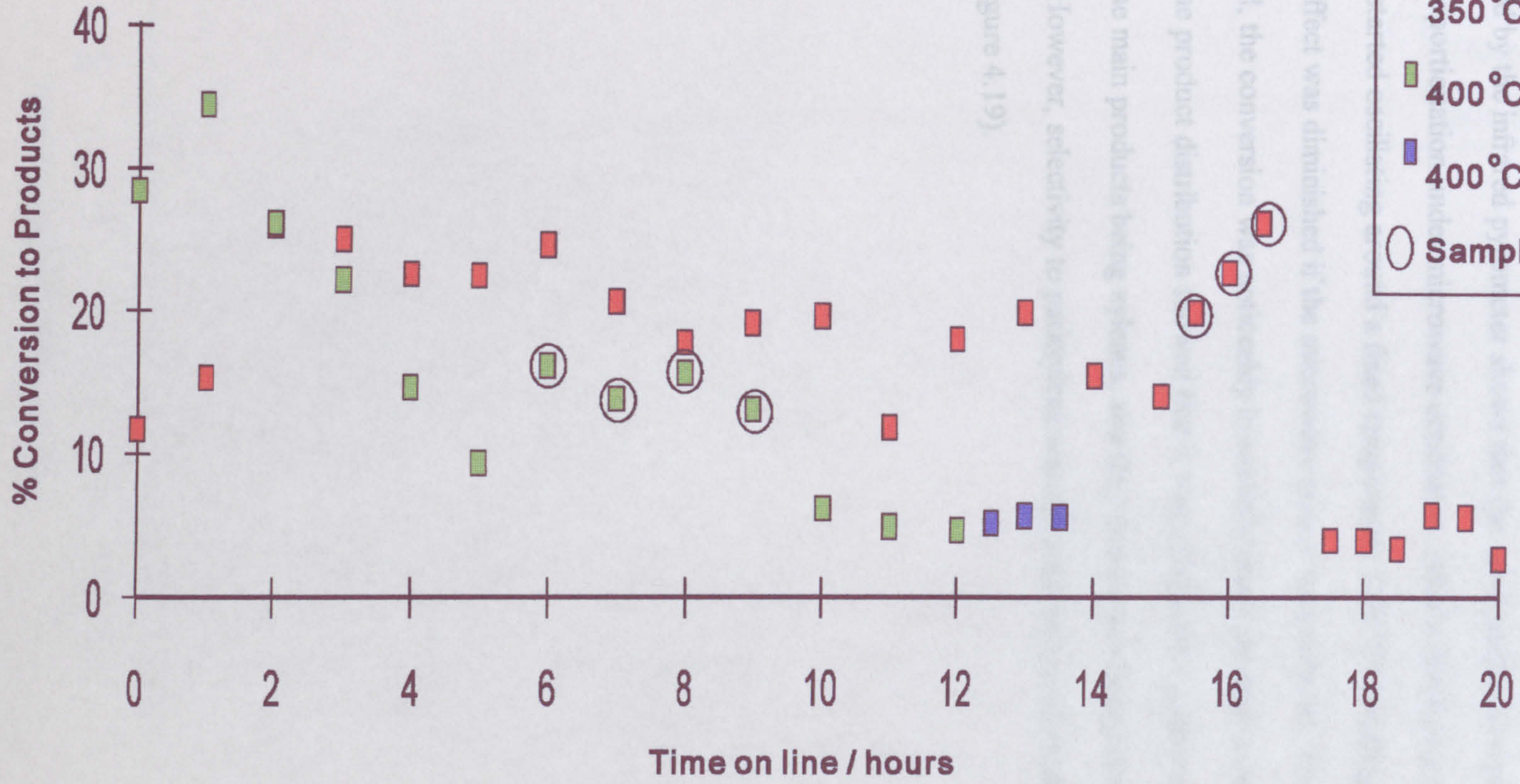

Figure 4.17. Conversion to products from alkylation of toluene with methanol over hydrogen mordenite (Strem Chemicals) under microwave conditions. (Toluene:Methanol 3:1).

Figures 4.18 and 4.19 presents the results from alkylation of toluene with methanol (toluene:methanol ratio 3:1) over HZSM-5 (BDH) under thermal and microwave conditions. Figure 4.18 shows the total conversion to products under thermal and microwave conditions. The results show that initially conversion was the same under microwave conditions compared with thermal conditions. Observation of the trace recorded by the infrared pyrometer shows that the same pattern is repeated as for toluene disproportionation under microwave conditions. After a few hours on line the temperature started oscillating around a fixed temperature (350°C) resulting in a "spiky" trace. This effect was diminished if the microwave power was reduced. However, when this happened, the conversion was noticeably lower than under thermal conditions.. Analysis of the product distribution showed that it was comparable to thermal conditions, the main products being xylenes, and the benzene to xylene ratio was very low (0.01). However, selectivity to paraxylene was reduced compared to thermal conditions (figure 4.19).

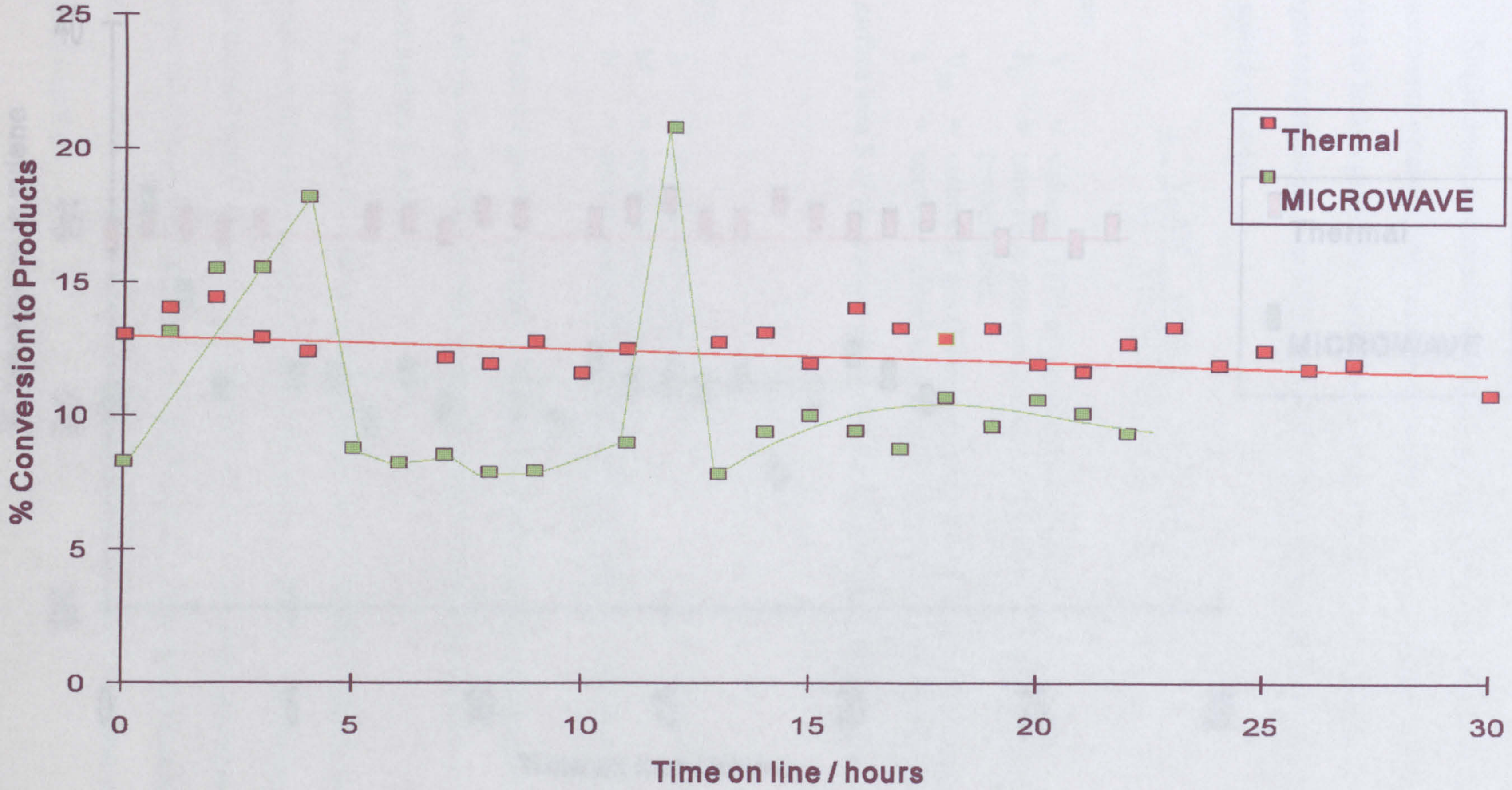

Figure 4.18. Conversion to products from alkylation of toluene with methanol over HZSM-5 (BDH) under thermal and microwave conditions at 350°C. (Toluene:Methanol 3:1).

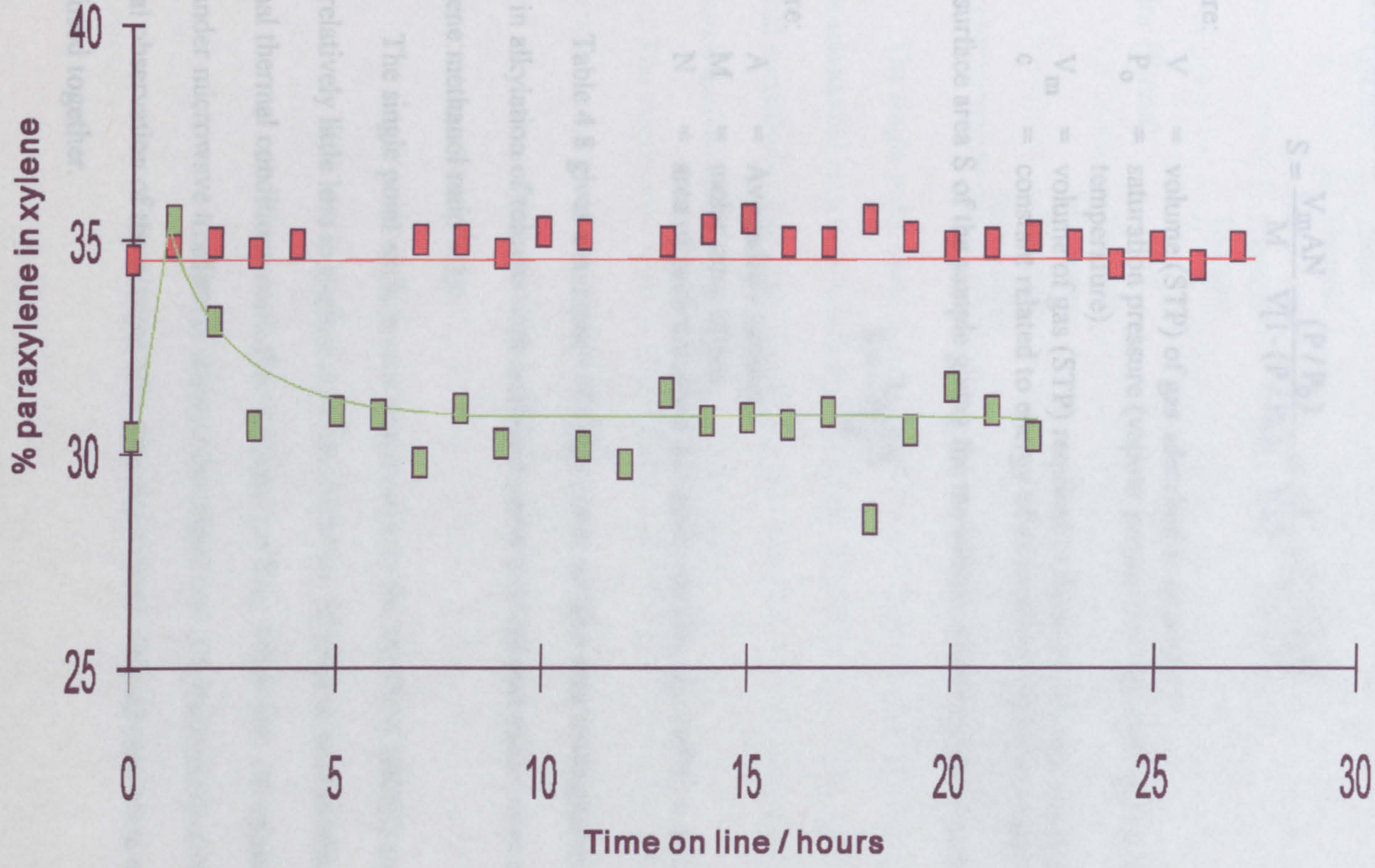

Figure 4.19. Selectivity to paraxylene from alkylation of toluene with methanol over HZSM-5 (BDH) under thermal and microwave conditions at 350 °C. (Toluene:Methanol 3:1).

4.3.3. Characterisation of catalysts.

4.3.3.1 Single point Surface Area Measurements.

Single point surface area measurements are not usually as precise as measurements obtained from multi point techniques. The technique uses a special nitrogen in helium gas mixture and the fact that nitrogen will physically adsorb at liquid nitrogen temperatures. The BET equation[42] that describes physical adsorption of gas on to a solid surface is

$$S = \frac{V_m A N}{M} \frac{(P/P_o)}{V[1-(P/P_o)} = \frac{1}{V_m c} + \frac{(c-1)}{V_m c} \frac{P}{P_o} \qquad (4.2).$$

Where:

V = volume (STP) of gas adsorbed at pressure P.
P_o = saturation pressure (vapour pressure of liquefied gas at the adsorbing temperature).
V_m = volume of gas (STP) required to form an adsorbed monolayer.
c = constant related to energy of adsorption (typically large).

The surface area S of the sample giving the monolayer adsorbed gas volume V_m (STP) is

$$S = \frac{V_m A N}{M} \qquad (4.3).$$

Where:

A = Avogadro's number.
M = molar mass of gas.
N = area of each adsorbed gas molecule (N_2 @ -195°C = 16.2×10^{-20} m^2).

Table 4.8 gives a summary of single point surface area measurements on catalysts used in alkylation of toluene with methanol under thermal and microwave conditions (toluene:methanol ratio 3:1).

The single point surface area measurements for HZSM-5 (BDH) show that there was relatively little loss in surface area for alkylation of toluene with methanol under normal thermal conditions even after 50 hours on line. However, the experiment carried out under microwave irradiation showed that there was a substantial loss in surface area. Visual observation of the catalyst after this experiment showed that some of the spheres had fused together.

Table 4.8.
Single point surface area measurements of zeolite catalysts under different conditions.

Catalyst	Conditions	Temperature / °C	Surface Area / m^2g^{-1}	Time on line / hours
HZSM-5	blank	----	298	----
	Thermal	350	287	50
	Thermal	400	289	50
	Thermal	450	288	50
	Thermal	500	282	50
	Microwave	350	142	20
H-Mor (BDH)	blank	---	304	----
	Thermal	350	175	50
	Microwave	350	106	35
	Thermal	220	160	25
	Thermal	450	161	50
H-Mor (Strem)	blank	---	356	----
	Thermal	350	158	50
	Microwave	350	13	20
	Thermal	450	218	50
	Microwave	450	42	15

The single point surface area measurements for mordenite (BDH) show that there was a substantial area loss following alkylation of toluene with methanol under normal thermal conditions. The sample heated under microwave irradiation had the lowest measured surface area for this catalyst (106 m^2g^{-1}).

The single point surface area measurements for the Strem mordenite show that there was a substantial area loss following alkylation of toluene with methanol under normal thermal conditions. However, there was a massive loss in surface area from the samples strongly heated under microwave irradiation (356 to 13 and 42 m^2g^{-1}).

4.3.3.3 X-ray Diffraction Measurements.

X-ray diffraction is well established for identification of solid phases. Monochromatic X-rays were deflected from the sample with the diffraction lines produced from the crystal planes (lattice structure) according to Bragg's law.

$$n\lambda = 2d \sin\theta \qquad (4.4).$$

Where:

λ = wavelength of x-ray radiation.
d = spacing between crystal planes.
θ = angle of incidence (and reflection) of the X-rays.
n = an integer.

Since each crystal type gives a characteristic pattern, comparison with standards was used to detect the presence of a particular compound.

The X-ray diffraction measurements for the blank HZSM-5 (BDH) sample agreed very well with the standard crystal data from the literature[43]. The main features are illustrated in table 4.9.

Table 4.9.
Comparison of major peaks for ZSM-5 (BDH).

ZSM-5 (BDH)			ZSM-5 Standard[43]		
2θ	d	rel Intensity	2θ	d	rel Intensity
8.01	11.02	43.6	7.95	11.13	63.4
23.13	3.84	99	7.96	11.12	7.96
23.31	3.81	100	23.19	3.84	100
24.0	3.70	56.6	23.32	3.82	78.5
24.1	3.69	47.1	23.99	3.70	48.2

The HZSM-5 (BDH) sample which had been run at 350°C under normal conditions was compared with the unused blank sample. The sample looked the same as the blank except there was an apparent enhancement of the low angle peaks compared with the midangle peaks. A possible reason for this could be that water was not present in the sample.

A HZSM-5 (BDH) sample which had been run under microwave conditions was compared with the blank. The first immediate observation was that the that the most intense peak had been vastly reduced (by 80%). Another observation was that there was an additional peak at the beginning of the spectrum ($2\theta = 4.14$, $d = 21.19$), which suggested a change to another zeolite form (analcime[44]). The middle peaks compared well with the blank, but there seems to be some small changes at the low angle peaks. The major conclusions from the HZSM-5 samples were that the samples were uncontaminated (i.e. agreed with standard) and that there was a major loss in crystalline material when the sample was subjected to microwave radiation.

The X-ray diffraction measurements for the blank mordenite (BDH) sample showed good agreement with the standard crystal data from the literature[45]. The mordenite (BDH) sample which had been run at 350°C under normal conditions was compared with the blank. The sample looked the same as the blank except there seemed to be some minor intensity changes with some of the major peaks. The possible reasons for this are that a species, such as water, could have been removed or that there was dealumination of the lattice. However, these were not major changes.

A mordenite (BDH) sample which had been run under microwave conditions was compared with the blank. The first immediate observation was that, although all the major peaks were present, they were drastically reduced compared with the blank (by approximately 50-70%). The major conclusions from the mordenite (BDH) samples were that the samples were uncontaminated (agreed with standard) and that there was a major loss in crystalline material when the sample was subjected to microwave radiation.

The X-ray diffraction measurements for the blank Strem mordenite sample showed that it agreed with the standard crystal data from the literature[45]. However, when it was compared with the BDH mordenite blank it was observed that, although the major peaks were all present, there were differences in shifts and relative intensity (table 4.10). The possible reasons for this could be that the Si/Al ratio is different and that different binders were contributing effects.

Table 4.10.
Comparison of major peaks for hydrogen mordenite (Strem and BDH).

Hydrogen mordenite (Strem)			Hydrogen mordenite (BDH)		
2θ	d	rel Intensity	2θ	d	rel Intensity
9.86	8.96	37.7	9.86	8.96	75.7
13.61	6.50	45.23	13.59	6.51	51.7
19.75	4.49	37.35	19.78	4.49	56.5
22.46	3.96	68.47	22.48	3.95	84.6
25.83	3.45	100	25.82	3.45	100

A Strem mordenite sample which had been run at 350°C under thermal conditions was compared with the blank. The XRD data looked the same as the blank except that there were changes in relative intensities.

Mordenite (Strem Chemicals) samples which had been run under microwave conditions were compared with the blank. One microwave sample gave a XRD pattern which showed a major loss in the crystalline structure including an amorphous "hump", while the other sample seemed to be a half way structure (i.e. had not lost as much structure). The major conclusions from the mordenite (Strem Chemicals) samples were that the samples agreed with the BDH catalysts except that there were changes in intensities, and that there was a major loss of crystalline material when the sample was subjected to microwave radiation.

4.3.3.4 Scanning Electron Microscopy Measurements.

Scanning electron microscopy scans over a sample surface with a probe of electrons (5-50 kV). Electrons that are back scattered produce an image on a cathode ray tube which is scanning synchronously with the beam. Magnifications of 20-500 000 times are possible. The Scanning electron microscope is a powerful tool for studying topography and highly irregular structures can be minutely examined.

Figures 4.20-4.22 show the electron micrographs of samples of HZSM-5 blank (figure 4.20), heated under thermal conditions (figure 4.21), and heated under microwave irradiation (figure 4.22) at magnification 12500x. The structure appears to be nodule-like (a) and appears to be irregular. It is difficult to be certain, but there appears to be a definite formation to the nodule structure. The nodules appear to form around a hole, (possibly a cavity). The nodule formation is more pronounced in figure 4.21 where the sample has been heated. The nodules appear to be more fused together by the heat, but the formation of holes and cavities is more pronounced. In figure 4.22 where the sample had been heated under microwave irradiation, the formation of cavities appears to be less pronounced. The nodules are smaller and are not as fused together as in figure 4.21.

Figure 4.23-4.25 shows the electron micrographs, at magnification 2500x, of samples of BDH mordenite blank (figure 4.23), heated under thermal conditions (figure 4.24), and heated under microwave irradiation (figure 4.25). The nodule shape is initially less pronounced compared with the HZSM-5, although the thermal sample (figure 4.24) is more fused together. Again a definite structure in the zeolite is not clear, but the structure does appear to be irregular. The microwave sample (figure 4.25) is more interesting, here a very definite nodule shape can be seen. The nodules to be been fused together and have grown. The structure certainly appeared to have been "melted" in certain parts while the nodules have fused together.

Figures 4.26-4.28 show the electron micrographs, at magnification 2500x, of samples of the Strem mordenite blank (figure 4.26), heated under thermal conditions (figure 4.27), and heated under microwave irradiation (figure 4.28).

Figure 4.26 shows that the structure of the blank Strem mordenite is different to the BDH mordenite and ZSM-5. Instead of a nodule structure, the structure is more rod-like. The picture of the thermal sample (figure 4.27) indicates that this rod-like structure is more pronounced compared to the blank. The picture of the microwave sample (figure 4.28) shows that the amalgamation of the structure is more pronounced, and it resembles the thermal sample (figure 4.27) except that the rods have fused together. However, holes can be seen in the fused structure which are not evident in figure 4.27 or in any of the thermal samples. An explanation for this is that the holes are due to water vapour which has been trapped and when the sample is been heated under microwave irradiation the vapour has burst through the edge of the pellet.

The conclusions from these series of results is that the zeolite catalysts have a definite structure (nodule-like or rod-like). Under thermal conditions the nodules or rods appear to slightly fuse together, whilst under microwave irradiation, definite distortion of the structure is observed.

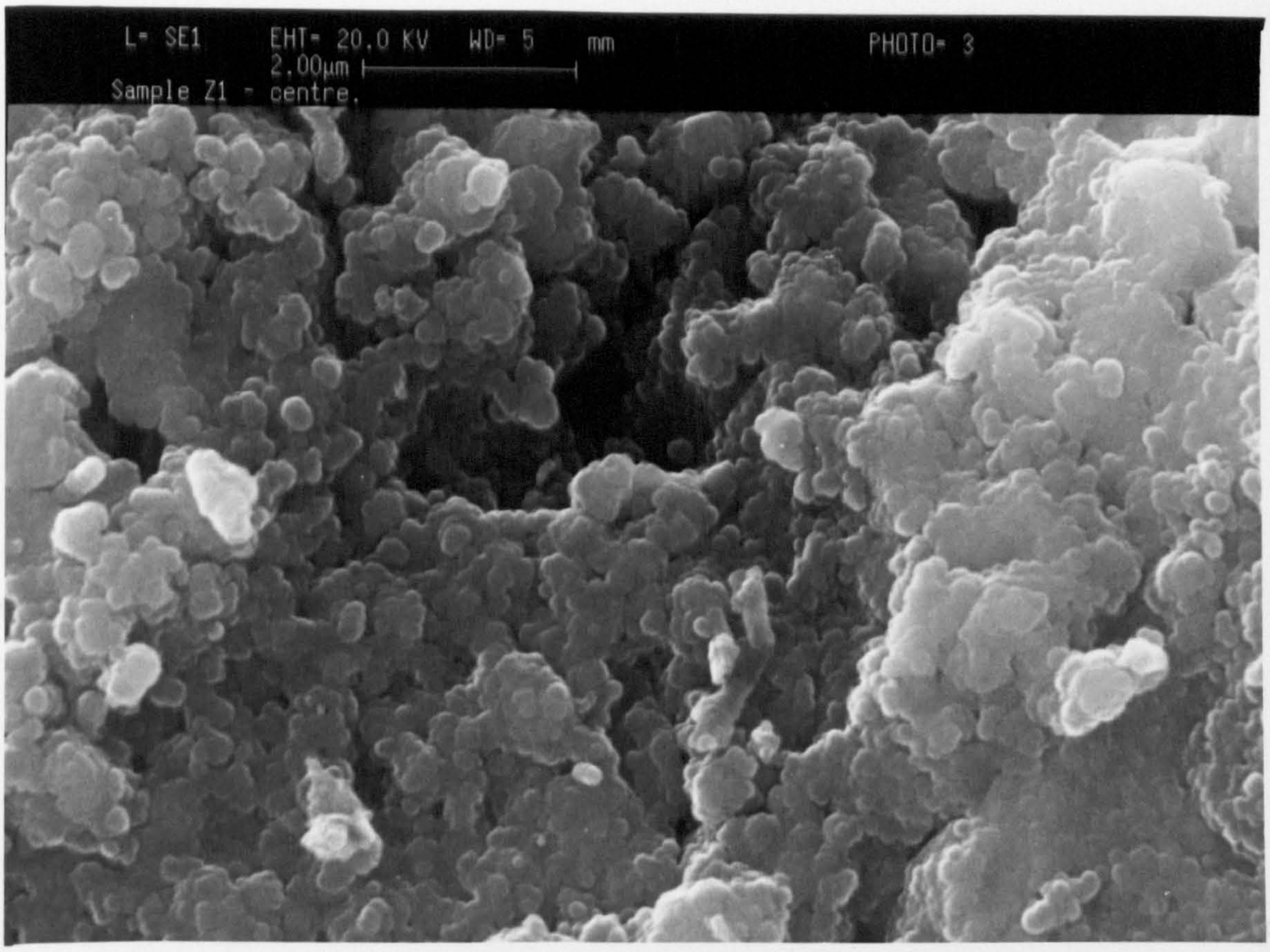

Figure 4.20. SEM picture of ZSM-5 (blank) x12500.

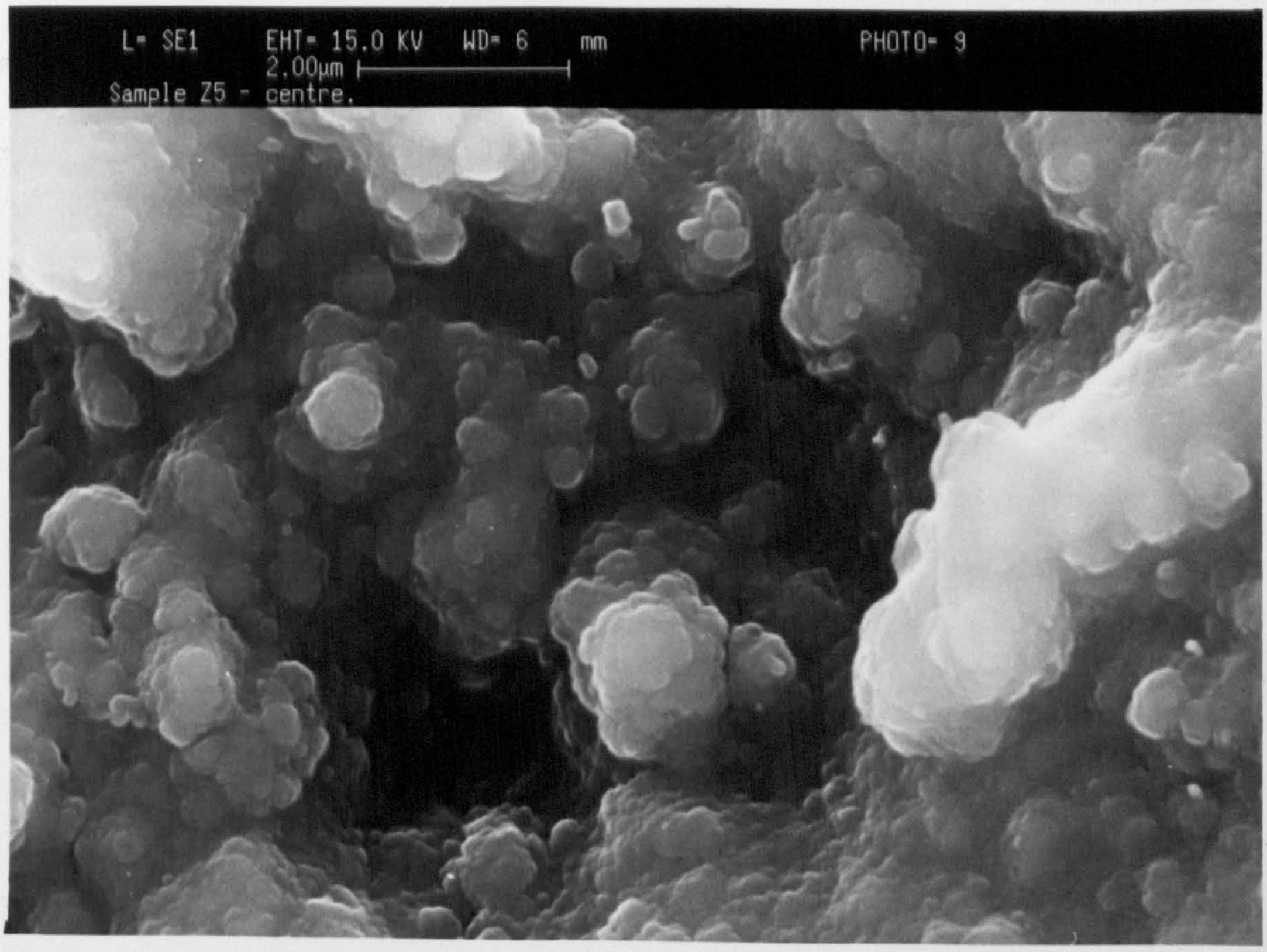

Figure 4.21. SEM picture of ZSM-5 (thermal) x12500.

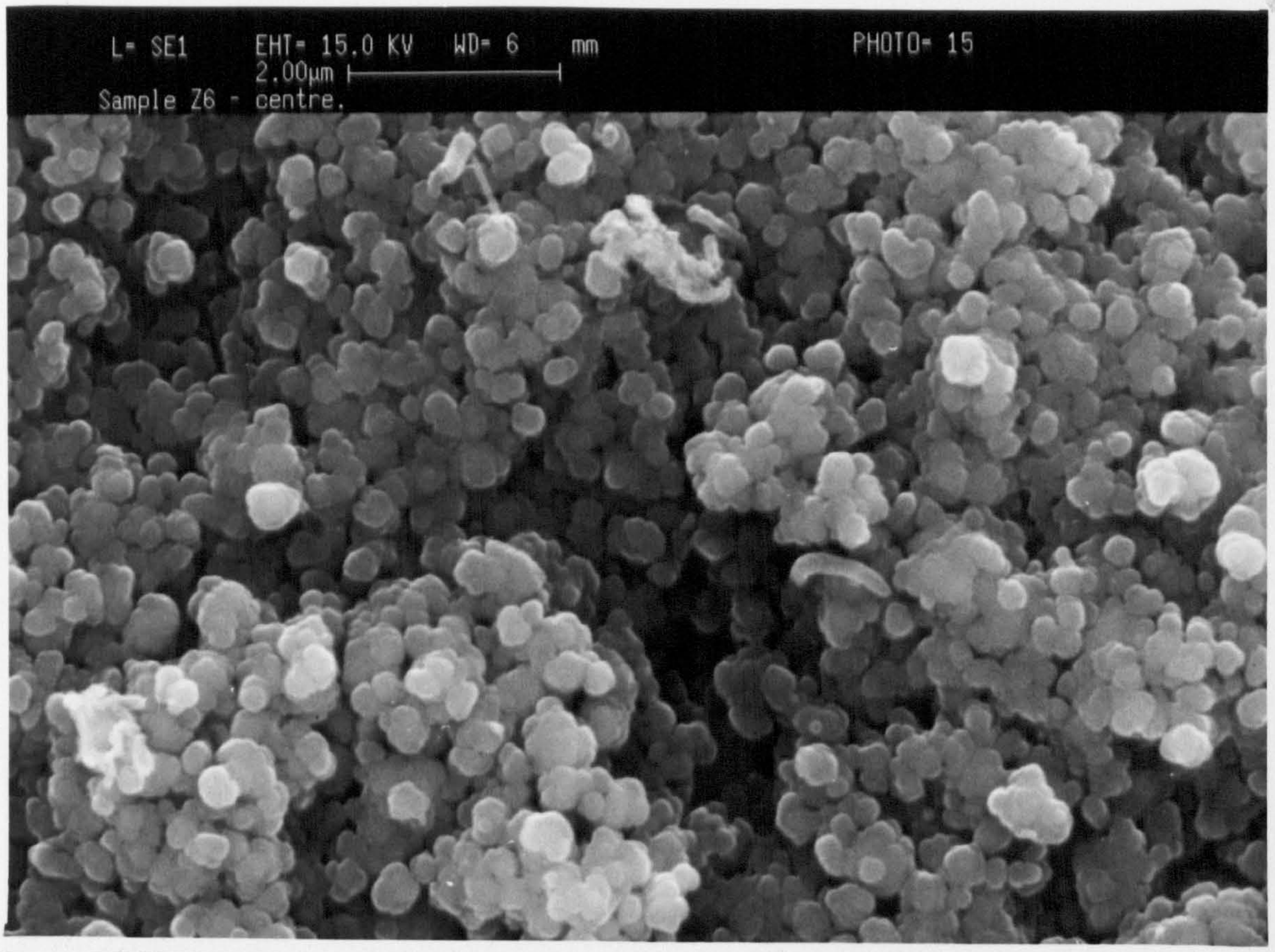

Figure 4.22. SEM picture of ZSM-5 (microwave) x12500.

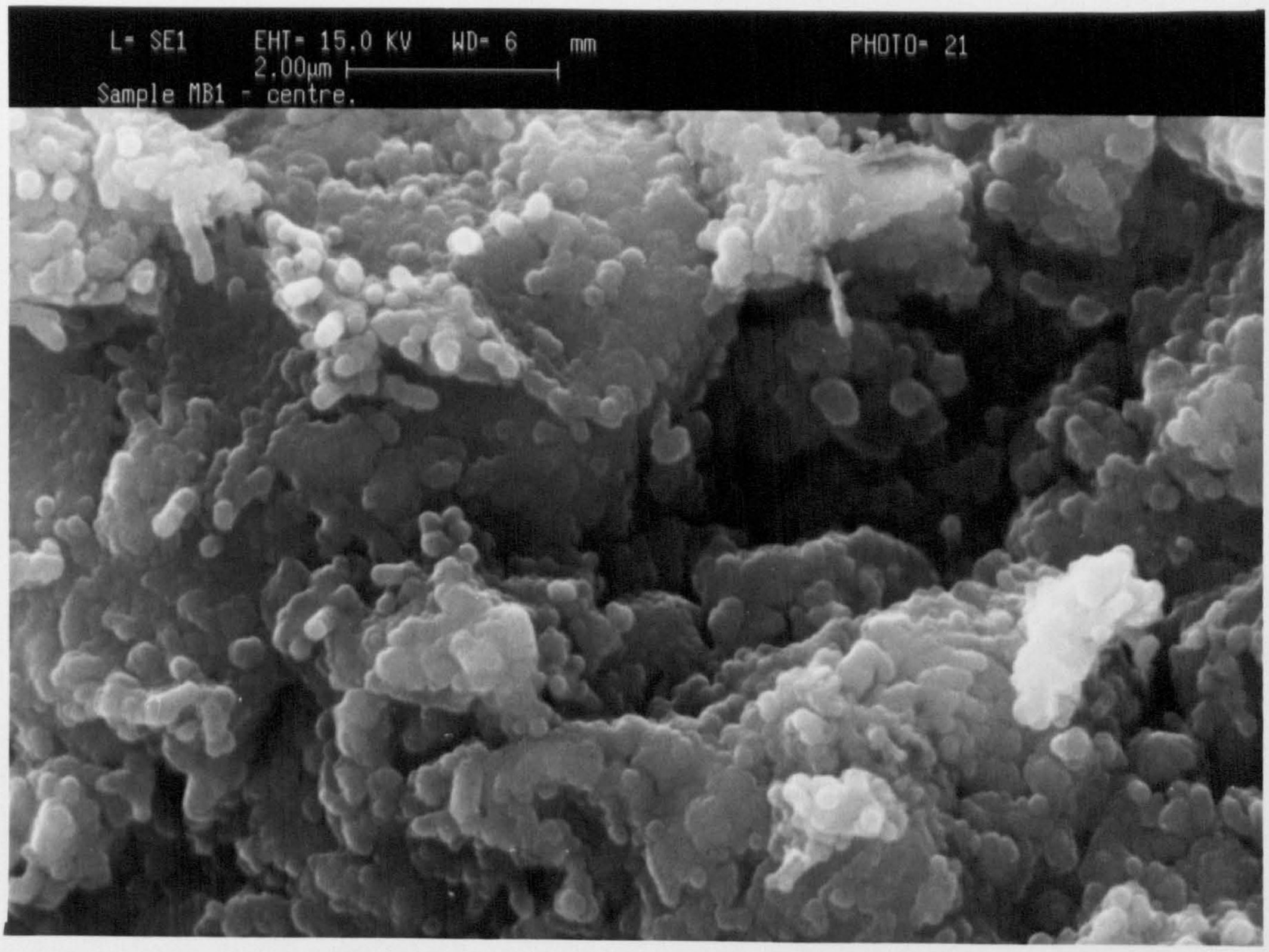

Figure 4.23. SEM picture of hydrogen mordenite (BDH). (blank) x 12500

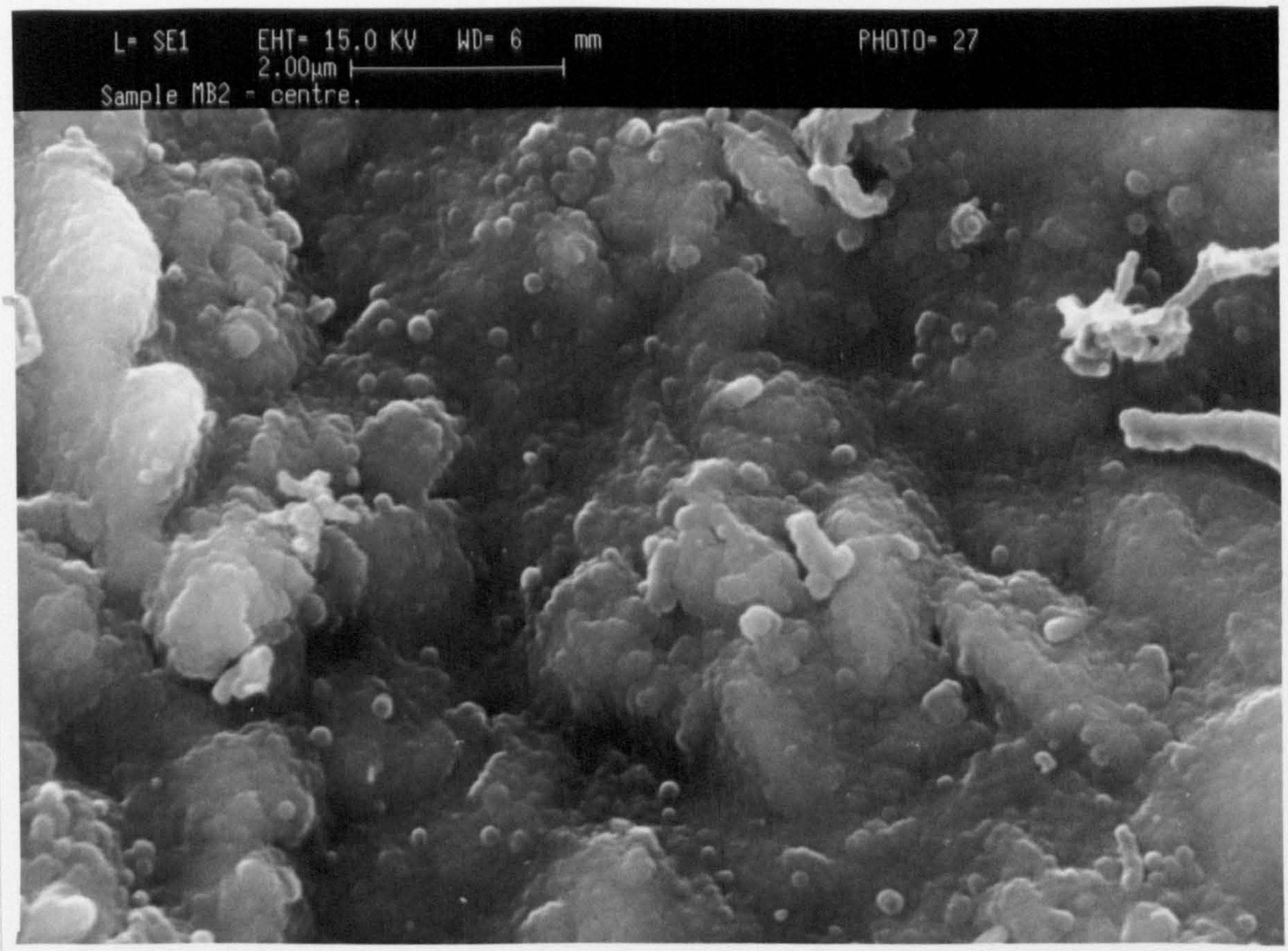

Figure 4.24. SEM picture of hydrogen mordenite (BDH) (thermal) x 12500.

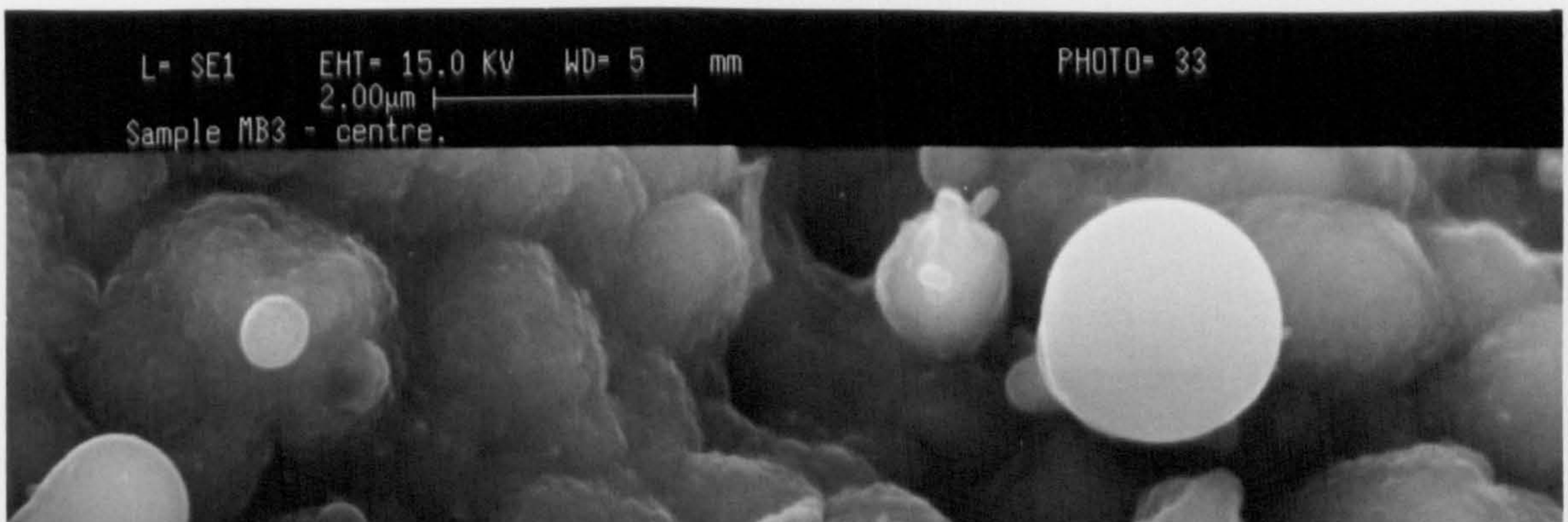

Figure 4.25. SEM picture of hydrogen mordenite (BDH) (microwave) x 12500.

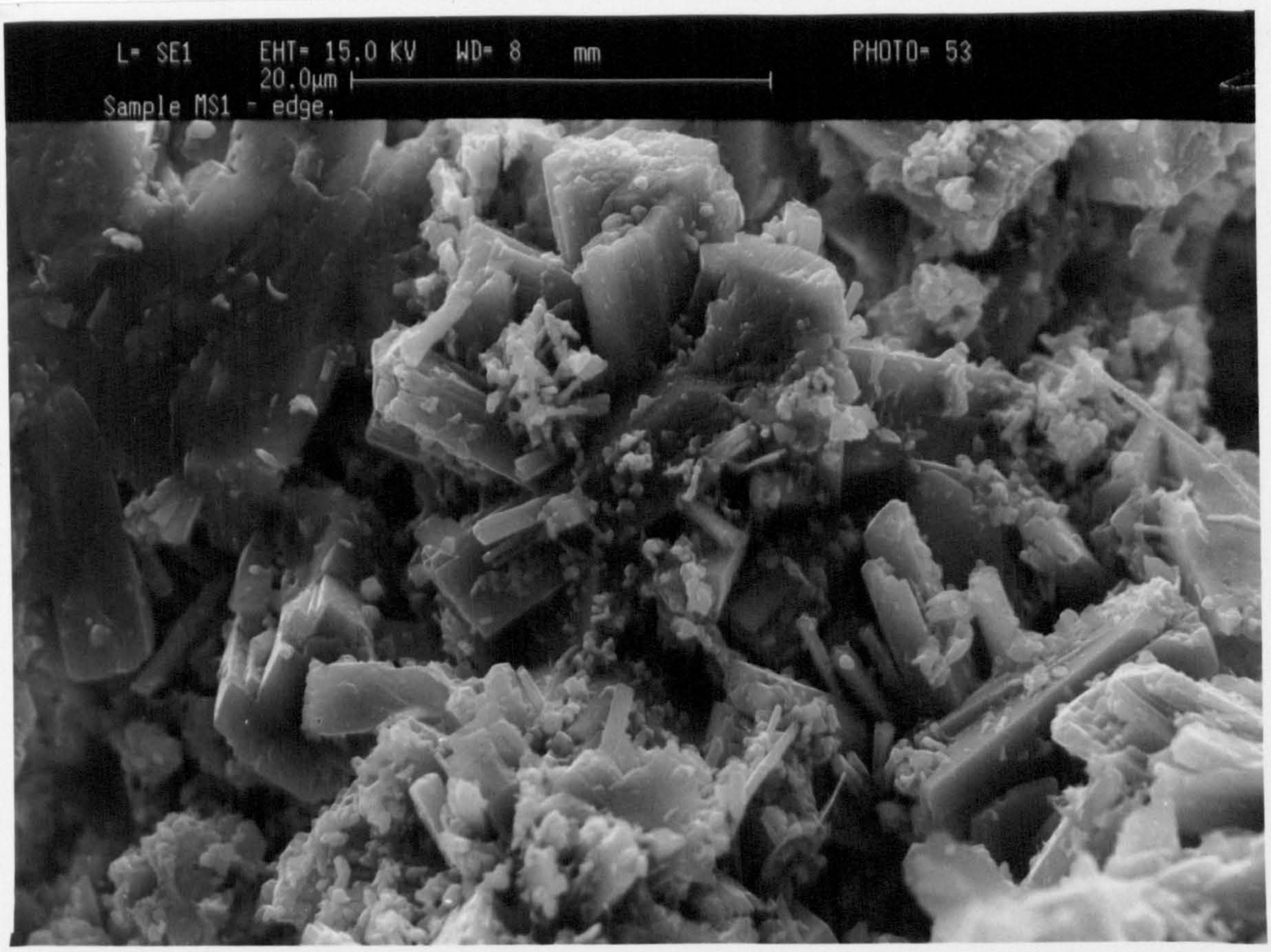

Figure 4.26. SEM picture of hydrogen mordenite (Strem) (blank) x 2500.

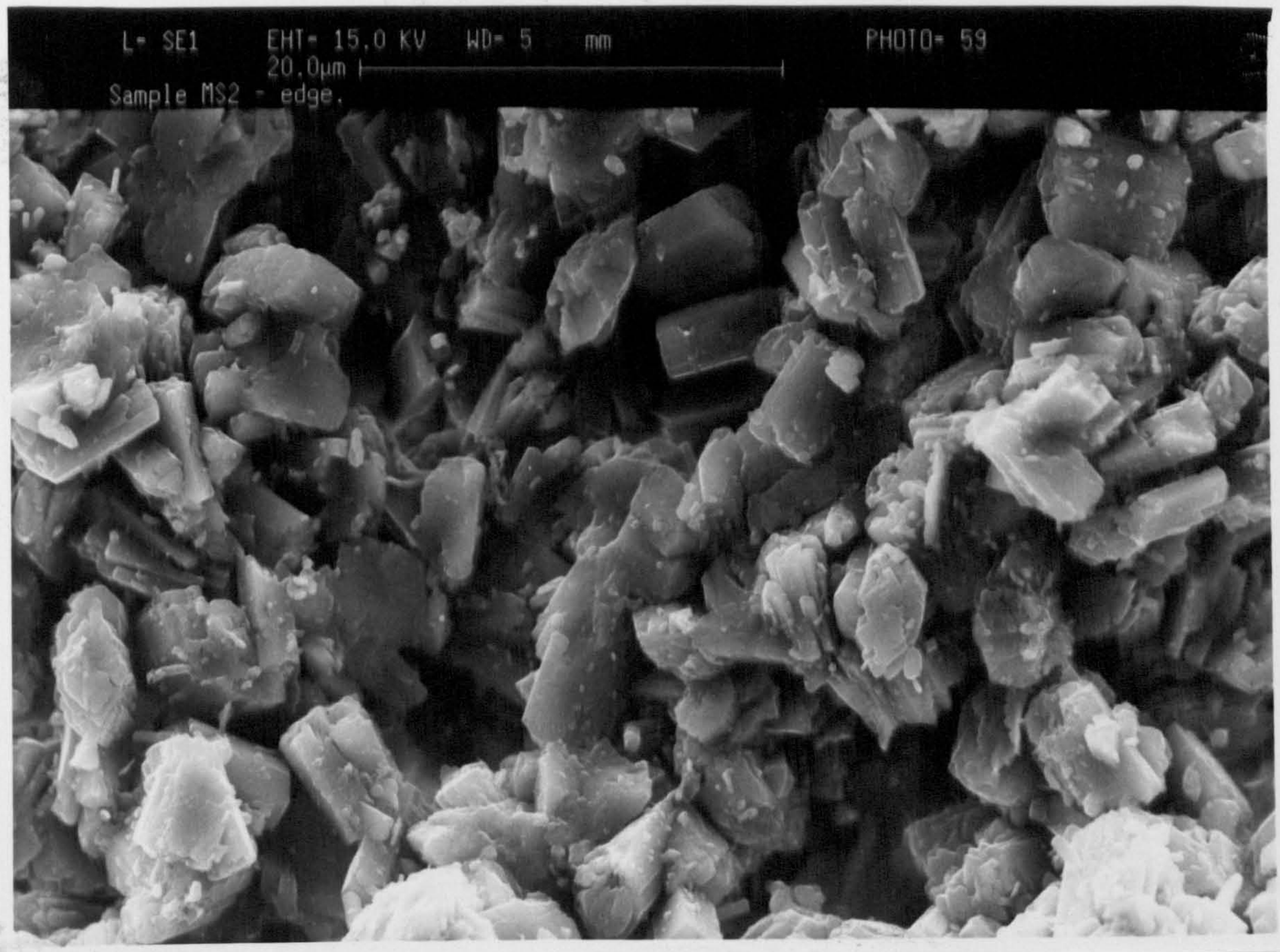

Figure 4.27. SEM picture of hydrogen mordenite (Strem) (thermal) x 2500.

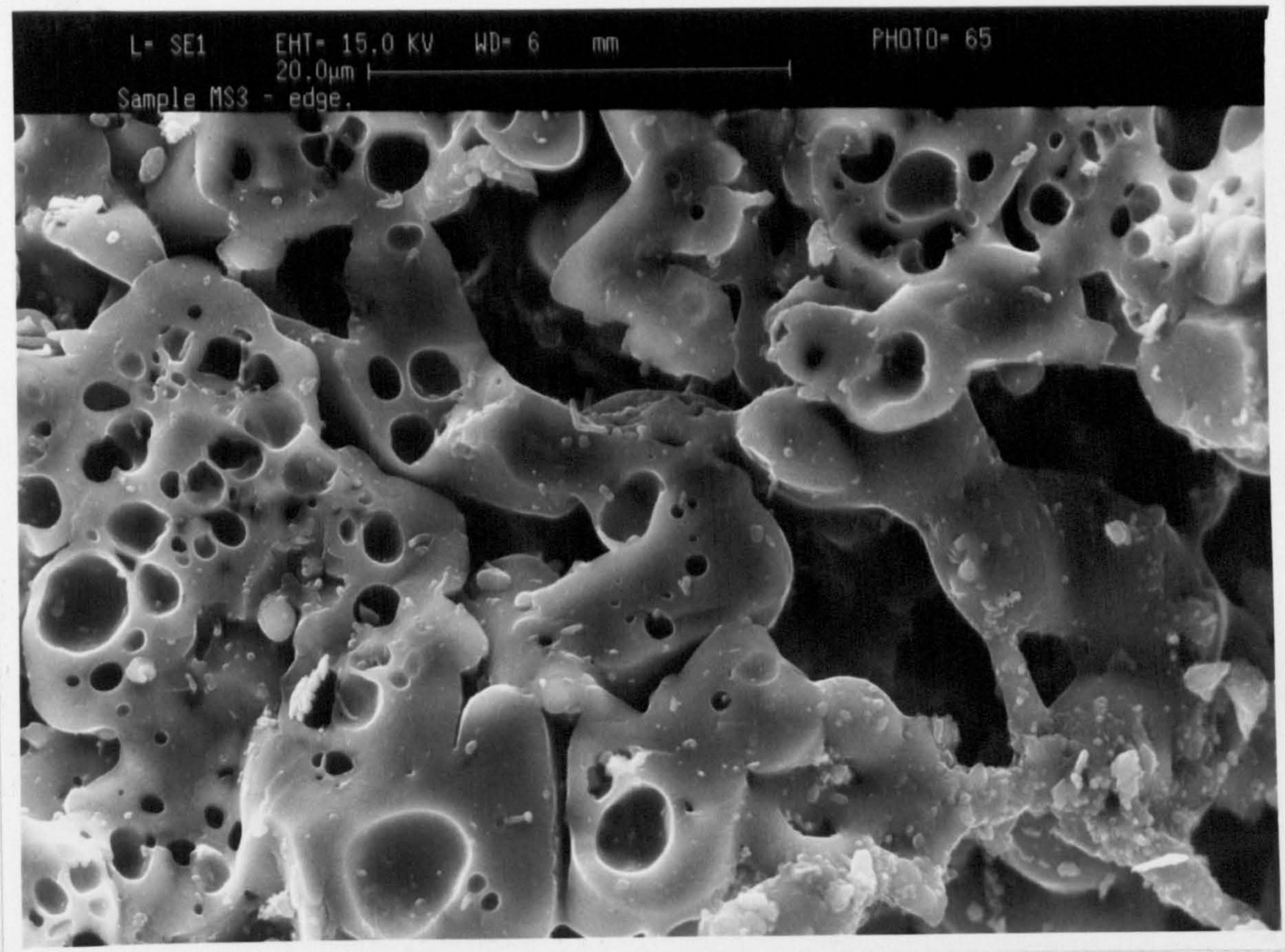

Figure 4.28. SEM picture of hydrogen mordenite (Strem) (microwave) x 2500.

4.4. Discussion.

4.4.1. Experiments using a molar ratio of 1 mole of toluene to 4 moles of methanol.

Since the experiments for disproportionation of toluene under microwave conditions were proving disappointing, it was decided to conduct further experiments on alkylation of toluene with methanol. Extensive modification of the analysis system was undesirable, so the first experiments were carried out by placing a mixture of 50% methanol:50% toluene in the bubbler. Under these conditions, the carrier gas is saturated with toluene and methanol vapour at a molar ratio of 1 to 4 (methanol in excess). Several reactions are occurring; one of which being the alkylation of toluene with methanol to produce para- or orthoxylene. However, there are several side reactions, such as isomerisation of xylenes, disproportionation of toluene, and alkylation of xylene by methanol to give tri- and tetramethylbenzenes (scheme 4.5).

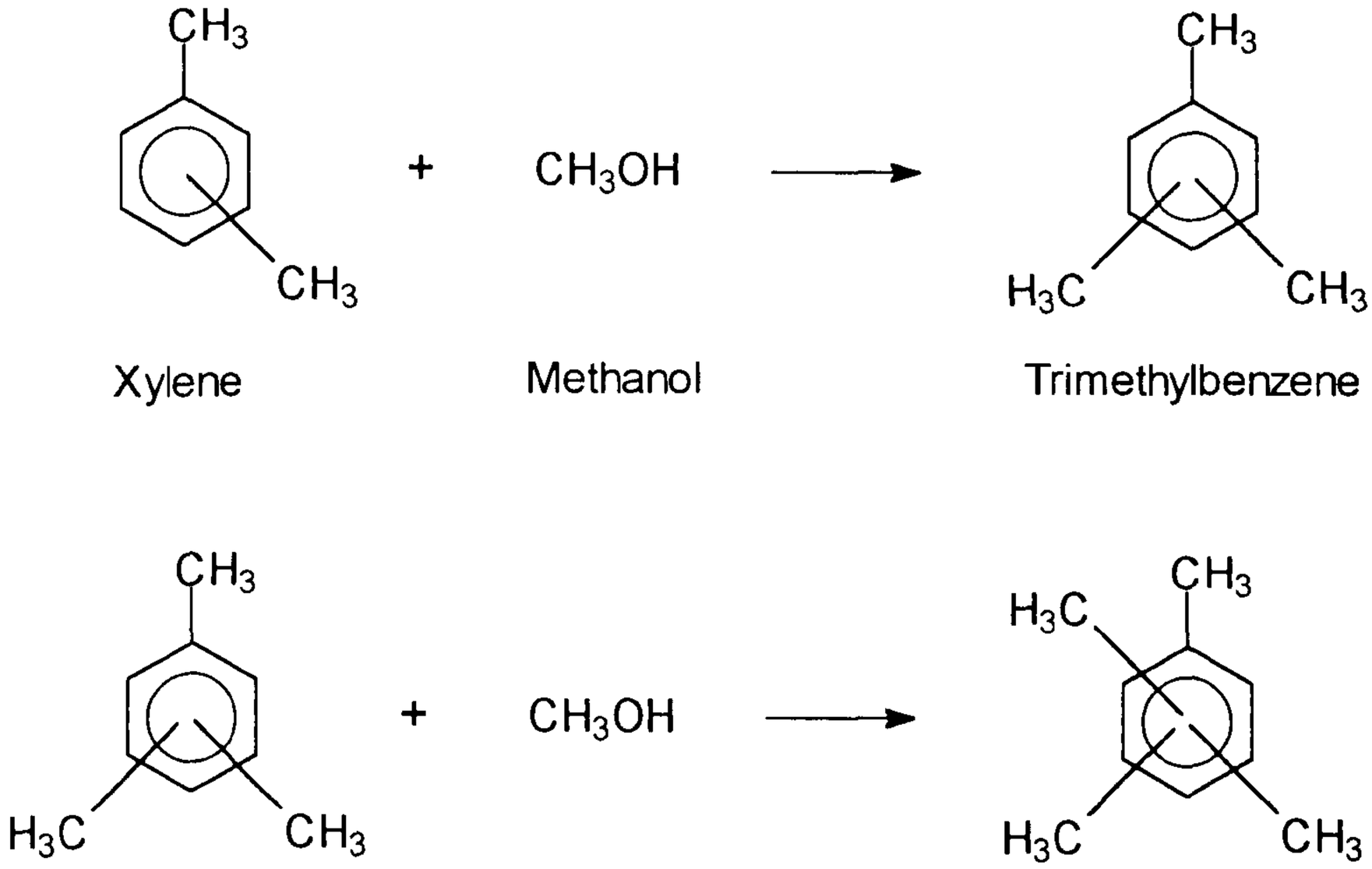

Scheme 4.5.
Alkylation of xylene to give tri- and tetramethylbenzene.

The conversion of methanol is much faster than the conversion of toluene[46-47]. Methanol mainly reacts to form aliphatic hydrocarbons (MTG process)[48].

4.4.1.1. Thermal experiments using a molar ratio of 1 mole of toluene to 4 moles of methanol.

The majority of the products under these conditions are light hydrocarbons. This indicates that dehydration of methanol is occurring to give aliphatic hydrocarbons. This agrees with Coughlan et al.[26], Beschmann et al.[46] and Pino et al.[47] who have observed that with high methanol concentrations, an excess of aliphatic hydrocarbons is formed. The column is not designed for separation of aliphatic light hydrocarbons, so further resolution is not possible. Alkylation of toluene with methanol is definitely occurring since the benzene to xylene ratio is small (<0.5:1). However, the analysis shows that a substantial amount of heavy end products have been formed which was confirmed by analysis of the substances extracted from the cold trap and reactor. This is due to further alkylation of xylenes to give tri- and tetramethylbenzenes because of the high concentration of methanol. When hydrogen mordenite was discharged from the reactor, a brown waxy substance was left. Analysis of this product by mass spectroscopy revealed it to be hexamethylbenzene. This means that excessive alkylation of toluene by methanol was occurring due to the high concentration of methanol.

The conversion to products from alkylation of toluene with methanol over hydrogen mordenite (BDH), under these conditions, is initially high (70%). However, as the experiments proceed, a steady decline in conversion is observed. The most rapid decline in conversion is shown at the higher temperatures (400-450°C). The experiments from alkylation of toluene over HZSM-5 (BDH) show that the catalyst is quite different to the mordenite catalyst. The conversion is similar (70-80%) but is maintained even after 30 hours while experiments on the mordenite catalyst have shown that the conversion is reduced drastically after the same amount of time (20-30%). This difference can be explained by the formation of coke within the pore structure of mordenite. Coke formation from alkylation of toluene with methanol over zeolite catalysts is thought to be a parallel type deactivation[16].

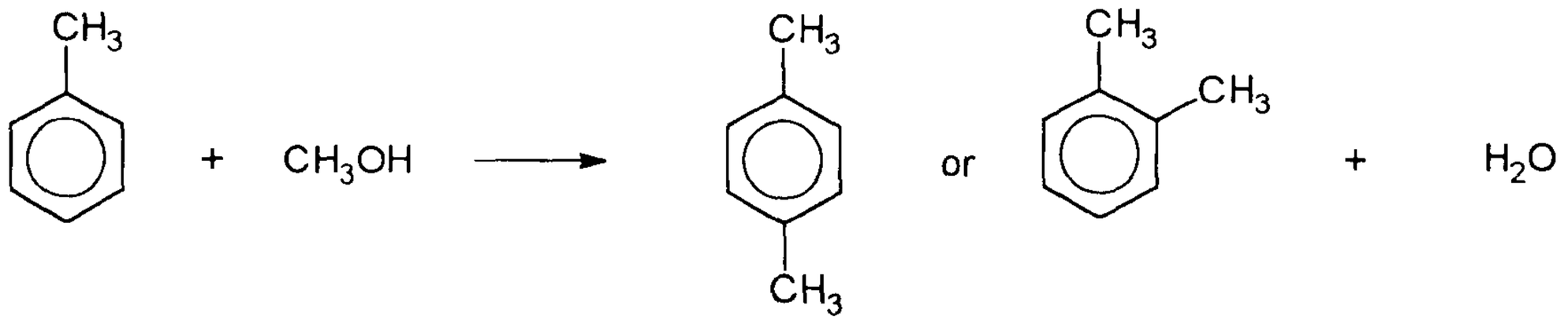

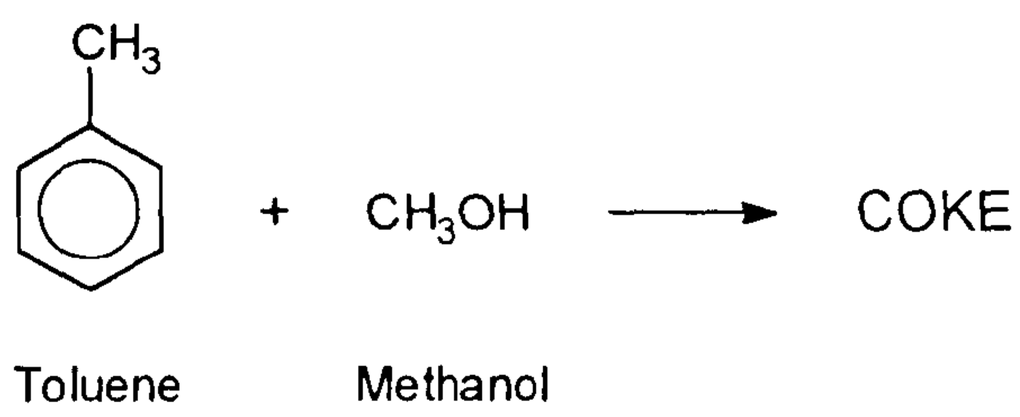

Scheme 4.6.
Coke formation from alkylation of toluene with methanol[16].

Although side reactions such as alkylation of xylenes and coke formation accompany toluene alkylation over ZSM-5, coking is not as drastic as in large pore zeolites such as mordenite because the pores in ZSM-5 are too small (as explained in chapter 3). Coke forms on the outer surface of ZSM-5, not within the pore structure, whereas in mordenite, most of the coke is formed within the pores.

The selectivity to paraxylene from alkylation of toluene with methanol over hydrogen mordenite is initially found to be near its equilibrium value of 24%. However, as the experiment proceeds, the selectivity decreases. This is due to an increase in selectivity to orthoxylene. Alkylation of toluene is para- or ortho- directing, isomersiation to give the equilibrium distribution of xylenes subsequently occurs. An ortho-rich distribution of xylenes has been observed for alkylation of toluene over large pore zeolites such as X, Y or L due to aromatic electrophilic substitution with a reactive alkylation agent[18, 28, 49]. The selectivity to paraxylene increases with temperature as observed by other workers[18, 24, 25, 39, 47]. The selectivity to paraxylene from alkylation of toluene with methanol over HZSM-5 is higher than the equilibrium value of 24% (typically 31-33%). This in agreement with Yashima et al.[24]. This enhanced selectivity is due to the small pore size of ZSM-5 (typically 6.3Å). The small pore size of ZSM-5 has a steric effect on the reaction giving preference to the para-form.

4.4.1.2. Microwave experiments using a molar ratio of 1 mole of toluene to 4 moles of methanol.

The experiments for alkylation of toluene with methanol over the catalysts under microwave irradiation have been disappointing. The conversion to toluene is very erratic but is comparable to experiments carried out under normal thermal conditions. The majority of the product distribution under microwave conditions is the formation of benzene and lighter hydrocarbons. There is only a very small amount of xylenes in the product distribution.

The experiments for alkylation of toluene with methanol behave in a similar fashion to experiments for disproportionation of toluene under microwave irradiation. The formation of carbon on the catalyst surface interacts with the microwave radiation. The carbon gets hot, thus raising the temperature of the catalyst and temperature measurement under these conditions is a problem. The temperature of the catalyst oscillates around a fixed temperature, resulting in the spiky trace from the infrared pyrometer. The results are very erratic under these conditions because the conversion of toluene depends on the temperature of the catalyst when the contents of the sample are injected into the gas chromatograph.

However, the conversion to products is comparable to the corresponding thermal experiment. The distribution of products, under these conditions, shows that the majority of the products are benzene and methane indicating that the temperature of the catalyst is significantly higher than that measured by the infrared pyrometer. After several hours under these conditions, the oscillation decreases, where the pyrometer is recording the temperature accurately. This indicates that carbon has been burnt off the surface of the catalyst. However, further analysis show that although conversion to products is comparable to the thermal experiment. (figure 4.8), there is still an excess of benzene and cracking products and xylene production is very low (figure 4.9).

Observation of the catalyst sample when the reactor is removed from the single mode cavity showed that some of the spheres had fused together and that in some cases there was distortion of the reactor, indicating that a very high temperature had been attained.

4.4.2. Experiments using a molar ratio of 3 moles of toluene to 1 mole of methanol.

4.4.2.1. Thermal experiments using a molar ratio of 3 moles of toluene to 1 mole of methanol.

A typical chromatographic trace from SUMMIT for alkylation of toluene, using a molar ratio of 3 moles of toluene to 1 mole of methanol under thermal conditions, shows that the distribution of products is different to alkylation of toluene using the previous ratio. Although the conversion to products is lower (40%) and methanol is completely converted, the majority of the products are xylenes. This indicates that further alkylation of xylene and dehydration of methanol is suppressed due to the lower concentration of methanol. This agrees with Beschmann et al.[46] and Pino et al.[47], who have observed that with lower methanol concentrations, conversion to products is reduced, but selectivity to xylenes increases. This agrees with the analysis of the products from the cold trap, which show that small amounts of trimethylbenzenes and only traces of tetramethylbenzenes are produced

The conversion to products from alkylation of toluene with methanol over hydrogen mordenite (BDH), under these conditions, increases with temperature. The conversion at 450°C is initially 40%. However, as the experiments proceeds, a gradual decline in conversion is observed (16% after 40 hours on line). The Strem mordenite shows a much lower conversion at the same temperatures (15%) but the same decline is observed. The experiments from alkylation of toluene over HZSM-5 (BDH) show that the catalyst is quite different to the mordenite catalyst. The conversion is lower than the BDH mordenite (20%) but the decline is much less (decreases to 14% after 40 hours).

The selectivity to paraxylene from alkylation of toluene with methanol over hydrogen mordenite is found to be near its equilibrium value of 24%. The selectivity did not decrease with time. This is in contrast to the previous experiments. This is due to the lower methanol concentration. Beschmann et al.[46] and Pino et al.[47] have observed that selectivity to paraxylene increases with decreasing methanol concentration. However, isomerisation of paraxylene occurs to give the equilibrium distribution of xylenes subsequently occurs. This is in agreement with Rakoczy et al.[28]. The selectivity

to paraxylene from alkylation of toluene with methanol over HZSM-5 is initially higher (46%) than the previous experiments (33%). However, as the experiments proceeds, a gradual decline in selectivity to paraxylene is observed (36% after 40 hours on line). Bhat[18] has performed studies on alkylation of toluene over HZSM-5 using both pulse and continuous flow methods and has observed that para- selectivity decreases with contact time. An explanation for this effect is that molecules entering the zeolite cavity will approach a surface already having an adsorbed layer of molecules. Adsorption of molecules in ZSM-5 is mainly concentrated on the acid sites. The first step in alkylation is thought to be the adsorption of the methanol molecule on the acid sites forming a carbonium ion with which the toluene molecule reacts to form the xylene. Due to steric hindrance, the para- position of toluene molecule would most easily react with the carbonium ion. With subsequent molecules entering the cavity, fewer strong acid sites would be accessible and the carbonium ion would be hindered less and more orthoxylene would be produced.

Observation of the benzene to xylenes ratio for the three catalysts show that for the mordenite catalysts, the ratio is high and declines. The Strem mordenite initially has a very high benzene to xylene ratio (1.9), which rapidly declines (0.6 after 5 hours). The BDH mordenite initially has a lower benzene to xylene ratio (0.8) which slowly declines (0.4 after 30 hours) and remains constant. The explanation for this is that side reactions such as disproportionation and dealkylation of toluene are occurring. This agrees with experiments on disproportionation of toluene, with dealkylation taking place on strong Bronsted acid sites. As these sites are covered (as the experiment proceeds), alkylation of toluene takes place. The benzene to xylene ratio for HZSM-5 is very small (0.01) and is constant. The explanation for this observation is the Si/Al ratio, HZSM-5 has the highest Si/Al ratio of 50, BDH mordenite has 20 and Strem mordenite 10. Strem mordenite has the highest aluminium content thus the highest acidity, and so dealkylation reactions are more prominent in the initial stages of the experiment. The conclusion from these experiments is that HZSM-5 (BDH) is a better catalyst for alkylation of toluene with methanol than mordenite.

4.4.2.2. Microwave experiments using a molar ratio of 3 moles of toluene to 1 mole of methanol.

The experiments for alkylation of toluene with methanol, using a molar ratio of 3 moles of toluene to 1 mole of methanol, over hydrogen mordenite (BDH) under microwave irradiation are similar to the previous microwave experiments for alkylation of toluene with methanol. Initially the conversion to toluene is very erratic but is comparable to experiments carried out under normal thermal conditions. The formation of carbon on the catalyst surface interacts with the microwave radiation. The carbon gets hot, thus raising the temperature of the catalyst and temperature measurement under these conditions is a problem. The sample is observed to be glowing under these conditions. The majority of the product distribution under microwave conditions is the formation of benzene and lighter hydrocarbons. There is only a very small amount of xylenes in the product distribution. To counteract this effect the microwave power is reduced until the sample is not glowing. Under these conditions, the infrared pyrometer reads a temperature of 214-220°C. Analysis of the products shows that conversion to products is comparable to the thermal run conducted at 350°C, although the selectivity to paraxylene is slightly higher. After 24 hours, under these conditions, there is no change in conversion (10%). The microwave power is then raised so the sample is glowing for 2 hours. When the conditions are restored the first analysis shows a massive decrease in orthoxylene and an increase in selectivity to paraxylene and total conversion to products is increased (figures 4.15 and 4.16, table 4.7). A conclusive reason for this effect is not immediately obvious, possibly the rise in microwave power causes carbon to be burnt off from the surface and inside the pore structure, leading to a partial regeneration of the catalyst resulting in an increase in conversion. The temperature of the catalyst could be much greater than 350°C although selectivity to dealkylation of toluene is not observed (table 4.7). The decrease in orthoxylene is more difficult to explain. Hydrogen mordenite is deactivated due to pore blockage, possibly the rise in microwave power causes part of the carbon deposits in the pore structure to be burnt off, and the formation of paraxylene is favoured due to steric hindrance. Paraxylene could then diffuse very quickly out of the pore, while orthoxylene diffuses more slowly

(increase in orthoxylene in subsequent analyses, table 4.7). A similar effect is observed with experiments performed under thermal conditions, after 24 hours the reactor is transferred to the single mode cavity and heated until the sample glows for 2 hours. Analysis of the products under these conditions shows only conversion to benzene and lighter hydrocarbons. The reactor is transferred to the furnace and heated up to reaction temperature, and results show that there is no dramatic change in conversion and selectivity to paraxylene.

These and previous experiments under microwave irradiation show that temperature measurement using the infrared pyrometer is a problem. Temperature measurement using gas thermometry is also a problem when the calibration is erroneous. Further experiments under microwave irradiation seemed fruitless unless this problem could be eradicated. Numerous experiments in gas thermometery were conducted with various pressure transducers and various types of seals. The major problem was that a careful calibration from room temperature to 500°C took a very long time (typically 10 hours). With various pressure transducers, there was a drift in the reading overnight, due to the long stem length of the thermometer being exposed to atmospheric changes overnight, leakage from the seal connecting the transducer to the thermometer, and possible drift in the electronics of the system. However, experiments using a EURO SENSOR OEM pressure Sensor Model 13, connected to the gas thermometer by a ¼" Drallim fitting proved very successful so this model was used for the microwave experiments.

The experiments for alkylation of toluene with methanol, using a molar ratio of 3 moles of toluene to 1 mole of methanol, over hydrogen mordenite (Strem) under microwave irradiation are similar to microwave experiments for alkylation of toluene over hydrogen mordenite (BDH). Because the infrared pyrometer is failing to read the temperature of the catalyst when a significant amount of carbon laydown produces a rapid rise in temperature, experiments are performed using the gas thermometer, so the temperature of the catalyst is read by both devices. At the start of the experiment they agree ($\pm$ 10°C), however, when the sample is observed to glow there is a significant difference in temperature recorded by each device. The infrared pyrometer read a

temperature of 350°C while with the gas thermometer, a temperature of 450°C is recorded. Analysis of the products show that only dealkylation of toluene is occurring. To counteract this effect the power is reduced until the temperature is 350°C (as read by the gas thermometer). The conversion to products and selectivity to paraxylene is comparable to the thermal experiments. After 24 hours, under these conditions, there is no change in conversion (10%). The microwave power is then raised so the sample is glowing for 2 hours. When the conditions are restored the first analysis shows only conversion to benzene and lighter hydrocarbons. Increasing the temperature produces no increase in conversion. A similar experiment at 400°C produces a similar result (figure 4.17) even when the reactor is replaced in the conventional furnace and heated up to 400°C only a very small conversion is observed, and the product distribution is mainly benzene and lighter hydrocarbons. An explanation for this effect is that raising the microwave power until the sample is glowing is detrimental to the pore structure of the Strem mordenite. Observation of the catalyst sample when the reactor is removed from the single mode cavity showed that some of the spheres had fused together and that in some cases distortion of the reactor occurred, indicating that a very high temperature had been attained.

4.4.3. Catalyst characterisation.

The single point surface area measurements show that there is substantial loss in surface area for the samples heated under microwave irradiation. The Strem mordenite shows the largest decrease. This agrees with the results from XRD and SEM, the XRD data from the thermal samples shows that they are not too different from the blank (unreacted) sample. The samples, which have been subjected to microwave radiation show a major loss in crystalline structure. The SEM data shows that the samples heated under thermal conditions are not so different compared to a blank sample. The mordenite samples heated under microwave radiation distortion of the structure is very evident (growth of nodules resulting in loss of surface area). The characterisation studies agree with each other in the fact that microwave radiation can have a detrimental effect upon the catalyst. The catalysts are very difficult to heat under microwave irradiation, however, once a carbon laydown has been established, the carbon absorbs the microwaves and gets very hot. Thermal tests up to 1000°C have revealed that very little change in surface area and crystalline structure is observed. The temperature attained by the catalysts under these conditions must be significantly be excess of 1000°C, since distortion of the silica reactor is observed with some experiments. The most striking results, measured by all techniques, are shown by the Strem mordenite. The samples heated under microwave radiation have the largest decrease in surface area and crystalline structure and are the most distorted. The most obvious difference between all the catalysts in the Si/Al ratio. The Strem mordenite has the lowest Si/Al ratio and hence contains the most aluminium and is thus the most acidic. This excess of aluminium could interact with the microwaves producing the very high temperatures, which the Strem mordenite samples obviously attain.

PAGE
MISSING
IN
ORIGINAL

17. Bhat Y. S., Halgeri A. B., and Prasada Rao T. S. R., Ind. Eng. Chem. Res., **28**, 890, (1989).

18. Bhat S. G. T., J. Catal., **75**, 196, (1982).

19. Venuto P. B., Hamilton L. A., Landis P. S., and Wise J. J., J. Catal., **4**, 81, (1966).

20. Venuto P. B., Hamilton L. A., and Landis P. S., J. Catal., **5**, 484, (1966).

21. Yashima T., Ahmad H., Yamazaki K., Katsuta M., and Hara N., J. Catal., **16**, 273, (1970).

22. Yashima T., Ahmad H., Yamazaki K., Katsuta M., and Hara N., J. Catal., **17**, 151, (1970).

23. Chen N. Y., and Garwood W. E., J. Catal., **52**, 453, (1978).

24. Yashima T., Sakaguchi Y., and Namba S., Proc. 7th Intern. Congr. Catal., Tokoyo 1980, Part A, p739, Elsevier, Amsterdam.

25. Kaeding W. W., Chu C., Young L. B., Weinstein B., and Butter S. A., J. Catal., **67**, 159, (1981).

26. Coughlan B., Carroll W. M., and Nunan J., J. Chem. Soc. Farad. Trans., I, **79**, 281, (1983).

27. Coughlan B., Carroll W. M., and Nunan J., J. Chem. Soc. Farad. Trans., I, **79**, 297, (1983).

28. Rakoczy J., Zadrozna G., and Krawczyk J., Hun. J. Ind. Chem., **19**, 211 (1991).

29. Yashima T., Sato K., Hayasaka T., and Hara N., J. Catal., **26**, 303, (1972).

30. Giordano N., Pino L., Cavallaro S., Vitarelli P., and Rao B. S., Zeolites, **7**, 131, (1987).

31. Englehardt J., Szanyi J.,and Valyon J., J. Catal., **107**, 296, (1987).

32. King S T., and Garces J. M., J. Catal., **104**, 59, (1987).

33. Nishi H., Nowinska K., and Moffat J. B., J. Catal., **116**, 480, (1989).

34. Blanco A., Campelo J. M., Garcia A., Luna D., Marinas J. M., and Romero A A., J. Catal., **137**, 51, (1992).

35. Dumitriu E., Oprea S., and Hulea V., Revue. Roumaine de Chemie, **32**, 2, 191, (1987).

36. Cavallaro S., Pino L., Tsiakaras P., Giordano N., and Rao B. S., Zeolites, **7**, 408, (1987).

37. Chen N. Y., Kaeding W. W., and Dwyer F. G., J. Am. Chem. Soc., **101**, 6783, (1979).

38. Lee C. S., Park T. J., and Lee W. Y., Appl. Catal., **96**, 151, (1993).

39. Wei J., J. Catal., **76**, 433, (1982).

40. Kodama H., and Okazaki S., J. Catal., **132**, 512, (1991).

41. Instruction Manual Pulse Chemisorb 2700. Micromeritics.

42. Brunauer S., Emmet P. H., and Teller E., J. Am. Chem. Soc., **60**, 309, (1938).

43. van Koningsveld H., van Bekkum H., and Jansen J. C., Acta Cryst., **B34**, 127, (1987).

44. Ferrais G., Jones D. W., and Yerkess., Z. Kristallogr., **135**, 240, (1972).

45. Gramlich V., PhD Dissertation, ETH, Zurich (1971).

46. Beschmann K., and Riekert L., J. Catal., **141**, 548, (1993).

47. Pino L., Giordano N., Cavallaro S., Rao B. S., Tsiakaras P., and Vitarelli P., Annaladi Chimica, **78**, 575, (1988).

48. Chen N. Y., J. Catal., **114**, 17, (1988).

49. Kaspa J., Montgomery D. D., and Olah G. A., J. Org. Chem., **43**, 3147, (1978).

Chapter Five.

General Conclusions and Future Work.

5.1. General Conclusions.

The conclusions that can be drawn from this study are:

5.1.1. Temperature measurement.

(1). Gas thermometry has shown to be an effective means of measuring the temperature within a microwave field.

5.1.2. Microwave Assisted Superheating Of Liquids.

(1). Polar solvents can superheat under microwave irradiation.

(2). The extent of superheating is a function of the dielectric properties of the material, the power, the surface area to volume ratio, the penetration depth, the state of the glassware and the surface tension of the liquid.

(3). Almost all of the literature claims regarding rate enhancement by microwave irradiation can be explained by the superheating phenomenon.

(4). The vapour phase has been shown to be significantly cooler than the bulk liquid.

5.1.3. Disproportionation and alkylation of toluene.

(1). Microwave radiation has no beneficial effect on the reaction selectivity.

(2). The problem is the carbon laydown which absorbs microwaves and raises the temperature of the catalyst.

(3). Experiments on disproportionation of toluene under high pressure conditions have shown that partial regeneration of the catalyst can be performed by raising the partial pressure of hydrogen.

5.2. Future Work.

5.2.1. Temperature measurement using gas thermometry.

Temperature measurement of the catalyst sample within a microwave field has been the major problem associated with this work. Infrared pyrometry can measure the temperature of the catalyst up to 500°C, beyond this temperature the radiation emission is in the visible part of the electromagnetic spectrum and the pyrometer fails to record the temperature accurately. Although the gas thermometer has shown to be an accurate means of determining the temperature within the catalyst bed there are inherent problems with the system. Leakage from the seal connecting the transducer to the thermometer makes the measurement futile and the physical problems of having a long stem length (for the gas thermometer to be incorporated into the reactor) affect the calibration. The thermometer is calibrated in a furnace and the response time of the thermometer is slower than the thermocouple so time is wasted leaving the system to equilibrate. A long section of the thermometer is open to the environment and this can affect the reading. However, preliminary experiments using the EURO SENSOR OEM pressure Sensor model 13 transducer, have shown that this system can be a viable method for recording the temperature. The problem of a long response time for rapid changes in temperature will have to be taken into consideration when planning future work using the thermometer. Since the transducers used in this study were not designed for the purposes of temperature measurement using a gas thermometer, future experiments could involve collaborative work with companies to develop a custom made pressure transducer for the purposes of temperature measurement in a microwave field. Work has been conducted by other workers in the microwave group at Hull using a fibre-optic probe and this has eased some of the problems with measuring temperature.

5.2.2. Microwave Assisted Superheating Of Liquids.

The benefits of this phenomenon are, at the moment, limited to small scale laboratory work. The effect is thermal so the rate enhancements are due to the temperature rise. If rate enhancements are required on a industrial scale, pressure vessels such as autoclaves can be employed. An area where microwave irradiation could be applicable is if high pressures are undesirable, particularly with regard to safety. One area which could be advantageous to industry could be the use of microwave irradiation with azeotropes. Water is only slightly superheated, while ethanol has been shown to be significantly superheated. However, the preliminary experiments have proved this does not occur.

Further work into this area could be directed on the following aspects. The extent of the microwave assisted superheating effect of solvents could be examined using different microwave frequencies. All the experiments performed in this work used a frequency of 2.45 GHz, so different effects could be observed at different frequencies. Further investigation of superheated boiling point compositions should be conducted, with regard to separation of liquid by fractional distillation where the condensation product can be removed. If the solvents have significantly different elevations of boiling points due to microwave irradiation, a different condensation product could be obtained in certain cases. Investigation of whether benefits of having the vapour phase significantly cooler than the bulk liquid phase could be studied. The effect of cooling the reaction vessel prior to the experiment should be studied. A better experiment for the azeotropic distillation of ethanol and water should be conducted. The water/ethanol solution has been shown to superheat under microwave irradiation. However, a different composition of distillate was not obtained due to the fact that the liquid condenses back into the vessel before it reaching the distilling column. A better experiment would be to lag the glassware so that condensation occurs only in the distillation column. The boiling points for water and ethanol are relatively the same under microwave conditions. A better system to investigate could be propan-1-ol and water. Under ordinary thermal conditions propan-1-ol boils at 96°C, while under

propan-1-ol and water under microwave conditions could have water being the first component to be distilled. The preliminary investigations with azeotropes has been with low boiling azeotropes (ethanol/water). Investigation of high boiling azeotropes (hydrochloric acid/water) could have different effects under microwave irradiation.

5.2.3. Disproportionation and alkylation of toluene.

Further investigation of the reactions could be to study the effect of incorporation of modifiers such as phosphorus, boron, or metals into the structure of the zeolite. This could change the selectivity in the reaction since the modifiers could preferentially absorb the microwave radiation. However, expectations would be that the temperature of the reaction would significantly rise where dealkylation of toluene would be the predominant process. Possible experiments could be using an injector type system where injections of toluene were passed through the catalyst. This would reduce the amount of coke build up. However, initial thermal experiments showed that resolution of the products was a problem.

Two interesting features have emerged during the course of this study which should both be pursued and involve regeneration of the catalyst. Experiments on disproportionation of toluene under high pressure conditions have shown that partial regeneration of the catalyst can be performed by raising the partial pressure of hydrogen. Preliminary experiments have indicated that hydrogen at high pressure is needed and that catalysts with lower Si/Al ratio need higher temperature for conversion to be restored. Further experiments are needed to quantify the initial results. Future experiments could investigate the effect of temperature, partial pressure of hydrogen, hydrogen to hydrocarbon ratio and the Si to Al ratio of the zeolite catalyst. The effect of modifiers could also be studied.

The experiments under microwave irradiation have indicated that partial regeneration of the catalyst could be performed by raising the microwave power to burn off the carbon. More extensive experiments are needed to see if this can be performed at a low temperature. Regeneration of zeolite under thermal conditions usually takes place at 500°C, so if carbon could preferentially absorb microwaves without

at a low temperature. Regeneration of zeolite under thermal conditions usually takes place at 500°C, so if carbon could preferentially absorb microwaves without substantially raising the temperature of the zeolite catalyst, it could have beneficial effects.

5.2.4. Catalytic reactions under microwave irradiation.

Although the experiments on disproportionation and alkylation of toluene under microwave conditions has proved unfruitful, this should not deter further research into effects of microwave radiation on catalytic reactions. Experiments on other catalytic reactions have shown that the effects of microwave radiation can be quite striking and further research and development is needed to exploit these effects and study other catalysed systems under microwave conditions. The fact that the only the catalyst is heated under microwave irradiation and that reactions take place at the surface sites and the temperature of these sites can be significantly in excess of the bulk means that reaction takes place at an apparently lower temperature. Thus, the overall temperature of the system can be lowered and gas phase reactions are quenched (due to the vessel being relatively cold) and this can result in different product selectivities. This effect should be explored further for different systems and different catalysts, where the dielectric properties of the catalyst can be changed by the incorporation of modifiers, and thus influence the chemistry of the reaction under investigation.